Finite Amplitude Resonant Acoustic Waves Without Shocks

by

Carlos Maria Celentano

Ingeniero Civil, Universidad de Buenos Aires (1986)

Submitted to the Department of Mathematics
in partial fulfillment of the requirements for the degree of

Doctor of Philosophy

at the

MASSACHUSETTS INSTITUTE OF TECHNOLOGY

January 1995

Signature of Author .....
Department of Mathematics
January 26, 1995

Certified by .....
Rodolfo R. Rosales
Professor of Applied Mathematics
Thesis Supervisor

Accepted by .....
Richard Stanley, Chairman
Applied Mathematics Committee

Accepted by .....
David Vogan, Chairman
Departmental Graduate Committee

Finite Amplitude Resonant Acoustic Waves Without Shocks

by

Carlos Maria Celentano

Submitted to the Department of Mathematics
on January 26, 1995, in partial fulfillment of the
requirements for the degree of
Doctor of Philosophy

Abstract

This thesis presents a new class of solutions in 1D inviscid Gas Dynamics having the remarkable property that they do not develop shocks at any time. These solutions are given as finite amplitude, continuous, time and space periodic acoustic waves propagating in a nonuniform entropy background.

A complete study of the formal conditions that guarantee the existence of small amplitude periodic acoustic waves is performed using weakly nonlinear and bifurcation theories. These analyses provide a detailed explanation concerning the interaction between acoustic and entropy modes that prevents hyperbolic wave breaking and shock formation. Our theoretical approach can be applied in problems involving very general entropy fields. Hence, these time periodic sound waves encompass a rich variety of solutions in nonlinear acoustics.

Numerical calculations reveal that periodic sound waves can occur only in a bounded range of acoustic amplitudes $0 < a \leq a_{max}$. At the maximum amplitude a_{max}, these standing acoustic waves exhibit corners in the flow quantities' profiles, similarly to free-surface gravity waves in water. The computations also show that extremely high intensity periodic sound waves are possible in the presence of relatively small entropy fluctuations.

While neutrally stable against infinitesimal perturbations, it appears that these solutions can be asymptotically stable when subject to small but finite disturbances: continuous waves for all times, with nontrivial acoustic content, may emerge after shocks have disappeared. This striking phenomenon enlarges substantially the class of continuous for all time solutions in nonlinear acoustics: in addition to the strictly periodic acoustic waves found by our theoretical and numerical studies, the stability calculations suggest that continuous, almost periodic solutions can also exist.

Thesis Supervisor: Rodolfo R. Rosales
Title: Professor of Applied Mathematics

Acknowledgements

I would like to thank my advisor, Ruben Rosales, for his guidance and very generous support during my years at MIT. I have learned a great deal from him, and his scientific views exerted a lasting influence on me. Above all, I sincerely appreciate his friendship.

I am grateful to Professors David Benney and Fabian Waleffe for accepting being part of my thesis committee, and to the faculty of the Applied Mathematics group for the quality of their courses and seminars. The research in this thesis was partially supported by NSF grants DMS-9008520 and DMS-9311438 and NASA grant NAG1-1519.

I would also like to thank Pablo Jacovkis, a friend and great mentor, who encouraged me to go back to academic life when I was working as a civil engineer. A particular note of appreciation is due to Rodney Worthing, with whom I shared my learning experience. His friendship is very dear to me.

My deepest gratitudes go to my wife, Albertina, and children, Agustin and Julia, for their love, patience and support. To them, and to my mother Irene, this work is dedicated.

Contents

Introduction

Nonlinear acoustics is concerned with the study of finite amplitude waves that result from the flow of compressible fluids. In terms of the range of wave amplitudes it covers, it is contiguous, from below, with classical (linear) acoustics, which considers infinitesimal perturbations around an equilibrium state. At the other end, it is bounded by the theory of shock waves, where finite jumps in the dependent variables occur across narrow fronts. In this thesis we will be concerned with some new and notable nonlinear acoustic waves, whose strength covers the whole range (from infinitesimal to fully nonlinear, comparable with weak shock waves). We will consider here only the case of 1D Gas Dynamics, though extensions to more dimensions seem possible. Below we include a brief review of some current related theoretical developments (also applying, mostly, to the 1D case only).

The study of nonlinear wave motion was initiated at the beginning of the last century by Poisson, Stokes, Earnshaw and Riemann. Further developments, particularly in the theory of shock waves, were provided by the work of Rankine, Hugoniot and Rayleigh. A detailed exposition of their ideas, along with historical remarks, can be found in Courant & Friedrichs (1948) and Whitham (1974). A broader perspective can be gained through the remarkable collection of original papers edited by Beyer (1984). This material covers the work of the authors mentioned above as well as more recent contributions, among them, Fubini's explicit solution for isentropic flow and Fay's theory of sound propagation in a dissipative medium.

A comprehensive review of theoretical analyses and experimental verifications for relevant practical problems in nonlinear acoustics can be found in Mason (1965) and Beyer (1974). Some current areas of active research include extensions of Burgers' equation for the study of finite amplitude plane waves in a viscous heat-conducting medium (see Rudenko & Soluyan (1977)), and a variety of analyses of sound produced by turbulence based on Lighthill's theory (see Goldstein (1976) and Hardin & Hussaini (1993)).

From a mathematical point of view, it is well-established that, in general, the Cauchy problem for genuinely nonlinear hyperbolic systems of conservation laws (such as the equations of Gas Dynamics) does not have a continuous solution valid for all times. Initial smooth conditions propagate for a while along the characteristic fields. Wave distortion then occurs due to the nonlinearities (i.e., characteristic velocities depend on the solution). Characteristic curves eventually "focus" and lead to the appearance of discontinuities in the flow quantities (shocks) at a finite time. This nonlinear build-up and shock formation process was long ago recognized as a distinctive feature of the theory of hyperbolic problems. It induced the development of notions such as that of generalized or weak solutions, entropy conditions, etc. (cf.

Lax (1957)). Rigorous proofs of existence and uniqueness of weak solutions for the equations of Isentropic Gas Dynamics, together with amplitude decay estimates, were given by Glimm (1965), Nishida & Smoller (1973), DiPerna (1973) and Liu (1977a). Similar studies for the non-isentropic compressible flow of a polytropic gas can be found in Liu (1977b) and Temple (1981). These results were derived for localized initial data in the unbounded line. In such a case, after some time, the solution decomposes into three regions in space — one corresponding to each characteristic field — and the nonlinear interactions between different modes cease to be relevant (see Liu (1977b)). Thus, in one dimensional problems with properly restricted initial data, the description of early stages in hyperbolic wave phenomena appears to be firmly grounded. (In several dimensions the situation is far less satisfactory.)

In contrast, the long time behavior of the solutions to the equations of compressible fluid flow is poorly understood — particularly in bounded geometries, such as the periodic case, where the excitations on the different characteristic fields can not separate in space and interact for all time. It is generally believed that, after shocks form and decay, the remaining solution will consist simply of an entropy wave, with trivial acoustic content: pressure and velocity reach constant values, whereas density may exhibit oscillations in space only[1]. More precisely, waves of genuinely nonlinear fields — in the sense of Lax (1957) — such as the two acoustic modes in Gas Dynamics, are expected to converge to N-waves that decay at the rate $t^{-1/2}$. Waves of linearly degenerate fields, such as the entropy mode, are expected to "remain" and converge to traveling waves. Numerical experiments performed by E & Yang (1991) on the Euler's equations in 1D with periodic initial data, appear to confirm this widely accepted point of view: wave structures with nontrivial acoustic content did not survive at the end of the shock decay process. It will be shown in this thesis that this need not be the case. We will do so by producing time periodic solutions (thus without shocks), but with a *nontrivial* acoustic content (see below). Obviously, the existence[2] of these waves runs counter to the widely held belief explained above.

Another aspect of this problem concerning the large time behavior of solutions, is given by the study of time periodic solutions to nonlinear hyperbolic partial differential equations, which has received considerable attention in recent years. Rigorous analyses have been given for certain types of equations, most of them formulated as perturbation problems, but the theory is far from complete (see, for example, Rabinowitz (1967)–(1978), Brezis & Nirenberg (1978) and references therein). In general,

[1]This belief is based on sound theoretical reasons: shocks form only on the acoustic modes, where they induce decay of the acoustic content. Further, in the case of special solutions where the other modes are not present (weakly nonlinear single mode acoustics, governed by Hopf's equation (inviscid Burgers'), see Whitham (1974)), the decay induced by the shocks completely obliterates the solution as $t \to \infty$. The reasoning, however, does not consider the effects of the nonlinear interactions between the different modes — which are very poorly understood.

[2]Our arguments will be both formal and numerical. Unfortunately, we were unable to produce a rigorous proof of existence. There appear to be some delicate issues regarding this, some of which we discuss in the main body of the thesis, see Section 2.6.

these perturbation problems have the form $Lu + \epsilon F = 0$, where L is a linear hyperbolic partial differential operator and F is a nonlinear function of x, t and u that satisfies certain restrictions to avoid non-smooth solutions. For such problems, the existence and uniqueness of classical (not weak) solutions, periodic in time and satisfying homogeneous boundary conditions in x was investigated. However, no attempt has been made to address this question in the specific context of Gas Dynamics, whose equations are more difficult to treat than the ones used in those theoretical studies.

Nevertheless, periodic solutions of the equations governing compressible fluid flow can be very important regarding the long time behavior of nonlinear acoustic waves. On the basis of recent studies reported below, it is reasonable to speculate that, under certain circumstances, the solution of an initial value problem for the Euler equations of compressible Gas Dynamics may converge, after the shocks have disappeared, towards a time periodic acoustic wave, or some more general solution with nontrivial acoustic content, but no shocks. In practical applications, this type of behavior may have profound implications, for example, in noise control problems arising in aero-acoustics.

The present work can be interpreted as an exploration of this last conjecture. The main objective of this thesis is to investigate the existence of time periodic solutions to the inviscid equations of Gas Dynamics in one space dimension. We will be concerned with finite amplitude sound waves propagating through a nonuniform medium inside a bounded domain. The focus will center on the interaction between the acoustic and entropy modes, and the conditions that may prevent wave breaking and shock formation. Physically, the problem can be visualized , in its simplest setting, as the interaction of plane sound waves inside a fluid-filled tube having a nonuniform density distribution and reflecting boundaries (acoustic cavity resonator).

Our work is based on the asymptotic theory for resonantly interacting, oscillatory weakly nonlinear hyperbolic waves developed by Majda & Rosales (1984). In the case of 1D compressible fluid flow, the time evolution of the leading order acoustic wave amplitudes $\rho(x,t)$ and $\sigma(x,t)$ is governed by a system of integro-differential equations, which can be written as

$$\frac{\partial \rho}{\partial t} + \frac{\partial}{\partial x}\left(\frac{1}{2}\rho^2\right) + \frac{1}{2\pi}\int_0^{2\pi} K(x-y)\ \sigma(y,t)\ dy = 0,$$

$$\frac{\partial \sigma}{\partial t} + \frac{\partial}{\partial x}\left(\frac{1}{2}\sigma^2\right) - \frac{1}{2\pi}\int_0^{2\pi} K(-x+y)\ \rho(y,t)\ dy = 0.$$

In these equations σ and ρ denote the amplitudes of the right and left moving acoustical modes, respectively, while K is the derivative of the entropy. Each wave is tracked in its own coordinate frame (thus x has different meanings as an argument in either σ, ρ or K) and t is a "slow" time. The equations constitute a pair of inviscid Burgers

equations coupled through a linear integral operator with a known kernel $K(x)$ — given by the initial conditions, as the evolution of the entropy is trivial in the limit the equations are derived. A detailed review of the derivation of these equations, together with their solutions is carried out in Section 1.5.

Numerical experiments done by Majda, Rosales & Schonbeck (1988) on these asymptotic equations displayed the behavior typically expected for solutions of the Gas Dynamic equations, namely, shock formation and fast temporal decay. These are well-known attributes of the basic nonlinear building block given by the inviscid Burgers equation. However, in many cases, striking periodic wave-trains emerged, eliminating completely the shock fronts. To explain this surprising outcome, it was argued that the interaction of acoustic waves coupled through an entropy wave background might balance the nonlinear terms and give rise to continuous, nontrivial waveforms. In fact, one can easily see that the linear part of the equations above, given by the integral coupling terms, is weakly[3] dispersive.

Furthermore, Pego (1988) found exact steady traveling wave solutions[4] of the integro-differential equations above that, of course, contain no shocks. This family of solutions only occurs for a range of amplitudes going from zero up to a maximum. They have smooth profiles for all the amplitudes, except the critical maximum one which exhibits corner singularities. This behavior can be understood in terms of a balance between the wave steepening nonlinear terms in the Burgers' part of the equations above and the dispersive integral coupling terms. As the amplitude increases, the steepening terms gain strength, while the dispersive terms cannot do so (due to its "weak" dispersive character: larger gradients — steeper waves — do not increase the amount of dispersion). Thus, the larger amplitude waves become "less smooth" till the balance reaches a breaking point at a critical amplitude. At that point the dispersion can no longer smooth out the wave completely and a singularity must occur. Why the singularity should be a corner is less clear, but this is typical for the balance between hyperbolic quadratic nonlinearities and weak dispersions.

Motivated by these results in weakly nonlinear acoustics, we have studied the possibility that the *full* set of Gas Dynamic equations may support time periodic solutions with nontrivial finite amplitude acoustical contents. These solutions must necessarily be continuous, with no shocks, as the dissipation produced by shocks is incompatible with time periodicity.

The plan of this thesis is as follows. In Chapter 1 we present a first approach to the problem of time periodic acoustic waves, in which the interaction of small amplitude sound and entropy waves is considered. Using perturbation techniques, formal series

[3]Namely: the amount of dispersion does not increase without bound with the wave-number k. This is related to the phenomena of "maximum amplitude" waves with corners, mentioned below.

[4]Precisely corresponding to the ones that emerged in the numerical experiments by Majda, Rosales and Schonbeck (1988).

solutions of Euler's equations will be derived. Though not exempt of certain limitations, this weakly nonlinear analysis will establish clearly the basic mechanism that may prevent shock formation. In Chapter 2, we reformulate the problem in a more fundamental way using bifurcation theory. This analysis will display all the essential elements that play a role in the sound-entropy interaction process. In particular, it will be shown that small amplitude standing acoustic waves can in fact exist when coupled with rather general entropy fields, and that they constitute a large class of solutions in 1D Gas Dynamics. In Chapter 3 we extend numerically the range of applicability of these analytical results, by computing large amplitude acoustic waves. First, we discuss in detail the essential components of our numerical algorithm, which is based upon the theoretical analysis of the previous chapter. Then, we present numerical results that show the dramatic effect a slightly wavy nonuniform medium can have in the generation of high intensity sound waves. As it turns out, time periodic acoustic waves can exist up to *extremely large acoustic amplitudes.* Finally, in Chapter 4, the stability problem for this new class of solutions is briefly addressed. Striking numerical experiments suggest that time periodic nonlinear acoustic waves can be asymptotically stable. Some practical implications arising from our analysis, as well as areas for further research, are suggested in the concluding remarks.

Chapter 1

Weakly Nonlinear Analysis

As a first step towards investigating the possibility of existence of acoustically nontrivial, continuous, time (and space) periodic solutions of the 1D Euler equations of inviscid compressible Gas Dynamics, we develop here a perturbation analysis for the case in which both sound and entropy waves have small amplitudes. More precisely, the purpose of this chapter is to characterize the evolution of weakly nonlinear doubly periodic — thus shock-less — acoustic waves moving through a given slightly nonuniform entropy background.

In this chapter we will consider, mostly, situations where the acoustic waves are second order relative to the (small) entropy variations. This assumption has the advantage of linearizing the equations, which then can be solved explicitly at all orders in the expansion. We will also (briefly) look at the case where the acoustic amplitudes are of the same order as the entropy variations. This is the situation, for general "oscillatory" initial values and general hyperbolic systems of conservation laws, first studied by Majda & Rosales (1984). For the particular case of Gas Dynamics, they found out that:

> Their asymptotic model equations allowed for solutions where the nonlinear wave deformation effects in the acoustic modes were balanced by the resonant coupling through the entropy mode in a dispersive way. Thus, wave breaking and shock formation was stopped.

This effect was found first numerically in Majda, Rosales & Schonbeck (1988). Exact solutions for special cases were also presented there and in Pego (1988). This work is the main motivation for the study in this thesis, where we wish to investigate these phenomena in depth. We will review this earlier work in some detail later in Section 1.5, where a comparison with the expansion in this chapter is also done.

As mentioned above, we are interested in situations where the acoustical component in the solution is nontrivial. If the acoustical and entropy modes have small amplitudes, we can use a "near linear" imagery to understand the physical picture. In this case, the acoustical wave moving to the left interacts with the entropy variations and produces (is "reflected" as) a wave moving to the right, and vice versa. Thus, each wave interacts with the other through the entropy field. It is this interaction that allows for the existence of continuous, time periodic solutions by balancing the

shock producing effects with a dispersive mechanism. As a result, there is no energy loss, since the system energy is merely exchanged between the acoustic modes.

Since we are looking for periodic shock-less solutions at any time, it seems appropriate to use the Poincare-Lindstedt method, which has been successfully employed in nonlinear mechanics of conservative systems. However, it is not trivial to extend this method, originally proposed to deal with systems described by ordinary differential equations, to the case where one has instead a system of hyperbolic partial differential equations. In the later situation, it is necessary to introduce several "strained" variables to follow the evolution of each wave present in the problem, a fact that usually originates such formal complications as to prevent the solution of the perturbation equations at higher orders (cf. Kevorkian & Cole (1981), Section 4.4). These difficulties arise, not surprisingly, when nonlinear interactions between different modes begin to take place. Fortunately, in our case, because of the fundamental symmetries in the Euler equations, it is possible to use two strained variables (corresponding to waves moving to the right or the left) involving only a *single* amplitude-dependent parameter obtained by a solvability condition at every order in the sequence of approximate equations. As mentioned earlier, these solutions consist of two acoustical waves (left and right moving) interacting through the entropy background. In mass-Lagrangian coordinates the entropy is given by the initial conditions, while the acoustical components must each be a reflection of the other via the entropy field. Thus, they must have the same amplitude and their phases will be very simply related (as the velocities must be equal in absolute value).

The material in this chapter is organized as follows. In Section 1.1, the basic equations are presented and nondimensionalized. Then the problem of continuous doubly periodic acoustic waves is formulated as a boundary value problem with periodic boundary conditions. Solutions are sought in the form of a perturbation series in powers of the entropy wave amplitude. Section 1.2 presents the solution of the perturbation equations for an arbitrary compressible fluid while their solvability is analyzed in detail in Section 1.3. Section 1.4 contains explicit solutions up to fourth order for the particular case of a simple entropy wave and a polytropic gas. In Section 1.5, a limiting case that shows continuous but non-smooth traveling wave solutions is presented. Finally, the merits and shortcomings of this approach are discussed in Section 1.6.

The main result from this analysis is that the proposed (formal) asymptotic solutions can be completely calculated to all orders (consistency of the expansion). We were unable to make a proof of convergence for the solution expansion. A reason for that impediment is discussed in Section 1.6 with the help of two problems arising in classical hydrodynamics (i.e., progressive and standing free surface waves in water) that have some strong mathematical and physical similarities with our case. Despite this drawback, the weakly nonlinear approach does provide a coherent frame for understanding the basic mechanisms at play in our problem. At the same time, the

limitations of the present method may also suggest possible cures, by making clear what kind of additional tools are in need.

1.1 Mathematical Formulation

The Euler equations governing inviscid 1D compressible Gas Dynamics constitute a nonlinear hyperbolic system of three conservation laws. In mass-Lagrangian coordinates they can be written as:

$$V_t - u_\xi = 0, \tag{1.a}$$

$$u_t + p_\xi = 0, \tag{1.b}$$

$$E_t + (pu)_\xi = 0, \tag{1.c}$$

where the independent variables are the time t and the mass coordinate ξ, related to the spatial coordinate x by

$$\xi(x,t) = \int_0^x \rho(s,t)ds - \int_0^t (\rho\, u)(0,s)ds,$$

so that $\xi_x = \rho$ and $\xi_t = -\rho u$. Here ρ denotes the density, $V = \rho^{-1}$ is the specific volume, u is the flow velocity, E is the specific total energy and p is the pressure. Equations (1.a) and (1.b) correspond to mass and momentum conservation, respectively, while equation (1.c) expresses conservation of energy. These are the conservation forms appropriate for solutions with discontinuities (shocks and contacts). But we will only deal with solutions that are continuous everywhere. Thus we will manipulate these equations freely and into forms not valid when shocks occur — e.g. see equation (1.3) below.

The specific total energy E is given in terms of the velocity u and the specific internal energy e by

$$E = e + \frac{1}{2}u^2.$$

To close the system, we must include an equation of state, which for an ideal (polytropic) gas can be written as

$$p(V,e) = (\gamma - 1)e/V,$$

where $1 < \gamma < 2$ denotes the ratio of specific heats[5].

For continuous flow fields, using the first and second laws of thermodynamics, it is possible to rewrite the energy equation (1.c) in a simpler form involving only the specific entropy S (cf. Courant & Friedrichs (1948), ch. 1). Namely: use (1.a) and (1.b) to eliminate u in (1.c). Then use $TdS = de + pdV$ (where T is the temperature) to obtain:

$$S_t = 0.$$

This form of the energy equation expresses the fact that changes of state are adiabatic and reversible in this limit where transport effects are neglected and no shocks are present. The equation of state for a polytropic gas with an adiabatic exponent γ can now be put in the form

$$p = p(S, V) = \kappa e^{\gamma S} V^{-\gamma},$$

where κ is a positive constant. In general, we have that p is a smooth function $p = p(S, V)$ where the proper monotonicity and convexity restrictions apply: $p_V < 0$, $p_S > 0$ and $p_{VV} > 0$. Then the system is strictly hyperbolic and either linearly degenerate (particle paths) or genuinely nonlinear (acoustics) in each characteristic field (cf. Lax (1957)). The quantity $C = [-p_V]^{1/2}$ is the Lagrangian sound speed, and it is related to the spatial sound speed c by $c = CV$. For an ideal gas, $C^2 = \gamma p/V$.

Let us now consider small deviations from a basic constant state given by $(V, u, S) = (V_0, 0, S_0)$; let $C_0 = [-p_V(V_0, S_0)]^{1/2}$ and $\delta = p_S(V_0, S_0)$. We then define the following dimensionless quantities:

$$\xi' = \frac{\xi}{L}, \quad t' = \frac{C_0}{L}t, \quad V' = \frac{V}{V_0}, \quad u' = \frac{u}{C_0 V_0}, \quad p' = \frac{p}{C_0^2 V_0}, \quad S' = \frac{(S - S_0)\delta}{C_0^2 V_0},$$

where $L = \frac{\mathcal{L}}{V_0}$, with $\mathcal{L}$ a typical length scale of the actual physical domain[6]. If we substitute these new variables in the equations of motion while dropping the primes and making the change in notation $\xi \to x$, the equations of inviscid 1D Gas Dynamics in mass-Lagrangian coordinates (in dimensionless form) become:

$$V_t - u_x = 0, \tag{1.1}$$

$$u_t + p_x = 0, \tag{1.2}$$

[5]In our actual calculations we assume an ideal gas law, but the expansions are valid for arbitrary equations of state, satisfying the usual physical restrictions.

[6]i.e.: $2\pi\mathcal{L}$ is the wavelength (space period). Thus, in the nondimensional variables the space period is 2π.

$$S_t = 0, \tag{1.3}$$

$$p = p(S,V) = \frac{1}{\gamma} e^{\gamma S} V^{-\gamma}. \tag{1.4}$$

The derivation of the perturbation method in Sections 1.2 and 1.3 will be valid for a general equation of state $p = p(S,V)$; in such a case, the nondimensionalization above yields, for the basic constant state, $p_V(0,1) = -1$ and $p_S(0,1) = 1$ in (1.4) above. Explicit analytic solutions will be given later in Section 1.4, and in that instance the polytropic gas law stated in the right side of (1.4) will be utilized.

It is clear, from equation (1.3), that the entropy function depends only on the mass-Lagrangian coordinate x, and in fact this is the reason for choosing this form of the equations of motion, more suitable from an analytical point of view. Throughout this work, then, the entropy wave is going to be thought of as a given background upon which the nonlinear interaction of sound waves takes place. We consider bounded domains with periodic boundary conditions, which correspond, in physical terms, to the practically important case of sound propagation inside a closed cavity with reflecting boundaries.

The entropy wave is given by

$$S(x) = \epsilon K(2x), \tag{1.5}$$

where $K(\xi)$ is assumed known[7], $O(1)$ and has period 2π with vanishing mean. The entropy wave amplitude ϵ, with $0 < \epsilon \ll 1$, is a measure of the effects introduced by a nonuniform background. (The case for which $\epsilon = 0$ and the sound waves have an infinitesimal amplitude corresponds, of course, to classical acoustics.)

Notice that the entropy has then period π, equal to $1/2$ the acoustical period. The reason for this is explained in Majda & Rosales (1984). Namely: the coupling between the two acoustical waves and the entropy is basically a three wave resonant interaction at the level of each harmonic in the Fourier expansion of the waves (see Ablowitz & Segur (1981), Sec. 4.2). Thus, for each integer n, the wave numbers and wave frequencies must satisfy

$$k_l + k_r = k_e \qquad \text{and} \qquad \omega_l + \omega_r = \omega_e,$$

where the subscripts l, r and e indicate the left moving acoustical wave, the right moving acoustical wave and the entropy wave, respectively. But we have $k_l = k_r = n$ and $\omega_l = -\omega_r = -n$. Thus $k_e = 2n$ and $\omega_e = 0$.

Consider now the Fourier series for K, which can be written as

[7] i.e.: K is given by the initial conditions. Any nonzero mean can be included in S_0 above.

$$K(\xi) = 2cos(\xi) + \sum_{n=2}^{\infty} \hat{k_n}\, cos[\, n\, (\xi - 2\, \xi_n)\,], \qquad (1.5')$$

for some phase shifts ξ_n and Fourier coefficients $\hat{k_n} \geq 0$. Without loss of generality we have assumed $\xi_0 = 0$, as this can be arranged by a change in the origin of the coordinate ξ. Assuming $\hat{k_1} \neq 0$, we kave normalized $\hat{k_1} = 2$ (this defines ϵ uniquely in terms of S in (1.5)). The following restriction will be needed for the validity of the expansion in this chapter: *in the Fourier expansion (1.5') above, there is at least one coefficient* $\hat{k_n} > 0$ *distinct from all the others.*

No additional restrictions on $K(\xi)$ are necessary. However, in later developments, it will be shown that if $K(\xi)$ is an even function, the solutions display certain symmetries in x that are convenient for clarity in the exposition. Thus, this last condition, though not essential in our developments, will be used to facilitate the analysis of our results. Further discussion is postponed until Section 2.3. We note that in all our explicit analytic calculations of Section 1.4 and in the numerical examples of Chapter 3 we will use the simple choice

$$K(2x) = 2\, cos\, (2x), \qquad (1.5'')$$

which is by no means crucial for the validity of the perturbation expansions.

Let us now introduce the characteristic variables:

$$\mu = x - \tau \qquad\qquad \lambda = -x - \tau$$

with $\tau = \omega t$, where the characteristic velocity ω is given by

$$\omega = 1 + \epsilon\omega_1 + \epsilon^2\omega_2 + \epsilon^3\omega_3 + ...$$

These characteristic variables will correspond to the right and left moving acoustical waves, respectively. The corrections ω_i modify the linear velocity $\omega = 1$ due to the nonlinearity at the various orders of approximation, and these constants will be determined along with the asymptotic solution. We then propose as a formal solution to (1.1) and (1.2) the following perturbation expansion:

$$V(x,t) \;=\; V(\mu,\lambda) \;=\; 1 + \sum_{i=1}^{\infty} V_i(\mu,\lambda)\, \epsilon^i, \qquad (1.6)$$

$$u(x,t) \;=\; u(\mu,\lambda) \;=\; \sum_{i=2}^{\infty} u_i(\mu,\lambda)\, \epsilon^i. \qquad (1.7)$$

To complete the formulation of the problem, we impose that V_i and u_i have period 2π in x and τ (thus, period $2\pi/\omega$ in time t). Since the equations of motion preserve the mean values of V and u, as a normalization condition we require zero average over one period in x for all perturbations. (In dimensionless form, we chose the mean of V to be 1, and since we can add any arbitrary constant to u, there is no loss of generality in selecting the mean of u to vanish.) In addition, exploiting the symmetry with respect to time exhibited by the Euler equations — namely, if $[V(x,t), u(x,t)]$ is a smooth solution, so is $[V(x,-t), -u(x,-t)]$ — we will also require that the specific volume V and flow velocity u be even and odd functions of time, respectively. This condition, in fact, picks out a time origin, as the solutions of (1.1)–(1.2) are invariant under time translation. It will also make the solution expansion depend on a single parameter.

Let us emphasize clearly the meaning of the formulation just laid out: our primary objective is to find continuous solutions to the system (1.1)–(1.2), periodic in x and, more importantly, periodic in time, with a period that is going to depend on the solution itself. In this sense, the formulation defines a boundary value problem, with periodic boundary conditions both in x and t, although the period $T = 2\pi/\omega$ is unknown a priori. We point out that the fact that the solution is periodic in time guarantees that the process of nonlinear wave distortion does not lead to shocks. This is because shocks are dissipative and no solution with shocks can be periodic. Note also that the solution will have a nontrivial acoustic component, as it has nontrivial time dependence and $p_x \neq 0$.

For later reference, we state here the form of the pressure expansion, a direct consequence of the fact that p is a smooth function of S and V, $p = p(S,V)$, with $p_S(0,1) = -p_V(0,1) = 1$. Then, from (1.5) and (1.6) we obtain (upon expanding p in Taylor series and collecting powers of ϵ)

$$p(S,V) \;=\; \sum_{i=0}^{\infty} p_i\, \epsilon^i, \tag{1.8}$$

where

$$p_0 = p(0,1), \qquad p_1 = -V_1 + K, \qquad p_2 = -V_2 + \frac{1}{2}\Gamma_{02}\, V_1^2 + \Gamma_{11}\, K\, V_1 + \frac{1}{2}\Gamma_{20}\, K^2,$$

and in general, for $i > 2$,

$$p_i = -V_i + \hat{p}_i, \qquad \hat{p}_i = \Gamma_{02}\, V_1\, V_{i-1} + \Gamma_{11}\, K\, V_{i-1} + P_i,$$

with

$$P_i = f(K, V_1, V_2, ..., V_{i-2}), \qquad \Gamma_{lm} = \left(\frac{\partial}{\partial S}\right)^l \left(\frac{\partial}{\partial V}\right)^m p(0,1).$$

The pressure expansion for the particular case of a polytropic gas used in our detailed calculations, is given in Appendix 1.1.

1.2 Perturbation Solution

In the analysis that follows, it will be convenient to work some of the aspects in the primary independent variables x and τ, while others will be handled in the characteristic variables μ and λ. This possibility of switching between both sets of independent variables relies on the important fact, to be shown below, that 2π–periodicity in x and τ is equivalent, not only to 4π–periodicity in μ and λ as the definition of the characteristic variables indicates, but indeed to 2π–periodicity in μ and λ. The reason that guarantees this property has to do with the entropy mode having a period in x half of that corresponding to the acoustic modes. This the way that the three wave resonant interaction mentioned below (1.5) shows up in this expansion.

The analyses of this and the next sections will be valid for a general equation of state $p = p(S, V)$. Thus, introducing expansions (1.6) to (1.8) in the equations for conservation of mass and momentum (1.1)–(1.2) — recall that the energy equation (1.3) is automatically satisfied by an entropy background of the form (1.5) — we obtain the following sequence of linear inhomogeneous equations:

At order $O(\epsilon)$:

$$V_{1\tau} = 0, \tag{1.9}$$

$$p_{1x} = 0. \tag{1.10}$$

At order $O(\epsilon^2)$:

$$V_{2\tau} - u_{2x} = -\omega_1 \, V_{1\tau}, \tag{1.11}$$

$$u_{2\tau} - V_{2x} = -\hat{p}_{2x}, \tag{1.12}$$

and in general, at order $O(\epsilon^n)$, for $n \geq 2$:

$$V_{n\tau} - u_{nx} = -A_n(x, \tau), \tag{1.13}$$

$$u_{n\tau} - V_{nx} = -B_n(x, \tau), \tag{1.14}$$

where

$$A_n(x,\tau) \;=\; \sum_{i=1}^{n-1} \omega_i \; V_{n-i_\tau}, \tag{1.15}$$

$$B_n(x,\tau) \;=\; \sum_{i=1}^{n-2} \omega_i \; u_{n-i_\tau} \;+\; \hat{p_{n_x}}. \tag{1.16}$$

Given the form of the pressure expansion (1.8), the first order solution is simply given by

$$V_1 \;=\; K(\mu - \lambda), \tag{1.17}$$

where we recall that $S = \epsilon K(\mu - \lambda)$ is the assumed form of the entropy background.

The second order equations can now be written as

$$V_{2_\tau} - u_{2_x} = 0, \tag{1.18}$$

$$u_{2_\tau} - V_{2_x} = -\Big\{ \Gamma_{11}\, K\, V_1 + \frac{1}{2}\,\Gamma_{02}\, V_1^2 + + \frac{1}{2}\,\Gamma_{20}\, K^2 \Big\}_x. \tag{1.19}$$

Substituting the known functions in the right hand sides they reduce to

$$V_{2_\tau} - u_{2_x} = 0, \tag{1.20}$$

$$u_{2_\tau} - V_{2_x} = -\Big\{ \Lambda\, K^2 \Big\}_x, \tag{1.21}$$

where $\Lambda = \Gamma_{11} + 1/2\ \Gamma_{02} + 1/2\ \Gamma_{20}$. The general solution of (1.20)–(1.21) can be written as

$$V_2 = \mathcal{V}_2(\mu,\lambda) - \sigma_2(\mu) - \rho_2(\lambda), \tag{1.22}$$

$$u_2 = \mathcal{U}_2(\mu,\lambda) + \sigma_2(\mu) - \rho_2(\lambda), \tag{1.23}$$

where

$$\mathcal{V}_2(\mu,\lambda) = \Lambda\,(K^2 - \overline{K^2}), \qquad\qquad \mathcal{U}_2(\mu,\lambda) \equiv 0,$$

and σ_2 and ρ_2 are arbitrary. Here a bar denotes the average over x of a 2π–periodic function. To satisfy the requirements of periodicity, time symmetry and zero average over one period in x, the functions $\sigma_2(\mu)$ and $\rho_2(\lambda)$ must be 2π–periodic in μ and λ, with zero mean, and satisfy $\rho_2(\xi) = \sigma_2(-\xi)$. As usual, the determination of σ_2 and ρ_2 must wait until the $O(\epsilon^3)$ terms are treated, at which time the frequency correction ω_1 will also be obtained.

In general, at $O(\epsilon^n)$, $n \geq 2$, the solutions $V_n(\mu,\lambda)$, $u_n(\mu,\lambda)$ will be determined up to two free functions, $\sigma_n(\mu)$ and $\rho_n(\lambda)$, satisfying the same conditions stated above for σ_2 and ρ_2. These unidirectional waves $\sigma_n(\mu)$ and $\rho_n(\lambda)$ will be obtained at $O(\epsilon^{n+1})$, while the velocity perturbation ω_n will follow from the solution of the $O(\epsilon^{n+2})$ equations.

Let us now prove the statements in the previous paragraph, in particular showing that the expansion is consistent at all orders. We will do this by induction. Assume $n \geq 3$ and that the perturbation equations have been solved up to $O(\epsilon^{n-1})$ (inductive hypothesis). From equations (1.13)–(1.14), we have

$$(V_n + u_n)_\tau - (V_n + u_n)_x = -(A_n + B_n), \tag{1.24}$$

$$(V_n - u_n)_\tau + (V_n - u_n)_x = -(A_n - B_n), \tag{1.25}$$

where

$$A_n = \sum_{i=1}^{n-2} \omega_i \, (V_{n-i})_\tau,$$

$$B_n = \sum_{i=1}^{n-2} \omega_i \, (u_{n-i})_\tau + (\hat{p}_n)_x.$$

From the pressure expansion (1.8) and the first order solution (1.17), the pressure term appearing in B_n is given by

$$\hat{p}_n = \beta \, K \, V_{n-1} + P_n(K, V_1, V_2, ..., V_{n-2}),$$

where $\beta = \Gamma_{02} + \Gamma_{11}$. Notice that A_n and B_n are both 2π–periodic functions of x and τ, with zero mean in x. Furthermore, from our inductive hypothesis, the only terms in A_n and B_n not fully determined are those involving ω_{n-2} or $V_{n-1}(\mu,\lambda)$, $u_{n-1}(\mu,\lambda)$. In particular, P_n is known at this stage. It should be pointed out that no terms involving ω_{n-1} appear since equation (1.9) holds and there is no u_1.

The general solution of (1.24)–(1.25) can be written as

$$V_n + u_n = -2 \int_0^\tau M_n(x + \tau - s, s) \, ds - 2\rho_n(\lambda), \tag{1.26}$$

$$V_n - u_n = -2 \int_0^\tau N_n(x - \tau + s, s)\, ds - 2\sigma_n(\mu), \tag{1.27}$$

where $\sigma_n(\mu)$ and $\rho_n(\lambda)$ are arbitrary functions, and M_n and N_n are obtained from

$$M_n = \frac{1}{2}\,(\,A_n + B_n\,), \qquad N_n = \frac{1}{2}\,(\,A_n - B_n\,).$$

The complete solution of the perturbation equations at $O(\epsilon^n)$ will be given by

$$V_n(\mu, \lambda) = \mathcal{V}_n(\mu, \lambda) - \sigma_n(\mu) - \rho_n(\lambda), \tag{1.28}$$

$$u_n(\mu, \lambda) = \mathcal{U}_n(\mu, \lambda) + \sigma_n(\mu) - \rho_n(\lambda), \tag{1.29}$$

where

$$\mathcal{V}_n = -\int_0^\tau \{\, M_n(x + \tau - s, s) + N_n(x - \tau + s, s)\,\}\, ds, \tag{1.30}$$

$$\mathcal{U}_n = -\int_0^\tau \{\, M_n(x + \tau - s, s) - N_n(x - \tau + s, s)\,\}\, ds. \tag{1.31}$$

In (1.30)–(1.31), $\mathcal{V}_n$ and $\mathcal{U}_n$ are a particular solution of the perturbation equations at $O(\epsilon^n)$ defined by $\mathcal{V}_n = \mathcal{U}_n = 0$ for $\tau = 0$. This is a convenient normalization, but others are possible. In Section 1.4 we calculate a solution up to fourth order for a particular entropy field and a polytropic gas, and in that case, a different normalization will be used for $\mathcal{V}_n$ and $\mathcal{U}_n$.

Thus, the solutions (1.28)–(1.29) are given by the superposition of two unidirectional waves $\sigma_n(\mu)$ and $\rho_n(\lambda)$, moving to the right and left, respectively, *plus* some interaction terms $\mathcal{V}_n(\mu, \lambda)$ and $\mathcal{U}_n(\mu, \lambda)$ due to weakly nonlinear effects. Since each mode is "produced" by reflection of the other on the entropy field, it is clear that both should have the same velocity. Strictly, ω defines the period of the stationary wave; but in a loose sense, it can also be interpreted as the average velocity with which $\sigma_n(\mu)$ and $\rho_n(\lambda)$ move to the right and left, respectively. These standing waves constitute a nonlinear solution that cannot result simply from the superposition of unidirectional modes $\sigma_n(\mu)$ and $\rho_n(\lambda)$; this is, ultimately, the reason why the interaction terms $\mathcal{V}_n(\mu, \lambda)$ and $\mathcal{U}_n(\mu, \lambda)$ are needed.

Notice that in (1.28)–(1.29), the functions $\mathcal{V}_n(\mu, \lambda)$ and $\mathcal{U}_n(\mu, \lambda)$ — except for the unknown contributions of V_{n-1} and u_{n-1} — are 2π–periodic in x, with zero mean, as follows from the definition of M_n and N_n and the induction hypothesis. In addition, up to $O(\epsilon^{n-1})$, the perturbation solutions satisfy the symmetric properties with respect to time, namely, for $i = 2, 3, ..., n - 1$

$$V_i(\mu,\lambda) = V_i(-\lambda,-\mu), \qquad u_i(\mu,\lambda) = -u_i(-\lambda,-\mu),$$

as $t \to -t$ translates into $(\mu,\lambda) \to (-\lambda,-\mu)$. These properties follow from the explicit requirement on the traveling modes $\rho_{i-1}(\xi) = \sigma_{i-1}(-\xi)$ imposed at any $O(\epsilon^i)$. By starting with $\rho_2(\xi) = \sigma_2(-\xi)$ at the first nontrivial order $n = 2$, time symmetries will be passed on to the higher order solutions through equations (1.28)-(1.31) and explicitly enforced for $\sigma_{n-1}(\mu)$ and $\rho_{n-1}(\lambda)$ in equation (1.33) below. Then, it is easy to see that A_n is odd in time and B_n is even. Thus

$$M_n(x,-\tau) = -N_n(x,\tau). \tag{1.32}$$

Hence, using (1.30)-(1.31), we can conclude that $\mathcal{V}_n(\mu,\lambda)$ and $\mathcal{U}_n(\mu,\lambda)$ are even and odd functions of time, respectively.

Therefore, the solution V_n, u_n will satisfy all the desired conditions if $\mathcal{V}_n$ and $\mathcal{U}_n$ are 2π-periodic in τ and $\rho_n(\xi) = \sigma_n(-\xi)$ are also 2π-periodic functions of mean zero. $\mathcal{V}_n$ and $\mathcal{U}_n$ will be 2π-periodic in τ if and only if they vanish at $\tau = 0$. Thus, we have the equations

$$\int_0^{2\pi} M_n(x+\tau-s,s)\,ds \;\equiv\; \int_0^{2\pi} N_n(x-\tau+s,s)\,ds \;\equiv\; 0,$$

which are equivalent, in characteristic coordinates, to

$$\int_0^{2\pi} M_n(\mu,\lambda)\,d\mu \equiv \int_0^{2\pi} N_n(\mu,\lambda)\,d\lambda \equiv 0. \tag{1.33}$$

These equations constitute the *solvability conditions* for time periodic solutions of (1.13)-(1.14), and we must show that they can be satisfied. They will be analyzed in detail in the next section in order to show that the sequence of linear inhomogeneous equations (1.13)-(1.14) can be solved at any order. We will show there that (1.33) can be satisfied if ω_{n-2} is chosen properly.

Strictly speaking, the integrals in (1.33) should be from 0 to 4π, as $x = (\mu-\lambda)/2$ and $\tau = (-\mu-\lambda)/2$, so that 2π-periodicity in x and τ generally guarantees only 4π-periodicity in μ and λ. We now show, however, that all the functions involved are 2π-periodic in each one of μ and λ.

The proof is by induction. Clearly, V_1, V_2 and u_2 satisfy the previous claim. Let $n \geq 3$ and assume that the proposition applies for V_j and u_j, $j < n$. Then A_n and B_n, and consequently M_n and N_n also satisfy the proposition. To complete the argument, we must show that $\mathcal{V}_n$ and $\mathcal{U}_n$ have that property. In terms of the characteristic variables, (1.30)-(1.31) are

$$\mathcal{V}_n = \frac{1}{2}\left\{ \int_{-\lambda}^{\mu} M_n(s,\lambda)\, ds + \int_{-\mu}^{\lambda} N_n(\mu,s)\, ds \right\}$$

$$\mathcal{U}_n = \frac{1}{2}\left\{ \int_{-\lambda}^{\mu} M_n(s,\lambda)\, ds - \int_{-\mu}^{\lambda} N_n(\mu,s)\, ds \right\}$$

But these functions are clearly 2π–periodic in μ and λ, given the periodicity conditions (1.33) and the fact that M_n and N_n are 2π–periodic in μ and λ. Hence, all the functions defining the perturbation solution are 2π–periodic in x, τ and *also* μ and λ.

1.3 Solvability of the perturbation equations

As advanced before, the basic strategy in the present perturbation scheme can be expressed as follows: at $O(\epsilon^n)$, the solution V_n, u_n will be calculated, using (1.28)–(1.31), except for two undetermined traveling modes $\sigma_n(\mu)$ and $\rho_n(\lambda)$ — which will be obtained when solving the equations at $O(\epsilon^{n+1})$ — and the frequency correction ω_n — calculated at $O(\epsilon^{n+2})$. To show that this argument holds — and thus that the expansion (1.6)–(1.7) is consistent to all orders — we must now investigate under what conditions the requirements in (1.33) are satisfied. We will also demonstrate that the whole expansion, subject to the conditions enunciated in Section 1.1, depends on a single parameter given by the fundamental characteristic velocity of the periodic acoustic waves.

As in last section, we proceed here inductively. It was mentioned earlier that it is convenient to work some aspects of the theory in the primary independent variables x and τ, while others are more clear in the characteristic variables μ and λ. In the previous section, 2π–periodicity and mean zero in x were shown to hold at any order in the perturbation equations by working essentially with the equations expressed in terms of x and τ. Here, as suggested by the form of (1.33), periodicity in time will be handled more easily using μ and λ.

The first solvability conditions occur at $O(\epsilon^3)$. Recalling that $\partial_x = \partial_\mu - \partial_\lambda$ and $\partial_\tau = -\partial_\mu - \partial_\lambda$, from the third order equations of motion we have

$$(\, V_3 + u_3 \,)_\mu = \frac{1}{2}\,(\, A_3 + B_3 \,), \tag{1.34}$$

$$(\, V_3 - u_3 \,)_\lambda = \frac{1}{2}\,(\, A_3 - B_3 \,), \tag{1.35}$$

where

$$A_3 = \omega_1 \, V_{2\tau} = -\omega_1 \, (\, V_{2\mu} + V_{2\lambda} \,),$$

$$B_3 = \omega_1 \, u_{2\tau} + \hat{p}_{3_x} = -\omega_1 \, (\, u_{2\mu} + u_{2\lambda} \,) + \hat{p}_{3_\mu} - \hat{p}_{3_\lambda}.$$

To insure boundedness of the solutions, we have to eliminate "secular" terms appearing in the right hand side of equations (1.34)-(1.35). Thus, our periodicity conditions (1.33) require:

$$\int_0^{2\pi} [\, \omega_1 \, (\, V_{2\lambda} + u_{2\lambda} \,) + \hat{p}_{3_\lambda} \,] \, d\mu = 0, \tag{1.36}$$

$$\int_0^{2\pi} \left[\omega_1 \, \left(V_{2\mu} - u_{2\mu} \right) + \hat{p}_{3_\mu} \right] \, d\lambda = 0. \tag{1.37}$$

Expanding these equations we obtain:

$$-\omega_1 \, \rho_2'(\lambda) - \frac{\beta}{4\pi} \int_0^{2\pi} \frac{\partial K}{\partial \lambda} \, \sigma_2(\mu) d\mu =$$

$$= -\frac{1}{4\pi} \, \omega_1 \, \frac{\partial}{\partial \lambda} \int_0^{2\pi} [\, \mathcal{V}_2 + \mathcal{U}_2 \,] \, d\mu - \frac{1}{4\pi} \frac{\partial}{\partial \lambda} \int_0^{2\pi} [\, \beta \, K \mathcal{V}_2 + P_3 \,] \, d\mu, \tag{1.38}$$

$$-\omega_1 \, \sigma_2'(\mu) - \frac{\beta}{4\pi} \int_0^{2\pi} \frac{\partial K}{\partial \mu} \, \rho_2(\lambda) d\lambda =$$

$$= -\frac{1}{4\pi} \, \omega_1 \, \frac{\partial}{\partial \mu} \int_0^{2\pi} [\, \mathcal{V}_2 - \mathcal{U}_2 \,] \, d\lambda - \frac{1}{4\pi} \frac{\partial}{\partial \mu} \int_0^{2\pi} [\, \beta \, K \mathcal{V}_2 + P_3 \,] \, d\lambda. \tag{1.39}$$

These integro-differential equations describe the evolution in characteristic variables of two unidirectional waves, $\sigma_2(\mu)$ and $\rho_2(\lambda)$ — propagating to the right and left, respectively — and represent a linearized version of the system derived by Majda & Rosales (1984). The coupling between these acoustic modes is given by the linear integral operator, whose kernel is the derivative of the known entropy field. The forcing terms include functions already obtained at previous order, and a little calculation shows that they vanish at this order. Furthermore, it is easy to see that equations (1.38)-(1.39) are compatible with the requirement concerning time symmetries, i.e., $\rho_2(\xi) = \sigma_2(-\xi)$, so that in (1.22)-(1.23) the specific volume V_2 and velocity u_2 are even and odd functions of time, respectively. These results imply that, in fact, we have a *single* solvability equation

$$\omega_1 \, \sigma_2'(\mu) + \frac{\beta}{4\pi} \int_0^{2\pi} \, K'(\mu + s) \, \sigma_2(s) \, ds = 0. \tag{1.40}$$

Consider (1.40) and let

$$y_2(\mu) = \sigma_2'(\mu) \tag{1.41}$$

We note that, since σ_2 must have zero mean, it is completely determined by its derivative. A simple integration by parts then shows that (1.40) is equivalent to the eigenvalue problem:

$$L[y_2] = \omega_1\, y_2, \qquad L[y] = \frac{\beta}{4\pi}\int_0^{2\pi} K(\mu + s)\, y(s)\, ds. \tag{1.42}$$

Notice that any solution of (1.42) will automatically have mean zero — provided $\omega_1 \neq 0$, which will be shown soon — as K does, and that the operator L is self-adjoint relative to the standard inner (scalar) product.

The eigenvalues of L can be found using Fourier series. Let the entropy field K be given, as in (1.5'), by

$$K(\xi) = 2cos(\xi) + \sum_{n=2}^{\infty} \hat{k_n}\, cos[\, n\,(\xi - 2\,\xi_n)\,], \tag{1.43}$$

for some phase shifts ξ_n and Fourier coefficients $\hat{k_n} \geq 0$. Then the eigenvalues and eigenvectors of (1.42) are

$$(1.44)\quad \begin{cases} \omega_1 = \ \ \beta/2, & y_2(\mu) = \ \ \alpha\, cos(\mu), & \Longrightarrow \quad \sigma_2(\mu) = \alpha\, sin(\mu), \\ \omega_1 = -\beta/2, & y_2(\mu) = -\alpha\, sin(\mu), & \Longrightarrow \quad \sigma_2(\mu) = \alpha\, cos(\mu), \end{cases}$$

$$(1.45)\quad \begin{cases} \omega_1 = \ \ \hat{k_n}\beta/4,\ y_2(\mu) = \ \ n\alpha cos[n(\mu - \xi_n)], \Longrightarrow \sigma_2(\mu) = \alpha sin[n(\mu - \xi_n)], \\ \omega_1 = -\hat{k_n}\beta/4,\ y_2(\mu) = -n\alpha sin[n(\mu - \xi_n)], \Longrightarrow \sigma_2(\mu) = \alpha cos[n(\mu - \xi_n)], \end{cases}$$

where $n \geq 2$ and α is arbitrary. The free parameter α appears as a consequence of the periodicity equations (1.38)–(1.39) being homogeneous at this order. Together with ϵ, the entropy wave amplitude, α is going to define the amplitude of the weakly nonlinear acoustic waves, in the form $O(\epsilon^2\alpha)$ — see equations (1.6)–(1.7). Notice that if the time symmetry condition is not imposed, namely, $\rho_2(\xi) = \sigma_2(-\xi)$, then other pairs of solutions $[\sigma_2(\mu), \rho_2(\lambda)]$ satisfying (1.38)–(1.39) can be found. These only differ from the solutions (1.44) and (1.45) in a phase shift, due to the translationally-invariant character of the original equations of motion with respect to time.

In the solutions (1.44)–(1.45) of the homogeneous problem (1.40), for any positive $\hat{k_n}$ *distinct* from the others, the eigenvalues $\omega_1 = \pm\hat{k_n}\,\beta/4$ will be simple. We then choose ω_1 and $y_2(\mu)$ as a simple eigenvalue and eigenfunction, respectively. This fact

is very important for the solution of the perturbation equations, as it will be shown below. Notice that when $\omega_1 > 0$ the nonlinear effects accelerate the modes relative to the linearized speed 1; the opposite occurs for $\omega_1 < 0$.

Having analyzed the solvability conditions (1.33) that appear first at $O(\epsilon^3)$, we proceed now with our inductive argument, assuming that these conditions have been satisfied up to $(n-1)$, for $n > 3$.

From the equations of motion (1.13)–(1.14) at $O(\epsilon^n)$, we obtained equations (1.24)–(1.25), which expressed in characteristic variables take the form

$$(V_n + u_n)_\mu = \frac{1}{2} (A_n + B_n), \tag{1.24'}$$

$$(V_n - u_n)_\lambda = \frac{1}{2} (A_n - B_n), \tag{1.25'}$$

where

$$A_n = -\sum_{i=1}^{n-2} \omega_i \left[(V_{n-i})_\mu + (V_{n-i})_\lambda \right],$$

$$B_n = -\sum_{i=1}^{n-2} \omega_i \left[(u_{n-i})_\mu + (u_{n-i})_\lambda \right] + (\hat{p}_n)_\mu - (\hat{p}_n)_\lambda.$$

Then we impose the solvability condition (1.33), namely

$$\int_0^{2\pi} \left\{ \sum_{i=1}^{n-2} \omega_i [(V_{n-i})_\lambda + (u_{n-i})_\lambda] + (\hat{p}_n)_\lambda \right\} d\mu = 0, \tag{1.46}$$

$$\int_0^{2\pi} \left\{ \sum_{i=1}^{n-2} \omega_i \left[(V_{n-i})_\mu - (u_{n-i})_\mu\right] + (\hat{p}_n)_\mu \right\} d\lambda = 0. \tag{1.47}$$

Expanding above, we obtain the coupled integro-differential equations:

$$-\omega_1 \rho'_{n-1}(\lambda) - \frac{\beta}{4\pi} \int_0^{2\pi} \frac{\partial K}{\partial \lambda} \sigma_{n-1}(\mu) d\mu = \omega_{n-2} \rho'_2(\lambda) + R_n(\lambda), \tag{1.48}$$

$$-\omega_1 \sigma'_{n-1}(\mu) - \frac{\beta}{4\pi} \int_0^{2\pi} \frac{\partial K}{\partial \mu} \rho_{n-1}(\lambda) d\lambda = \omega_{n-2} \sigma'_2(\mu) + T_n(\mu), \tag{1.49}$$

where $R_n(\lambda)$ and $T_n(\mu)$ are known functions, 2π–periodic with zero mean, and given by

$$R_n(\lambda) = \sum_{i=1}^{n-3} -\frac{1}{4\pi}\,\omega_i\,\frac{\partial}{\partial\lambda}\int_0^{2\pi}\left[\,\mathcal{V}_{n-i}+\mathcal{U}_{n-i}\,\right]d\mu + \sum_{i=2}^{n-3}\omega_i\,\rho'_{n-i}(\lambda)$$
$$-\frac{1}{4\pi}\frac{\partial}{\partial\lambda}\int_0^{2\pi}\left[\,\beta\,K\mathcal{V}_{n-1}+P_n\,\right]d\mu, \tag{1.50}$$

$$T_n(\mu) = \sum_{i=1}^{n-3} -\frac{1}{4\pi}\,\omega_i\,\frac{\partial}{\partial\mu}\int_0^{2\pi}\left[\,\mathcal{V}_{n-i}-\mathcal{U}_{n-i}\,\right]d\lambda + \sum_{i=2}^{n-3}\omega_i\,\sigma'_{n-i}(\mu)$$
$$-\frac{1}{4\pi}\frac{\partial}{\partial\mu}\int_0^{2\pi}\left[\,\beta\,K\mathcal{V}_{n-1}+P_n\,\right]d\lambda. \tag{1.51}$$

Now, considering the constructive equations (1.28)–(1.31) and the symmetric property (1.32), we can easily show that the following relation between the known forcing terms R_n and T_n must also hold:

$$R_n(-\mu) \;=\; -\,T_n(\mu). \tag{1.52}$$

In addition, implementing time symmetric properties at $O(\epsilon^n)$, we take

$$\rho_{n-1}(\lambda) \;=\; \sigma_{n-1}(-\lambda). \tag{1.53}$$

Then, as we did in equation (1.40), using (1.52) and (1.53) above we can reduce equations (1.48)–(1.49) to a *single* solvability condition, from which we will obtain the unidirectional wave $\sigma_{n-1}(\mu)$, 2π–periodic with mean zero, satisfying

$$\omega_1\,\sigma'_{n-1}(\mu) + \frac{\beta}{4\pi}\int_0^{2\pi} K'(\mu+s)\,\sigma_{n-1}(s)ds = -\omega_{n-2}\,\sigma'_2(\mu) - T_n(\mu). \tag{1.54}$$

As before, let us introduce

$$y_{n-1}(\mu) \;=\; \sigma'_{n-1}(\mu). \tag{1.55}$$

The function $y_{n-1}(\mu)$ is 2π–periodic with zero mean, and determines $\sigma_{n-1}(\mu)$ uniquely. Then, the inhomogeneous problem (1.54) takes the form

$$\omega_1\,y_{n-1} \;-\; L[y_{n-1}] \;=\; -\omega_{n-2}\,y_2 \;-\; T_n, \tag{1.56}$$

where the operator $L[y]$ has been defined in (1.42). To solve equation (1.56), we use Fredholm's alternative: this equation will have a periodic solution — which will automatically be zero mean, as the right side and the range of L are — provided that

$$\omega_{n-2}\int_0^{2\pi} y_2^2(\mu)\,d\mu \;=\; -\int_0^{2\pi} T_n(\mu)\,y_2(\mu)\,d\mu. \tag{1.57}$$

Equation (1.57) determines the frequency correction ω_{n-2} necessary to avoid secular terms in the equations of motion at $O(\epsilon^n)$. Then, the function $y_{n-1}(\mu)$ is obtained from (1.56), up to a multiple of the homogeneous solution $y_2(\mu)$. Without loss of generality, we can normalize y_{n-1} by requiring it to be orthogonal to y_2, for any $n > 3$. Through (1.55) and (1.53), we thus complete the periodic solution $[V_n(\mu, \lambda), u_n(\mu, \lambda)]$.

A final remark concerning the solvability of the perturbation equations. Recall that when solving the periodicity equation (1.42), we assume the existence of a simple eigenvalue ω_1 that defines the first order frequency correction in the form $\omega = 1 + \epsilon\,\omega_1 + O(\epsilon^2)$. If the eigenvalue ω_1 were not simple, there would be more than a single Fredholm condition at $O(\epsilon^n)$, and they could not be satisfied with a single parameter ω_{n-2}. It is not even clear whether we can make an expansion that would work in such a case. This difficulty justifies the assumptions on the entropy wave $K(\xi)$ made at the beginning, following equation (1.5').

The fact that the perturbation solution can be calculated for every order, gives a solid basis to speculate that for sufficiently small values of the parameters ϵ and α , the asymptotic solutions would indeed become convergent series defining continuous solutions that would not develop shock fronts. Although it seems difficult to carry the series summation in any particular case, the result that there are no formal obstacles (i.e., no hidden breakdowns of the asymptotic series at higher orders) constitutes a necessary condition upon which other methods can be brought to remedy the limitations of the weakly nonlinear approach.

Remark 1.1: we notice that if in (1.40)–(1.45) we select $\omega_1 = \pm\hat{k}_n\beta/4$ for some $n \geq 2$ then, up to leading order, the expansion has period $2\pi/n$ in τ. If n is even, then the period in x is π. In fact, it can be shown that these results apply to all orders, but we will not show it here as these issues are better understood in the context of the expansion in Chapter 2.

1.4 Explicit solutions for a simple entropy wave

The sequence of linear inhomogeneous equations (1.13)–(1.14) can be solved at any order using the method developed in Sections 1.3 and 1.4, valid for arbitrary entropy fields of the form (1.5') and a general equation of state $p = p(S, V)$. In this section, we apply that method to calculate explicit analytical solutions for the particular case in which the entropy background is simply given by (1.5") and a polytropic gas law is employed, namely

$$S(x) = \epsilon\, 2\, cos(2x), \qquad 0 < \epsilon \ll 1,$$

and

$$p = p(S,V) = \frac{1}{\gamma} e^{\gamma S} V^{-\gamma}.$$

The solutions for the specific volume V and velocity u obtained in such a way have the form of double Fourier series in x and t (or μ and λ), with coefficients given as series in powers of the entropy wave amplitude ϵ that also depend on the amplitude-like parameter α (see homogeneous solutions (1.44)-(1.45)). To write down the series solutions in a compact form, the following notation is used for the Fourier coefficients: $\varphi_{j,k}^{(i)}$, where j and k refer to the order of the harmonic in $(\mu - \chi_0)$ and $(\lambda + \chi_0)$, respectively, and the super index i denotes the order of the function in the asymptotic expansion in powers of ϵ. The constant χ_0 is equal to $\pi/2$ for the branch with frequency correction $\omega_1 > 0$, while $\chi_0 = 0$ for the branch with $\omega_1 < 0$. The interaction terms $\mathcal{V}_n$ and $\mathcal{U}_n$ are computed by the method of undetermined coefficients, since in this case all the functions involved are trigonometric. Thus, the general structure of the solution is given by:

$$V(\mu,\lambda) = 1 + \sum_{i=1}^{\infty} V_i(\mu,\lambda)\,\epsilon^i, \qquad V_i(\mu,\lambda) = \mathcal{V}_i(\mu,\lambda) - \sigma_i(\mu) - \rho_i(\lambda),$$

$$u(\mu,\lambda) = \sum_{i=2}^{\infty} u_i(\mu,\lambda)\,\epsilon^i, \qquad u_i(\mu,\lambda) = \mathcal{U}_i(\mu,\lambda) + \sigma_i(\mu) - \rho_i(\lambda).$$

The unidirectional modes can be written

$$\sigma_i(\mu) = \sum_{j=2}^{i-1} \delta_{j,0}^{(i)}\, cos\,[j(\mu - \chi_0)], \qquad \rho_i(\lambda) = \sum_{j=2}^{i-1} \delta_{0,j}^{(i)}\, cos\,[j(\lambda + \chi_0)],$$

and the interaction terms take the form

$$\mathcal{V}_i(\mu,\lambda) = \sum_{j=1}^{i-2} \left\{ f_{j,0}^{(i)}\, cos\,[j(\mu - \chi_0)] + f_{0,j}^{(i)}\, cos\,[j(\lambda + \chi_0)] \right\}$$
$$+ \sum_{j=1}^{i} \sum_{k=-i}^{i} \varphi_{j,k}^{(i)}\, cos\,[j(\mu - \chi_0) - k(\lambda + \chi_0)],$$

$$\mathcal{U}_i(\mu,\lambda) = \sum_{j=1}^{i-2} \left\{ g_{j,0}^{(i)}\, cos\,[j(\mu - \chi_0)] + g_{0,j}^{(i)}\, cos\,[j(\lambda + \chi_0)] \right\}$$
$$+ \sum_{j=1}^{i} \sum_{k=-i}^{i} \psi_{j,k}^{(i)}\, cos\,[j(\mu - \chi_0) - k(\lambda + \chi_0)].$$

For later reference, we write down the series solutions up to $O(\epsilon^3)$. For the branch $\omega_1 < 0$ ($\chi_0 = 0$), we have

$$\omega = 1 - \epsilon\,\frac{1}{2} + \epsilon^2\left(\frac{5}{16} + \frac{\gamma}{2}\right) - \epsilon^3\left(\frac{459}{128} + \frac{41}{16}\,\gamma + \frac{(1+\gamma)^2}{16}\,\alpha^2\right) + O(\epsilon^4), \quad (1.58)$$

$$\begin{aligned} V(\mu,\lambda) &= 1 + \epsilon\, 2\, cos(\lambda-\mu) + \epsilon^2\{cos(2\lambda-2\mu) - \alpha\, cos(\mu) - \alpha\, cos(\lambda)\} \\ &\quad +\epsilon^3\,\{1/3\, cos(3\lambda-3\mu) - cos(\lambda-\mu) - 3/4\,\alpha\,[\,cos(\lambda)+cos(\mu)\,] \\ &\quad -9/8\,\alpha\,[\,cos(2\lambda-\mu)+cos(-\lambda+2\mu)\,] \\ &\quad +(1+\gamma)\,\alpha^2/4\,[\,cos(2\mu)+cos(2\lambda)\,]\,\} + O(\epsilon^4), \end{aligned} \quad (1.59)$$

$$\begin{aligned} u(\mu,\lambda) &= \epsilon^2\,\alpha\{cos(\mu) - cos(\lambda)\} + \epsilon^3\,\{-\alpha/4\,[\,cos(\lambda) - cos(\mu)\,] \\ &\quad -3/8\,\alpha\,[\,cos(2\lambda-\mu) - cos(-\lambda+2\mu)\,] \\ &\quad -(1+\gamma)\,\alpha^2/4\,[\,cos(2\mu) - cos(2\lambda)\,]\,\} + O(\epsilon^4). \end{aligned} \quad (1.60)$$

The solution branch corresponding to $\omega_1 > 0$ ($\chi_0 = \pi/2$) is given by

$$\omega = 1 + \epsilon\,\frac{1}{2} + \epsilon^2\left(\frac{5}{16} + \frac{\gamma}{2}\right) + \epsilon^3\left(\frac{459}{128} + \frac{41}{16}\,\gamma + \frac{(1+\gamma)^2}{16}\,\alpha^2\right) + O(\epsilon^4), \quad (1.61)$$

$$\begin{aligned} V(\mu,\lambda) &= 1 - \epsilon\, 2\, cos(\lambda-\mu+2\chi_0) + \epsilon^2\{cos(2\lambda-2\mu+4\chi_0) - \alpha\, cos(\mu-\chi_0) \\ &\quad -\alpha\, cos(\lambda+\chi_0)\} + \epsilon^3\,\{1/3\, cos(3\lambda-3\mu+6\chi_0) - cos(\lambda-\mu+2\chi_0) \\ &\quad +3/4\,\alpha\,[\,cos(\lambda+\chi_0)+cos(\mu-\chi_0)\,] \\ &\quad +9/8\,\alpha\,[\,cos(\lambda+2\mu+3\chi_0)+cos(2\lambda-\mu+3\chi_0)\,] \\ &\quad -(1+\gamma)\,\alpha^2/4\,[\,cos(2\mu-2\chi_0)+cos(2\lambda+2\chi_0)\,]\,\} + O(\epsilon^4), \end{aligned} \quad (1.62)$$

$$\begin{aligned} u(\mu,\lambda) &= \epsilon^2\,\alpha\{cos(\mu-\chi_0) - cos(\lambda+\chi_0)\} + \epsilon^3\,\{\alpha/4\,[\,cos(\lambda+\chi_0) \\ &\quad +cos(\mu-\chi_0)\,] - 3/8\,\alpha\,[\,cos(\lambda-2\mu+3\chi_0) - cos(2\lambda-\mu+3\chi_0)\,] \\ &\quad +(1+\gamma)\,\alpha^2/4\,[\,cos(2\mu-2\chi_0) - cos(2\lambda+2\chi_0)\,]\,\} + O(\epsilon^4). \end{aligned} \quad (1.63)$$

In dimensionless units, the period of the oscillations is given by $T = 2\pi/\omega$, with $\omega = 1 \mp \epsilon\, 1/2 + \epsilon^2\,(5/16 + \gamma/2) + O(\epsilon^3)$. It follows that the period of the weakly nonlinear acoustic waves increases with the entropy wave amplitude ϵ for the first branch ($\omega_1 = -1/2$) and decreases for the second solution branch ($\omega_1 = 1/2$). For linear acoustics, we simply have $\omega = 1$.

For completeness, we have displayed the frequency series including terms ω_3, although those corrections are calculated together with fourth order simple waves $\sigma_4(\mu)$, $\rho_4(\lambda)$. Detailed formulae for the calculation of the solutions up to fourth order can be found in Appendices 1.1 to 1.4.

1.5 Non-smooth traveling waves

Weakly nonlinear standing acoustic waves were obtained in Sections 1.2 and 1.3 for a fairly general small amplitude entropy wave, and explicit solutions were given for a simple choice of the entropy field in Section 1.4. These continuous, time periodic waves were expressed as power series that depend on two parameters, the entropy wave amplitude ϵ and the coefficient α. It seems natural, then, to inquire about the convergence of these asymptotic solutions and the form of waves of greatest amplitudes. These two issues, intimately connected, will be discussed in next section. We present now some complementary analyses that will prove helpful in understanding these matters.

The question concerning the shape of continuous waves of maximum amplitude is not easy to treat analytically for arbitrary entropy amplitudes ϵ. However, in the limiting case $\epsilon \to 0$, Pego (1988) found exact solutions to the leading order equations (see below, equations (1.68)–(1.69)) given by traveling waves of permanent form. Using a slight variation of his ideas, exact formulae will be derived here showing that continuous traveling waves exist in certain range of acoustic amplitudes.

The main goal of this section is to show that traveling waves of maximum acoustic amplitude display a non-smooth structure, with corners in their profiles. Although these solutions are only valid for small entropy wave amplitudes, they provide some insight into the breaking process associated with time periodic hyperbolic waves propagating through more general entropy fields, a problem that will be discussed in next chapter.

We begin by reviewing the general theory for hyperbolic systems of conservation laws proposed by Majda & Rosales (1984), adapted to the present case of Gas Dynamics. In so doing, we will not only prepare the terrain for the analysis mentioned above, but we will be able to contrast that theory with our perturbation method of Sections 1.2–1.3 as well.

As before, the equations of motion are given by (1.1)–(1.2), complemented by an equation of state for the pressure in the form of (1.4), corresponding to a polytropic gas. The slightly wavy entropy field is given again by (1.5)–(1.5'). We define the characteristic variables as those corresponding to linear acoustics, namely, $\mu = x - t$, $\lambda = -x - t$, and introduce a slow time given by $\tau = \epsilon t$, with $0 < \epsilon \ll 1$, ϵ being, as before, the entropy wave amplitude. The slow variable τ and the higher order terms in (1.64)–(1.65) below will take care of weak nonlinear effects appearing when ϵ is small but finite. Then, we look for solutions in the form

$$V(x,t) \;=\; V(\mu,\lambda,\tau) \;=\; 1 + \sum_{i=1}^{\infty} V_i(\mu,\lambda,\tau)\,\epsilon^i, \tag{1.64}$$

$$u(x,t) \;=\; u(\mu,\lambda,\tau) \;=\; \sum_{i=1}^{\infty} u_i(\mu,\lambda,\tau)\,\epsilon^i, \tag{1.65}$$

where the perturbations V_i, u_i are required to be 2π–periodic in x and t, with mean zero in x.

It should be noted that the general expansions in Majda & Rosales (1984) deal with oscillatory initial data and general hyperbolic systems. In that context, infinite series solutions like those in (1.64)–(1.65) do not appear viable. Those expansions can be carried out only up to $O(\epsilon^2)$ and the best one can ask for the "t-behavior" is sublinear growth. Here, in contrast, the special symmetries of Gas Dynamics and the periodicity of the initial data allow the "improved" expansions (1.64)–(1.65). Comparing the expansions (1.64)–(1.65) with those used in our previous perturbation method of Sections 1.2–1.3 (see equations (1.6)–(1.7)), we also note that they differ in two features: first, for (1.6)–(1.7), the characteristic variables μ and λ incorporate nonlinear effects through the frequency ω, while in (1.64)–(1.65) they simply correspond to the linear case. Second, the expansion for the velocity u begins at $O(\epsilon^2)$ in (1.6), while (1.65) starts at $O(\epsilon)$. Thus, acoustic amplitudes are second order relative to entropy variations in (1.6), while they are of the same order in (1.65).

The first order solution can be written as

$$V_1 \;=\; K(\mu - \lambda) \;-\; \sigma_1(\mu,\tau) \;-\; \rho_1(\lambda,\tau), \tag{1.66}$$

$$u_1 \;=\; \sigma_1(\mu,\tau) \;-\; \rho_1(\lambda,\tau), \tag{1.67}$$

where $K(\mu-\lambda)$ is the given entropy field and, as usual, σ_1 and ρ_1 must be determined at the next order.

By imposing periodicity at $O(\epsilon^2)$, we obtain a pair of integro-differential equations describing the evolution of σ_1 and ρ_1 in the form

$$\frac{\partial \rho_1}{\partial \tau} + \frac{\partial}{\partial \lambda}\left\{ \frac{(1+\gamma)}{4}\ \rho_1^2 - \frac{1}{4\pi}\int_0^{2\pi} K(\mu-\lambda)\ \sigma_1(\mu,\tau)\ d\mu \right\} = 0, \qquad (1.68)$$

$$\frac{\partial \sigma_1}{\partial \tau} + \frac{\partial}{\partial \mu}\left\{ \frac{(1+\gamma)}{4}\ \sigma_1^2 - \frac{1}{4\pi}\int_0^{2\pi} K(\mu-\lambda)\ \rho_1(\lambda,\tau)\ d\lambda \right\} = 0. \qquad (1.69)$$

These equations were first derived by Majda & Rosales (1984) and we already commented about their significance in the introductory notes. They are essentially a pair of inviscid Burgers equations coupled through an integral term whose kernel K is given by the known entropy wave. In the work by Majda, Rosales & Schonbeck (1988), it was pointed out that the linear integro-differential terms introduce a dispersive coupling of the acoustical waves through the entropy field.

One can look for traveling wave solutions of these equations, namely

$$\rho_1(\lambda,\tau) = \rho_1(\lambda - c\tau) = \rho_1(\xi), \qquad \sigma_1(\mu,\tau) = \sigma_1(\mu - c\tau) = \sigma_1(\eta),$$

for some constant c, the wave speed. Then the equations reduce to

$$\left\{ -c\,\rho_1 + \frac{(1+\gamma)}{4}\ \rho_1^2 - \frac{1}{4\pi}\int_0^{2\pi} K(\eta-\xi)\ \sigma_1(\eta)\ d\eta \right\}_\xi = 0, \qquad (1.70a)$$

$$\left\{ -c\,\sigma_1 + \frac{(1+\gamma)}{4}\ \sigma_1^2 - \frac{1}{4\pi}\int_0^{2\pi} K(\eta-\xi)\ \rho_1(\xi)\ d\xi \right\}_\eta = 0, \qquad (1.70b)$$

where σ_1 and ρ_1 represent waves propagating to the right and left, respectively. At this level of approximation, their velocities are given by $\pm(1+\epsilon c)$, respectively.

The expansion (1.64)–(1.65) can be continued to all higher orders without trouble. However, its validity is not guaranteed as $\tau \to \infty$, but only for $\tau \ll \epsilon^{-1}$. This is because we have imposed no particular conditions on the τ-behavior, and secularities may arise as $\tau \to \infty$. In particular, a continuation of the traveling wave solutions (1.70) to higher orders is not possible, unless we modify the expansion so that higher order corrections to the wave's speeds are allowed, beyond the first order $\pm(1+\epsilon c)$ above. This is easily done; in fact, the proper expansion has exactly the same form and restrictions as our expansion in (1.6)–(1.7), except that the expansion for u starts at $O(\epsilon)$ instead of $O(\epsilon^2)$. This expansion works up very much the same way as the expansion in (1.6)–(1.7), except that the leading order solvability conditions

— at $O(\epsilon^2)$ now instead of $O(\epsilon^3)$ — now yield (1.70), instead of the linear (1.38)–(1.40). The higher order solvability conditions yield forced versions of the variational equations for (1.70).

Generally, it is very hard to obtain explicit solutions for (1.70). Further, the variational-forced forms of (1.70) that would appear at higher orders in the expansion mentioned in the previous paragraph are very hard to analyze. This is the reason that in our expansion (1.6)–(1.7) we started the velocity at $O(\epsilon^2)$. This feature, by delaying the appearance of nonlinear (self-interaction) wave-breaking terms to higher orders, gives a simple sequence of problems to analyze and solve at each step of the expansion. The price we pay for this is that we appear to be limited to smaller acoustic amplitudes. Given our numerical calculations in Chapter 3, that go beyond the reach of either expansion, this does not seem to be too high a price.

For simple functions $K(\xi)$, it is possible to obtain explicit solutions of (1.70). For example, if $K(\xi)$ is a periodic sawtooth wave, the equations reduce to o.d.e's that can be solved by phase plane methods. This analysis was carried out in Majda, Rosales & Schonbeck (1988), where they found that periodic solutions exist in an amplitude range $0 \leq A \leq A_c$. For $A = A_c$, the solution waves display corners in their profiles. It was also shown in that work that (1.70) can be generally reduced to systems of ordinary differential equations when $K(x)$ consists of simple wave shapes connected by discontinuities (e.g., a square wave). Notice that discontinuities in $K(\xi)$ amount to contact discontinuities in the Euler equations. It is easy to see that they do not affect the validity of the expansion, thus we are allowed to consider this case.

A second class of explicit solutions of (1.70) can be obtained when the entropy wave is a simple Fourier mode. As in Section 1.4, let the entropy field in (1.70) be given by (1.5"), namely

$$K(2x) \;=\; 2\,cos(2x). \tag{1.71}$$

Based on the ideas of Pego (1988), we derive now explicit formulae to describe continuous traveling waves in the limit $\epsilon \to 0$ for the case (1.71). We restrict the calculation to the first solution branch (1.58)–(1.60), but totally equivalent ideas can be applied, of course, to the second solution branch (1.61)–(1.63).

First, in view of the form of the solution (1.58)–(1.60), it is reasonable to require that, in the Euler equations (1.1)–(1.2), the specific volume V and velocity u be even and odd functions of the mass coordinate x, respectively. Second, to explicitly impose time symmetries as before, V and u must be even and odd functions of time, respectively. Then, both conditions are satisfied if and only if the perturbations $\rho_1(\xi)$ and $\sigma_1(\eta)$ are taken as the same even function, written in the form

$$\rho_1(\xi) \;=\; P\,(\,cos(\xi)\,), \qquad\qquad \sigma_1(\eta) \;=\; P\,(\,cos(\eta)\,). \tag{1.72}$$

Thus, the two integro-differential equations (1.70) provide the same evolution equation. Introducing (1.72) in (1.70), we obtain (here $\zeta = cos(\xi)$ and a prime indicates derivation with respect to ζ)

$$-c\,P'(\zeta) + \left[\frac{(1+\gamma)}{4}\,P^2(\zeta)\right]' - \frac{1}{2\pi}\int_0^{2\pi} cos(\eta)\,P\,(cos(\eta))\;d\eta = 0,$$

that can be immediately integrated to get

$$P^2(\zeta) - 2\,s\,P(\zeta) - 2\,\bar{Q}\,\zeta - \kappa = 0, \tag{1.73}$$

where κ is a constant of integration, $s = 2c/(1+\gamma)$, $Q = (1/2\pi)\int_0^{2\pi} cos(\eta)P(cos(\eta))d\eta$ and $\bar{Q} = [2/(1+\gamma)]\,Q$.

The traveling wave solution can now be written in the form

$$P(\zeta) = s + \sqrt{A + 2\,\bar{Q}\,cos(\xi)}\,, \tag{1.74}$$

$$s = \frac{2\,c}{1+\gamma} = -\frac{1}{\pi}\int_0^{\pi} \sqrt{A + 2\,\bar{Q}\,cos(\eta)}\;d\eta, \tag{1.75}$$

where the formula for the wave speed s follows from the mean zero condition and the parameters $A = s^2 + \kappa$ and $\bar{Q}$ must satisfy the equation

$$\bar{Q} = \frac{2}{(1+\gamma)\pi}\int_0^{\pi} \sqrt{A + 2\,\bar{Q}\,cos(\eta)}\;cos(\eta)\;d\eta. \tag{1.76}$$

Notice that the coefficient A is also restricted by $A \geq 2|\bar{Q}|$.

Now, notice that if $(\bar{Q}, A)$ solves (1.76), so does $(-\bar{Q}, A)$. Thus, without loss of generality, we assume $\bar{Q} \geq 0$. Let us define $\delta = A/2\bar{Q} \geq 1$. Then, the amplitude-dependent coefficients (1.75)–(1.76) can be explicitly calculated, and the traveling wave solution, for any $\delta \geq 1$, is given by

$$P(\zeta) = s + q\,\sqrt{\delta + cos(\xi)}\,, \tag{1.77}$$

$$s = -\frac{q}{\pi}\int_0^{\pi} \sqrt{\delta + cos(\eta)}\;d\eta, \qquad q = \frac{4}{(1+\gamma)\pi}\int_0^{\pi} \sqrt{\delta + cos(\eta)}\;cos(\eta)\;d\eta, \tag{1.78}$$

and $A = \delta q^2$, $\bar{Q} = q^2/2$.

Equations (1.77)–(1.78) describe continuous traveling wave solutions for a certain range of amplitudes that depend on the parameter δ. Two distinct limits can be considered, i.e., $\delta \gg 1$ and $\delta = 1$.

First, for $\delta \gg 1$, we have the "linear" limit, with $P(\xi)$ having infinitesimal amplitude. In this case, let $\nu^2 = 1/\delta$, $0 < \nu \ll 1$. Then

$$q = \frac{\nu}{1+\gamma} + O(\nu^2), \qquad s \simeq -\frac{1}{1+\gamma}, \qquad A \simeq \frac{1}{(1+\gamma)^2}, \qquad \bar{Q} \simeq \frac{\nu^2}{2(1+\gamma)^2},$$

so that

$$P(\zeta) \simeq \frac{\nu^2}{2(1+\gamma)}\, cos(\xi) \;=\; \frac{\nu^2}{2(1+\gamma)}\, cos(\, x + t + c\tau\,), \qquad c \simeq -\frac{1}{2}, \qquad \tau = \epsilon t,$$

a result that matches the perturbation solution (1.58)–(1.60), except for the normalization constant.

More interesting, the second limit is given by the case $\delta = 1$. Then

$$q = \frac{8\sqrt{2}}{3\pi(1+\gamma)}, \qquad s = -\frac{32}{3\pi^2(1+\gamma)}, \qquad A = \frac{128}{9\pi^2(1+\gamma)^2}, \qquad \bar{Q} = \frac{64}{9\pi^2(1+\gamma)^2},$$

so that

$$P(\zeta) \;=\; -\frac{32}{3\pi^2(1+\gamma)} \;+\; \frac{8\sqrt{2}}{3\pi(1+\gamma)}\sqrt{1 \;+\; cos(\, x + t + c\tau\,)}, \quad c = -\frac{16}{3\pi^2}, \quad \tau = \epsilon t.$$

Thus, for the case of maximum amplitude, $\delta = 1$, the traveling waves display corners in their profiles, corresponding to the square root of the double zero in the radical sign. Figures 1 and 2, at the end of this chapter, show the leading order solutions V_1 and u_1 (see equations (1.66)–(1.67)) when $\delta = 1$. Notice that corners appear clearly in velocity, but are hidden in the specific volume profile because of the additional contribution coming from the entropy wave.

The significance of the preceding analysis can be stated as follows. Leading order solutions to Euler equations in the form (1.66)–(1.67) are given by weakly nonlinear hyperbolic waves whose traveling wave components are, in turn, solutions of the integro-differential system (1.68)–(1.69). It was shown that, a) these time periodic waves only exist for a bounded range of acoustic wave amplitudes, and b) for waves of greatest amplitude a singularity in their profiles appears.

It seems plausible that these two results might hold for the more complex case of acoustic waves coupled with a large amplitude entropy wave. However, it is not clear whether the mechanics of the interaction process valid for ϵ small — essentially given by a dynamic balance of dispersion and nonlinear distortion — would also apply to the case having arbitrary ϵ. Further analysis to elucidate this point will be performed in Chapters 2 and 3.

1.6 Discussion

We investigated the possibility that the full set of gas dynamic equations may support finite, continuous, time periodic solutions with nontrivial acoustical component and no shocks, in the presence of a slightly wavy entropy field.

From the mathematical point of view, our formal explicit solution obtained in Section 1.4 is given by double Fourier series that define a family of stationary waves for the specific volume V and flow velocity u, 2π–periodic in the characteristic variables. The Fourier coefficients depend on two free parameters, ϵ and α, which in turn are related to the frequency ω through a kind of "Dispersion Relation". Incidentally, it is worth noting that the relation $\omega = \omega(\epsilon, \alpha)$ involves dimensionless amplitudes, a typical feature in nonlinear phenomena. There is no wavenumber k appearing in this "Dispersion Relation" since we required 2π–periodic solutions in x, which is equivalent to the choice $k = 1$. It is trivial to put k back, as it is built into the nondimensionalization through the choice of $\mathcal{L}$ as a unit of length (see Section 1.1). Clearly, there are only two physically meaningful parameters: the entropy wave amplitude ϵ and the frequency ω. The parameter α, although contributing to the definition of the sound wave amplitude (i.e., $a = \epsilon^2\alpha$, cf. Section 1.3), has a clear meaning only in the asymptotic limit defined by the expansion. It is not a parameter one can easily pin down if the solution is given without reference to a particular expansion — for example, via a numerical calculation, as done later in this thesis.

In physical terms, this class of solutions consists of two nonlinear sound waves moving in opposite directions, while interacting with each other through a nonuniform medium given by the entropy wave. Furthermore, if the asymptotic series were to converge for sufficiently small values of the parameters ϵ and α, then the solution would explicitly display a periodic transfer of energy between resonant acoustic modes that produces a flow field free of discontinuities. In this case, the dispersion effect introduced by the entropy wave background balances the nonlinear distortion, giving rise to periodic waveforms.

Keeping in mind the atypical character of the solutions we are looking for (continuous, time periodic and shock-less waves in the context of a nonlinear system of

hyperbolic conservation laws), it is legitimate to raise doubts about the meaning of the family of solutions provided by the perturbation approach. Are these perturbation series divergent or convergent? In the later case, is it possible to carry their summation? In this sense, two important points should be addressed:

1) For what values of (ϵ, ω) — or equivalently, (ϵ, α) — do these asymptotic series, in fact, converge? It is well established that, even for smooth initial conditions, genuinely nonlinear hyperbolic waves inherently tend to break and form shocks (cf. Lax (1964)). Thus, it is clear that even if our continuous solutions exist in some region of (ϵ, ω) parameter space, they would do so in rather limited portions whose boundaries should be somehow determined. These boundaries in parameter space would separate regions where, on one side, the dispersive effect coming from the entropy background would be strong enough as to prevent wave breaking, while on the other side the acoustical waves tendency to distort and break would be too strong and solutions without shocks could not exist.

2) As follows from the last sentence in (1) above, it seems reasonable to expect a bounded range of sound wave amplitudes. What is the magnitude of the maximum continuous wave amplitude? What is the shape of the wave profile corresponding to the greatest amplitude?

None of these questions can be answered by the weakly nonlinear approach employed before. The task of obtaining bounds on the asymptotic series in order to define regions of convergence in (ϵ, ω) space appears hopeless. And by its very nature, the asymptotic approach cannot help when it comes to characterizing waves of (presumably) large amplitudes.

It is interesting to mention here two classical problems in hydrodynamic theory that also had to deal with the task of proving convergence of formal solutions obtained via asymptotic techniques: Stokes gravity waves and stationary (periodic) free-surface waves studied by Penney and Price (1952) and verified experimentally by Taylor (1953). As it happens in the later case, the presence in our problem of stationary rather than progressive waves makes very difficult the task of proving convergence by estimating bounds on the asymptotic terms, precisely the type of proof Levi Civita (1925) carried out for Stokes waves.

With regard to the second question raised above, in both problems of free surface waves in incompressible fluid the wave profile presents a discontinuity of slope at the greatest amplitude, with an angle of 120^o in the Stokes waves case and 90^o for the standing waves. It seems difficult to derive an analogous mechanical or formal criterion to characterize the limiting "profile" in our problem.

Nevertheless, by analogy with these studies, it seems safe to expect that the behavior observed in the Majda-Rosales theory reviewed in Section 1.5 will be general. At the maximum amplitude, some sort of singularity (keeping the waves continuous) must appear, and a corner seems quite common for "low order" dispersion systems like

the present one. That limiting stage would indicate the maximum permissible balance between dispersion and nonlinearity, beyond which continuous solutions would no longer exist.

In concluding this chapter, our weakly nonlinear analysis gave presumptive (but far from conclusive) evidence for the existence of continuous, time periodic solutions of the equations of Gas Dynamics. The issue concerning regions of existence in (ϵ, ω) parameter space will be addressed in Chapter 2, by reformulating the problem and using more powerful techniques from bifurcation theory. The task of calculating maximum amplitude waves can only be attacked numerically, and it will be treated at length in Chapter 3.

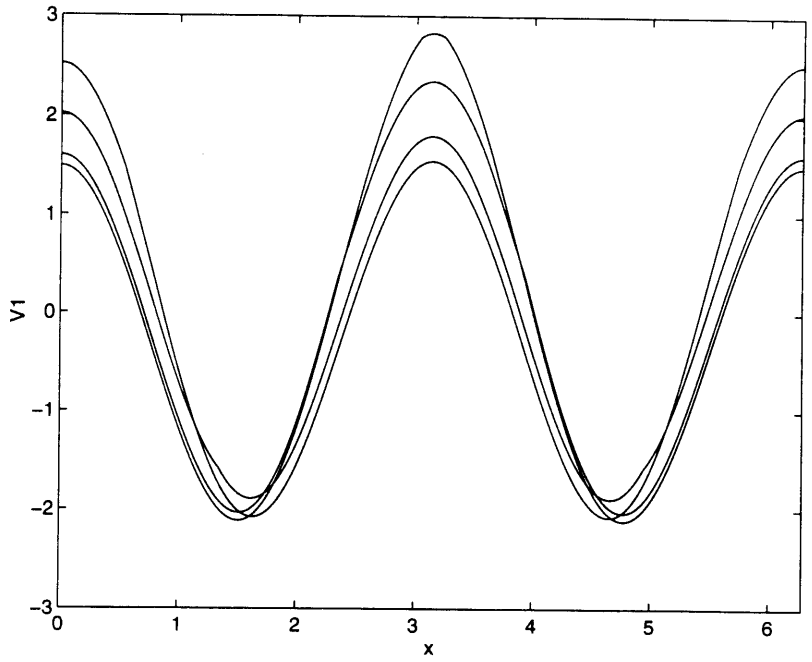

Figure 1: Leading order specific volume V_1 (equation (1.66)) at four different times, when traveling wave components have maximum amplitude $\delta = 1$ in (1.77)–(1.78).

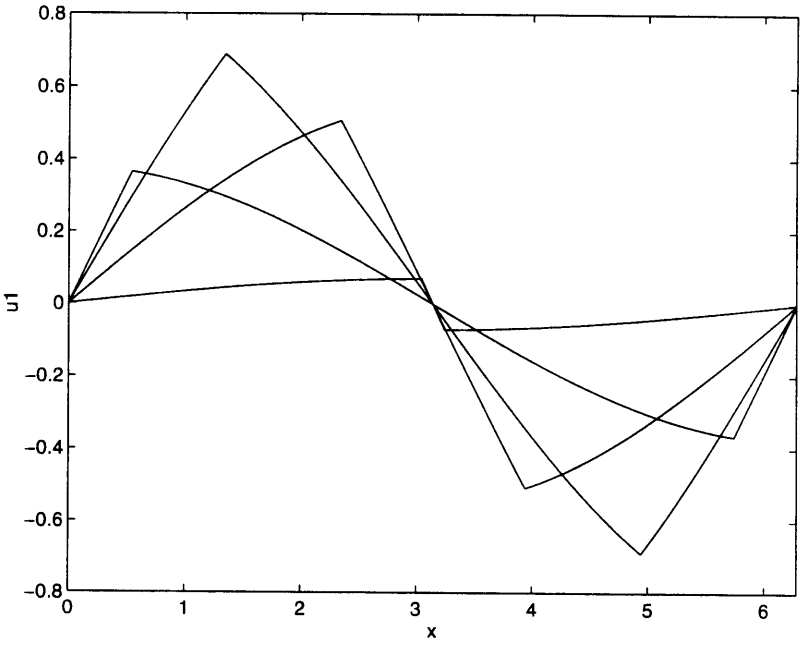

Figure 2: Leading order flow velocity u_1 (equation (1.67)) at four different times, when traveling wave components have maximum amplitude $\delta = 1$ in (1.77)–(1.78).

Bifurcation Analysis

In Chapter 1, a weakly nonlinear asymptotic analysis showed explicitly the basic mechanism that governs the interaction of small amplitude time periodic sound waves with a slightly wavy entropy background: a remarkable balance between nonlinear distortion and a nonlocal resonant term with a dispersive character involving the entropy background. It was also pointed out that we were unable to provide a rigorous proof of existence for these weakly nonlinear waves nor a theoretical method for delimiting the regions of existence of these solutions in parameter space (i.e., maximum allowed acoustic amplitudes, ranges of allowed entropy variations, etc.).

Building upon the insight gained through that preliminary analysis, our purpose in this chapter is to reformulate the problem in a more fundamental way in order to narrow the gap mentioned above. The objective is, in fact, twofold. On the theoretical side, the new approach introduced here will provide more evidence for the existence of time periodic nonlinear acoustic waves. Here the restriction to small variations in the entropy wave will be eliminated. Thus the results will have a much broader range of applicability. Equally important is the fact that the outcome of this analysis will form the basis for practical numerical calculations of large amplitude standing waves, the subject of next chapter.

To accomplish this plan, the asymptotic tools already used will be employed again, but with a new twist: the perspective here is going to be that of bifurcation theory applied to the study of the equilibrium solutions. For general expositions on the theory of bifurcations we remit the reader to Sattinger (1973), Joseph (1976), Rabinowitz (1977) and Ioos & Joseph (1980). Rigorous justifications of the kind of formal manipulations we will be using in our problem can be found in these publications. These are based on the use of the Implicit Function theorem — or equivalent results — in function spaces. Unfortunately, in the case of bifurcations for partial differential equations, either elliptic or parabolic equations are required. This is because the Implicit Function theorem does not usually apply when hyperbolic operators are involved. Thus, these rigorous results do not apply in our case here. In fact, given the rather complicated nature of the phase space structure of the periodic and multiply periodic solutions of conservative[8] systems[9], it is quite likely that the rigorous structure behind our expansions is very rich and intricate. See the discussion on convergence and small divisors in Section 2.6.

We remark here that the "usual" kind of bifurcations, as discussed in the refer-

[8]Notice that, for solutions without shocks, the Euler equations are non-dissipative. In fact, they can be written as a formal infinite dimensional Hamiltonian system, as shown in Appendix 2.1

[9]e.g.: KAM theory for Hamiltonian systems (Arnold (1978)).

ences in the prior paragraph, relate to the stability[10] of an equilibrium solution to a nonlinear system of evolution equations (as some parameter in the equations varies). As this equilibrium solution "looses stability", a bifurcation occurs — with either a single (real) eigenvalue crossing from $\lambda < 0$ to $\lambda > 0$ (steady state bifurcation) or a pair of complex conjugate eigenvalues crossing from $Re(\lambda) < 0$ to $Re(\lambda) > 0$ (Hopf bifurcation). Our case here is rather different, as all the eigenvalues are pure imaginary always (the linearized problem is a wave equation). Thus the analysis is not related in any way to the equilibrium solution "loosing" stability. In fact, what we will be doing is, formally, exactly equivalent to looking for periodic solutions of an infinite dimensional Hamiltonian system. The "bifurcation" parameter, rather than being "external" to the solutions, will in fact be their period.

Concerning our problem of nonlinear acoustic waves propagating through a nonuniform entropy background, we are going to construct time periodic continuous solutions as power series in a suitable defined amplitude and state general conditions for the solvability of the resulting asymptotic sequence of equations (Sections 2.1 and 2.2). The first order approximation will define an eigenvalue problem — having the form of a Hill's equation — that we will study using Floquet's theory for differential equations with periodic coefficients in Section 2.3. This analysis will establish general requirements on the eigenvalues of the problem that are equivalent to the solvability conditions under which the series solution can be calculated up to any order. The first few orders in the expansion are considered in some detail in Sections 2.4 and 2.5. Finally, in Section 2.6, we discuss some of the delicate issues concerning convergence for the formal asymptotic series expansion in this chapter, and the difficulties that the hyperbolic nature of the operators involved cause.

In Sections 2.7–2.8 it will be shown that the bifurcation solution here contains the weakly nonlinear solution of Chapter 1 as a limiting case. Though more powerful and general, the bifurcation analysis relies heavily on the findings and limitations of the weakly nonlinear technique, and both approaches should be seen as complementing rather than excluding each other. For example, the bifurcation asymptotic analysis provides no access to the structure of the maximum amplitude waves, while the weakly nonlinear one does so in the distinguished limit when both the sound and entropy disturbances have equal and small amplitudes. On the other hand, the bifurcation approach is not limited to small amplitude entropy variations, and provides a tool for the development of a numerical method for calculating these solutions (Chapter 3). Finally, in Section 2.9, an estimation of large eigenvalues using the WKBJ method is done.

[10]Consider a linearized stability analysis, where time is separated as $e^{\lambda t}$, so that one ends up with an eigenvalue problem for λ.

2.1 Basic potential equation

The equations of inviscid 1D Gas Dynamics in mass-Lagrangian coordinates (in dimensionless form) are, from Section 1.2 :

$$V_t - u_x = 0, \tag{2.1}$$

$$u_t + p_x = 0, \tag{2.2}$$

$$S(x) = \epsilon K(2x), \tag{2.3}$$

$$p = p(S,V) = \frac{1}{\gamma} e^{\gamma S} V^{-\gamma}. \tag{2.4}$$

In this chapter, for simplicity, we will restrict our considerations to a polytropic gas equation of state (though the analysis is fairly general and can trivially be extended to arbitrary equations of state). As in Chapter 1, we take here $S(x) = \epsilon K(2x)$ for the entropy background, with $K(\xi)$ of period 2π and mean zero — see equation (1.5). The case when K is even is particularly interesting, as certain symmetries in x arise that facilitate some of the analysis — as explained in Section 2.3. But this condition is not essential at all. We will also use $K(2x) = 2\,cos(2x)$ as an example for certain analytical calculations, as we did in Chapter 1. *The essential difference here is that the entropy amplitude ϵ is not assumed small*, in contrast with the assumption made in the weakly nonlinear analysis of Chapter 1.

The equilibrium solution for (2.1)–(2.2) is given by

$$V = V_f(x) = V_0\, e^{\epsilon K(2x)}, \qquad u \equiv 0 \qquad \textit{and} \qquad p \equiv \textit{constant} = \frac{1}{\gamma} V_0^{-\gamma},$$

where V_0 is a positive constant. As in Section 1.2, we require the normalization conditions of a mean value of one for $V(x,t)$ and zero for $u(x,t)$ over a 2π period in x. Hence, the specific volume amplitude for the basic solution is defined by

$$V_0(\epsilon) = 2\pi \left\{ \int_0^{2\pi} e^{\epsilon K(2x)} dx \right\}^{-1}.$$

We note that, for a general equation of state, $V_f = V_f(x)$ follows from solving the equation $p(S, V_f) = p_0$, where $S = S(x)$ is given as above in (2.3) and p_0 is a constant. This is solvable because the pressure is always a strictly monotone function of V ($p_V < 0$). The constant p_0 then follows upon requiring the mean of V_f to have a value of one.

Let us now consider small perturbations to the basic (equilibrium) solution:

$$V(x,t) = V_f(x) + \tilde{V}(x,t) \tag{2.5}$$

and

$$u(x,t) = \tilde{u}(x,t). \tag{2.6}$$

These are going to define time periodic solutions bifurcating from the basic state. Let us also introduce a potential function $\varphi(x,t)$ defined by

$$\tilde{V} = \varphi_x \qquad \textit{and} \qquad \tilde{u} = \varphi_t.$$

Substituting (2.5) and (2.6) into the equations of motion (2.1)–(2.2), and expanding the pressure term according to (2.4), we obtain a single nonlinear wave equation for the potential φ:

$$\varphi_{tt} - \left[b_1 \, e^{-\epsilon K(2x)} \, \varphi_x \right]_x = -\left\{ \sum_{n=2}^{\infty} (-1)^n \, b_n \, e^{-n\epsilon K(2x)} \, (\varphi_x)^n \right\}_x, \tag{2.7}$$

where the $b_n = b_n(\epsilon)$ are *positive* constants given by

$$b_n = \frac{1}{n} \begin{pmatrix} \gamma + n - 1 \\ n - 1 \end{pmatrix} V_0(\epsilon)^{-\gamma - n} \qquad \textit{for} \qquad n = 1, 2, 3, \ldots$$

In the derivation of (2.7) no simplifying assumptions have been made: it is an exact equation governing the potential function $\varphi(x,t)$. The entropy amplitude ϵ — not restricted to small values — enters the problem simply as an external parameter. Equation (2.7) is formally self-adjoint, a property that will be important in later developments.

Finally, we point out now that the only important feature of (2.7), as far as the expansion to follow is concerned, is that it has the form

$$\varphi_{tt} - \left[c^2(x) \, \varphi_x \right]_x = -\left\{ \sum_{n=2}^{\infty} \beta_n(x) \, (\varphi_x)^n \right\}_x, \tag{2.7$'$}$$

where c and the β_n are periodic of period π and $c > 0$. For a general equation of state this follows upon expanding the pressure term in (2.4), $p = p(S, V_f + \varphi_x)$, in a Taylor series in φ_x. Then $c^2 = -p_V(S, V_f) > 0$, $\beta_2 = (1/2)\, p_{VV}(S, V_f) > 0$, etc.

2.2 Series solution

We now look for solutions of (2.7) in terms of a formal power series in some amplitude "a" — defined below — of the form

$$\varphi(x,\tau) = a\,\varphi_1(x,\tau) + a^2\,\varphi_2(x,\tau) + a^3\,\varphi_3(x,\tau) + ..., \tag{2.8}$$

where a new variable $\tau = \omega t$ has been introduced. Here $\omega > 0$ denotes the fundamental frequency of the periodic bifurcating solutions: we require these solutions to have a minimal period of 2π in τ, or $2\pi/\omega$ in t. The frequency ω is expanded as

$$\omega = \omega_0 + a\,\omega_1 + a^2\,\omega_2 + a^3\,\omega_3 + ... \tag{2.9}$$

This frequency ω plays here a role similar to the ω introduced in Chapter 1. However, note that in Chapter 1, ω was introduced as an overall characteristic speed for the solution. There the fundamental frequency was given by $n\omega$ with $n = 1, 2, 3, ...$ — depending on the mode selected in solving the equations for σ_2 and ρ_2, see equations (1.43), (1.44), (1.45) and the remark at the end of Section 1.3.

As in the weakly nonlinear case, all the perturbation potentials $\varphi_n(x,\tau)$ will be required to have period 2π and mean zero in x. This condition is equivalent to having both perturbations in (2.5) and (2.6) periodic of period 2π and mean zero in x. Furthermore, again as in the weakly nonlinear case, we impose a time symmetry by requiring the potential $\varphi(x,\tau)$ to be an even function in τ. This requirement is a normalization condition to avoid arbitrary translations in time, making the solution unique given a period[11] $2\pi/\omega$ in t.

The mathematical problem (2.7) to (2.9) posed in this way constitutes, as in Chapter 1, a boundary-value problem with periodic boundary conditions. Each branch of nontrivial solutions will depend on two parameters: an arbitrary entropy amplitude ϵ, representing an external forcing to the system, and the frequency ω, which is, as before, an intrinsic, solution-dependent quantity. However, in a strict formal sense, here we have only a one parameter family of solutions given by $\varphi = \varphi(a)$ and $\omega = \omega(a)$, with ϵ known, fixed and playing no particular role in the asymptotic solution process.

In the usual way of bifurcation analysis we normalize[12] the amplitude a of the potential series by projection on the first term φ_1, as follows

$$a = \langle\, \varphi\,,\, \varphi_1 \,\rangle, \tag{2.10}$$

where

[11] Else, for each "allowed" frequency ω, a whole one parameter set of solutions would exist.

[12] This gives a definition of a independent of the asymptotic expansion, and will be useful when φ is calculated numerically.

$$\langle \varphi , \varphi_1 \rangle = \frac{1}{(2\pi)^2} \int_0^{2\pi} \int_0^{2\pi} \varphi(x,\tau)\, \varphi_1^*(x,\tau)\, dx d\tau$$

is the scalar product in the Hilbert space H of square integrable 2π doubly periodic functions in x and τ, and $*$ denotes complex conjugation[13]. Then, substituting (2.8) into (2.10) and equating equal powers of a, we see that φ_1 must have length one (in the norm defined by the scalar product above) and the higher order terms in (2.8) must all be orthogonal to the first — see (2.17).

Inserting (2.8) and (2.9) in the wave equation (2.7), we obtain a hierarchy of equations for the perturbation potentials $\varphi_n(x,\tau)$

$O(a)$:

$$\omega_0^2\, \varphi_{1_{\tau\tau}} - \left[\, b_1\, e^{-\epsilon K(2x)}\, \varphi_{1_x} \,\right]_x = L[\varphi_1] = 0, \tag{2.11}$$

$O(a^2)$:

$$\begin{aligned} \omega_0^2\, \varphi_{2_{\tau\tau}} - \left[\, b_1\, e^{-\epsilon K(2x)}\, \varphi_{2_x} \,\right]_x &= L[\varphi_2] = F_2 = \\ - 2\,\omega_0\,\omega_1\, \varphi_{1_{\tau\tau}} &- \left[\, b_2\, e^{-2\epsilon K(2x)}\, (\varphi_{1_x})^2 \,\right]_x, \end{aligned} \tag{2.12}$$

$O(a^3)$:

$$\begin{aligned} \omega_0^2\, \varphi_{3_{\tau\tau}} - \left[\, b_1\, e^{-\epsilon K(2x)}\, \varphi_{3_x} \,\right]_x &= L[\varphi_3] = F_3 = \\ - 2\,\omega_0\,\omega_1\, \varphi_{2_{\tau\tau}} &- \left(\omega_1^2 + 2\,\omega_0\,\omega_2\right)\, \varphi_{1_{\tau\tau}} \\ - \left[\, 2\, b_2\, e^{-2\epsilon K(2x)}\, \varphi_{1_x}\, \varphi_{2_x} \,\right]_x &- \left[\, b_3\, e^{-3\epsilon K(2x)}\, \varphi_{1_x}\, \varphi_{2_x} \,\right]_x, \end{aligned} \tag{2.13}$$

$O(a^4)$:

$$\begin{aligned} \omega_0^2\, \varphi_{4_{\tau\tau}} - \left[\, b_1\, e^{-\epsilon K(2x)}\, \varphi_{4_x} \,\right]_x &= L[\varphi_4] = F_4 = \\ - 2\,\omega_0\,\omega_1\, \varphi_{3_{\tau\tau}} - \left(\omega_1^2 + 2\,\omega_0\,\omega_2\right) \varphi_{2_{\tau\tau}} &- \left(2\,\omega_0\,\omega_3 + 2\,\omega_1\,\omega_2\right)\, \varphi_{1_{\tau\tau}} \\ - \left[\, b_2\, e^{-2\epsilon K(2x)}\, \left((\varphi_{2_x})^2 + 2\,\varphi_{1_x}\,\varphi_{3_x}\right) \,\right]_x &+ \left[\, b_3\, e^{-3\epsilon K(2x)}\, 3\,(\varphi_{1_x})^2\, \varphi_{2_x} \,\right]_x \\ - \left[\, b_4\, e^{-4\epsilon K(2x)}\, (\varphi_{1_x})^4 \,\right]_x, \end{aligned} \tag{2.14}$$

where the linear operator L and right hand sides F_n are defined by the formulas. Generally, at $O(a^n)$ for $n > 1$, we have

$$\omega_0^2\, \varphi_{n_{\tau\tau}} - \left[\, b_1\, e^{-\epsilon K(2x)}\, \varphi_{n_x} \,\right]_x = L[\varphi_n] = F_n. \tag{2.15}$$

[13]Notice that the linear part (left hand side) of (2.7) is formally self-adjoint with respect to this inner product.

We notice that F_n has the form

$$F_n = F_n(\omega_0, \omega_1, ..., \omega_{n-1}, \varphi_1, \varphi_2, ..., \varphi_{n-1}) = -2\omega_0\,\omega_{n-1}\,\varphi_{1\tau\tau} + G_n\,,$$

where G_n *does not depend on* ω_{n-1}.

Equation (2.11) is a self-adjoint linear generalized eigenvalue problem, with eigenvalue ω_0^2 and associated eigenfunction $\varphi_1(x,\tau)$. The other problems are linear inhomogeneous equations that will have a solution with the required properties only if the right hand sides F_n satisfy certain compatibility conditions that we can find using the Fredholm alternative (see, for example, Friedman (1990)).

Consider the set H_0 of all the square integrable 2π doubly periodic functions in x and τ, of mean zero in x and even in τ. This is a (Hilbert) subspace of H in (2.10), it is an invariant space for L as defined in (2.11) and it is clear that F_n is in H_0 if all the φ_j, for $j < n$, are in H_0. Thus we can consider all the linear problems above within the context of H_0 only.

Assume now that ω_0^2 in (2.11) is a simple eigenvalue. Then the compatibility condition at level n is that F_n should be orthogonal to the eigenfunction φ_1. Because of the observation below (2.15) on the form of F_n, this orthogonality condition can always be satisfied and determines ω_{n-1} uniquely[14] from

$$0 = \langle\, F_n\,,\, \varphi_1\,\rangle = 2\omega_0\omega_{n-1} + \langle\, G_n\,,\, \varphi_1\,\rangle\,.$$

Then φ_n is completely determined by the equation and the fact that it must be orthogonal to φ_1. This shows that the expansion can be carried to all orders, provided that a simple eigenvalue exists. We will look at this question and related ones in what follows.

Finally, we point out that the requirement that the eigenvalue be simple is crucial. The situation for bifurcations in the case of multiple eigenvalues is poorly understood. Even in the best of cases one should expect several solution curves arising from the bifurcation point (cf. Sattinger (1973)) and then a "simple" expansion, such as the one we are proposing, will certainly not work. Worse still, there is not even a guarantee that a solution will exist at all. For example, when $\epsilon = 0$ the eigenvalues of (2.11) are given by $\omega_0^2 = m^2/n^2$ with $\varphi_1 = cos(n\tau)\,cos(m(x - x_0))$ and n, m natural numbers. This is a highly degenerate set, with each eigenvalue having infinite multiplicity, and in this case *no* periodic time solution exists.

[14]We will soon show that $\omega_0 > 0$ and that $\varphi_{1\tau\tau} = -\varphi_1$. We have also used (2.17) here.

2.3 Eigenvalue problem and Floquet theory

Equation (2.11) is separable in time. Since 2π must be the minimal period in τ and φ must be even in τ , we must have

$$\varphi_1(x,\tau) \;=\; cos\,\tau \;\; \phi_1(x),$$

where $\phi_1(x)$ is periodic of period 2π, mean zero and satisfies the following linear eigenvalue problem:

$$L_x\,[\phi_1] \;=\; \Big[\, b_1\, e^{-\epsilon K(2x)}\, \phi_1'(x) \,\Big]' \;+\; \omega_0^2\, \phi_1(x) \;=\; 0. \tag{2.16}$$

As mentioned earlier, the normalization in (2.10) implies that

$$\langle\, \varphi_1\,,\, \varphi_1 \,\rangle \;=\; 1 \qquad and \qquad \langle\, \varphi_n\,,\, \varphi_1 \,\rangle \;=\; 0 \qquad for \qquad n \geq 2, \tag{2.17}$$

so that the eigenvector $\phi_1(x)$ is normalized by

$$\int_0^{2\pi} \phi_1^2(x)\, dx \;=\; 4\pi. \tag{2.18}$$

We notice now that

(a) The self-adjoint operator defined by $D[\phi] = -\Big[\, b_1\, e^{-\epsilon K(2x)}\, \phi'(x) \,\Big]'$ is non-negative. Thus ω_0^2 is non-negative.

(b) The only periodic solutions of (2.16) for $\omega_0 = 0$ are constants.

Thus, given that ϕ_1 must have mean zero, we see that we can take ω_0 positive, as it should be (given its meaning as a fundamental frequency). Vice versa, any 2π–periodic solution of (2.16) for a nonvanishing ω_0, is automatically of mean zero.

Generally, consider the problem

$$D[\phi] = \lambda\, \phi \tag{2.16'}$$

for ϕ periodic of period 2π and D defined[15] as in **(a)**. For $\lambda = \omega_0^2$ and $\phi = \phi_1$ of mean zero (which will apply any time $\lambda \neq 0$) this is (2.16).

Equation (2.16') is a standard periodic Sturm-Liouville eigenvalue problem. Thus we know that

[15]For a general equation of state, take $D[\phi] = -[c^2\phi']'$, with c as in (2.7'). Then everything said here applies.

(c) (2.16') has a complete orthonormal[16] set of eigenfunctions $\{\Phi_n(x)\}_{n=0}^{\infty}$ with corresponding eigenvalues that can be ordered as follows[17]

$$0 = \lambda_0 < \lambda_1 \leq \lambda_2 < \lambda_3 \leq \lambda_4 < ... < \lambda_{2m-1} \leq \lambda_{2m} < ... \qquad (2.16a)$$

(d) If $\lambda_{2m-1} = \lambda_{2m}$ then the eigenvalue is double, else both λ_{2m-1} and λ_{2m} are simple (generic case).

Thus, candidates for ω_0 and ϕ_1 in (2.16) are given by

$$\omega_0 = \sqrt{\lambda_n} \qquad and \qquad \phi_1 = \sqrt{2}\,\Phi_n, \qquad (2.16b)$$

for some $n = 1, 2, ...$ But we must still check that ω_0^2 is a simple eigenvalue of (2.11). We do this below.

We rewrite now the generalized eigenvalue problem (2.11) in the form

$$D[\varphi] + \lambda\,\varphi = 0, \qquad (2.11')$$

where φ is in H_0 (i.e., 2π–periodic in both x and τ, of mean zero in x and even in τ). It is then easy to see that the eigenfunctions and eigenvalues for this problem are

$$\varphi = \varphi_{mn} = \sqrt{2}\,\Phi_n\, cos(m\tau) \qquad and \qquad \lambda = \lambda_{mn} = m^{-2}\,\lambda_n, \qquad (2.16c)$$

where $m = 1, 2, 3, ...$, $n = 1, 2, 3, ...$ and the Φ_n and λ_n are as above in (2.16a). Notice then that $\{\varphi_{mn}\}$ is an orthonormal complete set of eigenfunctions for H_0.

The condition that ω_0^2 be a simple eigenvalue of (2.11) is now rather simple to state in terms of the eigenvalues of (2.16') — see (2.16b) above.

(e) λ_n must be a simple eigenvalue of (2.16'). Thus, if $n = 2m - 1$ or $n = 2m$, then $\lambda_{2m-1} < \lambda_{2m}$.

(f) For any $m = 2, 3, 4...$, $m^2\lambda_n$ is *not* an eigenvalue of (2.16').

Let us now consider these two conditions, particularly the second one **(f)** — which appears hard to check.

First of all, we notice that for $\epsilon = 0$ (2.16') is a trivial problem with $\lambda_{2m-1} = \lambda_{2m} = m^2$ and corresponding eigenfunctions $sin(mx)$ and $cos(mx)$. In this case, *both* conditions **(e)** and **(f)** above fail, grandly! However, as soon as $\epsilon > 0$, typically the eigenvalues will split (so **(e)** will apply) and they would do so at different rates (so **(f)** will also apply).

---

[16] Relative to the scalar product $\langle f, g\rangle = 1/2\pi \int_0^{2\pi} f(x)g^*(x)dx$.

[17] Of course, $\lambda_0 = 0$ corresponds to the eigenfunction $\Phi_0 = const.$. The other eigenfunctions have zero mean.

Second, we note that (even for large ϵ, where the eigenvalues cannot be computed by any sort of asymptotic method) **(f)** does not in fact require us to know all the eigenvalues of (2.16'). If we want to verify the condition for, say, λ_1 or λ_2, it is enough if we (numerically, say) compute the first few of them. This is because, for "large" n — which in practice is usually not that large — the eigenvalues are very well approximated[18] by WKBJ theory. Namely (see Section 2.9)

$$\lambda_{2m-1} \simeq \lambda_{2m} = m^2\, \bar{c}^2, \tag{2.16d}$$

where $\bar{c}$ is the harmonic mean of c, $\bar{c} = \{1/2\pi \int_0^{2\pi} dx/c(x)\}^{-1}$, c as in (2.7'). Thus, condition **(f)** above reduces to

$$m^2\, r \neq s^2, \tag{2.16e}$$

for m ans s "large" enough integers, where $r = \lambda_n/(\bar{c})^2$.

Remark 2.1 The question arises as to for which r's does (2.16e) apply. This is a complicated one, related to the issue of convergence of the expansion (and small divisors), which we will mention again in Section 2.6. Let us mention here, however, that the set is not empty. For example, if $r = 2$, then $|2m^2 - s^2| \geq 1$ since, clearly, $2m^2 - s^2$ is a nonzero integer.

Finally, in view of the discussion above, it is clear that in the context of this problem it is important to know — in the "$\lambda - \epsilon$ plane" — the position of the eigenvalues $\lambda_n = \lambda_n(\epsilon)$ as they split from their double values when $\epsilon = 0$. We will call these curves "transition curves". The reason for this name has to do with viewing (2.16') in terms of Floquet theory, a review of which is done below. In this theory the eigenvalues correspond to the values of λ for which the solutions of (2.16') — considered now as a second order differential equation, with no restrictions on the solutions — switch from all being unbounded in x to all being bounded.

Next we study the eigenvalue problem (2.16) from a point of view complementary to that provided by the Sturm-Liouville theory. This new approach (Floquet theory) is the basis for the method we actually used to compute the eigenvalues, transition curves and eigenfunctions numerically.

Equation (2.16) is a linear ordinary differential equation with periodic coefficients whose study can be done with the help of Floquet theory. For a detailed exposition of this theory, see (for example) Ince (1956), Stoker (1950), Hayashi (1964) and Jordan & Smith (1987). For the sake of completeness and clarity, we summarize below some of the main elements of Floquet theory, as they pertain to the solution of (2.16).

A non-autonomous first order system

[18] Better than any $O(n^{-s})$, any $s > 0$.

$$\mathbf{v}'(x) \;=\; H(x)\,\mathbf{v}(x), \tag{2.19}$$

where $H(x)$ is an $n \times n$ matrix whose coefficients are periodic functions with minimal period $\mathcal{X}$, has at least one (possibly complex) non-trivial n-vector solution $\mathbf{v} = \Psi(x)$ such that $\Psi(x+\mathcal{X}) = \nu\Psi(x)$, where ν is a (possibly complex) non–zero constant that depends on the parameters of the system (Floquet Theorem). This is shown below.

A *fundamental solution* of the system (2.19) is an $n \times n$ matrix function whose columns are n linearly independent solutions of (2.19). Any two fundamental solutions differ by post-multiplication by a nonsingular constant matrix. If $\Phi(x)$ is a fundamental solution of (2.19), so is $\Phi(x + \mathcal{X})$, because of the periodicity of $H(x)$. Thus, we can write

$$\Phi(x + \mathcal{X}) \;=\; \Phi(x)\,E, \tag{2.20}$$

where E is a nonsingular $n \times n$ matrix called the *monodromy matrix.* Clearly, monodromy matrices obtained from different fundamental solutions are similar. Let now ν and $\mathbf{e}$ be an eigenvalue[19] and corresponding eigenvector of E. Then, taking the solution $\Psi = \Phi\,\mathbf{e}$, it is easy to see that it satisfies the Floquet Theorem above:

$$\Psi(x + \mathcal{X}) = \Phi(x + \mathcal{X})\,\mathbf{e} = \Phi(x)\,E\,\mathbf{e} = \Phi(x)\,\nu\,\mathbf{e} = \nu\,\Psi(x).$$

The eigenvalues ν of E are called the characteristic numbers or Floquet multipliers of (2.19). They are independent of the choice of any particular fundamental solution. Let us now introduce the characteristic (or Floquet) exponents ρ by $e^{\rho\mathcal{X}} = \nu$. Then it is easy to see that $h(x) = e^{-\rho x}\,\Psi(x)$ is periodic of period $\mathcal{X}$. In general, if E is diagonalizable, we can find n linearly independent solutions of the form $\Psi_i = h_i(x)\,e^{\rho_i x}$, with $h_i(x)$ being $\mathcal{X}$–periodic. If E is not diagonalizable, one needs to consider solutions of the form $\Psi = h(x)\,e^{\rho x}$, where now $h(x)$ is a polynomial in x, with the coefficients periodic functions of x of period $\mathcal{X}$.

The important result for us concerns the existence of periodic solutions: if E has an eigenvalue ν which is one of the mth roots of unity, $\nu = 1^{1/m}$, m being a positive integer, then there is a periodic solution of period $m\mathcal{X}$:

$$\Psi(x + m\mathcal{X}) = \nu\,\Psi(x + (m-1)\mathcal{X}) = \ldots = \nu^m\,\Psi(x) = \Psi(x).$$

Let us complete this digression on Floquet theory with some remarks about the calculation of characteristic numbers. For systems of the form (2.19), it can be proved that the constant term in the characteristic equation $det(E - \nu I) = 0$ is given by

[19]Note that ν is non–zero, as E is nonsingular.

$$\nu_1\,\nu_2\,...\nu_n = exp\left(\int_0^{\mathcal{X}} tr\,[H(x)]\,dx\right),$$

where $tr\,[H(x)]$ is the trace of the matrix $H(x)$ and the eigenvalues are counted according to their multiplicity. Furthermore, for second order equations of the form $\ddot{\xi}(x) + F(x)\dot{\xi}(x) + G(x)\xi(x) = 0$, with F and G being $\mathcal{X}$-periodic and F of mean zero, it is always possible to eliminate the term containing the first derivative (without loosing periodicity). Using Sturm's transformation, where we notice that the integral of F is also periodic (given that its mean vanishes), $\xi = \left\{exp\left[-\frac{1}{2}\int F(x)dx\right]\right\}\eta$ we obtain $\ddot{\eta}(x) + \{G(x) - \frac{1}{2}F'(x) - \frac{1}{4}F^2(x)\}\,\eta(x) = 0$. Writing this equation as a first order system

$$\begin{cases} \eta_1'(x) = \eta_2(x), \\ \\ \eta_2'(x) = \left[\,-G(x) + \frac{1}{2}F'(x) + \frac{1}{4}F^2(x)\,\right]\,\eta_1(x), \end{cases}$$

we see that in this case $tr\,[H(x)] = 0$. From these remarks, we conclude that the constant term in the characteristic equation for second order systems with no first derivative terms is simply one.

To obtain the characteristic numbers, it is common practice to choose the fundamental matrix $\Phi(x)$ defined by $\Phi(0) = I$. Then, applying Floquet's relation (2.20), we have the result $\Phi(\mathcal{X}) = E$. Using the properties and the notation just stated, this relation means that the characteristic equation (in the case above) is given by

$$\nu^2 - (\eta_{11} + \eta_{22})\,\nu + 1 = 0,$$

where η_{11} and η_{22} result from the integration of the following initial value problems:

$$IVP\,1: \begin{cases} \eta_1(0) = 1 & \rightarrow & \eta_1(\mathcal{X}) = \eta_{11} \\ \eta_2(0) = 0 & \rightarrow & \eta_2(\mathcal{X}) = \eta_{21} \end{cases}$$

$$IVP\,2: \begin{cases} \eta_1(0) = 0 & \rightarrow & \eta_1(\mathcal{X}) = \eta_{12} \\ \eta_2(0) = 1 & \rightarrow & \eta_2(\mathcal{X}) = \eta_{22} \end{cases}$$

Remark 2.2 We see then that[20] in this case either ν_1 and ν_2 are both real with $\nu_1\nu_2 = 1$, or they are both complex conjugate and on the unit circle. In terms of $\Delta = \eta_{11} + \eta_{22} = \nu_1 + \nu_2$ we have then that: **(i)** If $\Delta > 2$, then ν_1 and ν_2 are both positive and one of them is bigger than one. **(ii)** If $\Delta = 2$, then $\nu_1 = \nu_2 = 1$. **(iii)** If $-2 < \Delta < 2$, then ν_1 and ν_2 are complex conjugate and on the unit circle. **(iv)** If $\Delta = -2$ then $\nu_1 = \nu_2 = -1$. **(v)** If $\Delta < -2$, then ν_1 and ν_2 are both negative and one of them is smaller than minus one.

[20]Assume that G and F are real valued, so that E is a real 2×2 matrix.

Let us return now to the eigenvalue problem (2.16) :

$$L_x[\phi_1] = \left[b_1 e^{-\epsilon K(2x)} \phi_1'(x) \right]' + \omega_0^2 \phi_1(x) = 0, \qquad (2.16)$$

where the eigenfunction $\phi_1(x)$ is 2π–periodic of mean zero, and

$$b_1 = V_0^{-\gamma-1}(\epsilon), \qquad V_0(\epsilon) = 2\pi \left\{ \int_0^{2\pi} e^{\epsilon K(2x)} dx \right\}^{-1}.$$

As we have seen, it is convenient to eliminate the first derivative term in (2.16). Introducing $\phi_1(x) = exp\left\{\frac{1}{2}\epsilon K(2x)\right\} \beta(x)$ we obtain Hill's equation :

$$\beta''(x) + \left\{ \frac{\omega_0^2}{b_1} e^{\epsilon K(2x)} + 2\,\epsilon\, K''(2x) - \epsilon^2 [K'(2x)]^2 \right\} \beta(x) = 0. \qquad (2.21)$$

This second order differential equation with periodic coefficients and its simpler companion, known as Mathieu's equation, have been studied extensively (e.g., McLachlan (1947), Arscott (1964)). They arise in a variety of physical problems, ranging from mechanical oscillations in systems with periodic forces to electronic circuits with time periodic capacitance. From the mathematical point of view, they are often derived in the stability analysis of nonlinear systems, and also in the solution of the wave equation in elliptic coordinates (Mathieu's equation) and paraboloidal coordinates (so called Hill's equation with three terms). Historically, Hill's equation was first derived in the investigation of the stability of the motion of the moon.

In general, (2.21) has two linearly independent solutions that, depending on parameter values[21], can be classified as follows, see Remark 2.2 above: two bounded solutions corresponding to the so-called stable region in parameter space ($-2 < \Delta < 2$); two unbounded solutions, in the unstable region ($|\Delta| > 2$); and finally, one periodic solution while the other is unbounded, corresponding to the transition curves separating regions of stability and instability ($|\Delta| = 2$).

Let us recall that in equation (2.21) ϵ is a fixed parameter corresponding to the entropy amplitude, while $K(2x)$ is a known periodic function defining the entropy wave. Hence, our objective is to determine the transition curves in (ϵ, ω_0) space associated with periodic solutions $\beta(x)$. In view of the previous discussion, if the coefficients appearing in (2.21) have minimal period $\mathcal{X}$, there are two possible cases in which the characteristic numbers will originate periodic solutions (of periods $\mathcal{X}$ or $2\mathcal{X}$):

If $\nu_1 = \nu_2 = 1$ (i.e., $\rho_1 = \rho_2 = 0$): one solution $\beta(x)$ of period $\mathcal{X}$.

If $\nu_1 = \nu_2 = -1$ (i.e., $\rho_1 = \rho_2 = \frac{i\pi}{\mathcal{X}}$): one solution $\beta(x)$ of period $2\,\mathcal{X}$.

[21] Here the parameters are ϵ and ω_0^2/b_1.

Note: This is the generic case. Exceptionally it can happen that two linearly independent solutions of period $\mathcal{X}$ (resp. $2\mathcal{X}$) occur (cf. Arscott (1964), Sec. 7.3). This corresponds to two transition curves crossing and to ω_0^2 being a double eigenvalue in (2.16).

In Chapter 1 we chose as an example $K(\xi) = 2\,cos(\xi)$ for the entropy wave. Thus, the minimal period of the coefficients appearing in (2.21) is $\mathcal{X} = \pi$, and accordingly we can expect periodic solutions with periods π and 2π . More precisely, it can be shown (cf. Arscott (1964)) that, if the coefficients in (2.21) are π–periodic even functions of x, then there are in fact four "basically-periodic" solutions given by even and odd functions $\beta(x)$, each one having in turn a period π or 2π. Generically, these basically-periodic solutions cannot coexist for the same parameter values: if the equation possesses one of these basically-periodic solutions, the other solution is unbounded. In the exceptional cases when they coexist, both have the same period, with one even and the other odd.

Thus, the requirement that $K(\xi)$ be even, though not essential for the expansion and Floquet theory, introduces clear symmetries in x that are exhibited by the solutions in different branches. For example, solutions with $\beta(x)$ odd, having period 2π, will be associated with a velocity function u odd in x and an even specific volume V. If $\beta(x)$ is even and 2π–periodic, then u will be even in x at leading order (and the first perturbation to V_f will be odd). But the full solution will present no symmetry, because of the contribution coming from the equilibrium solution, which is even in x. Similar relations hold for the solutions branching off π–periodic transition curves.

The solution of (2.21) for arbitrary values of ϵ can only be obtained numerically; this problem is treated in Chapter 3 following the guidelines sketched above. However, for small values of ϵ it is possible to determine the transition curves approximately by perturbation methods. This analysis is carried out in Section 2.8, and brings out an interesting connection between the weakly nonlinear approach and the bifurcation analysis.

To further advance this analysis, let us assume that we have actually found a pair $(\epsilon, \omega_0(\epsilon))$ such that $\beta(x)$ is either π or 2π periodic and the other solution is unbounded. Then, with $\phi_1(x)$ satisfying (2.18) we have, in principle, the first term $\varphi_1(x,\tau)$ in the potential series that defines a solution bifurcating from the equilibrium state, 2π periodic in x and τ. Then, provided that $n\omega_0$ is not in a transition curve for any $n = 2, 3, ...$, we have the basic elements to proceed with the expansion. Next we examine the first few terms in some detail.

2.4 Second order solution

Having studied in detail the eigenvalue problem (2.11), which gives the transition curves in the (ϵ, ω_0) plane and the periodic function $\varphi_1(x,\tau)$, we now turn our attention to the second order problem (2.12).

From the theory of linear operators in linear vector spaces (see Friedman (1990)) it is known that the non-homogeneous equation

$$L[\varphi] = F$$

has a solution, if and only if, F is orthogonal to every solution of the adjoint homogeneous equation $L^*[\varphi^*] = 0$. Since the operator L in (2.11) is formally self-adjoint, this solvability condition reduces to

$$\langle F_2 , \varphi_1 \rangle = 0. \tag{2.22}$$

Substituting $\varphi_1(x,\tau) = cos\,\tau\ \phi_1(x)$ in the forcing term F_2 we have:

$$F_2 = 2\,\omega_0\,\omega_1\,cos\,\tau\ \phi_1(x) - b_2\,cos^2\tau \left\{ e^{-2\epsilon K(2x)}\,[\phi_1'(x)]^2 \right\}'.$$

With the inner product as defined below (2.10), from (2.22) we then obtain

$$\omega_1 = 0.$$

Equation (2.12) can now be written

$$L[\varphi_2] = \omega_0^2\,\varphi_{2\tau\tau} - \left[b_1\,e^{-\epsilon K(2x)}\,\varphi_{2x} \right]_x = -\frac{b_2}{2}\,(1 + cos\,2\tau) \left\{ e^{-2\epsilon K(2x)}\,[\phi_1'(x)]^2 \right\}'.$$

The normalization condition (2.17), namely $\langle \varphi_2, \varphi_1 \rangle = 0$, removes the homogeneous part from the general solution $\varphi_2(x,\tau)$. Hence, upon separating time, φ_2 will have the form

$$\varphi_2(x,\tau) = \psi_2(x) + cos\,2\tau\ \phi_2(x), \tag{2.23}$$

where $\psi_2(x)$ and $\phi_2(x)$ have period 2π with zero mean, and they are the solutions of the following boundary-value problems:

$$\left[b_1\,e^{-\epsilon K(2x)}\,\psi_2'(x) \right]' = \frac{b_2}{2} \left\{ e^{-2\epsilon K(2x)}\,[\phi_1'(x)]^2 \right\}', \tag{2.24}$$

$$\left[b_1 \, e^{-\epsilon K(2x)} \, \phi_2'(x) \right]' + 4\,\omega_0^2 \, \phi_2(x) = \frac{b_2}{2} \left\{ e^{-2\epsilon K(2x)} \, [\phi_1'(x)]^2 \right\}'. \tag{2.25}$$

Having completed the second order solution $\varphi_2(x,\tau)$ for the bifurcating potential series, it seems appropriate to pause for a moment in the algebraic solution of the perturbation equations and comment upon the general conditions for the validity of the bifurcation approach.

At any order, after eliminating the temporal part of the solution, we will end up with boundary-value problems in x similar to (2.24) and (2.25). The first one presents no difficulty. The second type of problem will have the same linear operator L_x as in (2.16), but with $m^2\omega_0^2$, m being a positive integer, instead of the eigenvalue ω_0^2, and a forcing term with known functions. When $m > 1$, $m^2\omega_0^2$ is not an eigenvalue, as explained in Section 2.3, and L_x has an inverse. Thus, the problem will have a unique solution. When $m = 1$, then the Fredholm alternative that determines ω_n at each level — see the end of Section 2.2 — will guarantee that the right hand side is orthogonal to ϕ_1. But this is the Fredholm alternative at the level of $L_x[\phi]$ =forcing. Thus, the equation will again have a unique solution, since its solution will have to be orthogonal to ϕ_1 (this is what $\langle \varphi_n, \varphi_1 \rangle = 0$ in (2.17) translates into at the level of these equations where time τ has been separated). Therefore, applying the Fredholm condition to (2.25), or in general, to similar problems at higher orders, uniqueness of their solutions will be assured if and only if the quantity $n^2\omega_0^2$ is not an eigenvalue of L_x.

As a closing remark about formal conditions that justify the bifurcation series solution, it should be stated here that existence and uniqueness of solutions to boundary-value problems (2.24)–(2.25) (and, by extension, to those that will appear at higher orders having a similar structure, see next section) are guaranteed under relatively mild conditions on the coefficients (see Keller (1990)). For example, continuity of K will be enough. Therefore, existence and uniqueness of all boundary-value problems that define the eigenfunctions in mass coordinate x for the bifurcation series solution, are completely assured.

It should also be mentioned that efficient numerical methods for boundary-value problems have been developed based on the ideas employed to prove existence and uniqueness of solutions. We will pick up this topic again in Chapter 3.

2.5 Higher order solutions: general form

In this section, we look at the third order terms in the bifurcating potential series, in order to further illustrate the structure already pointed out in the previous section.

This will also give us a precise description of the bifurcation expansion up to a high order.

Inserting the solutions $\varphi_1(x,\tau)$ and $\varphi_2(x,\tau)$ in the right hand side of equation (2.13), the forcing term may be written as

$$F_3 = 2\,\omega_0\,\omega_2\,cos\,\tau\,\phi_1(x) \;-\; 2\,b_2\,cos\,\tau\,\left\{e^{-2\epsilon K(2x)}\,\phi_1'(x)\,\psi_2'(x)\right\}'$$

$$-\,b_2\,cos\,3\tau\,\left\{e^{-2\epsilon K(2x)}\,\phi_1'(x)\,\phi_2'(x)\right\}' \;+\; b_3\,(\frac{3}{4}\,cos\,\tau \;+\; \frac{1}{4}\,cos\,3\tau)\,\left\{e^{-3\epsilon K(2x)}\,[\phi_1'(x)]^3\,\right\}'.$$

The solvability condition at this order is given by

$$\langle\, F_3\,,\,\varphi_1\,\rangle = \langle\, F_3\,,\,cos\,\tau\,\phi_1(x)\,\rangle \;=\; 0.$$

Carrying out the algebraic operations, we thus obtain the second term in the frequency expansion:

$$\omega_2 \;=\; \frac{1}{4\pi\omega_0}\,\left\{\,-\,b_2\,\int_0^{2\pi}\,[\phi_1'(x)]^2\,\psi_2'(x)\,e^{-2\epsilon K(2x)}\,dx \;+\; \frac{3}{8}\,b_3\,\int_0^{2\pi}\,[\phi_1'(x)]^4\,e^{-3\epsilon K(2x)}\,dx\right\}.$$

Equation (2.13) now takes the form:

$$L\,[\varphi_3] = \omega_0^2\,\varphi_{3\tau\tau} - \left[b_1\,e^{-\epsilon K(2x)}\,\varphi_{3x}\right]_x = -f_3^{(1)}(x)\,cos\,\tau - f_3^{(3)}(x)\,cos\,3\tau,$$

where

$$f_3^{(1)}(x) = -2\,\omega_0\,\omega_2\,\phi_1(x) + 2\,b_2\,\left\{e^{-2\epsilon K(2x)}\,\phi_1'(x)\,\psi_2'(x)\right\}' - \frac{3}{4}\,b_3\,\left\{e^{-3\epsilon K(2x)}\,[\phi_1'(x)]^3\,\right\}',$$

$$f_3^{(3)}(x) = b_2\,\left\{\,e^{-2\epsilon K(2x)}\,\phi_1'(x)\,\phi_2'(x)\right\}' - \frac{b_3}{4}\,\left\{\,e^{-3\epsilon K(2x)}\,[\phi_1'(x)]^3\,\right\}'.$$

Then, we can write for φ_3

$$\varphi_3(x,\tau) \;=\; cos\,\tau\;\psi_3(x) \;+\; cos\,3\tau\;\phi_3(x),$$

where $\psi_3(x)$ and $\phi_3(x)$ have period 2π with zero mean and ψ_3 is orthogonal to ϕ_1; these functions satisfy the boundary-value problems:

$$\left[b_1\,e^{-\epsilon K(2x)}\,\psi_3'(x)\right]' \;+\; \omega_0^2\,\psi_3(x) \;=\; f_3^{(1)}(x),$$

and

$$\left[b_1\, e^{-\epsilon K(2x)}\, \phi_3'(x)\right]' \,+\, 9\,\omega_0^2\, \phi_3(x) \,=\, f_3^{(3)}(x).$$

As in the previous section, we note that there is no difficulty with the second problem, since $9\,\omega_0^2$ is not an eigenvalue. Regarding the first problem, the choice of ω_2 exactly guarantees that $f_3^{(1)}$ is orthogonal to ϕ_1. Since ψ_3 must be orthogonal to ϕ_1 also, this equation determines it uniquely.

It should be now obvious that at any stage in the solution of the sequence of inhomogeneous equations (2.15), the following structure occurs. At $O(a^n)$, F_n takes the form

$$F_n = -2\,\omega_0\,\omega_{n-1}\,\phi_1(x)\,cos\,\tau - \sum_{j=0}^{m} f_n^{(2j)}(x)\,cos\,2j\tau,$$

if $n = 2m$ is even, and

$$F_n = -2\,\omega_0\,\omega_{n-1}\,\phi_1(x)\,cos\,\tau - \sum_{j=0}^{m} f_n^{(2j+1)}(x)\,cos\,(2j+1)\tau,$$

if $n = 2m+1$ is odd. Clearly then, $\omega_{n-1} = 0$ if n is even ($\omega_1 = \omega_3 = \omega_5 = \ldots = 0$) while, for n odd, the condition $\langle F_n, \varphi_1\rangle = 0$ reduces to (use here $\varphi_1 = cos\,\tau\,\phi_1(x)$ and (2.18))

$$\omega_{n-1} = -\frac{1}{8\pi\omega_0}\int_0^{2\pi} f_n^{(1)}(x)\,\phi_1(x)\,dx.$$

Then, we can write for $\varphi_n(x,\tau)$

$$\varphi_n(x,\tau) \,=\, \sum_{i=0}^{n} \phi_n^{(i)}(x)\;\; cos(i\,\tau),$$

where $\phi_n^{(i)}(x)$ vanishes if n is even and i is odd or if n is odd and i is even. Furthermore, for n odd, $\phi_n^{(1)}(x)$ is orthogonal to ϕ_1. Of course, all the $\phi_n^{(i)}(x)$ are 2π–periodic of mean zero. They satisfy the equations (where i and n are either both odd or both even, and $0 \le i \le n$)

$$\left[\, b_1\, e^{-\epsilon K(2x)}\, \left(\phi_n^{(i)}(x)\right)'\,\right]' \;+\; i^2\,\omega_0^2\,\phi_n^{(i)}(x) \;=\; f_n^{(i)}(x), \qquad\qquad i \neq 1,$$

$$\left[\, b_1\, e^{-\epsilon K(2x)}\, \left(\phi_n^{(1)}(x)\right)'\,\right]' \;+\; \omega_0^2\,\phi_n^{(1)}(x) \;=\; 2\,\omega_0\,\omega_{n-1}\,\phi_1(x) + f_n^{(1)}(x).$$

Here the forcing terms $f_n^{(i)}$ are given in terms of quantities calculated at prior orders. As stated before, the equations for $i \neq 1$ present no difficulties because $i^2\omega_0^2$ is not an eigenvalue. When $i = 1$, the right hand side is orthogonal to the single homogeneous solution ϕ_1 by the choice ω_{n-1}, and again there is no difficulty.

Using the notation just introduced, we can now write the bifurcating potential function in the form

$$\varphi(x,\tau) = \left(a^2\,\phi_2^{(0)} + a^4\,\phi_4^{(0)} + a^6\,\phi_6^{(0)} + ...\right) + cos\,\tau\left(a\,\phi_1^{(1)} + a^3\,\phi_3^{(1)} + a^5\,\phi_3^{(5)} + ...\right) +$$

$$cos\,2\tau\left(a^2\,\phi_2^{(2)} + a^4\,\phi_4^{(2)} + a^6\,\phi_6^{(2)} + ...\right) + cos\,3\tau\left(a^3\,\phi_3^{(3)} + a^5\,\phi_5^{(3)} + a^7\,\phi_7^{(3)} + ...\right) +$$

$$cos\,4\tau\left(a^4\,\phi_4^{(4)} + a^6\,\phi_6^{(4)} + a^8\,\phi_8^{(4)} + ...\right) + cos\,5\tau\left(a^5\,\phi_5^{(5)} + a^7\,\phi_7^{(5)} + a^9\,\phi_9^{(5)} + ...\right) +$$

$$+...$$

In compact notation, φ and the frequency ω take the form

$$\varphi(x,\tau) = \sum_{j=0}^{\infty} cos\,j\tau \sum_{i=0}^{\infty} a^{j+2i}\ \phi_{j+2i}^{(j)}(x), \tag{2.26}$$

$$\omega(a) = \omega(-a) = \sum_{i=0}^{\infty} a^{2i}\,\omega_{2i}, \tag{2.27}$$

where $\phi_0^{(0)} \equiv 0$.

In summary, we have found time periodic solutions of the equations of motion (2.1)–(2.2) — or, equivalently, to the exact wave equation (2.7) — governing 1D compressible fluid flow, that arise as a bifurcation from an equilibrium state. In terms of the potential function (2.26), these nonlinear acoustic waves are given as Fourier series in time, with coefficients expanded in powers of an amplitude a defined by (2.10), with periods $2\pi/\omega$ in time t and 2π in the mass-Lagrangian coordinate x. The physical quantities specific volume V and flow velocity u can be recovered from

$$V(x,t) = V_0(\epsilon)\,e^{\epsilon K(2x)} + \varphi_x(x,t), \tag{2.28}$$

$$u(x,t) = \varphi_t(x,t), \tag{2.29}$$

where the normalized equilibrium amplitude $V_0(\epsilon)$ was defined in Section 2.1, and the "strained" variable τ is related to the original dimensionless time by $\tau = \omega t$, ω being given by (2.27).

2.6 Convergence of the series solution

As mentioned earlier in this chapter, the usual results that rigorously justify bifurcation expansions, do not apply in cases like ours — where the operators involved are hyperbolic. Without going into any details, we will discuss in this section some of the issues and difficulties associated with convergence in the particular case of our expansion.

The key difficulty that makes any proof of convergence rather tricky, is the following. Consider the operator L in (2.15), restricted (in H_0) to the set of functions orthogonal to φ_1 — i.e. H_1, also a Hilbert space. While L in H_1 has an inverse, this inverse is, generally, *not bounded.* This means that one has then very little control over the rate at which the φ_n's grow with n. Thus, not only a proof of convergence becomes very difficult, but one may even doubt if convergence occurs at all.

Let us clarify the previous paragraph a bit. From the discussion in Section 2.3, it is clear that the set$\{\varphi_{ml}\}$ for $m = 1, 2, 3...$, $l = 1, 2, 3...$ and $m + l \geq 3$ is a complete set of orthonormal functions in H_1. Now, the solution of the problem

$$L[\varphi] = \varphi_{ml}, \qquad m + l \geq 3,$$

(with φ in H_1) is given by

$$\varphi = \frac{1}{\lambda_l - m^2\omega_0^2}\,\varphi_{ml}.$$

We assumed that $\lambda_l - m^2\omega_0^2$ was never zero, but (generally) *we cannot be sure it will not take arbitrarily small values as m and l become large.* This thus leads to a *"small divisors"* problem: notice that, in solving for φ_n in (2.15), typically F_n will involve terms with φ_{ml} in the range $1 \leq m \leq n$ and any l (see the discussions in Sections 2.4 and 2.5). Thus, as n increases, φ_n may involve terms with smaller and smaller denominators.

In fact, when considering this "small divisors" problem, we only need to worry about the behavior of $\lambda_l - m^2\omega_0^2$ for m and l large. But for l large λ_l can be approximated by the WKBJ formula $\lambda_l \simeq s^2(\bar{c})^2$, where $l = 2s$ or $l = 2s - 1$ and $\bar{c}$ was defined in Section 2.3. Thus introducing $r = \omega_0^2/(\bar{c})^2$, the question becomes: how fast can

$$D(m,r) = \min_s |m^2 r - s^2|$$

become small, as m grows? We note that, as pointed out in Section 2.3, for some r's, D is bounded from below (e.g. $D(m,2) \geq 1$). In this case, in fact, L would have a bounded inverse and a proof of convergence might be possible. Unfortunately, the set of r's with this property is rather thin (measure zero).

A possible strategy for proving convergence would involve: first, identifying a rate of vanishing of D (as $m \to \infty$) that is "slow enough" so that convergence is not destroyed (roughly $\sum a^n s_n / D(n,r) < \infty$ for a small enough, where s_n is a factor that depends on the structure of F_n). Second, identifying the set of r's for which this rate (or slower) is achieved. As $r = r(\epsilon)$ for a given K and choice of branch $\omega_0 = \omega_0(\epsilon)$, this would translate into a set of ϵ's. For this set, convergence would occur, at least for small enough a.

We note that the strategy suggested above (a highly non-trivial task) is motivated by the similar situation with small divisors that occurs in the question of existence of quasi-periodic solutions for finite dimensional Hamiltonian systems, studied by Kolmogorov, Arnold, Moser and others (KAM theory, see for example Arnold (1978) and Moser (1973)). If the experience there is any guide, we can expect the set of r's (thus ϵ's) for which convergence occurs, to be very "strange": rather dense and "thick" in some regions (say, for ϵ small) and sparse elsewhere (say, for ϵ large). We point out that our numerical experiments of Chapter 3 and 4 were not sufficiently precise to detect any such structure, though we found it very hard to compute solutions for large values of ϵ. In fact, in those chapters we proceeded as if a solution could be found branching out from every point along a transition curve $(\omega_0(\epsilon), \epsilon)$. As long as the set of ϵ's for which this happens is dense, in practice this is not a bad approximation. The next paragraph proceeds with this point of view.

It was shown before (if one ignores convergence issues) that bifurcating solutions arise from particular locations in (ω, ϵ) parameter space called transition curves. It is convenient to add to this picture the normalized amplitude a in order to visualize the regions of existence of these nonlinear waves in a three dimensional parameter space (ω, ϵ, a). Thus, transition curves obtained by Floquet analysis lie in the bottom of this parameter space, namely, the plane of zero bifurcation amplitude $a = 0$ corresponding to equilibrium solutions. As we move upwards, for a small but different from zero, there will be certain special locations in this space that will correspond to time periodic solutions of finite amplitude. The shape of these surfaces in (ω, ϵ, a) space can only be drawn numerically because perturbation techniques, though very powerful, are essentially local tools that cannot be employed for finite amplitudes far from the basic reference state. However, the theoretical analysis developed in this chapter will constitute the basis for a practical numerical approach aimed at exploring regions of existence of large amplitude periodic waves. For the moment, it may be helpful to think that, for a fixed value of the entropy wave amplitude ϵ, there will be

curves in (ω, a) plane along which periodic solutions exist. These non-trivial branches will begin, for $a = 0$, at special points $\omega_0(\epsilon)$ in ω axis — given by the Floquet theory analysis — and will continue for finite values of a until (presumably) a maximum amplitude a_{max} is reached, beyond which, the basic balance between dispersion and nonlinearity breaks down and periodic continuous solutions no longer exist.

In sum, we have presented analytical plausibility arguments regarding the existence of time periodic solutions bifurcating from equilibrium in a Hamiltonian system described by the inviscid equations of 1D Gas Dynamics. The bifurcation process results from the resonant interaction of nonlinear acoustic waves propagating in a nonuniform entropy background. The weakly nonlinear analysis of Chapter 1 considered small amplitude sound waves in a slightly nonuniform medium, and the associated physical picture consisted simply of two weakly nonlinear periodic acoustic waves moving in opposite directions with certain additional interaction terms. In this chapter, we studied again small amplitude sound waves, but here the entropy wave amplitude that controls the bifurcation can take arbitrary values. The bifurcation approach clearly includes the weakly nonlinear analysis as a special case, and we show that connection in Sections 2.7 and 2.8. Furthermore, if the power series solutions (2.26)–(2.27) do converge for small amplitudes a, it is readily possible to extend (numerically) these solutions for larger amplitudes. It will be shown in the next chapter that these large amplitude solutions will exhibit a richer and more complex structure than those obtained in Chapter 1 as a small departure from linear acoustics.

2.7 Matching between bifurcation and weakly nonlinear solutions

Let us review the formal assumptions under which time periodic solutions to 1D inviscid Gas Dynamics were obtained via bifurcation and weakly nonlinear methods.

The weakly nonlinear series solution was derived in Chapter 1 for small amplitude sound and entropy waves. In fact, the entropy wave amplitude ϵ was the expansion parameter, and a measure of nonlinear effects present in the problem. The perturbations were required to have an average value zero in x (i.e., the specific volume V and flow velocity u had means one and zero, respectively) and periods $2\pi/\omega$ in time t and 2π in mass coordinate x. Furthermore, time symmetries were imposed by asking V and u to be even and odd functions of time, respectively. Likewise, time periodic bifurcating solutions were obtained in the present chapter for small sound amplitudes a, but for arbitrary entropy amplitudes ϵ. The periodicity requirements were identical, and the potential φ satisfying (2.7) had to be even in time with zero mean in x.

Our purpose here is to show that both solutions coincide for small values of ϵ.

We do so using, as an example, the particular case for which analytical solutions were calculated in Section 1.4. In that case, we employed a single Fourier mode for the entropy field and a polytropic gas law for the pressure (see the equations at the beginning of Section 1.4).

It should be remembered that the solutions obtained in Section 1.4 were expressed in terms of the characteristic variables $\mu = x - \omega t$ and $\lambda = -x - \omega t$ that involved the characteristic velocity ω, which was also expressed as a series in powers of ϵ. There were two solutions, corresponding to two different branches of $\omega = \omega(\epsilon)$, defined by equations (1.58)-(1.60 and (1.61)-(1.63). Hence, expressing all those quantities in the original independent variables, the leading order weakly nonlinear solutions are

$$\begin{cases} V(x,t) = 1 + \epsilon\, 2\, cos\,(2x) + \epsilon^2\, cos\,(4x) - \epsilon^2\, \alpha\, 2\, cos\,(x)\, cos\,(\omega t) + O(\epsilon^3), \\ u(x,t) = \epsilon^2\, \alpha\, 2\, sin\,(x)\, sin\,(\omega t) + O(\epsilon^3), \\ \omega = 1 - \epsilon\, 1/2 + \epsilon^2\,(5/16 + \gamma/2) + O(\epsilon^3), \end{cases}$$

$$\begin{cases} V(x,t) = 1 + \epsilon\, 2\, cos\,(2x) + \epsilon^2\, cos\,(4x) - \epsilon^2\, \alpha\, 2\, sin\,(x)\, cos\,(\omega t) + O(\epsilon^3), \\ u(x,t) = -\epsilon^2\, \alpha\, 2\, cos\,(x)\, sin\,(\omega t) + O(\epsilon^3), \\ \omega = 1 + \epsilon\, 1/2 + \epsilon^2\,(5/16 + \gamma/2) + O(\epsilon^3), \end{cases}$$

where each set of equations defines a particular solution branch. A detailed matching calculation for the characteristic velocity ω is performed in next section.

On the other hand, the bifurcation approach is based on the equilibrium solution $V_f(x) = V_0(\epsilon)\, e^{\epsilon K(2x)}$ (cf. Section 2.1) that has a unitary average value. Expanding for small ϵ and imposing that normalization, we obtain

$$V_f(x) = 1 + \epsilon\, 2\, cos\,(2x) + \epsilon^2\, cos\,(4x) + O(\epsilon^3).$$

Next, we have to solve the eigenvalue problem (2.11), which in the limit $\epsilon \to 0$ turns out to be simply

$$\phi_1''(x) + \omega^2 \phi_1(x) = 0,$$

where $\phi_1(x)$ has period 2π and zero mean. Thus, it follows immediately that the complete bifurcating solution $V(x,t) = V_f(x) + \varphi_x(x,t)$ and $u(x,t) = \varphi_t(x,t)$ satisfying (2.11) and the normalization (2.18) will be given by

$$\begin{cases} V(x,t) = 1 + \epsilon\, 2\, cos\,(2x) + \epsilon^2\, cos\,(4x) - a\, 2\, cos\,(x)\, cos\,(\omega t) + O(\epsilon^3, a^2), \\ u(x,t) = a\, 2\, sin\,(x)\, sin\,(\omega t) + O(\epsilon^3, a^2), \\ \omega = 1 - \epsilon\, 1/2 + \epsilon^2\,(5/16 + \gamma/2) + O(\epsilon^3, a^2), \end{cases}$$

$$\begin{cases} V(x,t) = 1 + \epsilon\, 2\, cos\,(2x) + \epsilon^2\, cos\,(4x) - a\, 2\, sin\,(x)\, cos\,(\omega t) + O(\epsilon^3, a^2), \\ u(x,t) = -a\, 2\, cos\,(x)\, sin\,(\omega t) + O(\epsilon^3, a^2), \\ \omega = 1 + \epsilon\, 1/2 + \epsilon^2\,(5/16 + \gamma/2) + O(\epsilon^3, a^2), \end{cases}$$

which match the weakly nonlinear solutions upon identifying $\epsilon^2\alpha = a$ as an acoustic wave amplitude measure. We can conclude that both approaches, though conceptually different, provide the same time periodic solution in the limit $\epsilon \to 0$, $a \to 0$.

2.8 Transition curves by perturbation. Stability diagram

In this section, transition curves in (ω, ϵ) parameter plane are calculated using perturbation methods for the limit $\epsilon \to 0$. As we saw in Section 2.3, these curves correspond to time periodic bifurcating solutions of the eigenvalue problem (2.11), or equivalently, (2.21). Our purpose can be unfolded in three parts: in the first place, a complete determination of the transition curves in the (ω, ϵ) plane will provide an illuminating picture of that "Floquet bottom" in (ω, ϵ, a) space referred to in Section 2.6, a plane $a = 0$ that marks the birth of periodic waves bifurcating from equilibrium. In the second place, and as a by-product of that calculation, it will be shown that the bifurcation approach and the weakly nonlinear analysis yield the same asymptotic expansion for the frequency ω in the limit $\epsilon \to 0$, $a \to 0$; this will complete the asymptotic matching to leading order terms between both methods initiated in previous section. Finally, a multiple scales calculation will classify stability regions in (ω, ϵ) separated by transition curves.

The significance of the transition curves calculation should be stressed again. It is well known that for an initially constant entropy field ($\epsilon = 0$), smooth initial conditions of the Gas Dynamic equations become singular in finite time; hence, in such a case, there are no periodic solutions other than the state of rest (cf. Lax (1964)). It is precisely a nonconstant entropy background that couples the acoustic modes in such a way that, by a periodic exchange of energy between them, wave breaking is

prevented. On the mathematical side, the analysis shows that a nonuniform entropy field ($\epsilon \neq 0$) is necessary in order to have simple eigenvalues ω_0^2, a crucial requirement for the bifurcation theory. Simple eigenvalues that define transition curves result from the splitting of the double eigenvalues $\omega_0^2 = n^2$ that correspond to the case with no entropy coupling ($\epsilon = 0$). Moreover, as the splitting is of higher order for increasing values of n, the analysis also guarantees (at least for small ϵ) the other critical assumption that $n^2\omega_0^2$ are not eigenvalues of L_x in (2.16). Recall that this last condition was essential in obtaining the higher order solutions in the bifurcation series.

We begin by recalling that after eliminating time dependence, periodic bifurcating solutions of (2.11) must satisfy Hill's equation (2.21):

$$\beta''(x) + \left\{ \frac{\omega_0^2}{b_1} e^{\epsilon K(2x)} + 2\,\epsilon\, K''(x) - \epsilon^2 [K'(x)]^2 \right\} \beta(x) = 0. \qquad (2.21)$$

The entropy wave appearing in the periodic coefficients of (2.21) was chosen as $K(2x) = 2cos(2x)$. Hence, as we saw seen in Section 2.3, periodic bifurcating solutions of (2.11) (with periods $2\pi/\omega$ in time t and 2π in x) will be defined for certain combinations (ω, ϵ) — transition curves — that produce a π or 2π periodic $\beta(x)$.

We notice that for $\epsilon = 0$, $b_1 = 1$ and (2.21) reduces to

$$\beta''(x) + \omega_0^2\, \beta(x) = 0.$$

This equation only has periodic solutions (of period 2π) when $\omega_0 = n = 1, 2, ...$ Thus, these ω_0's are the starting points for the transition curves at $\epsilon = 0$. Two of them start for each $\omega_0 = n$, splitting the double eigenvalue $\omega_0^2 = n^2$ of the equation above for $\epsilon \neq 0$. One of them will have odd solutions (corresponding to $\beta(x) = sin(nx)$ above) and the other will be the even branch (corresponding to $\beta(x) = cos(nx)$ above). We note that this symmetric split into even and odd branches occurs only because we will be looking at the particular case of an even $K = K(2x) = 2\,cos(2x)$. Furthermore, the branches with n even will be actually π–periodic, while the branches with n odd will be 2π–periodic.

Having established that for $\epsilon = 0$ the transition curves start at $\omega_0 = n$, $n = 1, 2, 3, ...$ — a limit that, obviously, corresponds to linear acoustics — we proceed to calculate these curves for $0 < \epsilon \ll 1$. Since we are dealing with periodic solutions, we apply Poincare-Linstedt method and expand the function $\beta(x)$ and frequency ω_0 in the form

$$\beta(x) = \beta_0(x) + \epsilon\, \beta_1(x) + \epsilon^2\, \beta_2(x) + \cdots,$$

$$\omega_0 = \Omega_0 + \epsilon\, \Omega_1 + \epsilon^2\, \Omega_2 + \cdots,$$

where, according to the calculation above, $\Omega_0 = n$. To avoid confusion, let us remember that $\omega_0 = \omega_0(\epsilon)$ is, in turn, the first term in the full expansion of $\omega = \omega(\epsilon, a)$ in powers of a (cf. equations (2.9) and (2.21)); we are now expressing that first term as a series in powers of ϵ, for small entropy amplitudes ϵ. Since the coefficient b_1 is a function of ϵ (cf. equation (2.7)), we can expand it as $b_1(\epsilon) = 1 + (\gamma + 1)\epsilon^2 + O(\epsilon^3)$, with γ the ratio of specific heats, and express the eigenvalues in the form

$$\frac{\omega_0^2}{b_1(\epsilon)} = \Omega_0^2 + \epsilon\, 2\,\Omega_0\,\Omega_1 + \epsilon^2\,(\Omega_1^2 + 2\,\Omega_0\,\Omega_2 - (\gamma+1)\,\Omega_0) + O(\epsilon^3).$$

Introducing these expansions in equation (2.21) we obtain the sequence of equations

$$\begin{aligned}
\beta_0''(x) + \Omega_0^2\,\beta_0(x) &= 0, \\
\beta_1''(x) + \Omega_0^2\,\beta_1(x) &= -\,[\,2\,\Omega_0^2\,cos(2x) + 2\,\Omega_0\,\Omega_1 - 4\,cos(2x)\,]\;\beta_0(x), \\
\beta_2''(x) + \Omega_0^2\,\beta_2(x) &= -\,[\,2\,\Omega_0^2\,cos(2x) + 2\,\Omega_0\,\Omega_1 - 4\,cos(2x)\,]\;\beta_1(x) \\
&\quad -[\,\Omega_0^2\,(1 + cos(4x)) + 4\,\Omega_0\,\Omega_1\,cos(2x) + \Omega_1^2 + 2\,\Omega_0\,\Omega_2 \\
&\quad -(\gamma+1)\,\Omega_0 - 2\,(1 - cos(4x))\,]\,\beta_0(x), \\
&\vdots
\end{aligned}$$

Let us investigate the periodic solutions arising near $\Omega_0 = 1$. According to the general theory of Hill's equation (see remarks accompanying equation (2.21) in Section 2.3), if the coefficients are even and π–periodic there is a couple of solutions, one even and the other odd, branching off every bifurcation point $\omega = n$, $n = 1, 2, 3, ...$; for more general periodic coefficients, the theory applies as well, but the symmetries in x do not hold. This detail was, in fact, the reason for choosing an entropy wave $K(2x) = 2cos(2x)$ that would allow a more clear distinction between different solutions of the equation (2.21), and simplify expansions like the one here.

We begin then by calculating the even branch $\beta(x)$ arising from $\Omega_0 = 1$. The leading order solution that is 2π–periodic is simply given by $\beta_0(x) = 2cos(x)$. Eliminating secular terms in the second equation, we obtain $\Omega_1 = 1/2$, and the first order solution is $\beta_1(x) = -cos(x) - 1/4\,cos(3x)$. In a similar way, we obtain, from the third equation, the frequency correction Ω_2 and $\beta_2(x)$. Therefore, the transition curves corresponding to 2π–periodic and even $\beta(x)$ solutions bifurcating from $\omega_0 = 1$ have the following form for $0 < \epsilon \ll 1$:

$$\beta(x) = 2\,cos\,(x) + \epsilon\,\left[-cos\,(x) - \frac{1}{4}\,cos\,(3x)\right]$$

$$+\epsilon^2 \left[-\frac{45}{64} cos\,(x) + \frac{19}{32} cos\,(3x) + \frac{13}{96} cos\,(5x) \right] + O(\epsilon^3),$$

$$\omega = 1 + \epsilon \frac{1}{2} + \epsilon^2 \left(\frac{5}{16} + \frac{\gamma}{2} \right) + O(\epsilon^3).$$

The 2π–periodic odd branch arising from $\omega_0 = 1$ can be calculated in the same way, and it is given by

$$\beta(x) = -2\,sin\,(x) + \epsilon \left[-sin\,(x) + \frac{1}{4} sin\,(3x) \right]$$

$$+\epsilon^2 \left[-\frac{23}{64} sin\,(x) + \frac{19}{32} sin\,(3x) - \frac{13}{96} sin\,(5x) \right] + O(\epsilon^3),$$

$$\omega = 1 - \epsilon \frac{1}{2} + \epsilon^2 \left(\frac{5}{16} + \frac{\gamma}{2} \right) + O(\epsilon^3).$$

At this stage, let us make two remarks: first, in Section 2.4 it was found that the second term in the frequency expansion (2.9), i.e., $\omega = \omega_0 + a\,\omega_1 + a^2\,\omega_2 + O(a^3)$ was identically zero, $\omega_1 \equiv 0$. Secondly, in Section 2.7 we identified $\epsilon^2\,\alpha = a$ in order to match asymptotic solutions obtained by bifurcation and weakly nonlinear methods. Hence, up to $O(\epsilon^3)$, the expansion for $\omega(\epsilon)$ will in fact be given by the expansion $\omega_0(\epsilon)$ calculated so far, since the next non-zero term in (2.9), namely, ω_2, will represent a contribution to $O(\epsilon^4)$. Thus, both formulas for the frequency ω arising from the bifurcation approach in the limit $\epsilon \to 0$, $a \to 0$ agree with their counterparts of Chapter 1 derived using weakly nonlinear techniques (see leading order solutions in Section 2.7). These results, together with those derived in the previous section, complete the proof that the more general bifurcation solution contains the weakly nonlinear solution as a limiting case for vanishing sound and entropy amplitudes.

A similar analysis around $\omega_0 = 2$ yields transition curves associated with π–periodic solutions $\beta(x)$. The even branch is given by

$$\beta(x) = 2\,cos\,(2x) + \epsilon \left[-1 + \frac{1}{3} cos\,(4x) \right]$$

$$+\epsilon^2 \left[-\frac{59}{36} cos\,(2x) + \frac{5}{24} cos\,(6x) \right] + O(\epsilon^3),$$

$$\omega = 2 + \epsilon^2 \left(-\frac{1}{3} + \frac{\gamma}{2} \right) + O(\epsilon^3),$$

while the odd branch is given by

$$\beta(x) = -2\,sin\,(2x) + \epsilon \left(-\frac{1}{3} \right) sin\,(4x)$$

$$+\epsilon^2 \left[\frac{13}{36} \, sin\,(2x) - \frac{5}{24} \, sin\,(6x) \right] + O(\epsilon^3),$$

$$\omega = 2 + \epsilon^2 \left(\frac{2}{3} + \frac{\gamma}{2} \right) + O(\epsilon^3).$$

Extending the analysis for subsequent $\omega_0 = n$, $n = 3, 4, 5, \ldots$, a complete chart of transition curves in (ω, ϵ) parameter plane can be drawn.

To complete the study of the solutions of (2.21) in the (ω, ϵ) plane, we perform now a multiple scales analysis to determine the "stability" properties of the regions separated by the transition curves. We focus our attention on the stability problem of solutions near $\omega = 1$.

As usual, we introduce a slow variable $X = \epsilon x$, $0 < \epsilon \ll 1$, and expand $\beta(x)$ of (2.21) and the frequency ω_0 in the form

$$\beta(x) = \beta_0(x, X) + \epsilon \, \beta_1(x, X) + \epsilon^2 \, \beta_2(x, X) + \cdots,$$

$$\omega_0 = 1 + \epsilon \, \Omega_1 + \epsilon^2 \, \Omega_2 + \cdots,$$

where we require periodicity in x of the functions β_n.

Substituting these expansions in (2.21) we obtain the equations

$$\frac{\partial^2 \beta_0}{\partial x^2} + \beta_0 = 0,$$

$$\frac{\partial^2 \beta_1}{\partial x^2} + \beta_1 = -\left[2\,\Omega_1 + 2\,sin(2x)\right] \beta_0 - 2\,\frac{\partial^2 \beta_0}{\partial x \partial X},$$

$$\frac{\partial^2 \beta_2}{\partial x^2} + \beta_2 = -\left[2\,\Omega_1 + 2\,sin(2x)\right] \beta_1 - \left[-2 - 3cos(4x) - 4\Omega_1 sin(2x) + \Omega_1^2 + 2\Omega_2 - \gamma\right] \beta_0(x)$$

$$-2\,\frac{\partial^2 \beta_1}{\partial x \partial X} - \frac{\partial^2 \beta_0}{\partial^2 X},$$

and so on. The zero order solution is $\beta_0 = A(X)\,cos(x) + B(X)\,sin(x)$, where the coefficients are functions of the slow variable X . Replacing β_0 in the forcing term of the second equation, we cancel secular terms and obtain the system

$$A'(X) = A(X)/2 + \Omega_1 \, B(X),$$
$$B'(X) = -B(X)/2 - \Omega_1 \, A(X),$$

which can be reduced to a single ordinary differential equation

$$A''(X) - \left(\frac{1}{4} - \Omega_1^2\right) A(X) = 0.$$

The solution will have the form $A(X) = Cexp\left(\pm\sqrt{1/4 - \Omega_1^2}X\right)$. Therefore, there would be an unbounded solution if $1/4 - \Omega_1^2 > 0$, or $| \Omega_1 | < 1/2$. Thus, regions between the transition curves arising from $\omega = 1$ and the ω axis correspond to "stable" (bounded) solutions $\beta(x)$, while those pairs (ω, ϵ) lying in between both branches induce "unstable" (unbounded) solutions.

A similar analysis can be carried out to study the "stability" of solutions around $\omega = 2$. In this case, the slow variable must be $X = \epsilon^2 x$, corresponding to the fact that in this case the perturbations to $\omega = 2$ only start at $O(\epsilon^2)$, as shown earlier for the periodic solutions. Proceeding as before, we find that to avoid secular terms Ω_1 must vanish. At second order, we obtain again a system of ordinary differential equations for the slowly varying coefficients, which reduces to an equation of the form

$$A''(X) - \left(-\frac{4}{3} + 2\gamma + 4\Omega_2\right)\left(\frac{8}{3} + 2\gamma - 4\Omega_2\right)\frac{1}{16} A(X) = 0.$$

Hence, unbounded solutions will exist for $-1/3 + \gamma/2 < \Omega_2 < 2/3 + \gamma/2$, in the region delimited by both transition curves, while bounded solutions will appear outside that wedge, giving a picture consistent with the stability characteristics found near $\omega = 1$.

The above calculations are graphically summarized in the stability diagram of figure 3, valid for $0 < \epsilon \ll 1$. In concluding this section, let us sum up how the Floquet analysis assures, for $0 < \epsilon \ll 1$, the necessary conditions for the solution of the bifurcating potential series stated in Section 2.6. First, the eigenvalues split as they branch off the axis $\epsilon = 0$, thus becoming simple. Second, the splitting of ω is of higher order in ϵ as we move up in the frequency axis ω, thus preventing $n^2\,\omega_0^2$ from becoming an eigenvalue.

For arbitrary values of the entropy wave amplitude ϵ, the stability diagram is obtained numerically in Chapter 3.

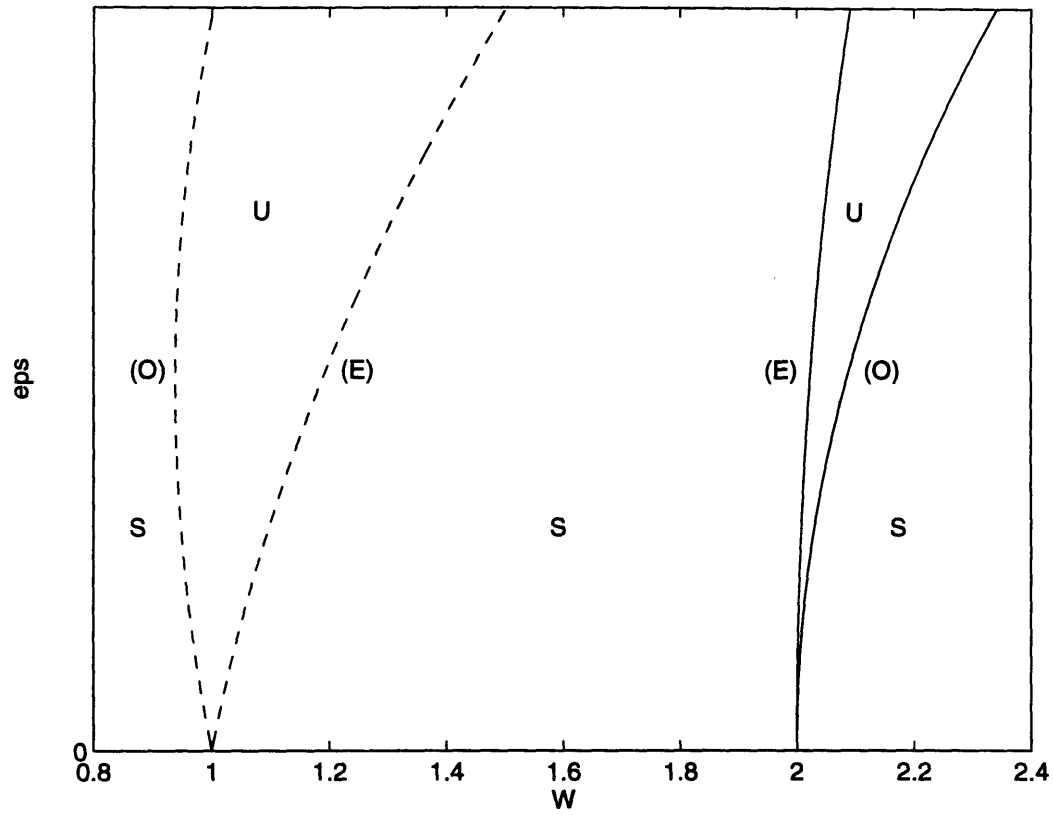

Figure 3: Stability diagram for small entropy amplitudes ϵ ; ω is the frequency of periodic acoustic waves. Dashed lines correspond to 2π–periodic transition curves (TC), solid lines depict π–periodic TC. Stability regions are denoted by U (two unstable solutions $\beta(x)$) and S (two stable but not periodic solutions $\beta(x)$). Simmetry of the eigenfunctions $\beta(x)$ is also indicated: (O) odd, (E) even. The ϵ axis is out of scale for illustrative purposes. Notation: (TC 1) to (TC 4), starting from the left.

2.9 Large eigenvalues by WKBJ method

In the previous section, approximate values for $\omega_0(\epsilon)$, the first term in the power series (2.9) for the frequency $\omega(\epsilon, a)$, together with periodic eigenfunctions $\beta(x)$ satisfying Hill's equation (2.21), were obtained by perturbation methods for $0 < \epsilon \ll 1$. The calculations showed the structure of transition curves in (ω, ϵ) parameter plane arising from the linear acoustic frequencies $\omega_0(\epsilon = 0) = n$, $n = 1, 2, ...$ Our purpose now is to estimate the value of $\omega_0(\epsilon)$ for large n, using the WKBJ method.

It was stated in Section 2.2 that our eigenvalue problem, given by Hill's equation (2.21), constitutes a Sturm-Liouville system

$$\beta''(x) + \left\{ \lambda^2 p(x) + q(x) \right\} \beta(x) = 0,$$

with periodic boundary conditions in $(0, 2\pi)$, where the eigenvalues $\lambda_n^2 = \omega_{0n}^2(\epsilon)/b_1(\epsilon)$ form an infinite sequence $\lambda_0 < \lambda_1 \leq \lambda_2 < \lambda_3 \leq ...$ such that $\lambda_n \to \infty$ as $n \to \infty$. Here, $p(x) = exp\{\epsilon K(2x)\}$, $p(x) > 0$, and $q(x) = 2\epsilon K''(2x) - \epsilon^2[K'(2x)]^2$ will be assumed to be continuous functions of x.

To estimate large eigenvalues λ_n as $n \to \infty$, let $\nu = 1/\lambda$, $0 < \nu \ll 1$. Hill's equation (2.21) now takes the form

$$\nu^2 \beta''(x) + \left\{ e^{\epsilon K(2x)} + \nu^2 \left[2\epsilon K''(2x) - \epsilon^2 \left(K'(2x)\right) \right] \right\} \beta(x) = 0. \qquad (2.30)$$

Notice that no restriction has been imposed on the value of the entropy wave amplitude ϵ; for this calculation, in contrast to the approximations derived in Section 2.8, ϵ can take arbitrary values.

A WKBJ approximation to (2.30) is given by

$$\beta(x) = e^{i\Theta_0(x)/\nu} A(x, \nu), \qquad (2.31)$$

where A has an expansion of the form $A(x, \nu) = A_0(x) + \nu A_1(x) + ...$ and $A_0(x)$ does not vanish identically. Substituting (2.31) in (2.30) we obtain

$$\left[e^{\epsilon K(2x)} - (\Theta_0')^2 \right] A + \nu \left[i \Theta_0'' A + 2 i \Theta_0' A_x \right] + \nu^2 \left[A_{xx} + q(x) A \right] = 0. \quad (2.32)$$

We collect now equal powers of ν. The zero order problem is called the eikonal equation; it gives $\Theta_0'(x) = \pm exp\{(\epsilon/2) K(2x)\}$. We take the plus sign, with a second (linearly independent) solution following by taking complex conjugates. Hence

$$\Theta_0(x) = \int e^{\frac{1}{2}\epsilon K(2x)} dx. \qquad (2.33)$$

This solution eliminates the first term in (2.32) at all orders. Considering now the remaining terms, and using the expansion for A we obtain the equations

$$2\,i\,A_0'\,\Theta_0' + i\,A_0\,\Theta_0'' = 0, \tag{2.34}$$

$$2\,i\,A_1'\,\Theta_0' + i\,A_1\,\Theta_0'' = -A_0'' - q(x)\,A_0, \tag{2.35}$$

$\vdots$

From (2.34), called the transport equation, we get

$$A_0(x) = [\Theta_0'(x)]^{-1/2} = e^{-\frac{1}{4}\epsilon K(2x)}. \tag{2.36}$$

Therefore, taking the real and imaginary parts in (2.31), two linearly independent real solutions of (2.30) can be written as

$$\beta_1(x) \simeq e^{-\frac{1}{4}\epsilon K(2x)}\,cos\left[\frac{1}{\nu}\int_0^x e^{\frac{1}{2}\epsilon K(2t)}\,dt\right], \tag{2.37}$$

$$\beta_2(x) \simeq e^{-\frac{1}{4}\epsilon K(2x)}\,sin\left[\frac{1}{\nu}\int_0^x e^{\frac{1}{2}\epsilon K(2t)}\,dt\right]. \tag{2.38}$$

Equations (2.37)–(2.38) will define approximate eigenfunctions $\beta(x)$ associated with even and odd branches in (ω_0, ϵ) parameter plane, respectively, arising from $\omega_0 = n$.

To find the eigenvalues $\lambda = 1/\nu$, we impose periodic boundary conditions on the solutions above. This yields

$$\frac{1}{\nu}\int_0^{2\pi} e^{\frac{1}{2}\epsilon K(2x)}\,dx = 2\,m\,\pi, \tag{2.39}$$

for some integer $m = 1, 2, 3, ...$ and then each of (2.37) and (2.38) yields an approximate eigenfunction. It is then clear that the associated eigenvalues can be written as

$$\frac{\omega_{0n}(\epsilon)}{b_1^{1/2}(\epsilon)} \simeq m\,2\,\pi\left\{\int_0^{2\pi} e^{\frac{1}{2}\epsilon K(2x)}\,dx\right\}^{-1}, \tag{2.40}$$

for some large integer m.

Thus, in this WKBJ approximation, it appears that the eigenvalues are double $\lambda_{2m-1} = \lambda_{2m}$ and that the transition curves coincide — with no unstable region between them. This is not quite true; it can be shown that, for large m, λ_{2m-1} and λ_{2m} are transcendentally close, but not necessarily equal. Thus, the WKBJ approximation (that can distinguish only inverse powers of λ) collapses the whole

unstable domain (with the two transition curves bounding it on each side) into a single curve.

Just to recall, the coefficient $b_1(\epsilon)$ is a function of the normalized specific volume for the equilibrium solution, and is given by

$$b_1 = V_0^{-\gamma-1}(\epsilon), \qquad V_0(\epsilon) = 2\pi \left\{ \int_0^{2\pi} e^{\epsilon K(2x)} dx \right\}^{-1},$$

with $1 < \gamma < 2$ the ratio of specific heats.

Equation (2.40) gives approximations to the frequency $\omega_{0n}(\epsilon)$ valid for arbitrary entropy amplitudes ϵ and vanishing acoustic amplitude a. Since (2.40) holds for small ν (or large $\lambda = \omega_0/b_1^{1/2}$), they will be more accurate for large n, indicating equal spacing between adjacent eigenvalues as $n \to \infty$. For $\epsilon = 0$, the classical acoustic frequencies $\omega_0 = n$ are recovered, which correspond, again, to points along the ω axis where transition curves branch off. From Section 2.8, transition curves having an odd value of n correspond to 2π–periodic solutions $\beta(x)$, while those with even values of n are associated with solutions of period π.

It can be readily seen in (2.40) that, for a fixed value of n, transition curves given by $(\omega_0(\epsilon)/b_1^{1/2}(\epsilon), \epsilon)$ will coalesce towards the axis $\omega = 0$ for increasing values of the entropy amplitude ϵ. This feature will be displayed in more detail by the numerical solution of the eigenvalue problem for arbitrary ϵ undertaken in Section 3.1.

Chapter 3

Numerical Calculations

Formal analytical evidence for the existence of small amplitude, time periodic continuous solutions to the equations of 1D inviscid Gas Dynamics was presented in Chapter 2 using concepts and tools from bifurcation theory. It was shown that there is, in fact, a two-parameter family of time periodic nonlinear acoustic waves bifurcating from equilibrium, the independent parameters being given by an arbitrary entropy wave amplitude ϵ and either the frequency ω that defines the minimal period of these striking hyperbolic waves or their acoustic wave amplitude a (defined in (2.10)). The convergence of our formal asymptotic expansions is an issue that remains open.

The purpose of this chapter is to numerically extend the range of validity of those theoretical results — which are limited to small acoustical amplitudes a. We want to explore the domain of existence in parameter space (ω, ϵ, a) of large amplitude time periodic acoustic waves, as well as their shape for different parameter values. More precisely, if the bifurcation solutions are expressed as power series in the (small) amplitude a (see (2.26)-(2.27)), the objective here is to calculate them for large values of a. Thus, the term "large amplitude" refers in this context only to the dynamic part of the solutions, and there should be no confusion with the fact that the static equilibrium solution, which depends on an arbitrary amplitude ϵ characterizing the nonuniform entropy field, can have itself quite large deviations from its mean value in the expansions of the prior chapter (see Section 2.1).

As was stated earlier, the numerical work here is based on the theoretical analysis of the preceding chapter. Thus, in Section 3.1, we will first solve the eigenvalue problem given by Hill's equation (2.21). We will determine the transition curves in the (ω, ϵ) plane where periodic solutions bifurcate from an equilibrium state corresponding to the plane $a = 0$. This calculation is an extension, for arbitrary entropy amplitudes ϵ, of the perturbative analysis done in Section 2.8 for the case $0 < \epsilon \ll 1$. Next, a brief discussion about possible methods for calculating nonlinear, periodic in time and space solutions to the 1D Gas Dynamic equations will be carried out in Section 3.2. We will review some of the problems and limitations that have appeared in similar studies for free surface waves. We present and describe in detail our own numerical approach in Section 3.3. This approach is based on formulating the equations as a boundary value problem for a nonlinear system of partial differential equations. This algorithm essentially comprises three elements. First, a discretization of the partial differential equations that is time reversible, second order accurate and has

limited artificial dissipation. Second, a shooting method to impose time periodicity. Computational savings can be gained by enforcing the temporal symmetries in the solutions. Third, an adaptation of Keller's pseudo-arclength continuation procedure to follow different bifurcation branches in parameter space. Finally, in Section 3.4, we present numerical computations of nonlinear acoustic waves in different regions of parameter space. To facilitate a physical appreciation of the large sound waves' intensities, their dimensionless amplitudes will also be expressed in the conventional decibel scale employed in technical acoustic measurements.

The issue raised in Chapter 1 concerning waves of greatest amplitude is addressed with particular interest, not only for its obvious significance in the present context of nonlinear acoustics, but also, in more general terms, because of the difficulties associated with the study of wave breaking phenomena. It was mentioned before that the acoustic waves of greatest amplitude would separate regions in parameter space where either dispersion or nonlinear distortion prevail, corresponding to two essentially different types of solutions: continuous, time periodic waves on one side — the main object of this work — and non-periodic waves containing discontinuities on the other side. It will be shown that our method can handle quite effectively the challenge of calculating large amplitude nonlinear acoustic waves up to the limiting state where continuous solutions cease to exist. It should be mentioned that at the breaking point, the continuous solutions display a non-smooth structure (corners) that poses a considerable obstacle to a robust numerical treatment.

The most important result that the numerical calculations consistently show is that the standing hyperbolic waves can have very large amplitudes, with variations in pressure of up to 10% relative to the mean value, p_f. It is also confirmed that continuous waves occur for a certain range of acoustical amplitudes a. At the maximum amplitude a_{max}, it appears that they develop corners in their profiles, just the same as the progressive and standing free surface waves in water referred to in Section 1.6.

3.1 Eigenvalue problem

Let us summarize the main results of the analysis carried out in Section 2.3 as they lay out the foundation for the numerical calculation of large amplitude acoustic waves.

The equilibrium solution to the equations of motion (2.1)–(2.2) is given by

$$V = V_f(x) = V_0\, e^{\epsilon K(x)}, \qquad u \equiv 0 \qquad \textit{and} \qquad p \equiv \textit{constant} = p_f = \frac{1}{\gamma}\, V_0^{-\gamma}, \quad (3.1)$$

with a normalized amplitude

$$V_0(\epsilon) = 2\pi \left\{ \int_0^{2\pi} e^{\epsilon K(x)} dx \right\}^{-1}$$

that depends on the arbitrary entropy amplitude ϵ.

The nonlinear acoustic waves bifurcating from equilibrium have the form

$$V(x,t) = V_f(x) + \varphi_x(x,t), \tag{3.2}$$

$$u(x,t) = \qquad \varphi_t(x,t), \tag{3.3}$$

where $\varphi(x,t)$ satisfies the nonlinear wave equation (2.7). The potential function φ and the frequency ω that characterizes periodic acoustic waves were expressed as series in powers of a suitable defined amplitude a (see (2.8)-(2.10)). Then, it was shown that the first order solution φ_1 could be obtained from the eigenvalue problem (2.11), where the eigenvalues depend on the arbitrary amplitude ϵ. Taking into account the symmetry with respect to time exhibited by the original equations of motion, the first order solution was given by $\varphi_1(x,\tau) = cos(\tau)\,\phi_1(x)$, with $\tau = \omega t$, where $\phi_1(x)$ satisfies equation (2.16). With the change of variables $\phi_1(x) = exp\{1/2\epsilon K(x)\}\beta(x)$ we finally obtained Hill's equation (2.21). Therefore, the eigenvalue problem corresponding to the first order solution for the bifurcation potential series is given by (2.21) and reproduced here for convenience:

$$\beta''(x) + \left\{ \frac{\omega_0^2}{b_1}\, e^{\epsilon K(x)} + \frac{1}{2}\,\epsilon\, K''(x) - \frac{1}{4}\,\epsilon^2\,[K'(x)]^2 \right\} \beta(x) = 0, \tag{3.4}$$

where $b_1(\epsilon) = V_0(\epsilon)^{-\gamma-1}$ and β is periodic of period 2π, normalized by

$$\int_0^{2\pi} {\phi_1}^2(x)\, dx = \int_0^{2\pi} e^{\epsilon K(x)}\, \beta^2(x)\, dx = 4\pi.$$

The mean zero property for ϕ_1 is guaranteed by the form of equation (2.16) whenever ω_0 does not vanish.

Thus, for a given entropy field $S(x) = \epsilon K(x)$, we want to find the eigenvalues $\omega_0^2(\epsilon)/b_1 > 0$ associated with the periodic eigenfunctions $\beta(x)$. From these follow the first order approximation to the periodic acoustic waves (3.2)-(3.3).

According to the discussion in Section 2.3 concerning Floquet's theory for Hill's equation (3.4), there are four periodic solutions $\beta(x)$, either even or odd in x and having periods π or 2π — since π is the minimal period of the coefficients in (3.4) — while the associated eigenvalues define so-called transition curves in parameter space $(\omega_0(\epsilon), \epsilon)$.

To find periodic solutions to (3.4), we rewrite Hill's equation as a first order system:

$$\begin{cases} \eta_1'(x) = \eta_2(x) \\ \eta_2'(x) = \left\{ -\frac{\omega_0^2}{b_1}\, e^{\epsilon K(x)} \;-\; \frac{1}{2}\,\epsilon\, K''(x) \;+\; \frac{1}{4}\,\epsilon^2\,[K'(x)]^2 \right\} \eta_1(x) \end{cases} \tag{3.5}$$

By Floquet's theory, periodic solutions to this system having period π correspond to the characteristic numbers $\nu_1 = \nu_2 = 1$, while those of period 2π are associated with $\nu_1 = \nu_2 = -1$. The characteristic numbers are obtained from the characteristic equation

$$\nu^2 \;-\; (\eta_{11} \;+\; \eta_{22})\;\nu \;+\; 1 \;=\; 0.$$

Here $\eta_{11} = \eta_1(\pi)$ for the solution of (3.5) with initial conditions $\eta_1(0) = 1$ and $\eta_2(0) = 0$. Similarly $\eta_{22} = \eta_2(\pi)$, starting with $\eta_1(0) = 0$ and $\eta_2(0) = 1$.

Observe that $b = \eta_{11} + \eta_{22}$ is a function of the parameters in (3.5). Specifically, $b = b(\lambda)$, where $\lambda = \omega_0^2(\epsilon)/b_1$, as ϵ will be considered as known and given for each calculation. Furthermore: $b = 2$ if and only if $\nu_1 = \nu_2 = 1$ (period π solution) and $b = -2$ if and only if $\nu_1 = \nu_2 = -1$ (period 2π solution).

For all the numerical calculations, we took $K(x) = 2\,cos(2x)$ for the entropy wave and $\gamma = 1.4$ for the ratio of specific heats (air). To solve (3.4), we integrated (3.5) with a fourth order Runge-Kutta method for both sets of initial conditions, thus obtaining η_{11} and η_{22}. Then we used Newton's method to solve the equations $b(\lambda) \mp 2 = 0$, for π or 2π–periodic solutions $\beta(x)$, respectively . The eigenfunctions themselves then followed easily as linear combinations of the two computed solutions, with coefficients given by the eigenvectors of the 2×2 matrix whose eigenvalues are the ν's. In this fashion, we obtained, for a given ϵ, a pair $(\omega_0(\epsilon), \epsilon)$ defining the transition curves as ϵ varies, together with the eigenfunctions $\phi_1(x)$ and $\phi_1'(x)$ with periods π or 2π and $\phi_1(x)$ even or odd. The stability diagram displaying transition curves is shown in Figure 4, which represents, of course, an extension of the chart in Figure 3 obtained for small ϵ by perturbation techniques. Notice that for large values of the entropy amplitude ϵ, the transition curves tend to coalesce towards the axis $\omega = 0$. This property was predicted by the WKB analysis of Section 2.9 and is displayed in full extent by the numerical solution of (3.5).

The eigenvalue problem provides the structure for the first order approximation to the potential $\varphi(x, \tau)$ and the combination of parameters $(\omega_0(\epsilon), \epsilon)$ associated with periodic solutions. But to calculate finite amplitude time periodic acoustic waves in the form (3.1)–(3.2) we will also need, for a fixed ϵ, an approximation to the frequency $\omega(a)$ for a small but nonzero value of the amplitude a that will produce solutions with non-trivial acoustic content. In a geometric way, a proper approximation of $\omega(a)$ for

$0 < a \ll 1$ will move us up and away from the "Floquet bottom" ($a = 0$) in (ω, ϵ, a) parameter space that corresponds to the equilibrium solution. At the same time it will keep the first order approximate solution inside the domain of attraction of the exact solution for that value of a.

A good approximation to $\omega(a)$ is given by $\omega(a) = \omega_0 + a^2\,\omega_2 + O(a^4)$, where the coefficient ω_2 was found in Section 2.5 as

$$\omega_2 \;=\; \frac{1}{4\pi\omega_0}\left\{ -\,b_2 \int_0^{2\pi} [\phi_1'(x)]^2\,\psi_2'(x)\,e^{-2\epsilon K(x)}\,dx \;+\; \frac{3}{8}\,b_3 \int_0^{2\pi} [\phi_1'(x)]^4\,e^{-3\epsilon K(x)}\,dx \right\}. \tag{3.6}$$

The coefficients b_2 and b_3, defined in Section 2.1, are given by $b_2 = (\gamma+1)/2\;V_0^{-\gamma-2}$ and $b_3 = (\gamma+2)(\gamma+1)/6\;V_0^{-\gamma-3}$. To calculate ω_2, we first have to determine $\psi_2(x)$, which is the solution of the inhomogeneous boundary value problem (2.24):

$$\left[b_1\,e^{-\epsilon K(x)}\,\psi_2'(x)\right]' \;=\; \frac{b_2}{2}\left\{\,e^{-2\epsilon K(x)}\,[\phi_1'(x)]^2\,\right\}', \tag{3.7}$$

where ψ_2 is periodic of period 2π and mean zero. In fact, only $\psi_2'(x)$ is needed in (3.6), and it is readily obtained as

$$\psi_2'(x) \;=\; \frac{b_2}{2\,b_1}\,e^{-\epsilon K(x)}\,(\phi_1'(x))^2 \;-\; \frac{C}{b_1}\,e^{\epsilon K(x)}.$$

The constant of integration C is determined by the fact that $\psi_2'(x)$ is necessarily of mean zero.

In sum, to obtain a *first order approximation* to the periodic acoustic waves for arbitrary entropy amplitudes ϵ and a small but nonzero acoustic amplitude a, we perform the following steps:

A) Solve the eigenvalue problem (3.4), using the formulation given by Floquet's theory. In so doing, we obtain the zeroth order term in the frequency series $\omega_0(\epsilon)$ and the normalized eigenfunctions $\phi_1(x)$, $\phi_1'(x)$ of period π or 2π.

B) Solve the boundary value problem (3.7), obtaining the periodic function $\psi_2(x)$. Then we calculate the frequency perturbation ω_2 using (3.6).

C) For a small amplitude a, we describe approximately the time periodic acoustic waves by

$$V(x,\tau) = V_f(x) + a\,cos(\tau)\,\phi_1'(x) + O(a^2), \tag{3.8}$$

$$u(x,\tau) = -a\,\omega(a)\,sin(\tau)\,\phi_1(x) + O(a^2), \tag{3.9}$$

where

$$\omega(a) = \omega_0 + a^2\,\omega_2 + O(a^4). \tag{3.10}$$

These expressions then provide accurate initial values for the iterative algorithm developed in Section 3.3 to calculate nonlinear periodic acoustic waves. Notice that, in fact, *the initial conditions for u given by (3.9) are exact* since u is odd in time —thus $u(x,0) \equiv 0$.

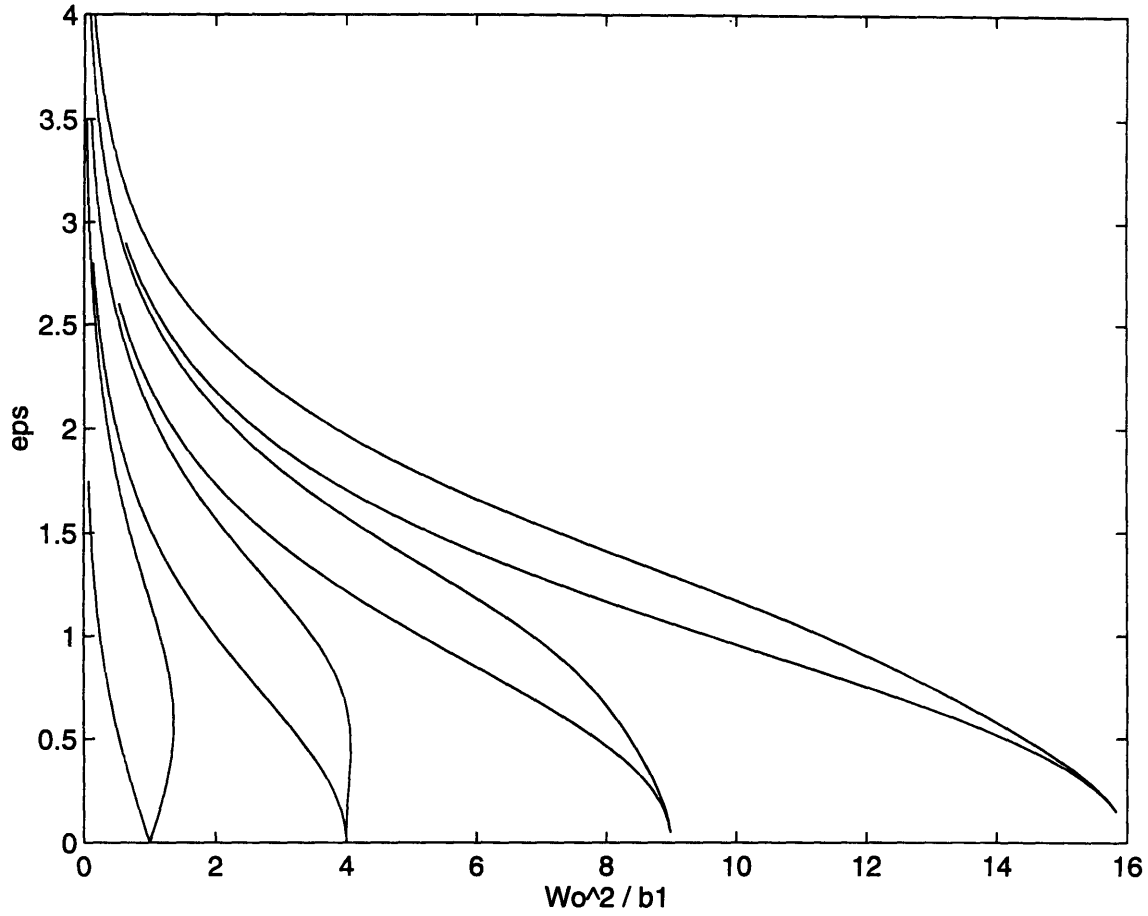

Figure 4: Stability diagram for arbitrary entropy amplitudes ϵ ; ω_0 is the frequency of periodic acoustic waves, and the coefficient $b_1(\epsilon)$ is defined in (3.4). The first four branches are denoted (TC 1) to (TC 4), starting from the left.

3.2 Numerical difficulties

Before turning our attention to the calculation of large amplitude waves, let us comment briefly about possible strategies and review previous attempts to solve similar problems in other fields.

If our objective were to compute a (asymptotically stable) time periodic solution for a (forced) dissipative system, then we could use the following approach: first, obtain initial conditions sufficiently close[22] to the ones corresponding to the (unknown) desired solution. Then integrate the equations in time with an initial value problem solver. In this case the time evolution would eventually converge the solution to the desired one. Even though this approach may not be very efficient, it would (at least in principle) work for a situation as outlined above. In our case, this method would be horrendously "expensive" (computationally). This is not, however, the only (not even the main) reason for not using it, as we explain next.

Our system of equations is not dissipative, or at least not exactly so. That is: when shocks occur, then there is dissipation (concentrated at the shocks). But for shock-less solutions, the equations behave in a conservative (in fact Hamiltonian) way. Thus, for example, the periodic solutions we are seeking to compute have a free (amplitude) continuous parameter in them. This contrasts sharply with the typical situation in dissipative systems, where the amplitude is unique[23]. It is, in fact, more along the lines of the expected behavior for dispersive, non-dissipative systems. Furthermore, in conservative systems, solutions like the ones we are looking for are, at best, neutrally stable —and this is, roughly, the situation we expect in our case[24].

If we were to attempt to implement the simple idea outlined above in our case, using (3.8)–(3.10) to produce the approximate initial conditions, then the (small) initial value errors would (typically) trigger small shocks in the solution. These shocks would produce dissipation (increase the entropy) and, we expect, eventually decay and become negligible. The solution would then converge (as $t \to \infty$) to one without shocks. But this limit solution would certainly not correspond to the one we used to produce the initial data —albeit it might be "close". In fact, not even the entropy would be the same we started with (as shocks produce entropy). Thus, this method would give us almost no control over the final product. Worse still, we have no guarantee that the final solution the method converges to will be one of the special type we are looking for! In fact, for Hamiltonian systems of more than two degrees of freedom, the set of periodic solutions is a very small subset of the total set of solutions. Here, within the set of solutions without shocks, the time evolution is

[22]Namely: within the basin of attraction of the desired solution.

[23]Achieved at the balance point between dissipation and forcing.

[24]This is a tricky issue, given the situation described earlier in this paragraph. We will consider it again in Chapter 4.

that of an infinite dimensional Hamiltonian system. This set contains the stationary periodic waves, but it may very well contain also such things as multiply periodic waves and other more complicated objects whose *complete* time evolution[25] is in the set. Any of these could be the final product of the approach above. We will return to some of these issues in Chapter 4.

Therefore, it seems clear that an initial value problem type of approach does not calculate time periodic waves in an intrinsic way, but as the final result of a decaying process in which no control can be exerted. In addition, for the reasons pointed out above, the probability that such a method may pick up a truly periodic wave, seems very low. Nevertheless, this approach can be profitably used to analyze the *stability* of the time periodic nonlinear acoustic waves. This issue will be also addressed in Chapter 4.

Another common method for calculating large amplitude waves is based on a high-order perturbation computation. The basic idea is to extend the domain of validity of a power series solution by summing up[26] small amplitude expansions carried to a very high order. This technique was applied for the calculation of steep gravity waves, one of the problems that we referred to in Chapter 1 as having some strong physical and mathematical similarities with our present case.

For steady, progressive free-surface waves, Schwartz (1974) performed an analytic continuation of the Stokes infinitesimal-wave expansion by using Pade approximants, complemented with some graphical procedures to determine the type and location of the singularities in the ("summed up") series solution. Further work along similar lines was done by Longuet-Higgins (1975) and Cokelet (1977) employing different parameters for the series expansions.

It is not clear whether these techniques can be successfully applied to our problem of large amplitude acoustic waves. The reason, as pointed out in Chapter 1 in connection with the problem of convergence of small amplitude asymptotic series solutions, is that we have stationary, rather than progressive, waves. This feature would make it very difficult to find appropriate recursive relations for the series coefficients that would allow their efficient computation to high orders. Furthermore, recent work by Drennan et al. (1992) presented solid evidence that computer extensions of small-amplitude expansions through Pade approximants may produce divergent results for large amplitudes. Since little is known about the convergence properties of Pade approximants of arbitrary series, these authors warned about using such an "empirical" technique that can lead to apparently convergent but incorrect solutions. Rather than attributing these non-convergent results to roundoff error, they stressed the increas-

[25]Any solution starting from smooth initial values is in this set, for a while —till shocks form. The interesting solutions are those for which shocks never form, such as the stationary periodic waves we are studying here.

[26]Specifically: re-casting the series solution into a form with, presumably, better convergence properties. For example, a rational function (Pade) approximation.

ing relative importance of high order harmonics as the wave amplitude increases, a fact that was not properly taken care of in those methods mentioned above.

Hence, because of the algebraic complexities involved and the dubious basis of ad hoc methods needed for accelerating the convergence at large amplitudes, we are not going to pursue this approach in our problem. Instead, in the next section we will take a more fundamental view to design a numerical method that does not relay on a small-amplitude Fourier series solution.

Needless to say, other methods (besides small-wave expansions) have been proposed and used to describe gravity waves of constant form. Notably among them the use of a nonlinear integral equation for the slope of the waves due to Nekrasov (cf. Milne-Thomson (1968)). But these depend on very specific peculiarities of the gravity waves problem. Our limited goal here was to refer to those formulations in free surface waves that, in principle, could be applied to our problem of standing hyperbolic waves, without attempting any survey of the vast literature on that subject.

3.3 A nonlinear boundary-value problem

We develop here an algorithm for the calculation of finite amplitude time periodic acoustic waves that flows almost "naturally" from the original equations of motion and the bifurcation theory formulated in Chapter 2.

The idea is to transform the problem into a nonlinear two-point boundary-value problem, where the governing equations (formally given by a nonlinear system of ordinary differential equations) result from a convenient space discretization of the original partial differential equations of motion. In a schematic way, we propose to solve the original boundary-value problem composed by equations (2.1)–(2.2) along with periodic boundary conditions both in the Lagrangian coordinate x and the time t, by an initial-value problem of the form

$$\dot{\mathbf{U}}(t) = \mathbf{F}(t, \mathbf{U}), \tag{3.11}$$

$$\mathbf{U}(0) = \mathbf{s},$$

where $\mathbf{s}$ is an approximation for the initial values of the exact periodic solution. Then we impose the periodicity condition[27] at a time equal to the (unknown) period T

$$\mathbf{f}(\mathbf{s}) = \mathbf{U}(T) - \mathbf{s} \equiv 0. \tag{3.12}$$

[27] Periodicity in x will be built into the system (3.11), as explained later.

These equations, where s and T are the unknowns, will be solved by an appropriate method.

There are, of course, several steps in this general plan that require careful examination, and we do so below. For a complete presentation of numerical methods for nonlinear boundary-value problems, we refer to Keller (1992) and Kubicek & Hlavacek (1983).

Once the numerical formulation is framed as a boundary-value problem, the first decision we have to make concerns the choice of a suitable method for our particular case. Generally speaking, there are basically two types of methods for the solution of boundary-value problems: shooting methods, based on the numerical integration of initial-value problems, and relaxation methods, which employ finite difference equations in a grid covering the whole domain. The former can handle highly oscillatory solutions, while the later are preferred for very smooth functions. Based on the theoretical analyses of Chapters 1 and 2, we know that nonlinear acoustic waves may present wild fluctuations, and for large amplitudes close to the critical maximum one, they can develop sharp peaks where the field variables have discontinuous first derivatives. Therefore, we choose to employ the shooting method with the hope that it can calculate solutions up to and including waves of greatest amplitude.

The truth of the matter is that, in fact, we will get a little bit more: a really good numerical method for our problem should be able to go beyond the limiting maximum amplitude, showing clearly a numerical change in the solutions that would correspond to the actual physical change that takes place when the solutions move from the dispersion-dominated region (where time periodic acoustic waves exist) to the region in parameter space where hyperbolic distortion prevails (and shock waves appear). This qualitative change in the nature of the solutions should be accompanied by, for example, the appearance of (fast) oscillations in the field variables, thus indicating a breakdown or threshold as we move in parameter space towards larger amplitudes. Such a numerical scheme is robust in the sense that it can find a solution in either region — a "converged" solution — although, of course, the solutions in the "dispersion-deficient" region, with fast oscillations in broad areas, will not correspond to solutions of the original problem. In particular, and this is the useful property, the scheme will not "break down" as the critical amplitude is reached.

Let us clarify the preceding paragraph a bit: equation (3.11) assumes a given space discretization, at a given level of resolution (in space). The numerical scheme would then produce a solution for this system (the "converged" solution above). As the space resolution is increased, we expect this solution to converge to a solution of the original P.D.E. problem. This should occur in the dispersion dominated region. Elsewhere (parameter values for which no solution exist for the P.D.E. problem) convergence cannot occur, and this would manifest itself by some "defect" in the computed solutions. Specifically, short wave oscillations (wave-length coupled to the space mesh size) whose amplitude does not vanish as the space mesh does would do

the trick — below we explain why this is what our scheme will do.

There still remains a point to be clarified in our argument. Namely: why do we expect the discretized equations to have "solutions" beyond the maximum amplitude allowed by the full P.D.E. system? Basically this is because the "maximum amplitude" phenomena amounts to an abrupt termination of a bifurcation branch; not merely a "turning back" of the branch that a re-parametrization would fix, but an *end* to the bifurcation curve itself[28]. This is, fundamentally, an infinite dimensional effect. No finite dimensional O.D.E. discretization, as (3.11), can exhibit it. There the bifurcation branches would continue without any abrupt ends. The effect appears only in the limit as the space grid vanishes. Then the numerical solutions beyond the threshold exhibit grid level oscillations (with amplitudes depending only on how far past the maximum amplitude they are; not the space discretization mesh size) and thus have no continuum limit.

The ability of the numerical formulation to go beyond the breaking point without suffering from non-convergence problems, would allow a consistent determination of the region in parameter space (ω, ϵ, a) where periodic acoustic waves exist, providing the answer for those issues raised in Section 1.6. Incidentally, notice that those methods based on some sort of analytic continuation of small-wave expansions described in Section 3.2 cannot satisfy this threshold requirement, precisely because of the convergence problems associated with a (finite) Fourier representation of functions having discontinuous derivatives.

The shooting method requires that the initial and final values of the integration interval be well defined. However, in our problem the numerical integration marching forward in time will comprise exactly one period of the nonlinear acoustic waves, which, as we know, is a function of the wave amplitude and a priori unknown. Thus, we introduce again the strained variable $\tau = \omega t$, with ω the wave frequency. In this way the numerical domain in (x, τ) coordinates becomes the square $(0, 2\pi) \times (0, 2\pi)$. The parameter ω (equivalent to the period T in (3.12)) has to be determined along with the solution and occurs now explicitly in the equation. As stated before, in this coordinate frame the acoustic waves will be 2π–periodic in both x and τ, with a period $2\pi/\omega$ in time t.

Let us consider now the discretization of the original partial differential equations of motion (2.1)-(2.2). To every coordinate $x_j = j\,\Delta x$, $j = 0, 1, 2, ..., J$, with $\Delta x = 2\pi/J$, there will be a corresponding vector field $\mathbf{U}(x_j, \tau) = \mathbf{U}_j(\tau) = [V_j(\tau), u_j(\tau)]$. (All vectors are column vectors, and for simplicity we don't indicate the transpose when displaying vector components.) Periodicity in x is imposed by requiring $\mathbf{U}_J = \mathbf{U}_0$, so we need to consider the index j only in the range from 0 to $(J-1)$. Thus, after a discretization of the flux terms, we will end up with a system of coupled nonlinear ordinary differential equations of the form (3.11) — as in the so-called method of lines.

[28]This can be seen easily in the "simple" example of the exact Pego solutions for the Majda-Rosales asymptotic resonant equations in Section 1.5.

In this rather simple conceptual approach, however, care must be taken regarding the following aspects.

First, it is important to keep in mind that (despite notation) in (3.11) we are in fact integrating a nonlinear system of hyperbolic partial differential equations. This means that we cannot simply pick up any good ODE solver and apply it in a straightforward way to the solution of (3.11)[29]. Were we interested in the calculation of solutions with shocks, we could rely in one of the well tested methods for this purpose that are available (see Leveque (1990)). These methods are, however, all dissipative to a larger or lesser extent — a deadly feature as far as our task is concerned[30]. Given the nature of our problem, we need a method that preserves a crucial feature of the original equations that allows the existence of periodic solutions. Namely: the method must be *nondissipative.* Another important feature we must preserve is the *time symmetry.*

Second, since one of the main goals of the numerical work is to calculate large amplitude waves that can display steep gradients and even sharp corners, there is no point in using high order schemes that assume the existence of smooth solutions with several continuous derivatives.

Third, the numerical scheme should be consistent and stable to guarantee convergence to the solution (whenever one exists). Consistency is trivial to check. For stability we will limit ourselves to a simple linearized analysis.

To fulfill these conditions, we decided to use a staggered "leapfrog" finite difference scheme, which besides having second order accuracy, produces no artificial dissipation (at least for linear systems). Equally important, it also guarantees time symmetric properties.

Thus, the discrete system corresponding to the equations of motion (2.1)-(2.2) is

$$V_j^{n+1} = V_j^{n-1} + \delta \left(u_{j+1}^n - u_{j-1}^n \right), \tag{3.13}$$

$$u_j^{n+1} = u_j^{n-1} - \delta \left(p_{j+1}^n - p_{j-1}^n \right), \tag{3.14}$$

where $\delta = \Delta\tau/(\omega\,\Delta x)$, $\Delta\tau = 2\pi/N$, $\Delta x = 2\pi/J$ and standard notation has been used for discrete variables: $u_j^n = u(x_j, \tau_n)$, with $x_j = j\,\Delta x$, $j = 0, 1, 2, ..., J$, and $\tau_n = n\,\Delta\tau$, $n = 0, 1, 2, ..., N$. In (3.14), the pressure terms are given by $p_j^n = p(x_j, \tau_n) = 1/\gamma\ exp(\gamma S_j)\,(V_j^n)^{-\gamma}$, with the entropy field defined as in Chapter 2 by $S_j = S(x_j) = \epsilon\,K(x_j)$. Notice that the equilibrium solution (3.1) is in fact an exact

[29]So far we have been speaking as if the solution of the "reduced" O.D.E. system (3.11) could be done exactly. In fact, we will have to discretize the system in time also. Then, for efficiency reasons, we will use a time step of roughly the same order as the space mesh size. This means that we cannot neglect the time discretization effects introduced by the O.D.E. solver.

[30]No periodic solutions can occur in this case.

solution of this discretized system — a good indication of the appropriateness of the discretization.

Next we apply a von Neumann stability analysis to the system (3.13)–(3.14) (see Press et al. (1992)). First we linearize the discrete equations of motion around the equilibrium solution. Thus, taking $V(x,\tau) = V_f(x) + \hat{V}(x,\tau)$, $u(x,\tau) = \hat{u}(x,\tau)$ and retaining only linear terms, we obtain the system

$$\hat{V}_j^{n+1} = \hat{V}_j^{n-1} + \delta\,(\hat{u}_{j+1}^n - \hat{u}_{j-1}^n), \tag{3.15}$$

$$\hat{u}_j^{n+1} = \hat{u}_j^{n-1} + \delta\,(C_{j+1}^2\,\hat{V}_{j+1}^n - C_{j-1}^2\hat{V}_{j-1}^n), \tag{3.16}$$

where $C = (\gamma p_f/V_f)^{1/2}$ is the Lagrangian sound speed for the equilibrium state. Then we "freeze" the variable coefficients in these equations (i.e.: take $C_j \equiv C = constant$) and express the eigenmodes of the difference equations as

$$\begin{bmatrix} \hat{V}_j^n \\ \\ \hat{u}_j^n \end{bmatrix} = \xi^n(k)\; e^{ikj\Delta x} \begin{bmatrix} \hat{V}^0 \\ \\ \hat{u}^0 \end{bmatrix}, \tag{3.17}$$

where $\xi(k)$ is the amplification factor that depends on the real wavenumber k. Substituting (3.17) in (3.15)–(3.16) we obtain the four roots

$$\xi(k) = \pm\, i\, C\, \delta\, sin(k\Delta x) \;\pm\; \Big\{\, 1 \;-\; [\, C\, \delta\, sin(k\Delta x)\,]^2 \,\Big\}^{1/2}. \tag{3.18}$$

The stability condition $|\xi|^2 \leq 1$ is then equivalent to the Courant-Friedrichs-Lewy criterion (or CFL condition, for short) $C\,\delta \leq 1$, that is

$$\left|\frac{\Delta\tau\, C}{\omega\, \Delta x}\right| \leq 1. \tag{3.19}$$

The CFL condition (3.19), is always a necessary condition for stability and guarantees that the domain of dependence of the numerical scheme includes the domain of dependence of the original partial differential equations. This ensures that there is no missing information for the correct propagation of waves (see Leveque (1990)).

For a stable scheme, i.e., for any $\Delta\tau \leq \omega\Delta x/C$, we can see in (3.18) that $|\xi|^2 \equiv 1$, confirming that, at least for the linearized equations, no numerical viscosity is introduced. We stress that our prior argument shows that the CFL condition (3.19) is sufficient for stability only in the case of the linearized equations (3.15)–(3.16) with frozen coefficients. In practice we found that stability for the nonlinear system (3.13)–(3.14) required a more restrictive $\Delta\tau$, smaller the larger the amplitudes in a and ϵ.

It should be noted here that the scheme (3.13)–(3.14) would be disastrous for the computation of solutions with shocks, precisely because it is purely dispersive. Instead of dissipating energy in the zone where a shock would form and large gradients occur, this scheme radiates that energy away from the area. Thus, when shocks "try" to form in the Euler equations, this scheme generates grid scale oscillations that radiate away from the area and whose amplitude is related to the "would-be" shock strength. This behavior is in fact, in some sense, the one responsible for the behavior of our overall scheme "beyond" the maximum amplitude allowed for the standing periodic waves (see the beginning of this section) as we roughly explain now.

Imagine that we are "moving" along a solution branch towards increasing amplitudes, computing with the scheme each solution. This calculation, as we explain below, involves producing a "first guess" for the initial conditions and ω (using the prior calculated solution) and then doing a Newton iteration on equation (3.12) to calculate the final values. This involves integrating the equations of motion using (3.13) and (3.14). However, once we are "past" the maximum allowed amplitude, there is no continuous periodic solution of the Euler equations anymore. Thus, when we integrate the equations numerically in the solution process, shocks will try to form. From the prior paragraph we see that, instead, we will get oscillations. The amplitude of these will be connected to how strong the shocks should have been, which in turn should be (roughly) related to how much past the threshold we have gone. Our numerical calculations confirm this (rather intuitive) argument.

Starting with appropriate initial values, we will thus integrate the system (3.13)–(3.14) up to $\tau = 2\pi$, at which point time periodicity will have to be imposed. Periodicity in the Lagrangian coordinate x will be automatically satisfied by equating $V_J^n = V_0^n$ and $u_J^n = u_0^n$ at every time τ_n. To start the integration, a second order Runge-Kutta method coupled with center differences for the fluxes will be used for the first iteration.

At the initial time $\tau = 0$, there are $2J$ values to be specified, J quantities corresponding to either the specific volume and the flow velocity, i.e., V_j and u_j for $j = 0, 1, 2, ..., J-1$. These initial values for problem (3.11) can then be written as

$$V_j(0, \omega, \mathbf{s}) = V_j^0 = s_{V_j} \qquad j = 0, 1, 2, ..., J-1 \tag{3.20}$$

and

$$u_j(0, \omega, \mathbf{s}) = u_j^0 = s_{u_j} \qquad j = 0, 1, 2, ..., J-1, \tag{3.21}$$

where a functional dependence upon time τ, frequency ω and free initial vector $\mathbf{s} = [\mathbf{s}_V, \mathbf{s}_u]$ has been assumed for the basic field variables $\mathbf{U}_j = [V_j(\tau, \omega, \mathbf{s}), u_j(\tau, \omega, \mathbf{s})]$. Time periodicity is then imposed through equation (3.12), which in scalar notation reads

$$f_{V_j}(\omega, \mathbf{s}) = V_j(2\pi, \omega, \mathbf{s}) - s_{V_j} \equiv 0 \qquad for \qquad j = 0, 1, 2, ..., J-1 \tag{3.22}$$

and

$$f_{u_j}(\omega, \mathbf{s}) = u_j(2\pi, \omega, \mathbf{s}) - s_{u_j} \equiv 0 \qquad for \qquad j = 0, 1, 2, ..., J-1. \tag{3.23}$$

To zero the discrepancy vector $\mathbf{f} = [\mathbf{f}_{V_j}, \mathbf{f}_{u_j}]$, we use Newton's method, which solves the system

$$\mathbf{J} \,.\, \Delta\mathbf{s} = -\mathbf{f}, \tag{3.24}$$

giving the improved vector of initial conditions as

$$\mathbf{s}^{new} = \mathbf{s}^{old} + \Delta\mathbf{s}. \tag{3.25}$$

In (3.24), $\mathbf{J}$ is the Jacobian matrix $\mathbf{J} = \partial\mathbf{f}/\partial\mathbf{s}$ of dimension $2J \times 2J$. It will be calculated by centered finite differences to assure the symmetric properties of the original equations, an operation that would demand $2 \times 2J$ integrations of (3.11) in the form of (3.13)–(3.14), in addition to one integration that provides the residuum $\mathbf{f}$. Equation (3.24) will be solved by LU decomposition with partial pivoting. A discussion concerning convergence properties of Newton's method can be found in Keller (1992). In the same reference, an error analysis of the noise in $\mathbf{s}$ introduced by the integration of the initial-value problems is developed, indicating a lower bound in the achievable accuracy of this "noisy" Newton's method that cannot be further improved unless the time integration solver is refined.

Another very important point that has to be addressed is related to the formulation of a continuation or embedding method to calculate solutions along different branches in parameter space (see Keller (1992)). In our problem, there are three parameters given by the entropy wave amplitude ϵ, the fundamental frequency ω and the normalized acoustic wave amplitude a. According to the analysis of Section 2.2, these parameters are related to each other in such a way that only two of them are truly independent: the independent pairs are (ω, ϵ) and (a, ϵ), with the entropy wave amplitude ϵ always present since it represents the external forcing to the system. The continuation problem can now be put in the following terms: suppose that, for a given ϵ, we have a periodic solution $\mathbf{U}(\tau, \omega)$ (or, if we prefer, $\mathbf{U}(\tau, a)$). Then, the task is to use that solution as an initial guess to calculate other solutions in (ω, a) parameter space, the so-called continuation branches, in such a way that we always keep those guesses inside the domain of attraction for Newton's method.

The most natural way to compute solution branches is by using a parameter appearing in the equations as the parameter that defines solution arcs. This regular

continuation method can be formulated as follows. Consider the initial-value problem (3.11) in the form

$$\dot{\mathbf{U}} = \mathbf{F}(\tau, \mathbf{U}, \omega), \tag{3.26}$$

$$\mathbf{U}(0) = \mathbf{s},$$

with the boundary condition enforcing time periodicity[31]

$$\mathbf{f}(\mathbf{s}, \omega) = \mathbf{U}(2\pi, \mathbf{s}, \omega) - \mathbf{s} \equiv 0. \tag{3.27}$$

If we now think of ω as the continuation parameter, such that $\mathbf{s} = \mathbf{s}(\omega)$, from (3.27) we get

$$\left[\frac{\partial \mathbf{U}(2\pi, \mathbf{s}, \omega)}{\partial \mathbf{s}} - \mathbf{I} \right] \frac{d\mathbf{s}}{d\omega} + \frac{\partial \mathbf{U}(2\pi, \mathbf{s}, \omega)}{\partial \omega} = 0. \tag{3.28}$$

Notice that in (3.28) the matrix $\partial \mathbf{U}(2\pi, \mathbf{s}, \omega)/\partial \mathbf{s}$ is available from the calculation of the Jacobian matrix $\partial \mathbf{f}/\partial \mathbf{s}$ needed in Newton's method for the solution of (3.26)–(3.27). To obtain $\partial \mathbf{U}(2\pi, \mathbf{s}, \omega)/\partial \omega$ in (3.28), we define $\mathbf{z} = \partial \mathbf{U}(\tau, \mathbf{s}, \omega)/\partial \omega$ and solve the variational problem associated with (3.26)–(3.27):

$$\dot{\mathbf{z}} = \frac{\partial \mathbf{F}}{\partial \omega} + \frac{\partial \mathbf{F}}{\partial \mathbf{U}} \mathbf{z}, \tag{3.29}$$

$$\mathbf{z}(0) = \mathbf{0}. \tag{3.30}$$

Thus, whence a periodic solution $\mathbf{s}(\omega)$ of (3.26)–(3.27) is found, a good initial guess along the continuation branch is given by

$$\mathbf{s}(\omega + \Delta\omega) = \mathbf{s}(\omega) + \frac{d\mathbf{s}}{d\omega} \Delta\omega + O(\Delta\omega^2), \tag{3.31}$$

at the additional computational cost of solving the initial-value problem (3.29)–(3.30), almost negligible when compared with the effort required to calculate $\partial \mathbf{f}/\partial \mathbf{s}$ for Newton's method.

Let us go back, for a moment, to the issue of oscillations in the scheme when past the maximum amplitude. As we pointed out earlier, these are related to the inability of a dispersive scheme to deal with shocks. We also pointed out that the amplitude of the generated oscillations would be roughly related to how far the solution is "past maximum". This would make them hard to be distinguished initially — a

[31]Notice that, even though ϵ is a parameter in the equations, it plays no role in the bifurcation analysis. Thus we do not display it here and treat it as a fixed constant.

bad feature for our purposes. On the other hand, we are actually not solving an initial value problem here, where the solution starts smooth and then develops the oscillations. Because of the time periodicity, we should expect the "initial conditions" themselves (i.e.: $\mathbf{s}$) to develop oscillations! Now, typically $\Delta\omega$ will be small. Thus (3.31) shows that the oscillations will in fact appear in an amplified manner (relative to the field variables $\mathbf{U}$) in the quantity $d\mathbf{s}/d\omega$ (or, equivalently $d\mathbf{r}/d\theta$ in (3.35)) by a factor of roughly $1/\Delta\omega$ ($1/\Delta\theta$, respectively). This quantity is thus the "best one" to watch for oscillations indicating the threshold. Furthermore: the oscillations will, in fact, occur everywhere (global). Roughly this follows because the oscillations (in the scheme (3.13)–(3.14)) spread from the point of formation of a "would-be-shock" in an initial value problem. But here, again because of the periodicity, the amount of time to spread is unbounded!

The above procedure can only deal with regular points in parameter space, where the Jacobian matrix is nonsingular. When the Jacobian matrix does become singular, we are in the presence of singular points that can be classified as bifurcation points or turning points. In our problem, the parameter space is comprised, for a fixed ϵ, by the acoustic amplitude a and frequency ω. Thus, bifurcation points will be those points where several solution branches $a = a(\omega)$ intersect, while at turning points a branch $a = a(\omega)$ will become multivalued (curve turns back — or forward — relative to the ω axis).

Our numerical goal is to calculate large amplitude periodic acoustic waves, starting from small amplitude waves and moving upwards in (ω, a) parameter space for increasing values of the acoustic amplitude a. Hence, we are not interested in bifurcation points per se, nor in the exploration of the bifurcating branches arising from them[32]. However, we cannot rule out the possibility of turning points in (ω, a) space, whose existence will prevent the use of a regular continuation procedure that can only work for monotonic branches $a = a(\omega)$ or $\omega = \omega(a)$. Therefore, we need another kind of parametrization of the solution arcs that, in contrast with regular continuation, can deal with turning points in parameter space.

For that purpose we employ Keller's (see Keller (1992)) continuation method where a new parameter is introduced to define solution arcs. The basic idea is to impose an additional constraint or normalization on the solution, in such a way that the "inflated" Jacobian matrix is no longer singular at the turning points. Leaving aside for a moment that part of our problem concerning the time integration (equation (3.26)), we seek to determine the zeros of the discrepancy function $\mathbf{f}$, equation (3.27). Following Keller, we add an arbitrary constraint in the form of a pseudo-arclength equation

$$\mathbf{f}(\mathbf{s}, \omega) = 0 \tag{3.32}$$

[32]In fact, as far as we have explored the parameter space, it appears that any bifurcation points would be beyond the critical maximum amplitude and are thus irrelevant.

and

$$N(\mathbf{s}, \omega, \theta) \;=\; 0, \tag{3.33}$$

where θ is the new parameter on the solution branch. Introducing $\mathbf{r}(\theta) = [\mathbf{s}(\theta), \omega(\theta)]$, a solution arc of (3.32)–(3.33) can be found using Newton's method:

$$\mathbf{J}_E \,.\, \Delta\mathbf{r} \;=\; -\,\mathbf{f}_E \tag{3.34}$$

or

$$\begin{bmatrix} \mathbf{f}_\mathbf{s} & \mathbf{f}_\omega \\ N_\mathbf{s} & N_\omega \end{bmatrix} \begin{bmatrix} \Delta\mathbf{s} \\ \Delta\omega \end{bmatrix} = \; - \begin{bmatrix} \mathbf{f} \\ N \end{bmatrix},$$

where the extended Jacobian matrix $\mathbf{J}_E$ can be nonsingular even if the regular Jacobian matrix $\mathbf{f}_\mathbf{s}$ is singular. (It can be shown that this is in fact the case for turning points). This is, clearly, a great advantage of the pseudo-arclength continuation method.

Having found a solution $\mathbf{r}(\theta) = [\mathbf{s}(\theta), \omega(\theta)]$ of (3.32)–(3.33), an initial estimate to move along the continuation branch is given by

$$\mathbf{r}(\theta + \Delta\theta) \;=\; \mathbf{r}(\theta) \;+\; \frac{d\mathbf{r}}{d\theta}\,\Delta\theta \;+\; O(\Delta\theta^2) \tag{3.35}$$

where $d\mathbf{r}/d\theta = [\,d\mathbf{s}/d\theta, d\omega/d\theta\,]$ is calculated as in the regular continuation procedure, namely, by solving the variational problem associated with (3.32)–(3.33):

$$\begin{bmatrix} \mathbf{f}_\mathbf{s} & \mathbf{f}_\omega \\ N_\mathbf{s} & N_\omega \end{bmatrix} \begin{bmatrix} \dot{\mathbf{s}}(\theta) \\ \dot{\omega}(\theta) \end{bmatrix} = \; - \begin{bmatrix} \mathbf{0} \\ N_\theta \end{bmatrix} \tag{3.36}$$

As before, the extra cost required to compute the estimate (3.35) is given by the solution of the linear system (3.36), since the extended Jacobian matrix $\mathbf{J}_E$ is available from Newton's method (equation (3.34)) — in fact, $\mathbf{J}_E$ is already decomposed in LU form.

Free from the difficulties associated with singular points, the pseudo-arclength continuation method represents an efficient procedure to calculate solution branches in parameter space that, generally speaking, will include a naturally occurring parameter and a suitable norm of the solutions. For our problem, in particular, a convenient parameter space is given, again, by ω, the frequency of the periodic acoustic waves, and a, a measure of wave amplitudes. It is necessary, then, that the pseudo-arclength normalization (3.33) reflect the structure of the particular parameter space that we want to depict. For a nonlinear boundary-value problem of the form (3.11)–(3.12)

that represents a system of coupled ordinary differential equations, Keller proposed for the parametrization of a solution branch $[\mathbf{s}(\theta), \omega(\theta)]$ a form of arclength:

$$N(\mathbf{s}, \omega, \theta) = \kappa \,||\, \dot{\mathbf{s}}(\theta) \,||^2 \,+\, (1 - \kappa) \,|\, \dot{\omega}(\theta) \,|^2 \,-\, 1 \,=\, 0, \tag{3.37}$$

for some $\kappa \in (0, 1)$. (Slight variations of (3.37), computationally more efficient, were also suggested). Equation (3.37) will allow the calculation of solution branches in the space $(\omega, ||\mathbf{s}||)$ even in the presence of turning points. But the application of (3.37) to our problem, whose governing equations are given as a PDE system, will not work, simply because $\mathbf{s}(\theta)$ is just a vector of field variables at discrete coordinates x_j but at a particular instant of time, $\tau = 0$ (see equations (3.20)–(3.21)). Hence, $||\dot{\mathbf{s}}||$ (or $||\mathbf{s}||$) is not a proper global norm for our solution space measuring acoustic wave amplitudes, and therefore, equation (3.37) will not provide a unique relation between ω and a.

A good constraint that involves a correct norm in $L^2[(0, 2\pi) \times (0, 2\pi)]$, appropriate for our system of partial differential equations with periodic boundary conditions, is given by

$$N(\mathbf{s}, \omega, \theta) = [\, a\,(\mathbf{s}(\theta), \omega(\theta)) \,-\, a_0\,] \,-\, [\,\theta \,-\, \theta_0\,] \,\equiv\, 0 \tag{3.38}$$

where $a_0 = a(\mathbf{s}_0, \omega_0) = a(\mathbf{s}(\theta_0), \omega(\theta_0))$ is the normalized acoustic wave amplitude corresponding to a known solution $[\mathbf{s}_0, \omega_0]$. The acoustic wave amplitude a was defined in (2.10) in terms of the potential function $\varphi(x, \tau)$. Integrating (2.10) by parts, we can express a in terms of the basic field variables (V and u) as

$$a \,=\, a\,(\mathbf{s}(\theta), \omega(\theta)) \,=\, -\frac{1}{(2\pi)^2} \int_0^{2\pi} \int_0^{2\pi} \frac{1}{\omega} u(x, \tau, \mathbf{s}(\theta), \omega(\theta))\, sin(\tau)\, \phi_1(x)\, dx\, d\tau, \tag{3.39}$$

where $\phi_1(x)$ is the eigenfunction of Floquet's eigenvalue problem solved in Section 3.1.

Equation (3.38) does provide a consistent parametrization of solution branches, in the sense that, for increasing values of the parameter θ, the solutions will have increasing amplitudes a, irrespective of the values taken by the frequency ω. Whether $\omega(\theta)$ increases or decreases monotonically or goes through a turning point, the important characteristic of (3.38) is that it makes possible a sequential calculation of the solution branches from small amplitude waves (close to that "Floquet bottom" referred to in Section 2.6) towards waves of greatest amplitudes[33] (near the breaking point) in (ω, ϵ, a) space, for a fixed ϵ.

[33]In our problem the difficulty with turning points arises because ω is not a good parameter for the branches — which are multiple valued relative to the ω axis, but not relative to the a axis.

So far we have formulated the problem for the Newton iteration as if the whole set of initial conditions in (3.20)–(3.21) was unknown. This is not so, as we know that u vanishes initially. A better implementation, that uses this information and reduces the amount of computational work by roughly a factor of two, follows. We start by observing that the total energy is conserved[34]

$$\bar{E} = \int_0^{2\pi} E(x,\tau)\,dx \;= const., \tag{3.40}$$

where $E = \frac{1}{2}u^2 + e$. Here $e = e(S,V)$ satisfies $e_V = -p$ and is given by

$$e = \frac{1}{\gamma(\gamma-1)}\, e^{\gamma S}\, V^{-\gamma+1}. \tag{3.41}$$

Therefore, if we require that $u(x,0) \equiv 0$ and $V(x,0) \equiv V(x,2\pi)$, then (3.40) — given the form of E above — automatically implies $u(x,2\pi) \equiv 0$ and 2π periodicity in τ follows. This is the actual strategy we will follow.

Some final remarks concerning the time symmetries of the solutions we seek seem in place now.

First of all, we notice that (using uniqueness for the initial value problem) *the condition $u(x,0) \equiv 0$ is equivalent to u being odd in time and V being even.* This is easily proved. Consider a solution $V = V(x,\tau)$ and $u = u(x,\tau)$ of the equations (2.1)–(2.2), satisfying $u(x,0) \equiv 0$. Then define V_* and u_* by

$$V_*(x,\tau) \;=\; V(x,-\tau) \qquad \textit{and} \qquad u_*(x,\tau) \;=\; -u(x,-\tau).$$

Clearly V_* and u_* also satisfy the equations, with the same initial conditions. Thus $V_* = V$ and $u_* = u$. The converse is trivial: if u is odd, then clearly $u(x,0) \equiv 0$! This simple observation shows that the *procedures described earlier for finding a solution will indeed produce one with the desired symmetries.*

Second, we observe that a 2π–periodic in τ solution of (2.1)–(2.2) which, furthermore, has u odd and V even in time satisfies the equations

$$V(x,\pi+\tau) \;=\; V(x,\pi-\tau) \qquad \textit{and} \qquad u(x,\pi+\tau) \;=\; -u(x,\pi-\tau). \tag{3.42}$$

That is, *V is even and u is odd in time τ relative to the time origin $\tau = \pi$.* Further, in view of the first observation above, (3.42) is in fact equivalent to the condition $u(x,\pi) \equiv 0$. The proof of (3.42) is, again rather simple. For, given the first observation above and the 2π periodicity, we have $V(x,\pi+\tau) \;=\; V(x,-\pi-\tau) \;=\; V(x,\pi-\tau)$ and similarly for u.

[34] As follows from the equation $E_t + (p\,u)_x = 0$.

Third, we point out that if we have a solution of (2.1)-(2.2) such that u vanishes at both $\tau = 0$ and $\tau = \pi$, then, this solution has period 2π in τ. Again, this is easily proved. From the first observation and $u(x,\pi) \equiv 0$, (3.42) must apply. Evaluating (3.42) at $\tau = \pi$, and using $u(x,0) \equiv 0$, periodicity follows.

Finally, we point out that we could use the last (third) observation above to further reduce the numerical work relative to the scheme we actually used (see below (3.41)). Namely, set $u(x,0) \equiv 0$ and then solve the equation $u(x,\pi) \equiv 0$ considering $u(x,\pi)$ as a function of $V(x,0) = \mathbf{s}_V$ and ω. This reduces the amount of time integration needed by a half. Unfortunately, in practice we found this scheme to be unreliable: it appears that small errors in $u(x,\pi) \equiv 0$ produce large errors[35] in $\mathbf{s}_V$. Thus an ill conditioned algorithm results.

From a numerical point of view, the problem may now be formulated as follows. With our usual compact notation ($\mathbf{V}(\tau) = [V_0(\tau), ..., V_j(\tau), ..., V_{J-1}(\tau)], \mathbf{u}(\tau) = [u_0(\tau), ..., u_j(\tau), ..., u_{J-1}(\tau)], \mathbf{F} = [\mathbf{F}_V, \mathbf{F}_u]$), the initial-value problem (3.11) takes the form

$$\dot{\mathbf{V}}(\tau) = \mathbf{F}_V(\tau, \mathbf{u}), \tag{3.43}$$

$$\dot{\mathbf{u}}(\tau) = \mathbf{F}_u(\tau, \mathbf{V}), \tag{3.44}$$

$$\mathbf{V}(0) = \mathbf{s}, \tag{3.45}$$

$$\mathbf{u}(0) = \mathbf{0}. \tag{3.46}$$

The boundary condition (3.12) enforcing periodicity in time will be

$$\mathbf{f}(\mathbf{s}) = \mathbf{V}(2\pi) - \mathbf{s} = \mathbf{0} \tag{3.47}$$

While (3.47) guarantees periodicity in time for the specific volume V, periodicity for the flow velocity u will be assured by initial condition (3.46) and energy conservation. In fact, the values of $\mathbf{u}(2\pi)$ can serve as a direct measure of the error of the whole numerical scheme: while $\mathbf{V}(2\pi)$ will differ from $\mathbf{s}$ by a prescribed tolerance, 10^{-5} say, $\mathbf{u}(2\pi)$ is not constrained, and hence, the value $max|u_j(2\pi)|$, not exactly equal to zero, is a reliable indicator of the accuracy of the numerical solution.

Let us summarize, then, the steps required for the numerical calculation of large amplitude time periodic acoustic waves.

[35]This is based purely on our computational experience. We have, presently, no analytical understanding of this phenomena.

For a given value of the entropy wave amplitude ϵ, we first solve the eigenvalue problem and auxiliary calculations as explained in Section 3.1, in order to obtain an approximate small amplitude periodic solution that will constitute a sufficiently accurate initial estimate for subsequent computations.

With those starting values, we then integrate the system (3.13)–(3.14), which, for $j = 0, 1, 2, ..., J-1$ we now write in the form

$$V_j^{n+1} = V_j^{n-1} + \delta \left[u_{j+1}^n - u_{j-1}^n \right], \tag{3.48}$$

$$u_j^{n+1} = u_j^{n-1} - \frac{\delta}{\gamma} \left[exp(\gamma S_{j+1}) \ (V_{j+1}^n)^{-\gamma} - exp(\gamma S_{j-1}) \ (V_{j-1}^n)^{-\gamma} \right], \tag{3.49}$$

$$V_j^0 = s_j, \tag{3.50}$$

$$u_j^0 = 0. \tag{3.51}$$

At $\tau = 2\pi$, periodicity in time and the additional constraint for continuation in (ω, a) parameter space are imposed:

$$f_j = V_j^N - s_j = 0, \tag{3.52}$$

$$N = [\, a - a_0 \,] - [\, \theta - \theta_0 \,] = 0, \tag{3.53}$$

with a calculated according to (3.39). Equations (3.52)–(3.53) are solved by Newton's method (equation (3.34)), and we thus obtain a periodic solution $[\, V_j^n, u_j^n, \omega, \epsilon \,]$ in the square domain $[(0, 2\pi) \times (0, 2\pi)]$. An important detail in the calculation of the extended Jacobian in (3.34) concerns the values given to the increments in the initial vector $\mathbf{s}$ and frequency ω. If we take $\Delta s \simeq \Delta a$, then, from the bifurcation series for $\omega(a)$, we can use consistently $\Delta\omega \simeq a \, \Delta s$. Finally, an initial guess for the next solution with a larger acoustic amplitude a is obtained by solving the linear system (3.36) and using the "continuation" equation (3.35). The direction along the regular branch $[\mathbf{s}(\theta), \omega(\theta)]$ is chosen so that $\dot{\mathbf{s}}(\theta).\dot{\mathbf{s}}(\theta_0) + \dot{\omega}(\theta)\dot{\omega}(\theta_0) > 0$.

3.4 Numerical results

In this section, we describe numerical computations obtained with the algorithm devised in Section 3.3.

Taking as an initial guess (for a small acoustic amplitude a) the approximate solution (3.8)–(3.10) computed in Section 3.1, we calculated, for a given entropy amplitude ϵ, time periodic solutions to the equations of motion. We used the continuation procedure comprised by equations (3.53), (3.34) and (3.35) on every newly found solution, to move to larger amplitudes the computational procedure. This sequence of solutions consists of continuous and smooth waves, 2π–periodic in τ and x, having increasing acoustic amplitudes a, as defined by (3.39). At the limiting stage or breaking point, the acoustic waves reach their maximum amplitude while remaining continuous. Beyond that, the balance between dispersion and nonlinear distortion can no longer be sustained and the periodic solutions cease to exist.

Figures 5 through 85 show the structure of the nonlinear time periodic acoustic waves close to the breaking point. There are basically three types of plots: the first and second types of figures display the profile of a field variable (specific volume V, flow velocity u or pressure p) as a function of either the mass coordinate x or the normalized time τ, passing through the point of maximum amplitude (V_{max}, u_{max} or p_{max}, respectively). The third type is a 3D plot that gives the shape of a field variable in its whole domain, the square $[(0, 2\pi) \times (0, 2\pi)]$. These waves of greatest amplitude a_{max} represent the end point of a regular branch $\omega = \omega(a)$ that started, for a given ϵ, at a particular location (ω, ϵ) in the Floquet bottom $a = 0$. For all figures, it has been indicated the transition curve (TC) from which a particular large amplitude wave bifurcated (see figure 4 for (TC)'s notation). Several combinations of the entropy wave amplitude ϵ and the frequency ω were selected along the first four transition curves in order to have representative solutions for each parameter region. All computations were performed using 128 points to discretize each dependent variable V_j^n and u_j^n, $j = 0, 1, ..., J$ ($\Delta x = 2\pi/J$ and $J = 127$). The time steps $\Delta\tau$ were roughly 5–10 times larger than the linear CFL limit (3.19) calculated for small a. The 3D figures are plotted on a 64×64 grid, which may smooth out a bit the sharp corners in velocity and pressure. The tolerance for Newton's method was 10^{-5} and the parameter $\Delta\theta = \theta - \theta_0$ appearing in the continuation constraint (3.53) varied between 0.0001 for small values of ϵ to 0.002 in regions with large ϵ. Typically it took about 10–20 intermediate steps — smooth, continuous solutions — to walk along a bifurcation branch (ω, a) up to the breaking point, from the starting point near $a = 0$.

A surprising result is that *even for a slightly nonuniform entropy background* (namely, small ϵ), *nonlinear acoustic waves have very large amplitudes.* For example, notice in Figures 18–19 waves with $\Delta p/p$ in the order of 8% for $\epsilon = 0.001$! And the waves in Figures 36–37, for $\epsilon = 0.1$, display a $\Delta p/p$ as large as 27%. Figure 86 shows the L^∞ norm of the velocity u as a function of ϵ for waves close to the breaking point, that bifurcate from the second transition curve (TC 2) with a frequency $\omega = 1 + \epsilon/2 + O(\epsilon^2)$ in the stability diagram of Fig. 4. Figure 87 displays the same relation for the acoustic amplitude a (equation (3.39)). To further appreciate the strength of these waves, their intensities are also displayed (in the figures) in the traditional decibel scale of acoustics — explained at the end of this section (equations

(3.54)-(3.56)).

Clearly, these stationary periodic acoustic waves can reach into a highly nonlinear regime. To gain some perspective, consider the propagation of a *single* nonlinear "periodic" acoustic wave on a *uniform background.* We can measure its amplitude by $A = \Delta p/p$. Let T be its period. Then, starting from a smooth initial shape, this wave will break and form shocks[36] in times of order T/A. When A is as large as 0.1, the wave shape deformation over a single "period" will be considerable. Nevertheless, the waves we are investigating — which achieve $A = 0.1$ and larger — experience *no* distortion over a period T. It is interesting that this strong effect can be produced by apparently inoffensive fluctuations in the entropy field, though the effect clearly extends to larger variations of rather general shapes. This balance between the nonlinear distortion inherent to the equations of motion and the dispersive effect introduced by the coupling between entropy and acoustic modes — needless to say, the leit motiv of this investigation — is displayed in its fullest extent by our numerical calculations.

Although our numerical computations were carried out for a particular entropy field (namely $S(x) = \epsilon\, K(x) = \epsilon\, 2\, cos(2x)$) and a polytropic gas law with $\gamma = 1.4$, similar results can be obtained for functions $K(x)$ of much more general structure and more general equations of state. Indeed, the analyses of Sections 2.3 and 2.8 showed that, as long as $K(x)$ satisfies certain simple symmetric and periodic properties, the existence of periodic acoustic waves bifurcating from equilibrium will be guaranteed by Floquet theory applied to Hill's equation (3.4) for quite general $K(x)$. This observation suggests a very large class of periodic solutions to Euler equations of 1D gas dynamics that should manifest itself in the large time asymptotic behavior of this system subject to arbitrary initial conditions. We will discuss this topic a bit further in Chapter 4.

Confirming our previous conjectures, the waves of greatest amplitudes present sharp peaks in the field variables that indicate the maximum allowable amplitudes for which continuous and periodic solutions to the 1D Gas Dynamic equations are possible. These peaks, representing discontinuities (corners[37]) in the first derivatives of the field quantities, must propagate along the characteristics, which in this system of coordinates are given by

$$\frac{dx}{d\tau} = \pm\, C(x, \tau, \epsilon, \omega),$$

[36]This follows from well known results in weakly nonlinear acoustic asymptotic theory, see Whitham (1974).

[37]Actually, this is an issue where further work is needed. The calculation of maximum amplitude stationary periodic waves is fairly expensive. Thus the resolutions we have been able to achieve preclude highly accurate evidence of corners. With a scheme of the type we have, it would be unreasonable to expect a "corner" to be sharper than about 10 mesh widths. Thus we would need far more than 128 points for a fully resolved picture.

where the Lagrangian sound speed is $C^2 = \gamma p/V$. This property is nicely captured in the 3D figures, where it can be seen that the peaks in the wave profiles propagate in (x, τ) plane following a slightly oscillatory pattern around the mean values $C \simeq \pm 1$. It is also interesting to observe the strong interaction between peaks moving along different characteristics, a very noticeable feature in the general picture of standing hyperbolic waves having nontrivial structures even in their smooth zones. In this respect, the figures give a vivid illustration of the geometrical complexities in the waves' profiles due to the nonuniformity of the underlying medium, in marked contrast with the stationary free surface waves mentioned in Section 1.4. Figures 88–96 are the result of a higher resolution calculation, where 256 points (instead of 128) were used in the space discretization. As before, the 3D plots are done using a 64×64 grid, but the other graphs reflect the increased resolution. Figure 97 displays a typical steepening pattern for the flow quantities as the acoustic amplitude increases.

Compared with those numerical methods based on the extrapolation of small amplitude wave expansions described in Section 3.3, our numerical algorithm exhibits clear advantages. First, the boundary-value problem formulation does not suffer from convergence problems when calculating large amplitude waves with non-smooth structure, a case that presents serious difficulties when handled using Fourier expansions. Our difficulties for a proper resolution of corners are, in fact, minor compared with those a Fourier based approach would face. Moreover, when our method goes beyond the breaking point, it still provides a converged solution, though not a physically realistic one. As mentioned before in Section 3.3, this is a very desirable feature for our purposes, since it gives a threshold in parameter space indicating maximum permissible wave amplitudes for continuous time periodic solutions. It is precisely this type of capability that is required for a systematic determination of the domains of existence in the (ω, ϵ, a) parameter space of periodic nonlinear acoustic waves.

As mentioned before in Section 3.3 (see the remark below equation (3.31)): the oscillations indicating that we are "beyond" the maximum amplitude should be more evident in the continuation procedure, when calculating $d\mathbf{r}/d\theta = [d\mathbf{s}/d\theta, d\omega/d\theta]$ in equation (3.36). This follows from equation (3.35), where the amplification factor $A_m = 1/\Delta\theta$ is seen to occur. This is illustrated in Figures 98–99, where the amplitude of the oscillations in $d\mathbf{s}/d\theta$ is about 3×10^5 larger than the amplitude of the oscillations in u. This is actually larger than A_m, but this is because the A_m factor applies to the comparison of $d\mathbf{s}/d\theta$ with the "next" solution[38] — not the "current" one as in these figures. We see then that the "oscillations test", when applied to $d\mathbf{s}/d\theta$, is quite sensitive.

In Section 3.3 (just below equation (3.47)), it was pointed out that the value $max|u_j(2\pi)|$, $j = 0, 1, ..., J-1$ could serve as a general measure for the error of the

[38]Which is further "beyond" the maximum amplitude and thus has larger amplitudes in the field variable's oscillations. The additional amplification this introduces is hard to estimate and we have not even attempted to do so

numerical scheme that takes advantage of fundamental symmetric properties in the original equations. In all numerical experiments, it was found that this error was comparable with the tolerance imposed in Newton's method (10^{-5}) for the solution of (3.52)–(3.53).

A more direct perception of the large intensities attainable by the standing periodic acoustic waves just described, can be gained by translating their amplitudes into actual physical units.

It is conventional in technical acoustics to measure the intensity of a sound wave by the sound pressure level (SPL) scale:

$$SPL \;=\; 20\, log_{10}\, \frac{p_{rms}}{p_{ref}}. \tag{3.54}$$

Here p_{ref} is a root-mean-square reference pressure, that for the case of sound waves propagating in air is usually taken as $p_{ref} = 2.04 \times 10^{-5}\ N/m^2$. The quantity p_{rms} is called effective sound pressure, and it is equal to the root-mean-square of the excess pressure — total instantaneous pressure at a point minus the static pressure — taken over one period. The dimensionless level provided by (3.54) is said to be in decibels (dB). Thus, the threshold of audibility, i.e., the lowest SPL of a particular frequency that can be heard by the human ear is about 20 dB at 1000 Hz (audible sound contains frequency components between 15 and 15000 Hz). At the other end of the hearing range, for extremely loud sound, the threshold of pain — which depends very little on frequency — is about 140–150 dB.

It should be mentioned that other quantities can sometimes be used to define the decibel scale, such as acoustic intensity, power and velocity ratios. However, conventional sound pressure meters (comprising a microphone, amplifier and indicating meter) usually measure p_{rms} in a complex sound wave, and that is why (3.54) is generally employed. For further details about acoustic measuring techniques, see Beranek (1949).

To quantify the intensity of our nonlinear periodic acoustic waves in the scale (3.54), the excess pressure is defined by

$$p_e(x,\tau) \;=\; p(x,\tau) \;-\; p_f \tag{3.55}$$

where $p(x,\tau)$ is the total instantaneous pressure as calculated by the numerical scheme according to the state equation (2.4), and p_f is the static pressure corresponding to the equilibrium solution (3.1). Taking an average in x and τ, the effective sound pressure can be written as

$$p_{rms} \;=\; \left\{ \frac{1}{(2\pi)^2} \int_0^{2\pi} \int_0^{2\pi} p_e^2(x,\tau)\, dx\, d\tau \right\}^{1/2} \tag{3.56}$$

Finally, to express p_{rms} in dimensional units, we have to multiply the number obtained via (3.56) by $C_0^2 V_0$ (see dimensionless variables in Section 1.1). For air at 273 K and 1 atm, we have that $\gamma = 1.4$, $V_0^{-1} = 1.293\, kg/m^3$ and $c_0 = 331\, m/s$ (recall that the spatial sound speed is related to the Lagrangian sound speed by $c = CV$).

The sound pressure level (SPL) calculated by (3.54)–(3.56) has been indicated in the 3D figures. As already pointed out, entropy waves of relatively small amplitude ϵ can induce periodic acoustic waves of extremely high intensity. Figures 100–101 show the relation between SPL, entropy amplitude ϵ and acoustic amplitude a (equation (3.39)) for waves close to the breaking point, along the second transition curve already mentioned.

Additional physical information can be obtained by defining the acoustic Mach number M as the ratio of the maximum particle velocity to the local sound speed, in a fashion similar to that used commonly in aerodynamics. Values of the Mach number M for waves close to the breaking point are also given in the 3D figures, and displayed in Figs. 102–103 as a function of ϵ and a for those waves (close to the maximum amplitude) bifurcating from the second transition curve. Notice that the sound of a jet engine at short range may have an intensity of $SPL \simeq 140\, dB$ in the scale (3.54), which translates into an acoustic Mach number $M \simeq 0.001$ (Beyer (1984)). Thus, the Mach numbers associated with our standing periodic acoustic waves are more in line with those found in the theory of weak shock waves than in acoustics or even nonlinear acoustics. Nevertheless, they have no shocks.

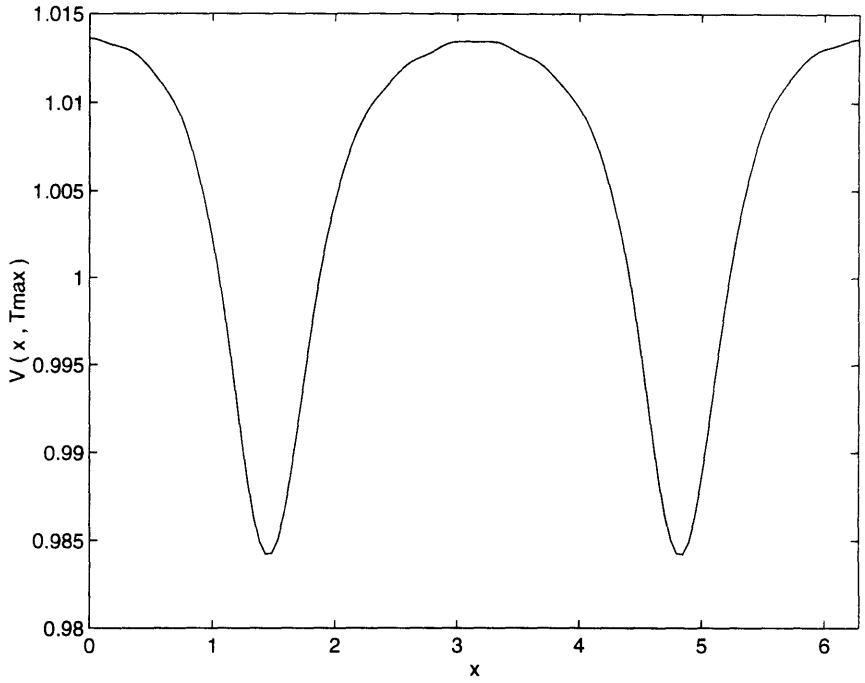

Figure 5: $V(x, \tau_{max})$ for $\epsilon = 0.001$, $\omega = 0.999664$ (TC 1).

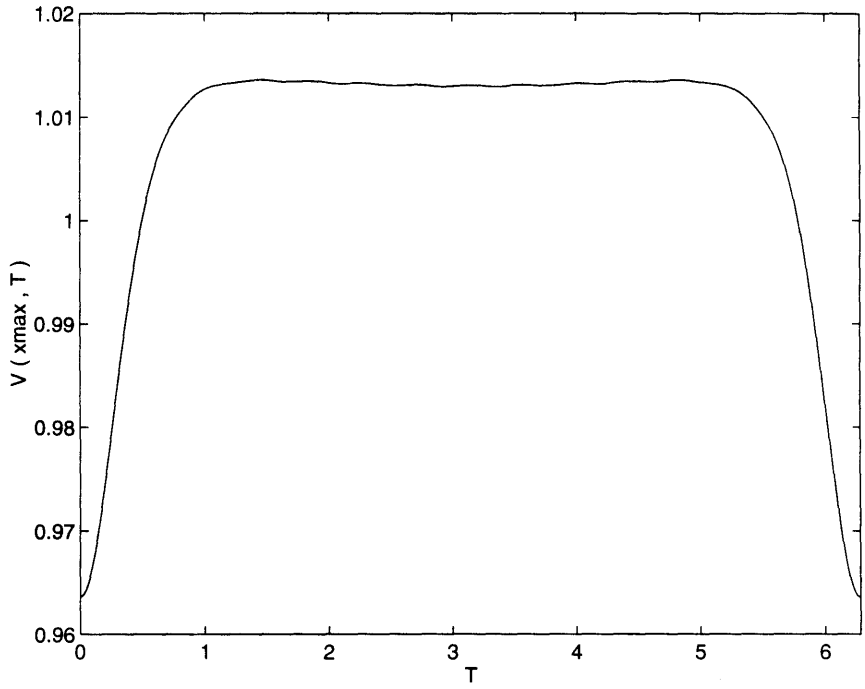

Figure 6: $V(x_{max}, \tau)$ for $\epsilon = 0.001$, $\omega = 0.999664$ (TC 1).

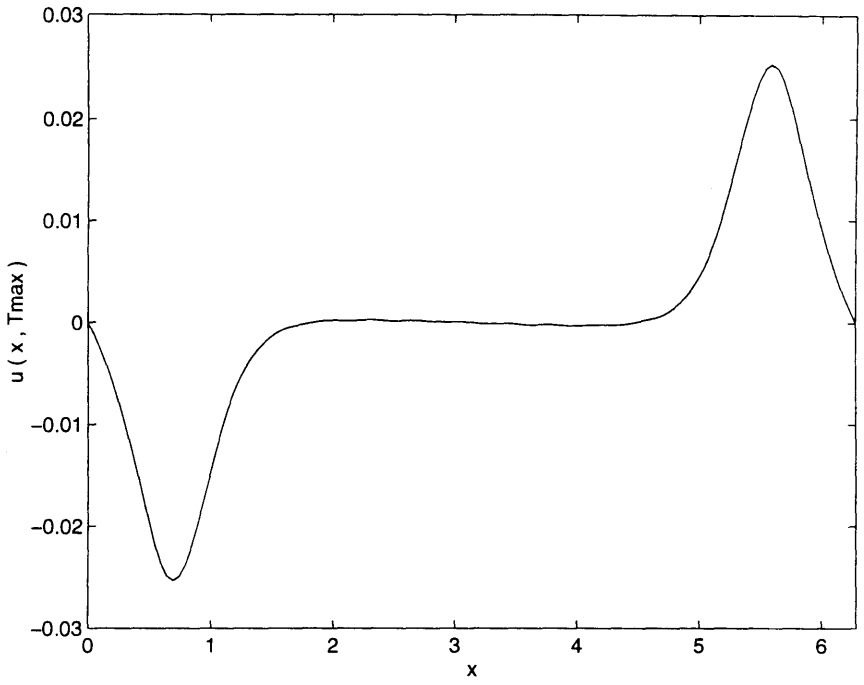

Figure 7: $u(x, \tau_{max})$ for $\epsilon = 0.001$, $\omega = 0.999664$ (TC 1).

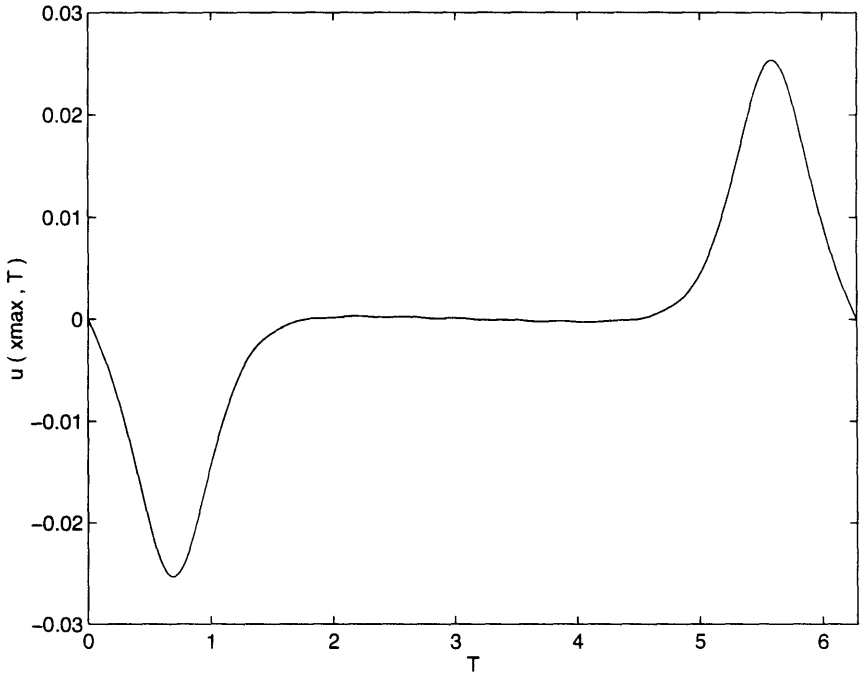

Figure 8: $u(x_{max}, \tau)$ for $\epsilon = 0.001$, $\omega = 0.999664$ (TC 1).

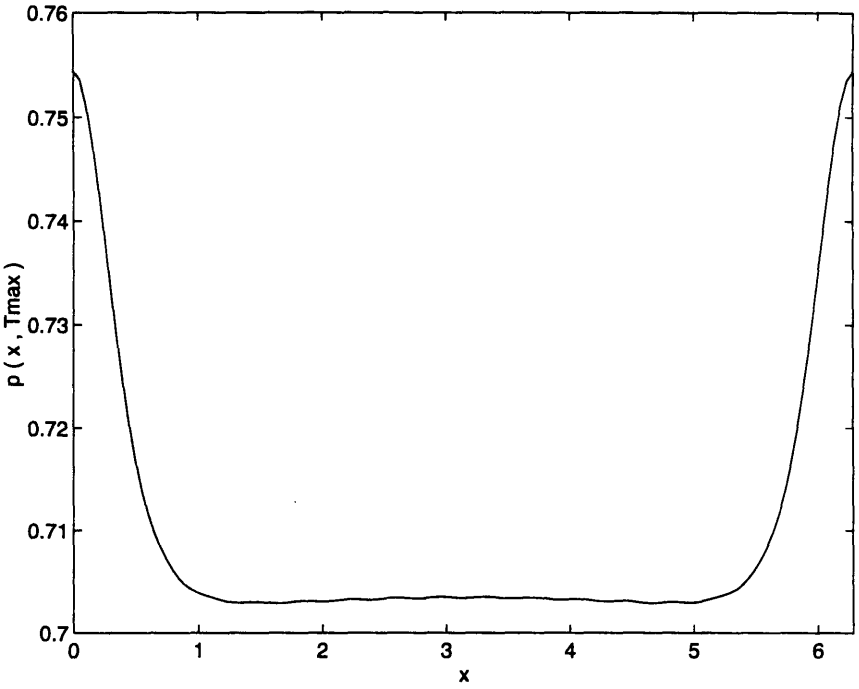

Figure 9: $p(x, \tau_{max})$ for $\epsilon = 0.001$, $\omega = 0.999664$ (TC 1).

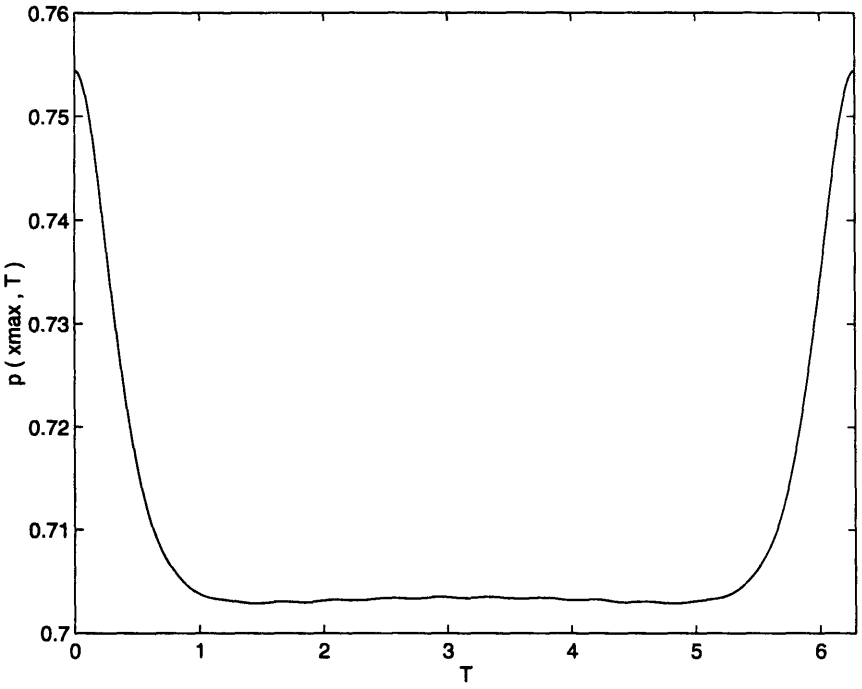

Figure 10: $p(x_{max}, \tau)$ for $\epsilon = 0.001$, $\omega = 0.999664$ (TC 1).

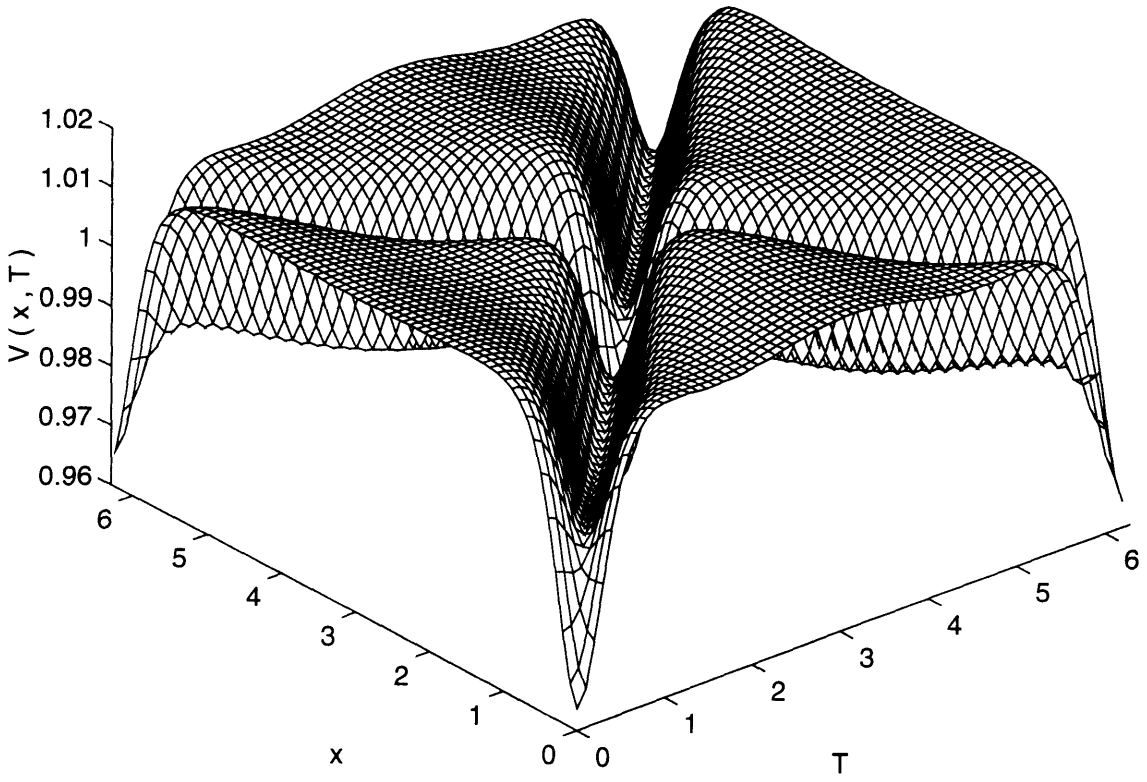

Figure 11: $V(x,\tau)$ for $\epsilon = 0.001$, $\omega = 0.999664$; $a = 0.00578$, $SPL = 157.3dB$, $M = 0.02492$, (TC 1).

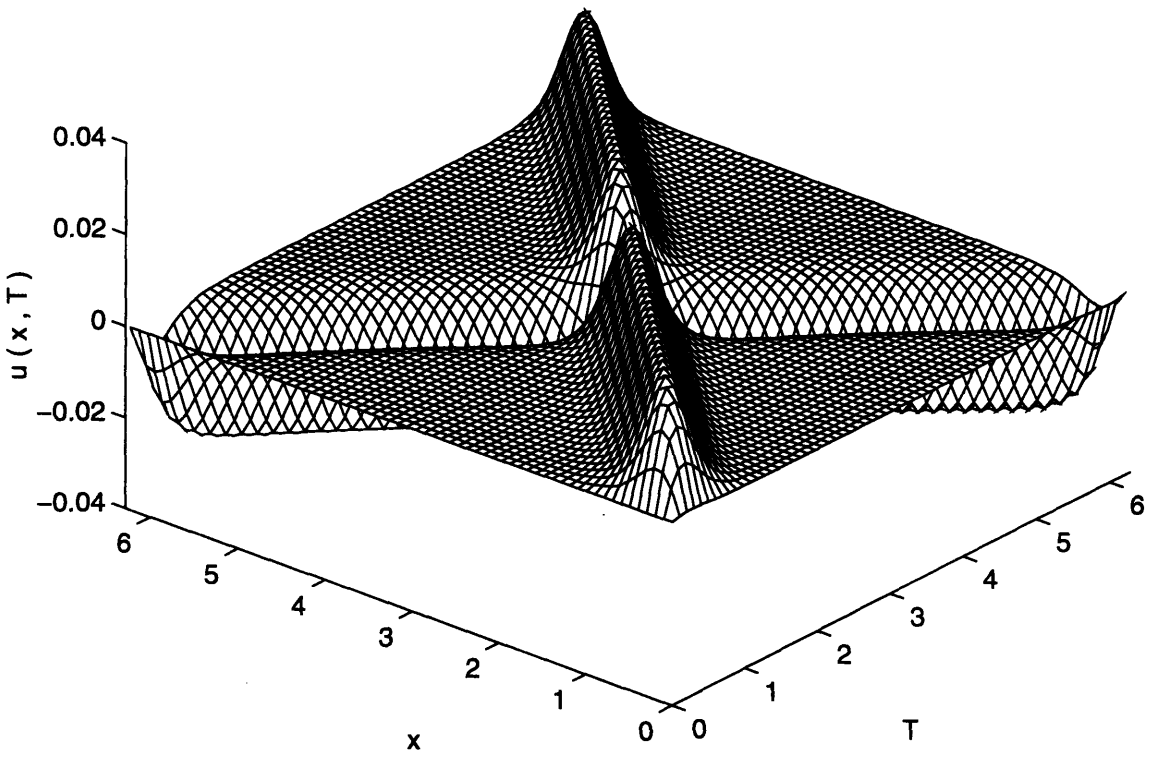

Figure 12: $u(x,\tau)$ for $\epsilon = 0.001$, $\omega = 0.999664$; $a = 0.00578$, $SPL = 157.3dB$, $M = 0.02492$, (TC 1).

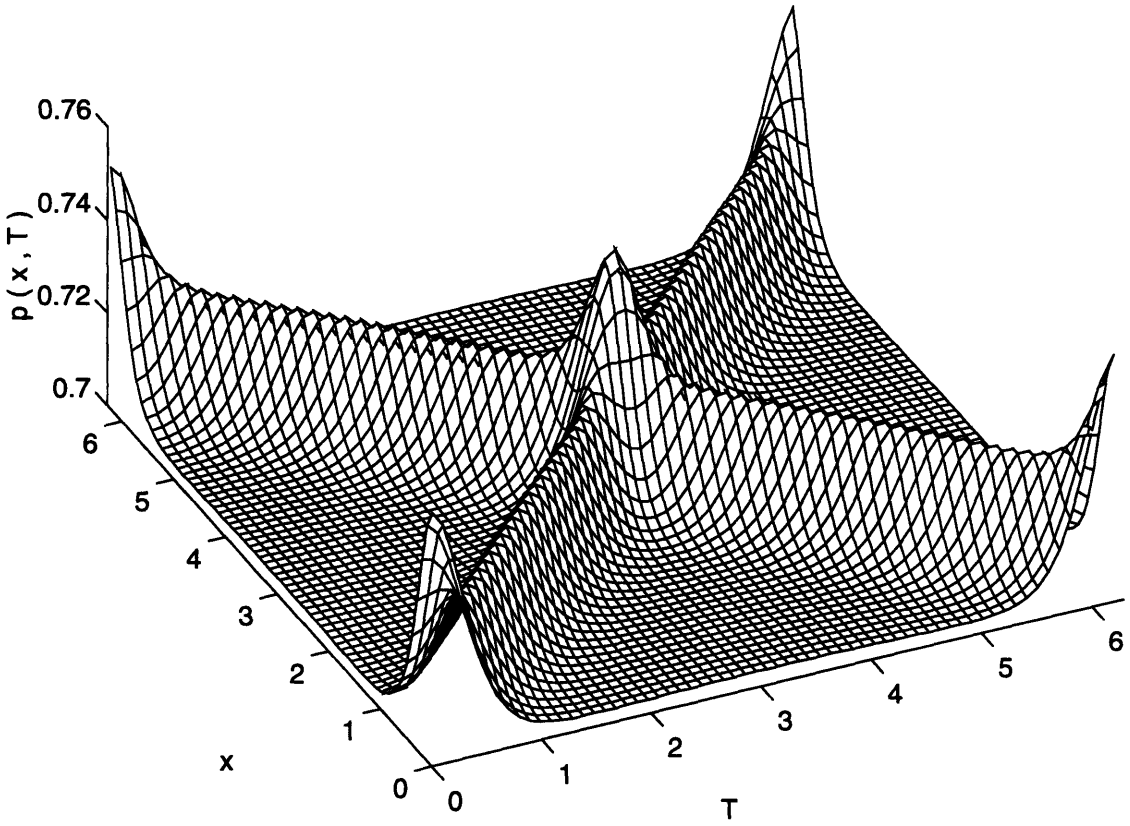

Figure 13: $p(x,\tau)$ for $\epsilon = 0.001$, $\omega = 0.999664$; $a = 0.00578$, $SPL = 157.3dB$, $M = 0.02492$, (TC 1).

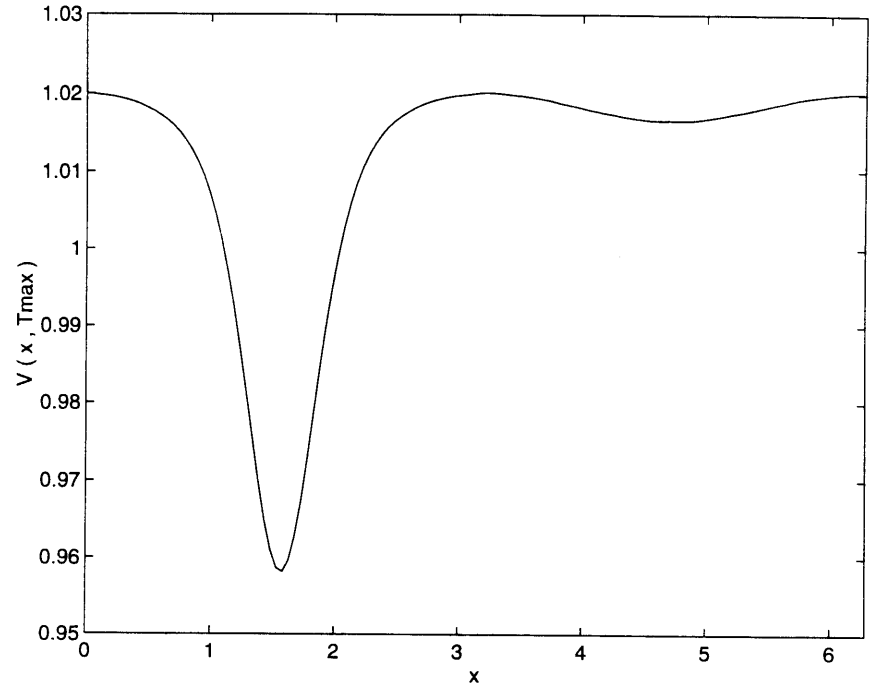

Figure 14: $V(x, \tau_{max})$ for $\epsilon = 0.001$, $\omega = 0.995341$ (TC 2).

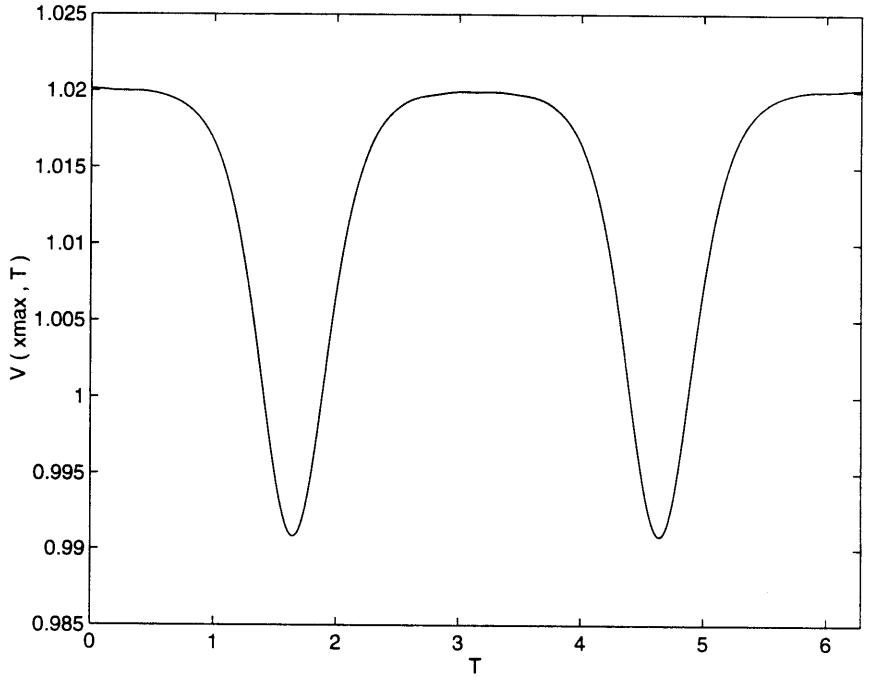

Figure 15: $V(x_{max}, \tau)$ for $\epsilon = 0.001$, $\omega = 0.995341$ (TC 2).

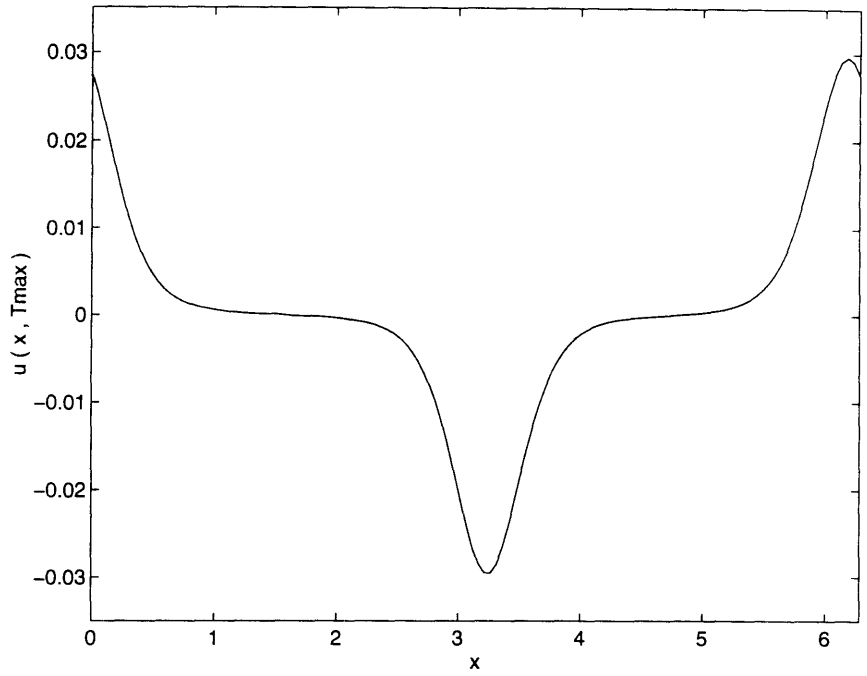

Figure 16: $u(x, \tau_{max})$ for $\epsilon = 0.001$, $\omega = 0.995341$ (TC 2).

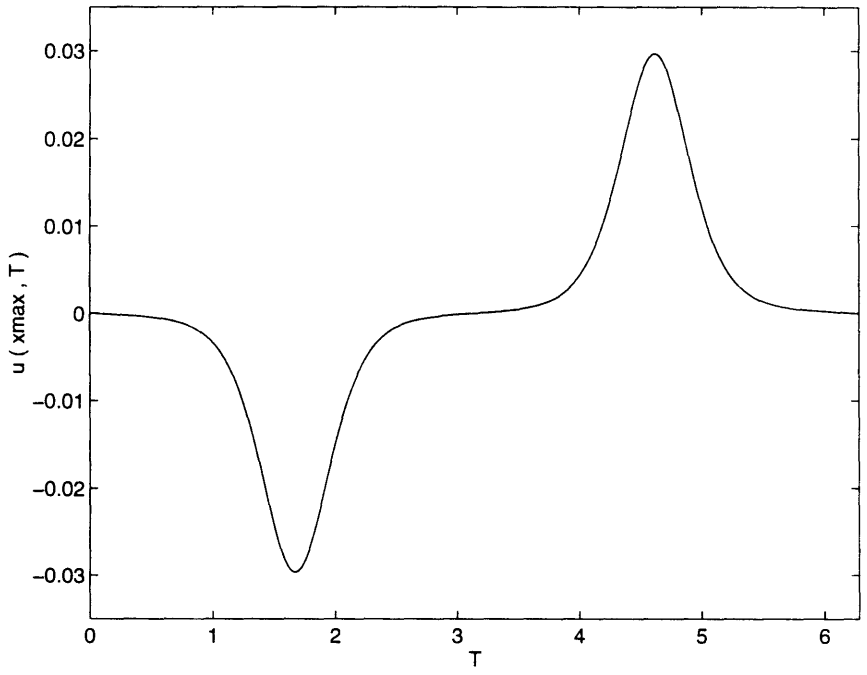

Figure 17: $u(x_{max}, \tau)$ for $\epsilon = 0.001$, $\omega = 0.995341$ (TC 2).

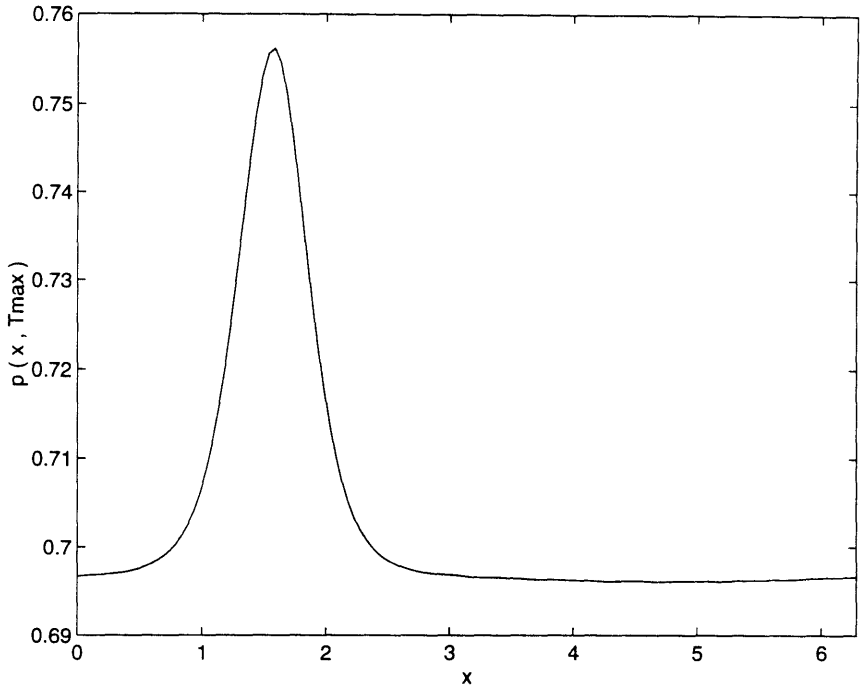

Figure 18: $p(x, \tau_{max})$ for $\epsilon = 0.001$, $\omega = 0.995341$ (TC 2).

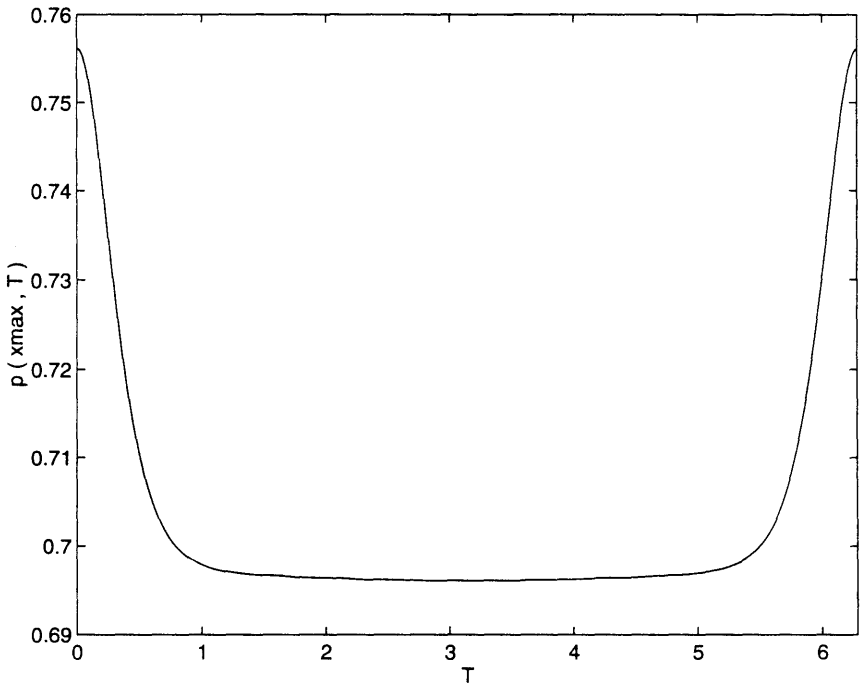

Figure 19: $p(x_{max}, \tau)$ for $\epsilon = 0.001$, $\omega = 0.995341$ (TC 2).

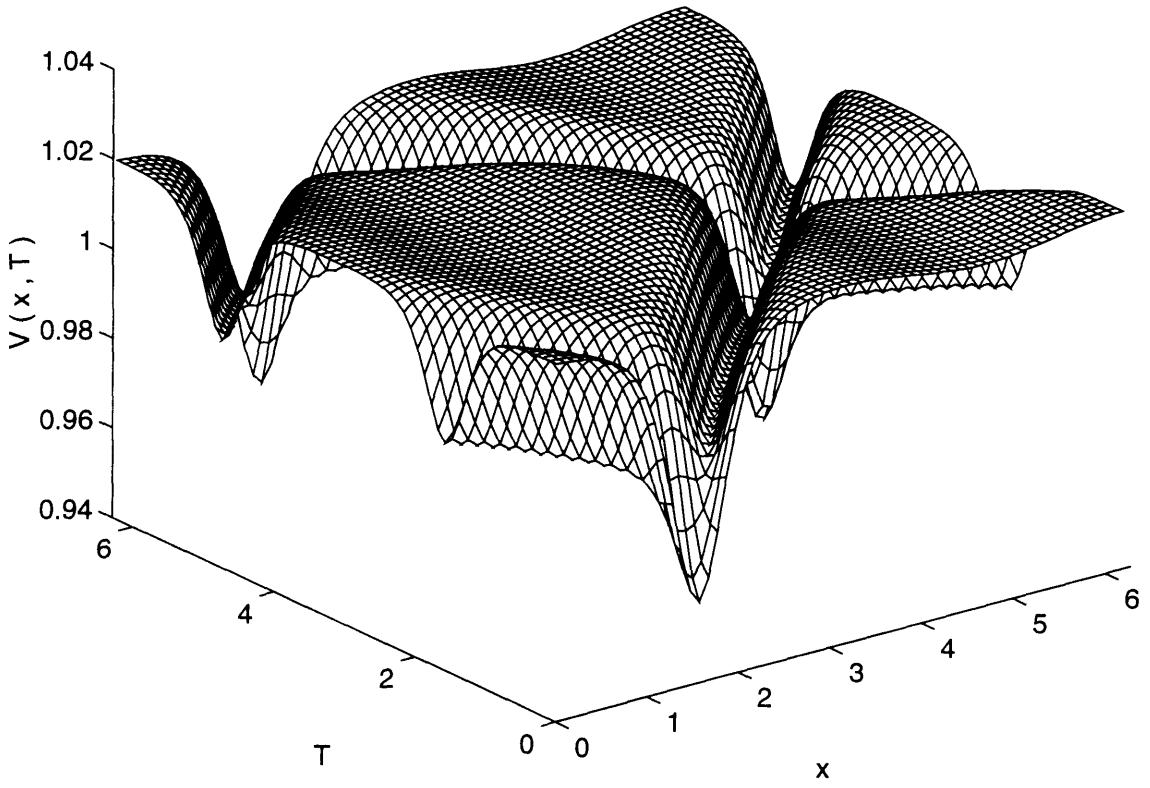

Figure 20: $V(x,\tau)$ for $\epsilon = 0.001$, $\omega = 0.995341$; $a = 0.00678$, $SPL = 160.5dB$, $M = 0.02928$, (TC 2).

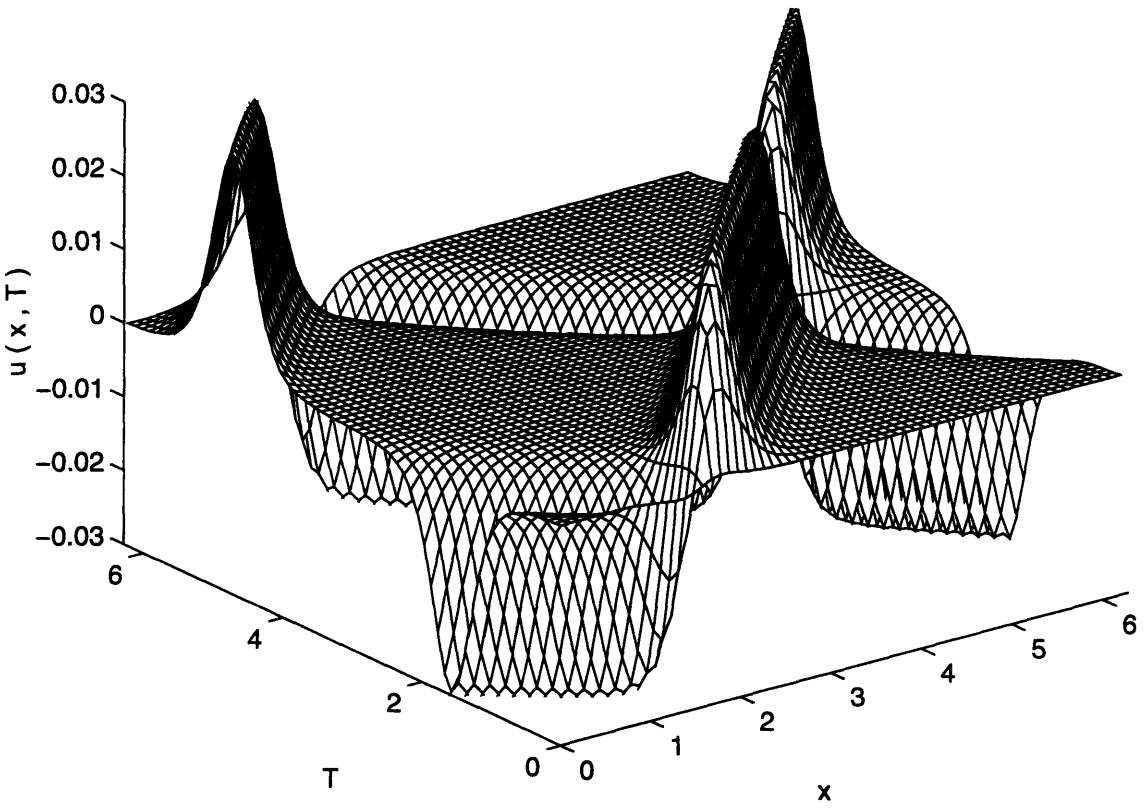

Figure 21: $u(x,\tau)$ for $\epsilon = 0.001$, $\omega = 0.995341$; $a = 0.00678$, $SPL = 160.5dB$, $M = 0.02928$, (TC 2).

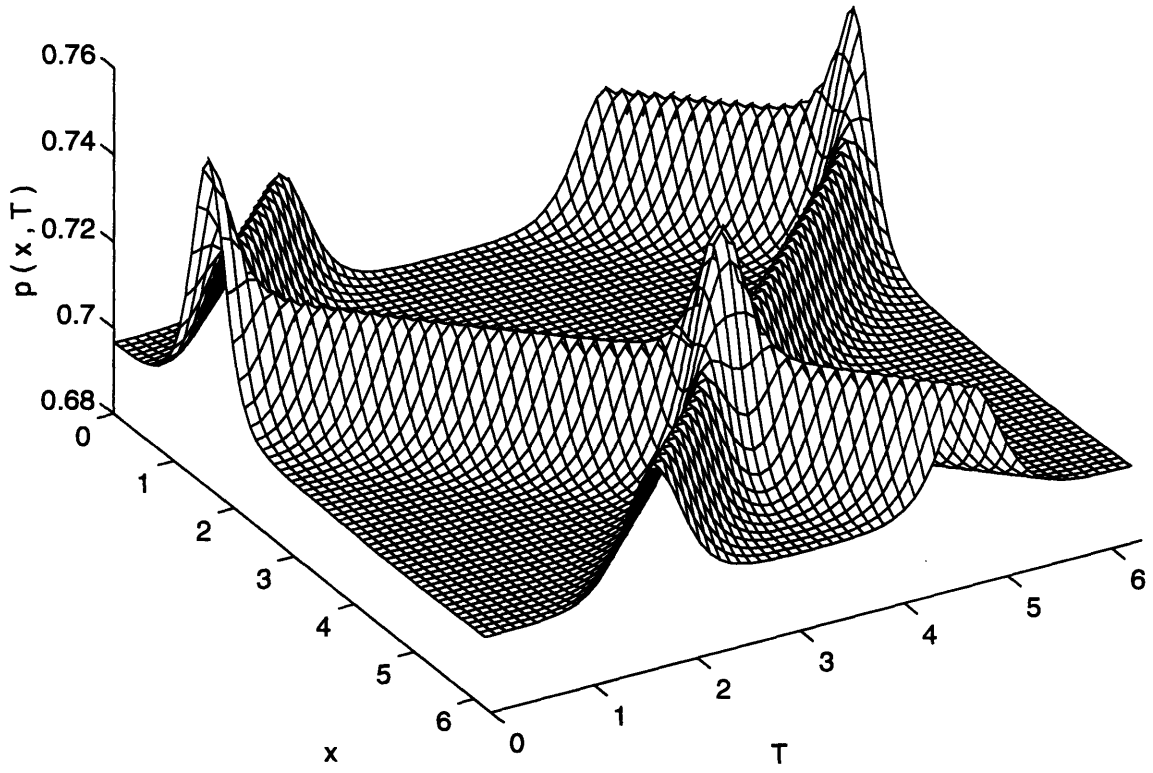

Figure 22: $p(x,\tau)$ for $\epsilon = 0.001$, $\omega = 0.995341$; $a = 0.00678$, $SPL = 160.5dB$, $M = 0.02928$, (TC 2).

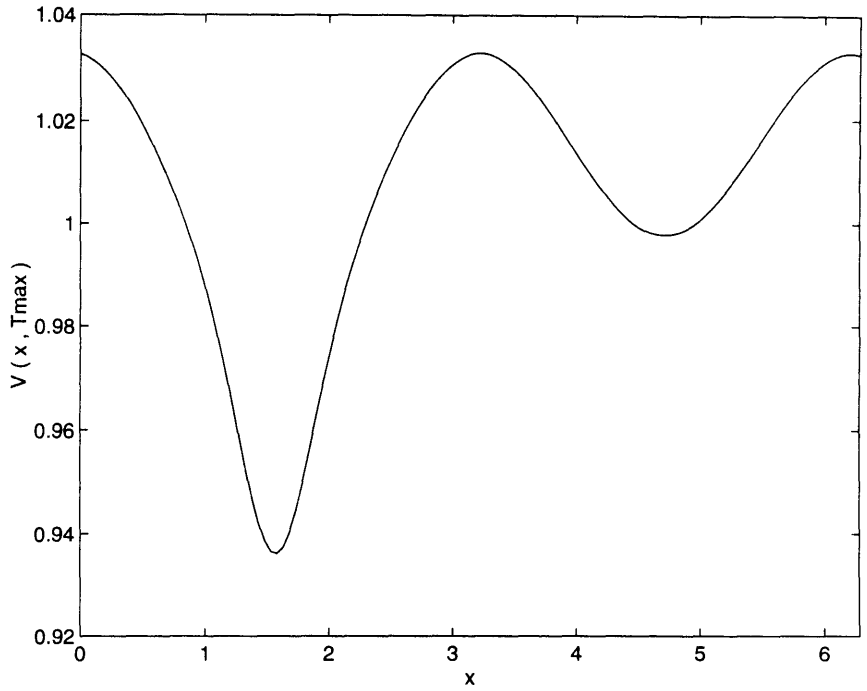

Figure 23: $V(x, \tau_{max})$ for $\epsilon = 0.01$, $\omega = 1.003630$ (TC 2).

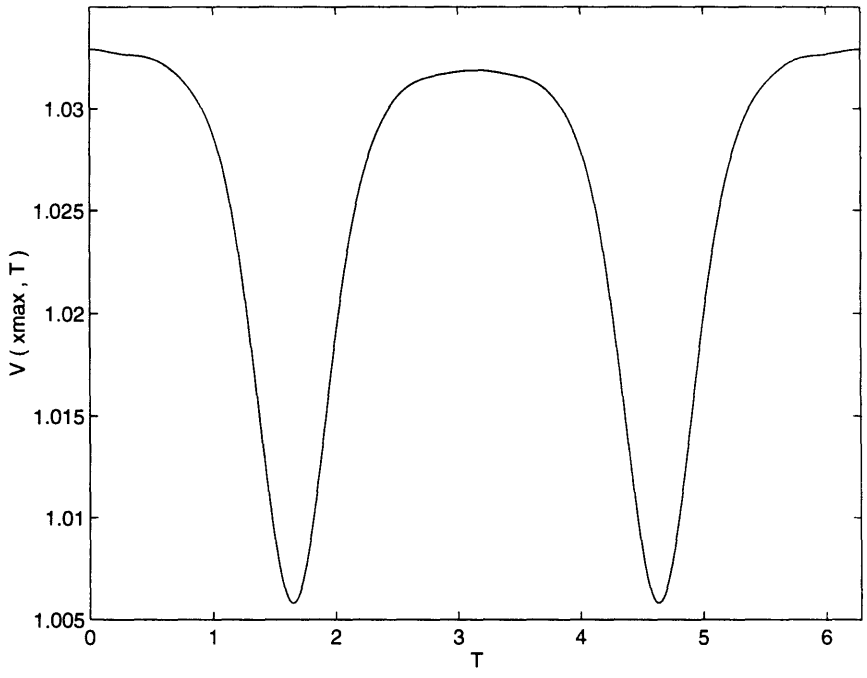

Figure 24: $V(x_{max}, \tau)$ for $\epsilon = 0.01$, $\omega = 1.003630$ (TC 2).

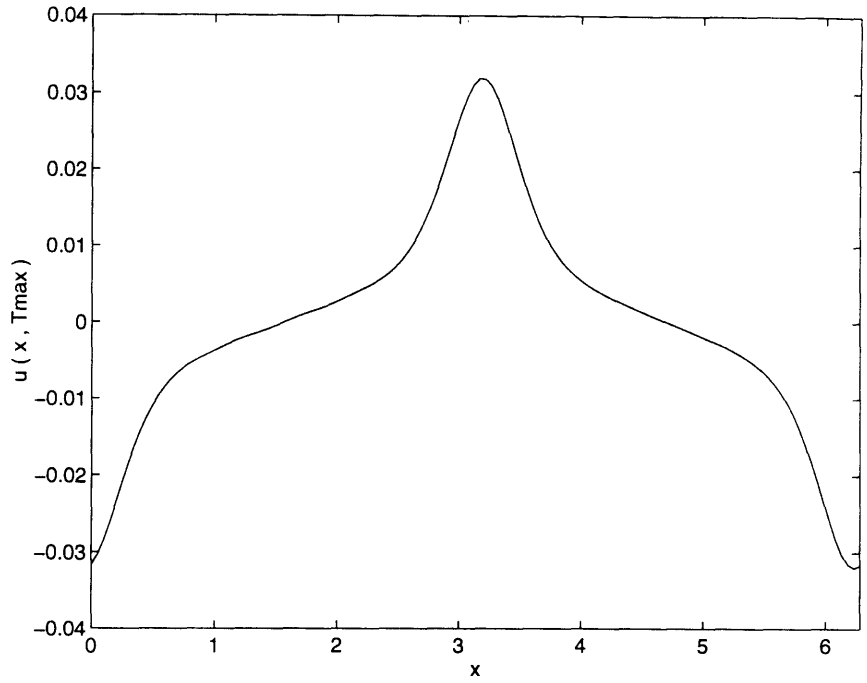

Figure 25: $u(x, \tau_{max})$ for $\epsilon = 0.01$, $\omega = 1.003630$ (TC 2).

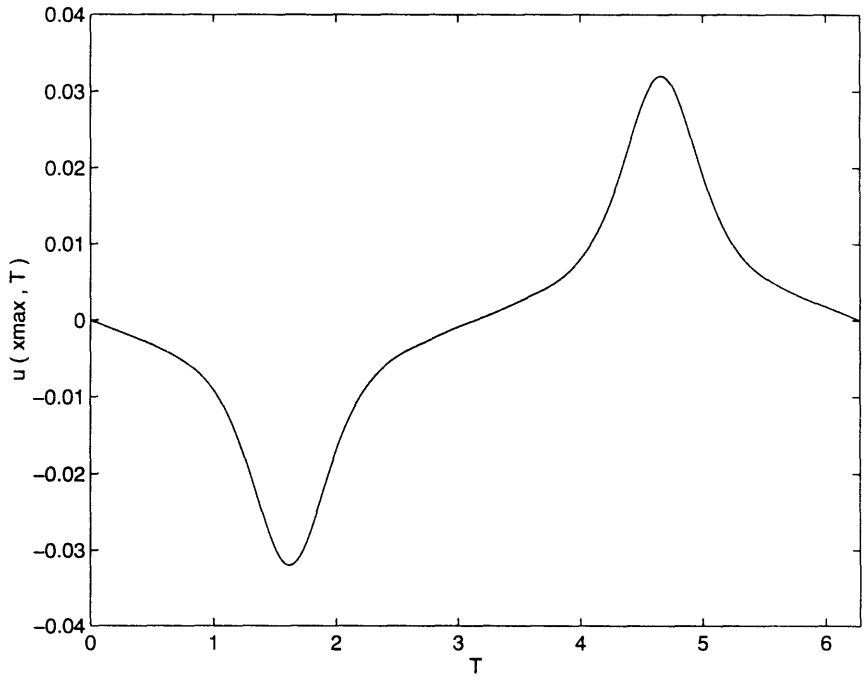

Figure 26: $u(x_{max}, \tau)$ for $\epsilon = 0.01$, $\omega = 1.003630$ (TC 2).

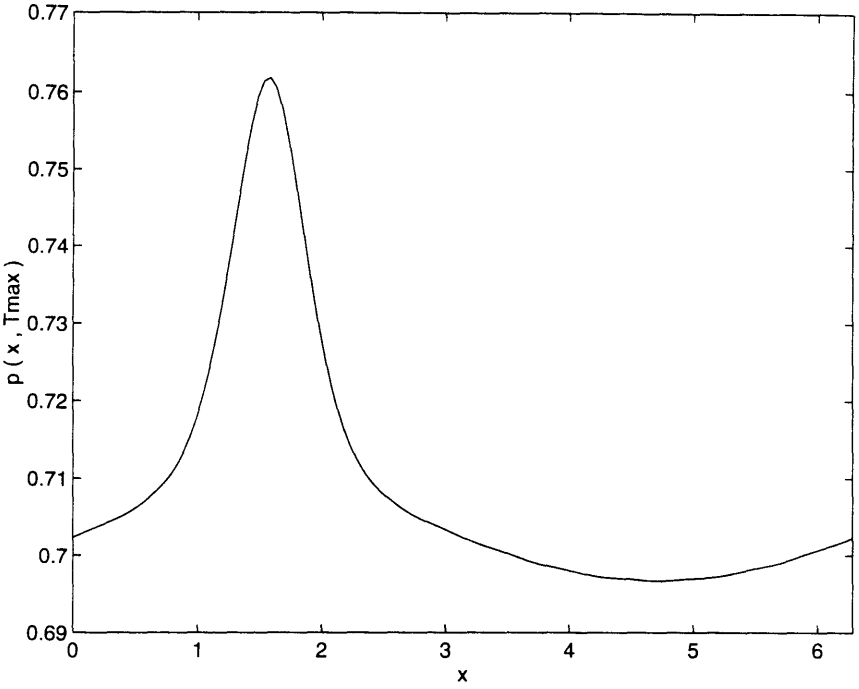

Figure 27: $p(x, \tau_{max})$ for $\epsilon = 0.01$, $\omega = 1.003630$ (TC 2).

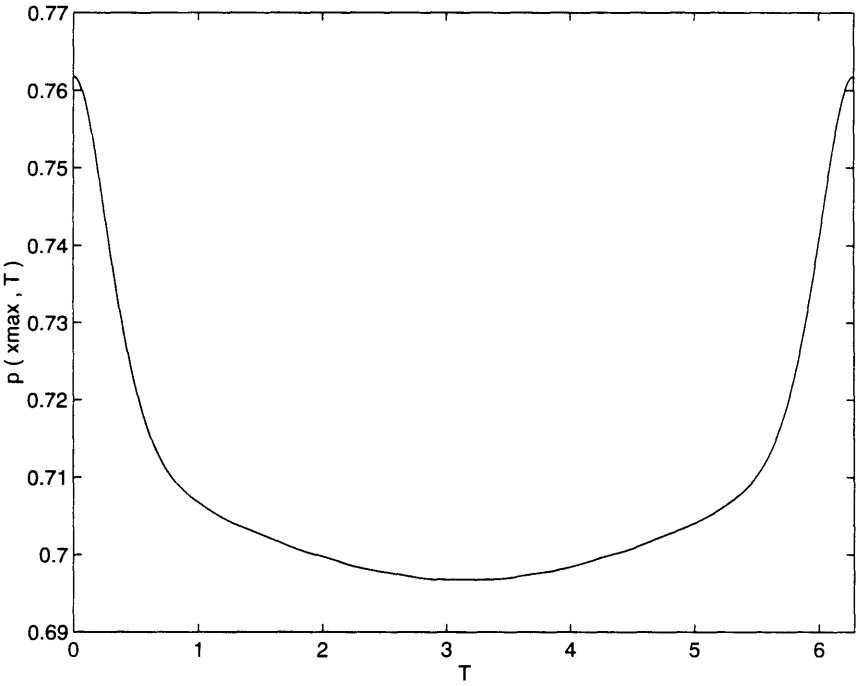

Figure 28: $p(x_{max}, \tau)$ for $\epsilon = 0.01$, $\omega = 1.003630$ (TC 2).

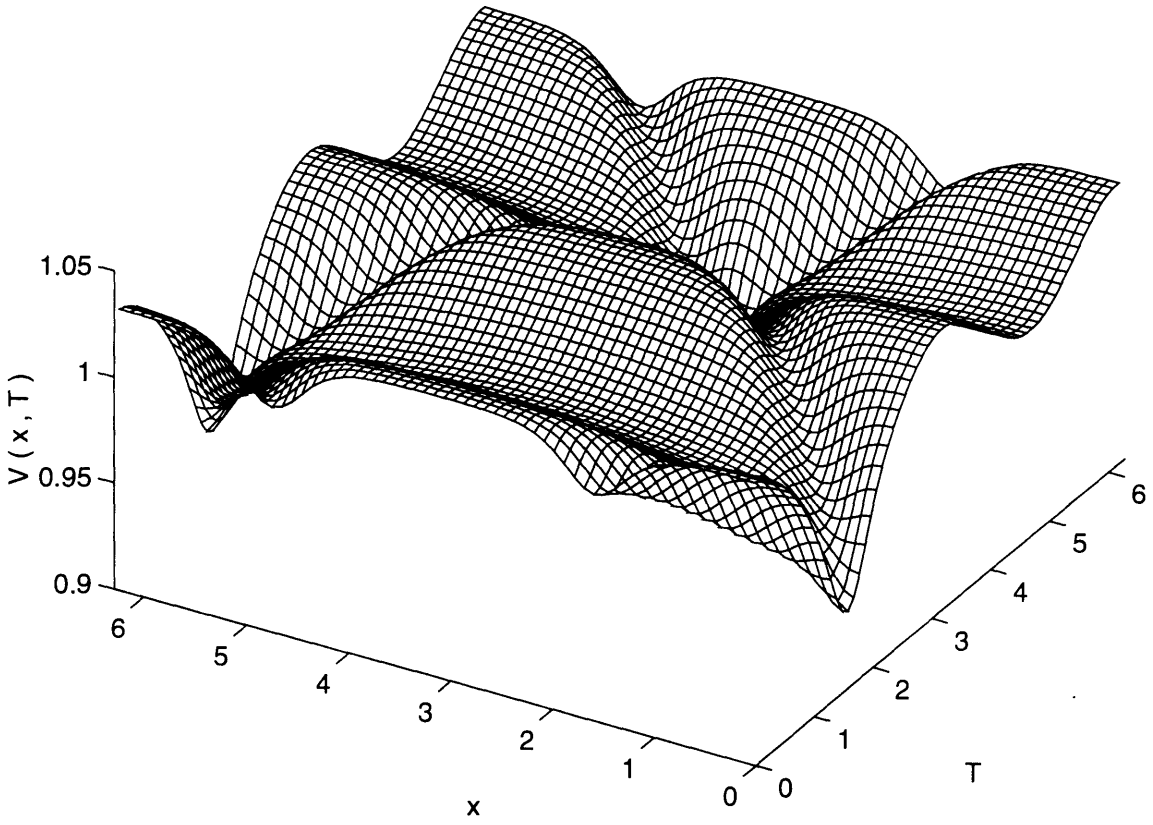

Figure 29: $V(x,\tau)$ for $\epsilon = 0.01$, $\omega = 1.003630$; $a = 0.00904$, $SPL = 159.1dB$, $M = 0.03178$, (TC 2).

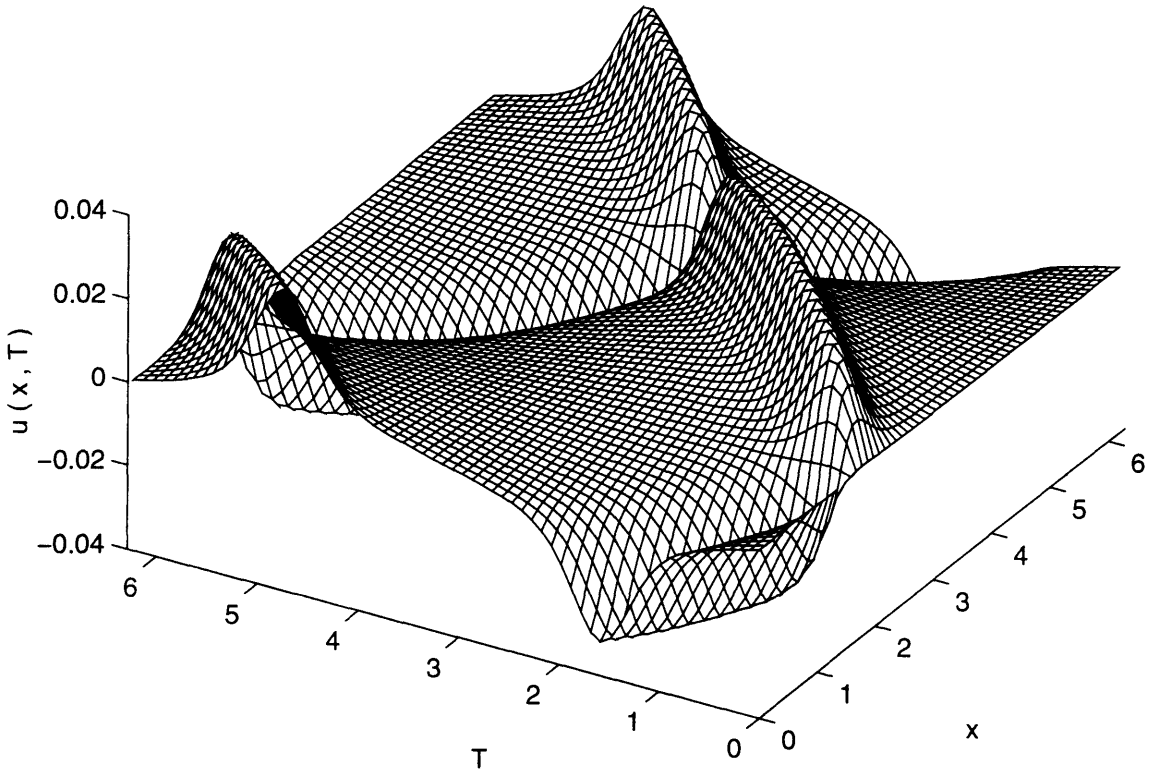

Figure 30: $u(x,\tau)$ for $\epsilon = 0.01$, $\omega = 1.003630$; $a = 0.00904$, $SPL = 159.1dB$, $M = 0.03178$, (TC 2).

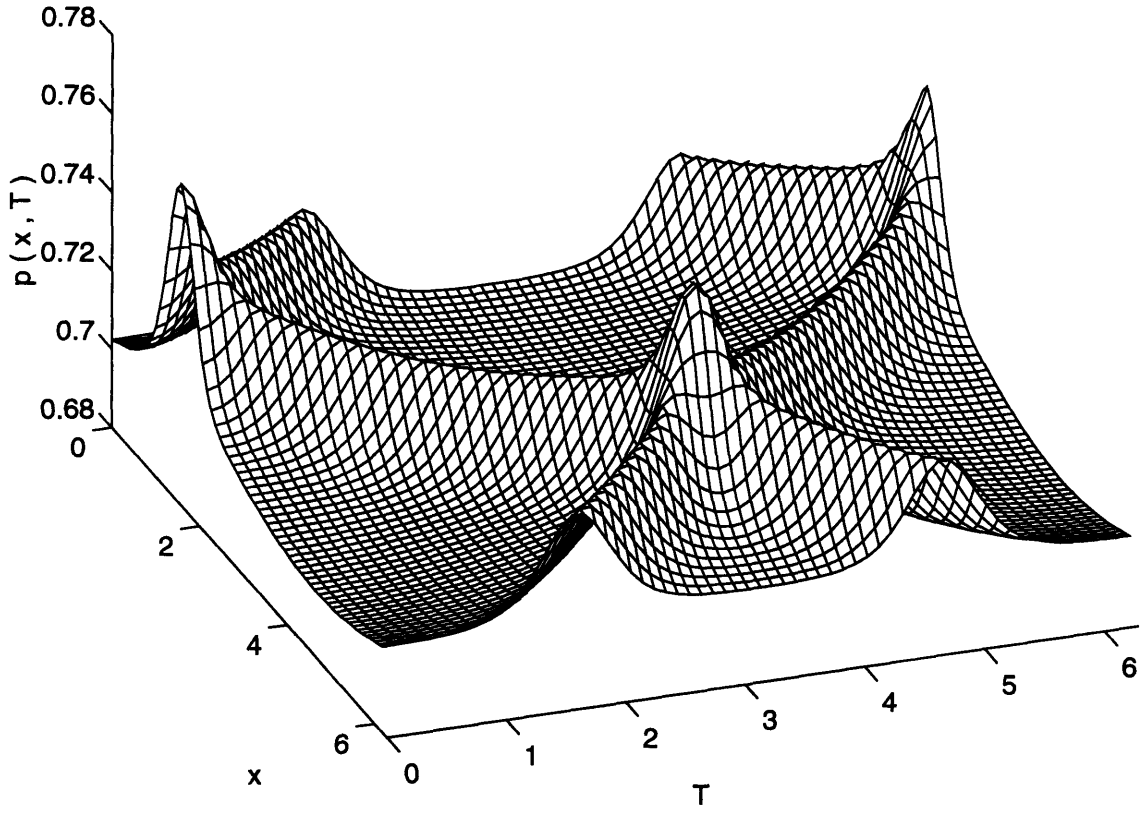

Figure 31: $p(x,\tau)$ for $\epsilon = 0.01$, $\omega = 1.003630$; $a = 0.00904$, $SPL = 159.1dB$, $M = 0.03178$, (TC 2).

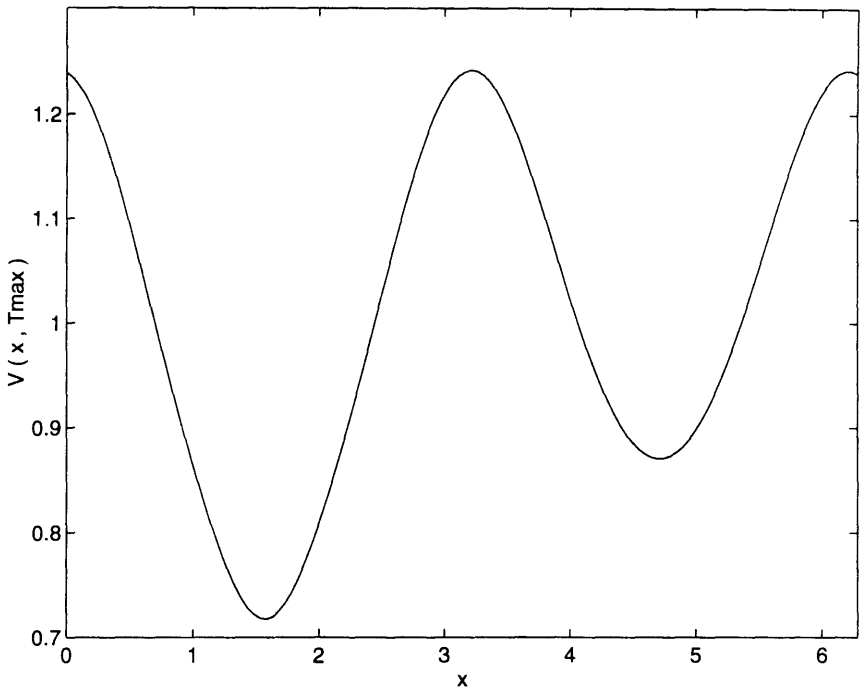

Figure 32: $V(x, \tau_{max})$ for $\epsilon = 0.1$, $\omega = 1.056186$ (TC 2).

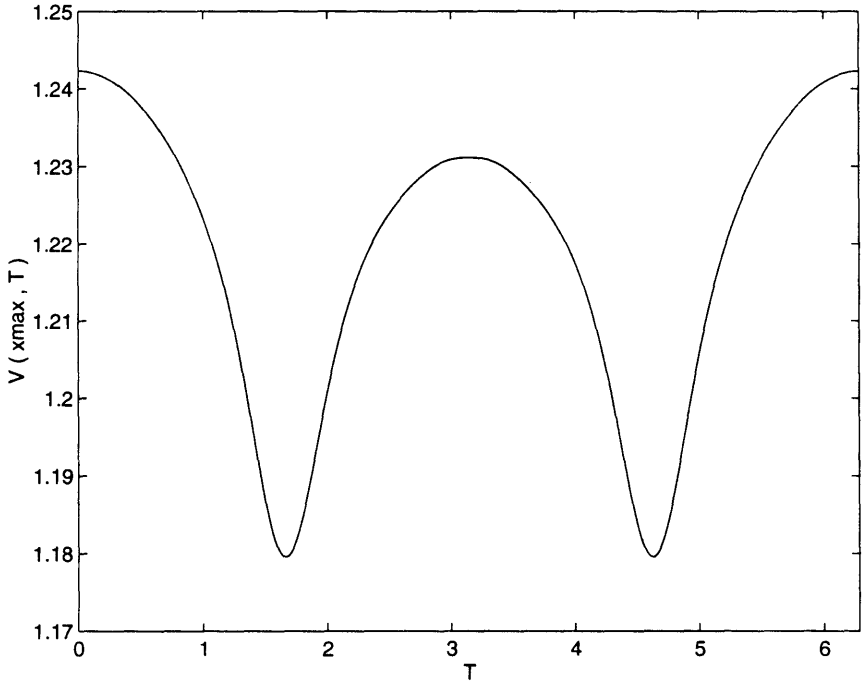

Figure 33: $V(x_{max}, \tau)$ for $\epsilon = 0.1$, $\omega = 1.056186$ (TC 2).

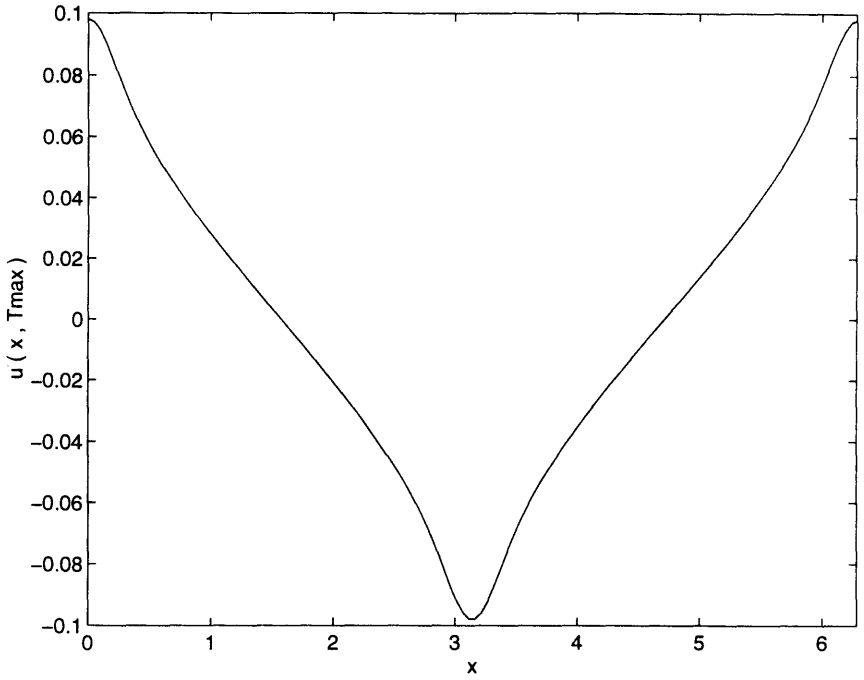

Figure 34: $u(x, \tau_{max})$ for $\epsilon = 0.1$, $\omega = 1.056186$ (TC 2).

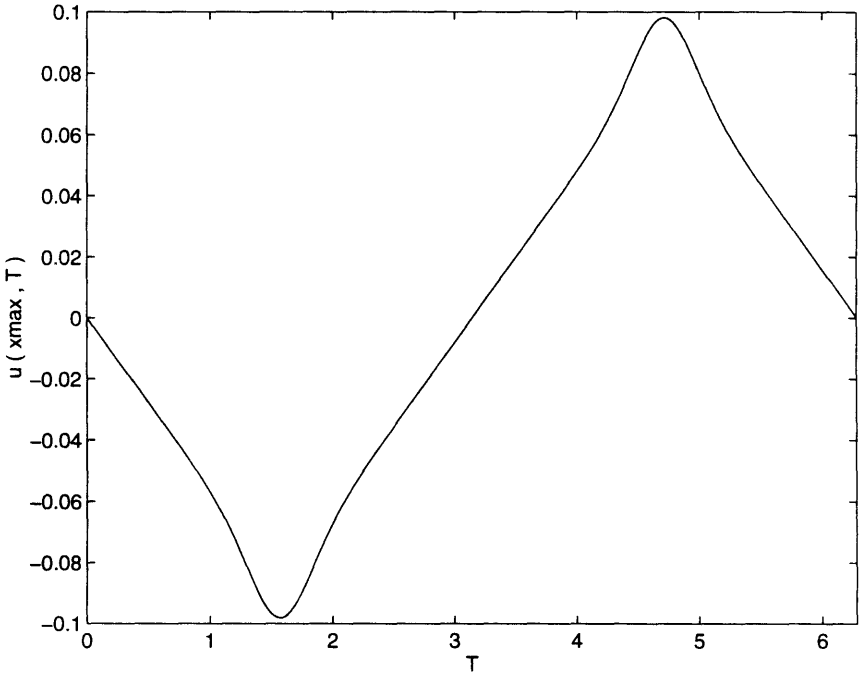

Figure 35: $u(x_{max}, \tau)$ for $\epsilon = 0.1$, $\omega = 1.056186$ (TC 2).

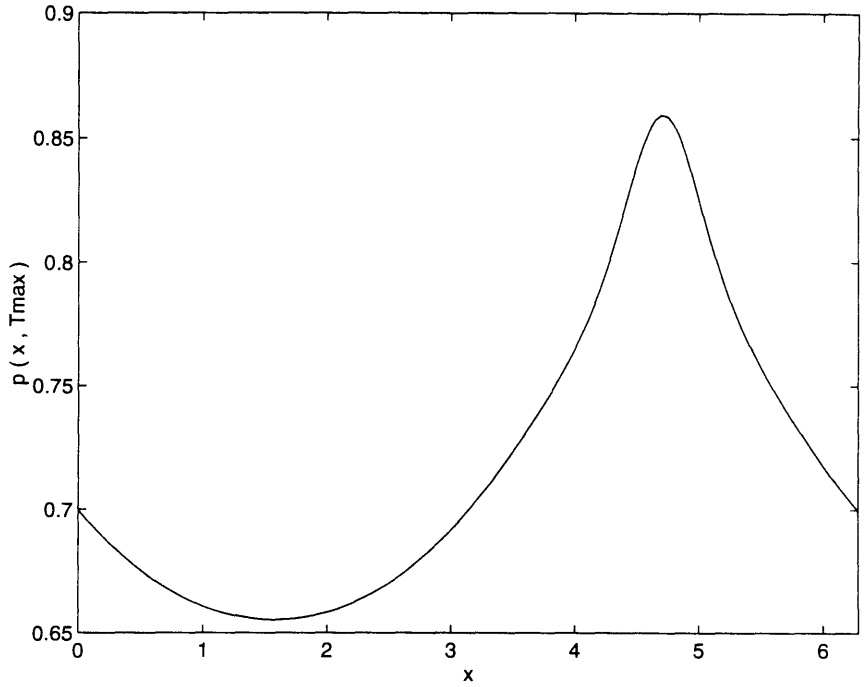

Figure 36: $p(x, \tau_{max})$ for $\epsilon = 0.1$, $\omega = 1.056186$ (TC 2).

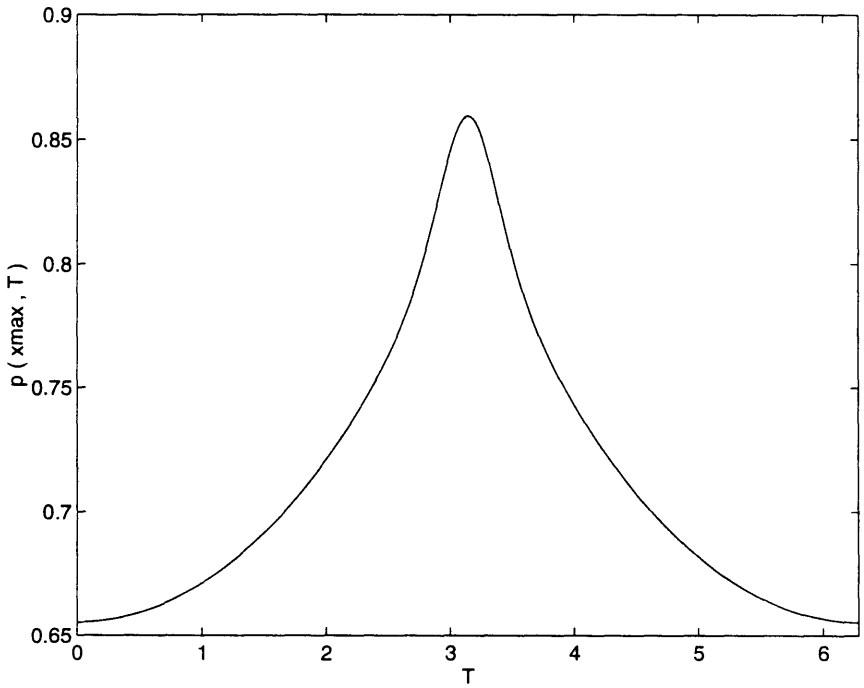

Figure 37: $p(x_{max}, \tau)$ for $\epsilon = 0.1$, $\omega = 1.056186$ (TC 2).

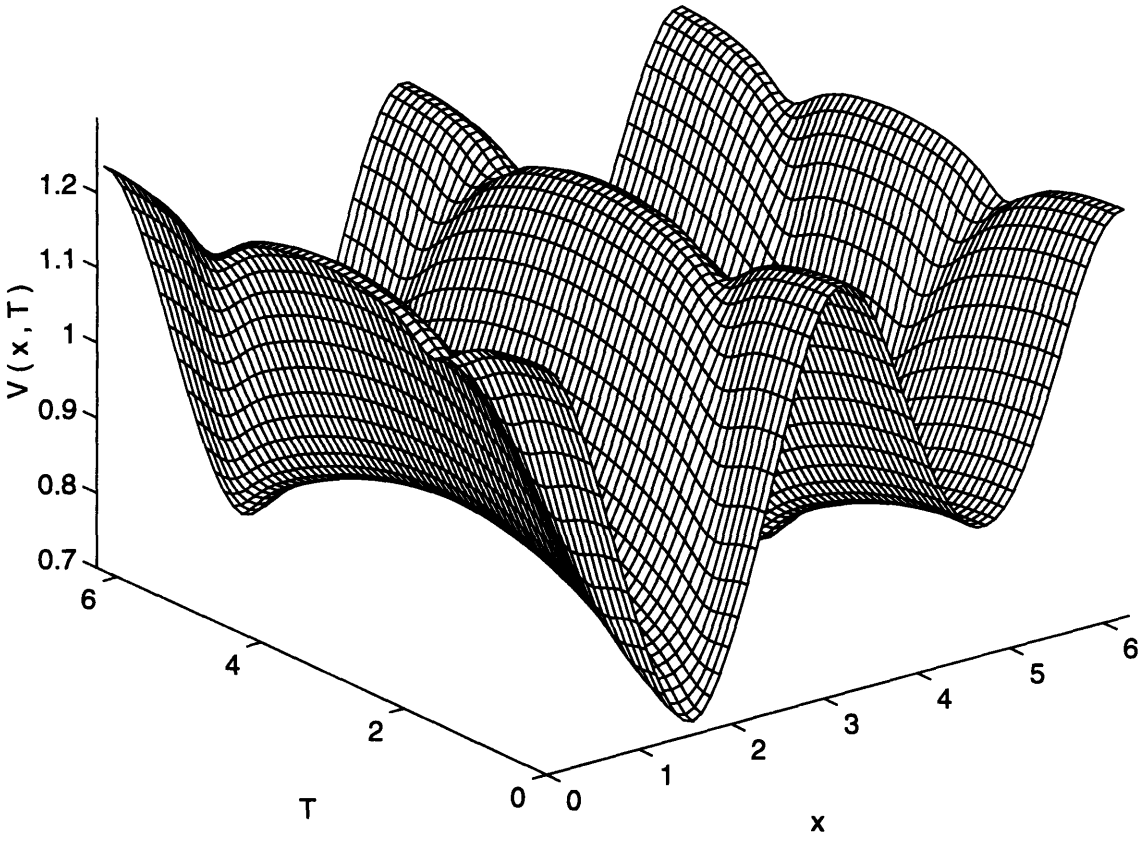

Figure 38: $V(x,\tau)$ for $\epsilon = 0.1$, $\omega = 1.056186$; $a = 0.03471$, $SPL = 169.4dB$, $M = 0.10430$, (TC 2).

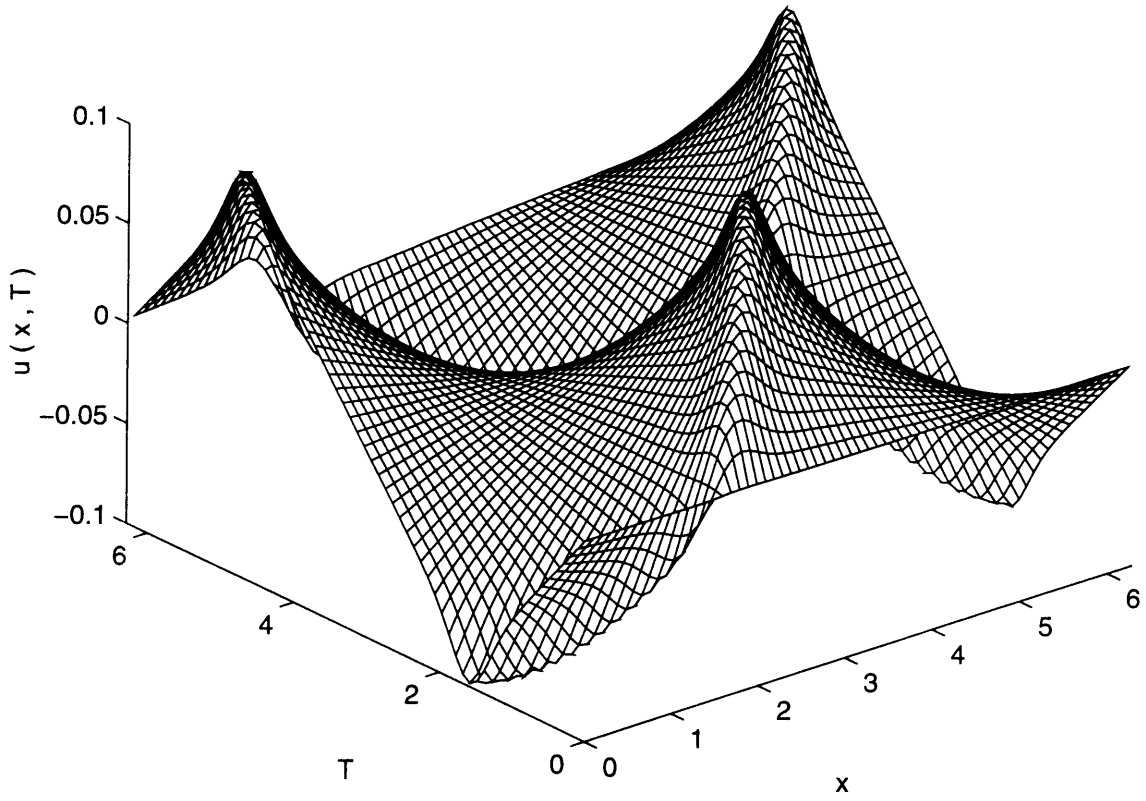

Figure 39: $u(x,\tau)$ for $\epsilon = 0.1$, $\omega = 1.056186$; $a = 0.03471$, $SPL = 169.4dB$, $M = 0.10430$, (TC 2).

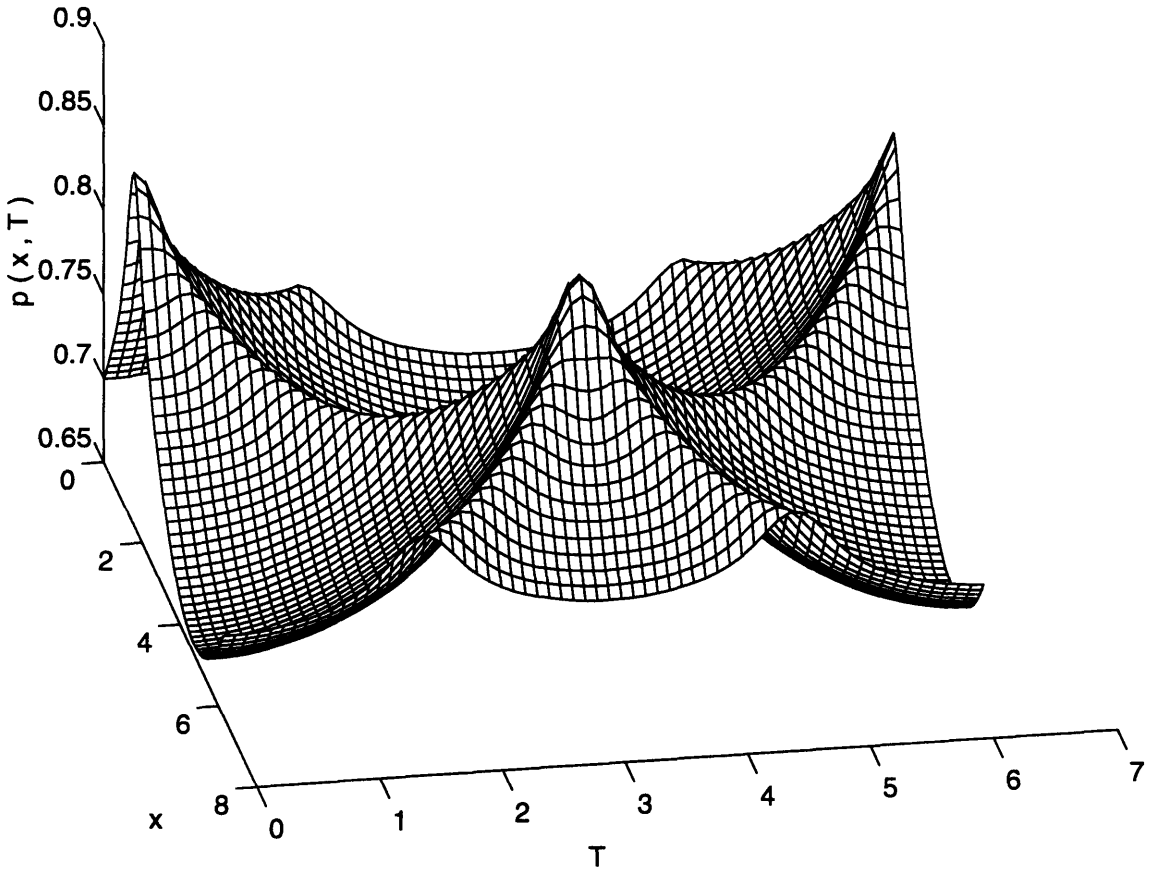

Figure 40: $p(x,\tau)$ for $\epsilon = 0.1$, $\omega = 1.056186$; $a = 0.03471$, $SPL = 169.4dB$, $M = 0.10430$, (TC 2).

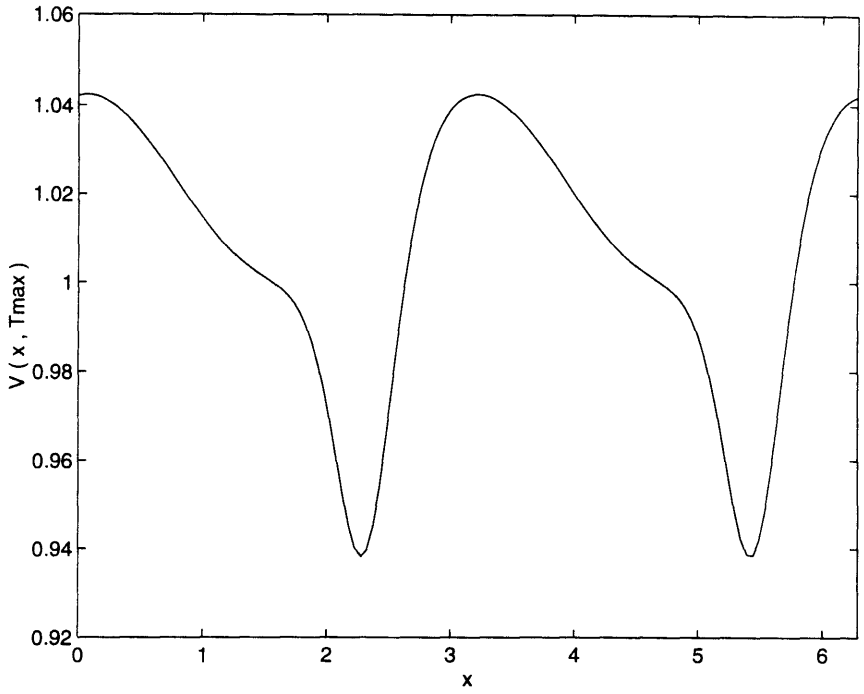

Figure 41: $V(x, \tau_{max})$ for $\epsilon = 0.01$, $\omega = 1.999307$ (TC 3).

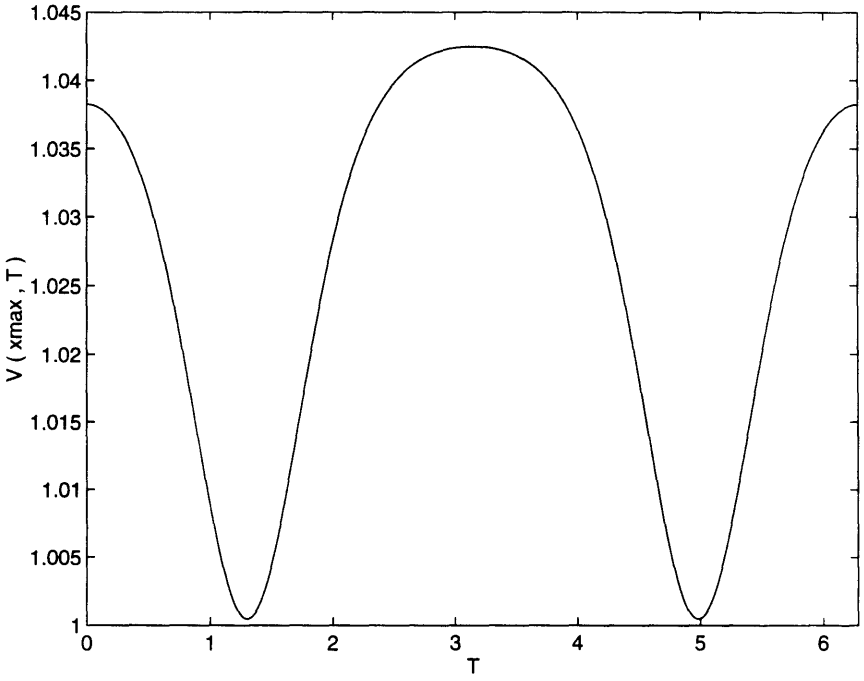

Figure 42: $V(x_{max}, \tau)$ for $\epsilon = 0.01$, $\omega = 1.999307$ (TC 3).

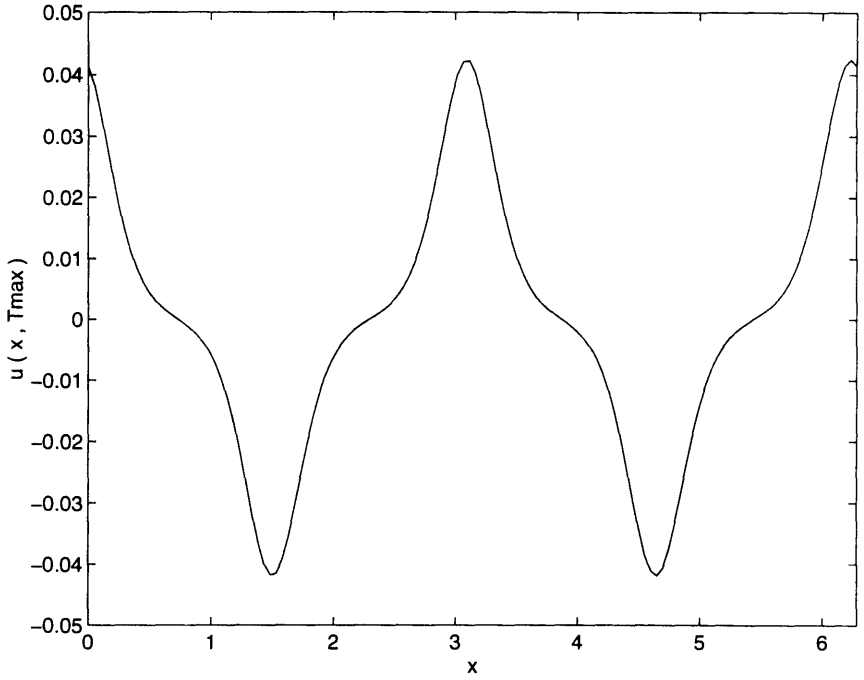

Figure 43: $u(x, \tau_{max})$ for $\epsilon = 0.01$, $\omega = 1.999307$ (TC 3).

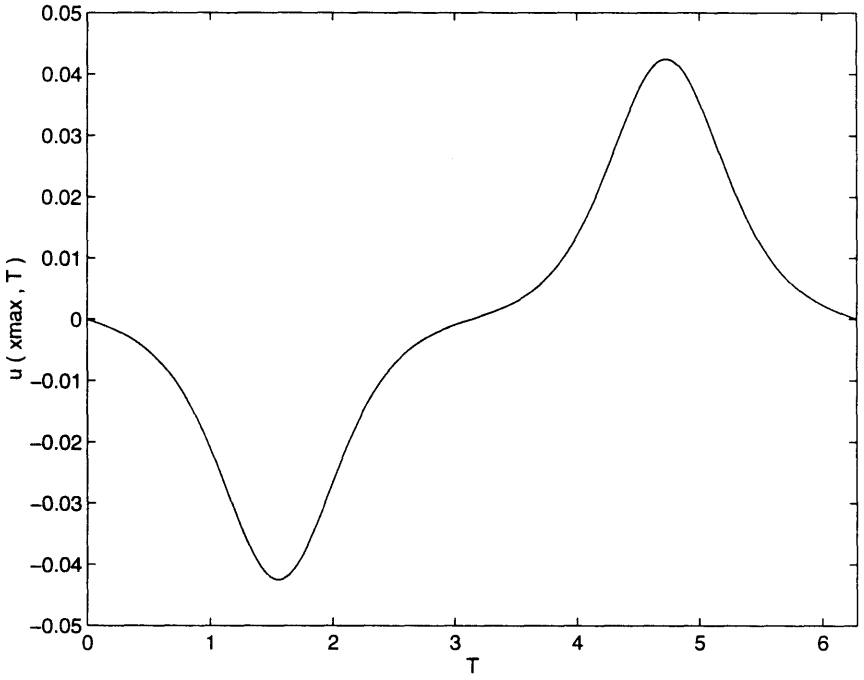

Figure 44: $u(x_{max}, \tau)$ for $\epsilon = 0.01$, $\omega = 1.999307$ (TC 3).

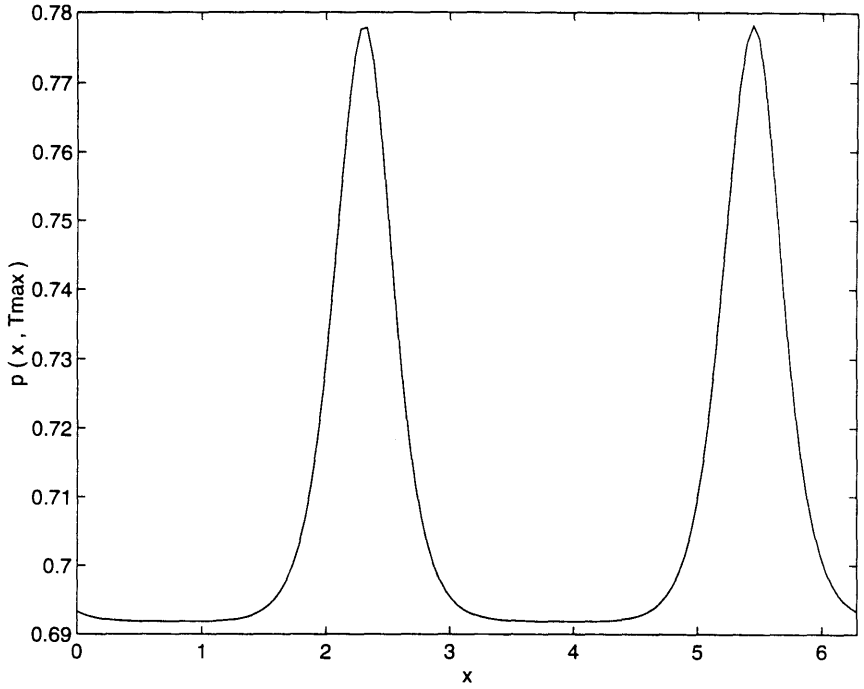

Figure 45: $p(x, \tau_{max})$ for $\epsilon = 0.01$, $\omega = 1.999307$ (TC 3).

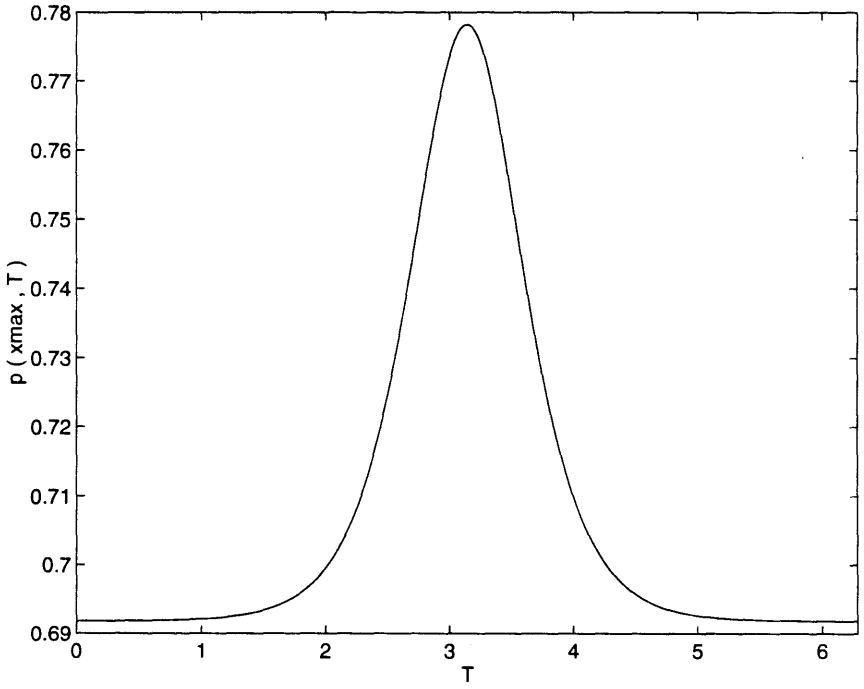

Figure 46: $p(x_{max}, \tau)$ for $\epsilon = 0.01$, $\omega = 1.999307$ (TC 3).

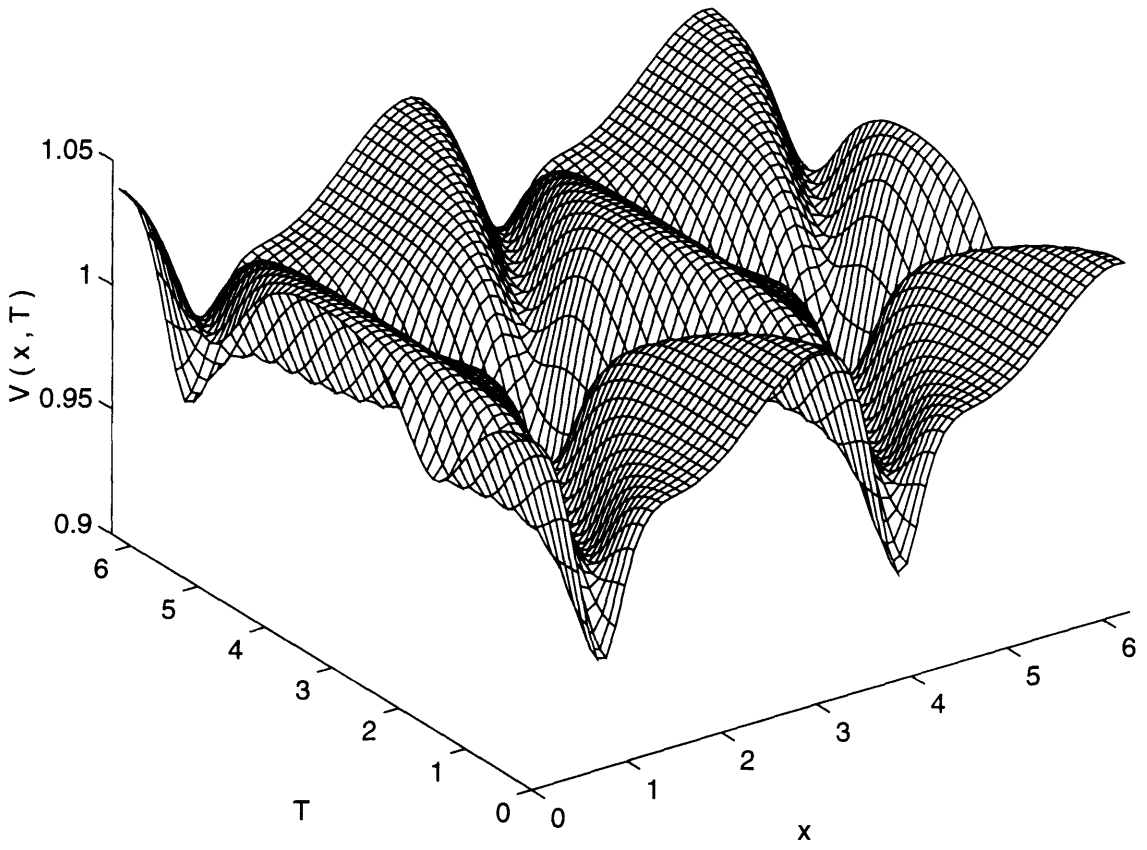

Figure 47: $V(x,\tau)$ for $\epsilon = 0.01$, $\omega = 1.999307$; $a = 0.00712$, $SPL = 162.5dB$, $M = 0.04191$, (TC 3).

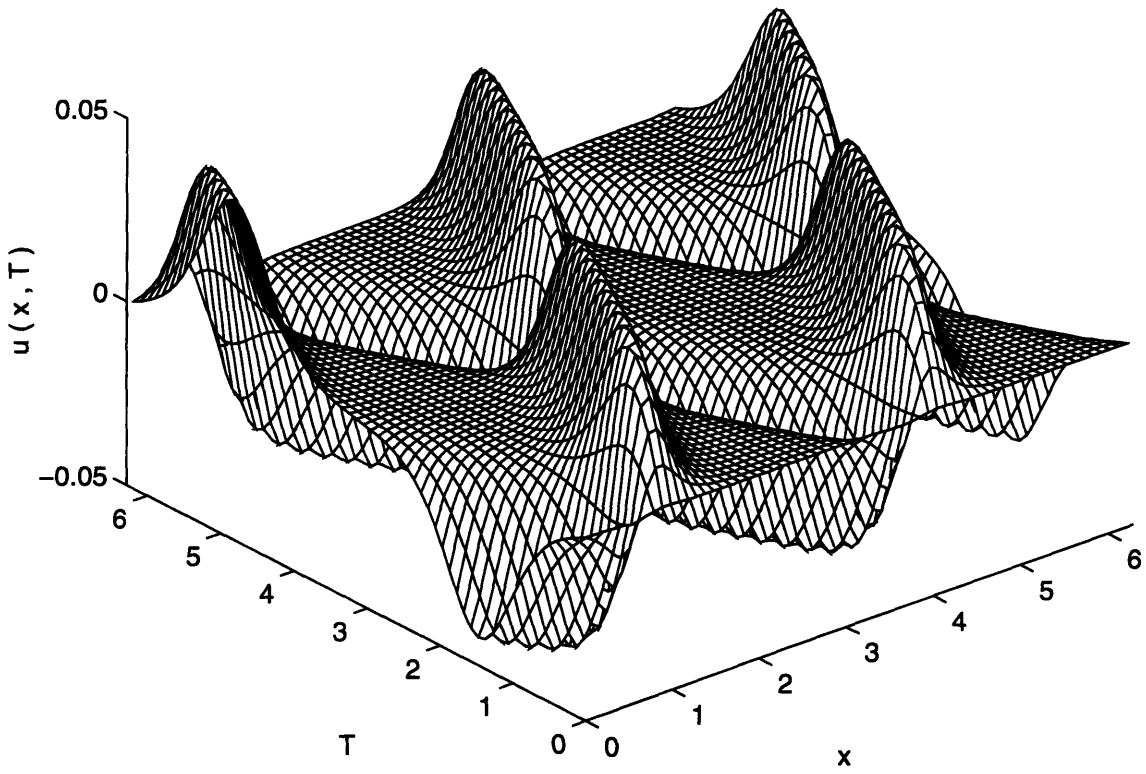

Figure 48: $u(x,\tau)$ for $\epsilon = 0.01$, $\omega = 1.999307$; $a = 0.00712$, $SPL = 162.5dB$, $M = 0.04191$, (TC 3).

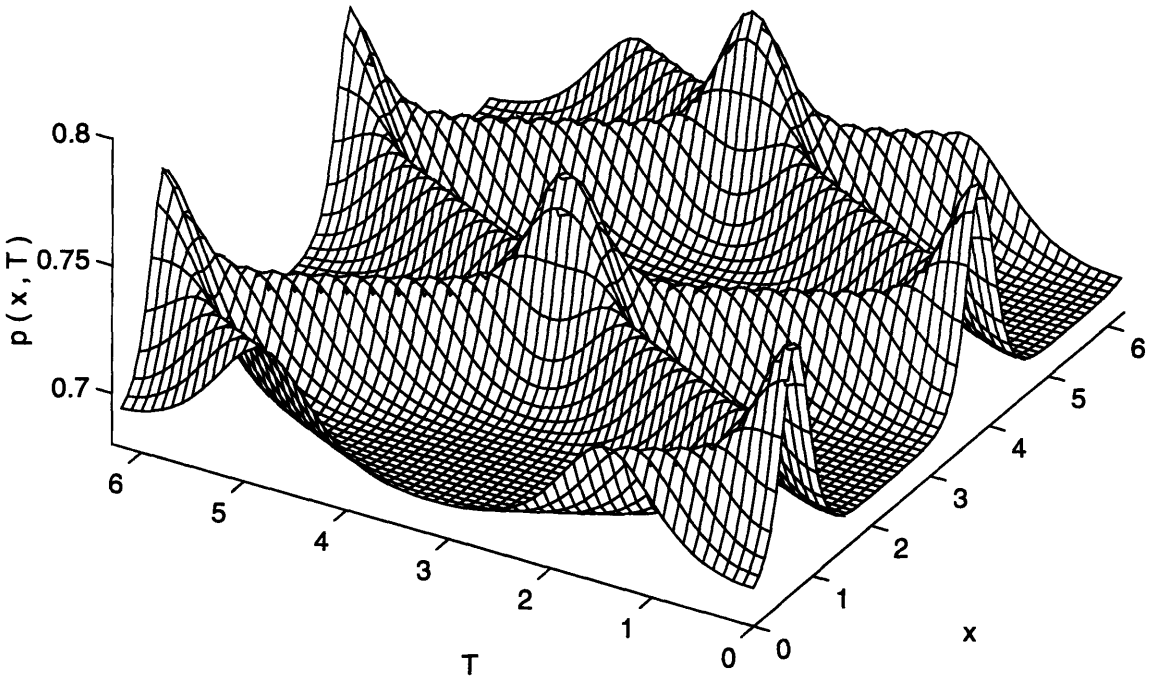

Figure 49: $p(x,\tau)$ for $\epsilon = 0.01$, $\omega = 1.999307$; $a = 0.00712$, $SPL = 162.5dB$, $M = 0.04191$, (TC 3).

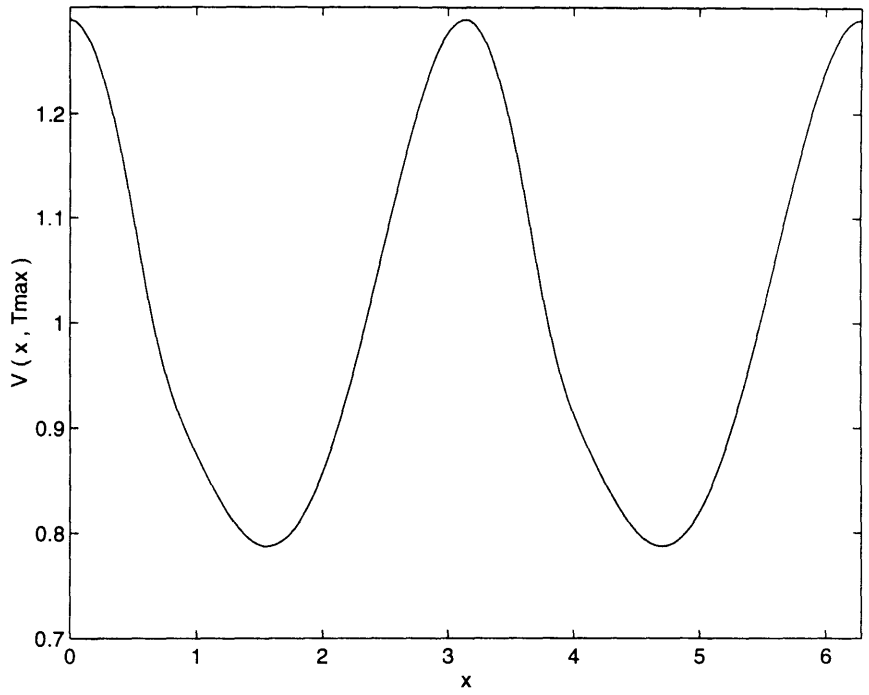

Figure 50: $V(x, \tau_{max})$ for $\epsilon = 0.1237$, $\omega = 2.01723$ (TC 3).

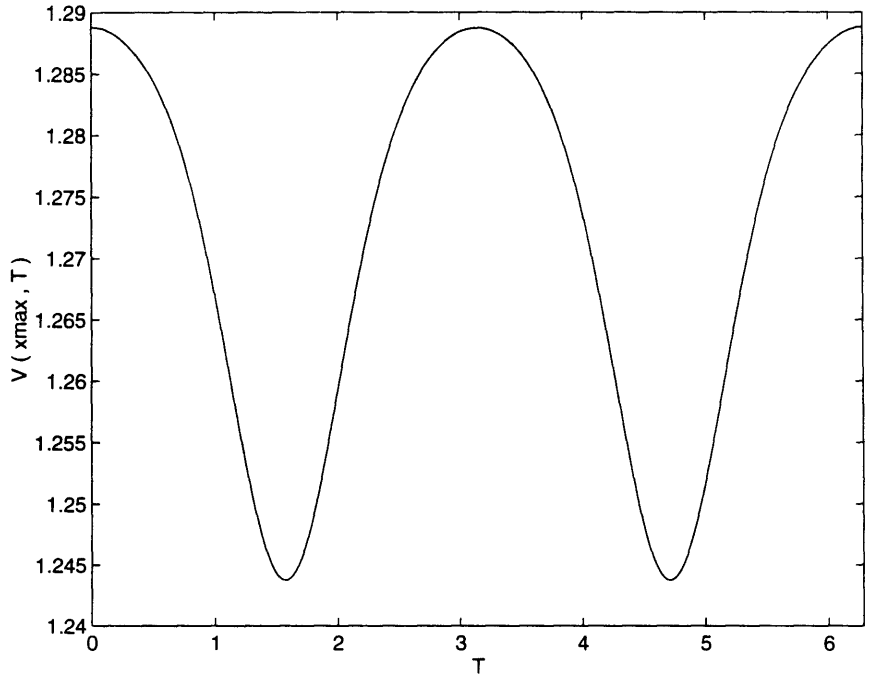

Figure 51: $V(x_{max}, \tau)$ for $\epsilon = 0.1237$, $\omega = 2.01723$ (TC 3).

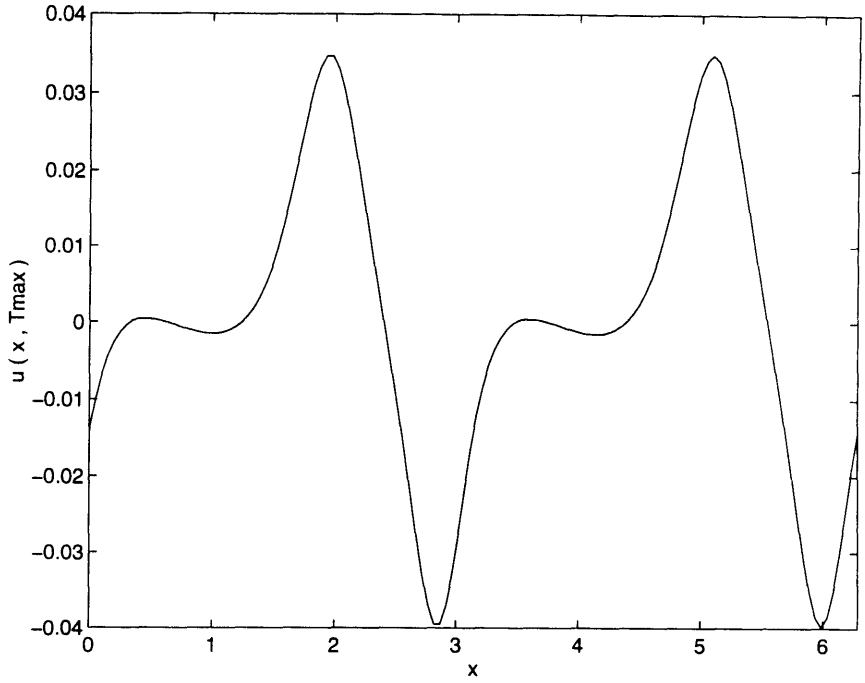

Figure 52: $u(x, \tau_{max})$ for $\epsilon = 0.1237$, $\omega = 2.01723$ (TC 3).

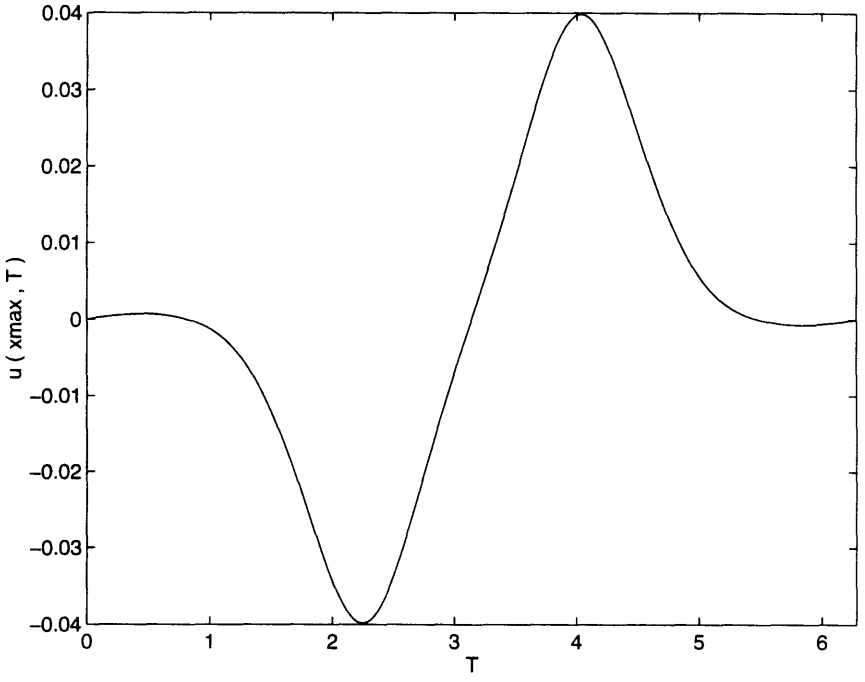

Figure 53: $u(x_{max}, \tau)$ for $\epsilon = 0.1237$, $\omega = 2.01723$ (TC 3).

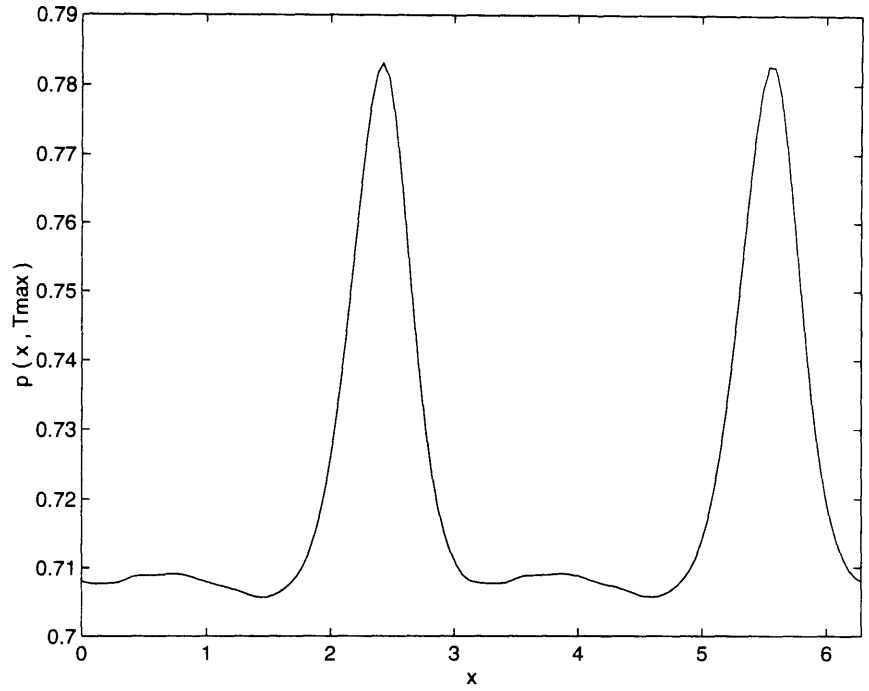

Figure 54: $p(x, \tau_{max})$ for $\epsilon = 0.1237$, $\omega = 2.01723$ (TC 3).

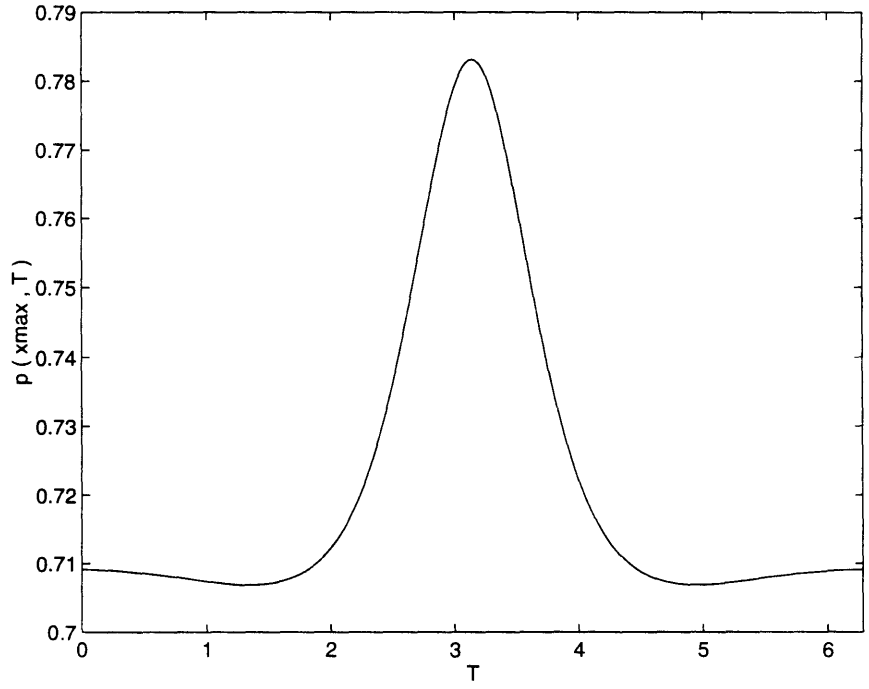

Figure 55: $p(x_{max}, \tau)$ for $\epsilon = 0.1237$, $\omega = 2.01723$ (TC 3).

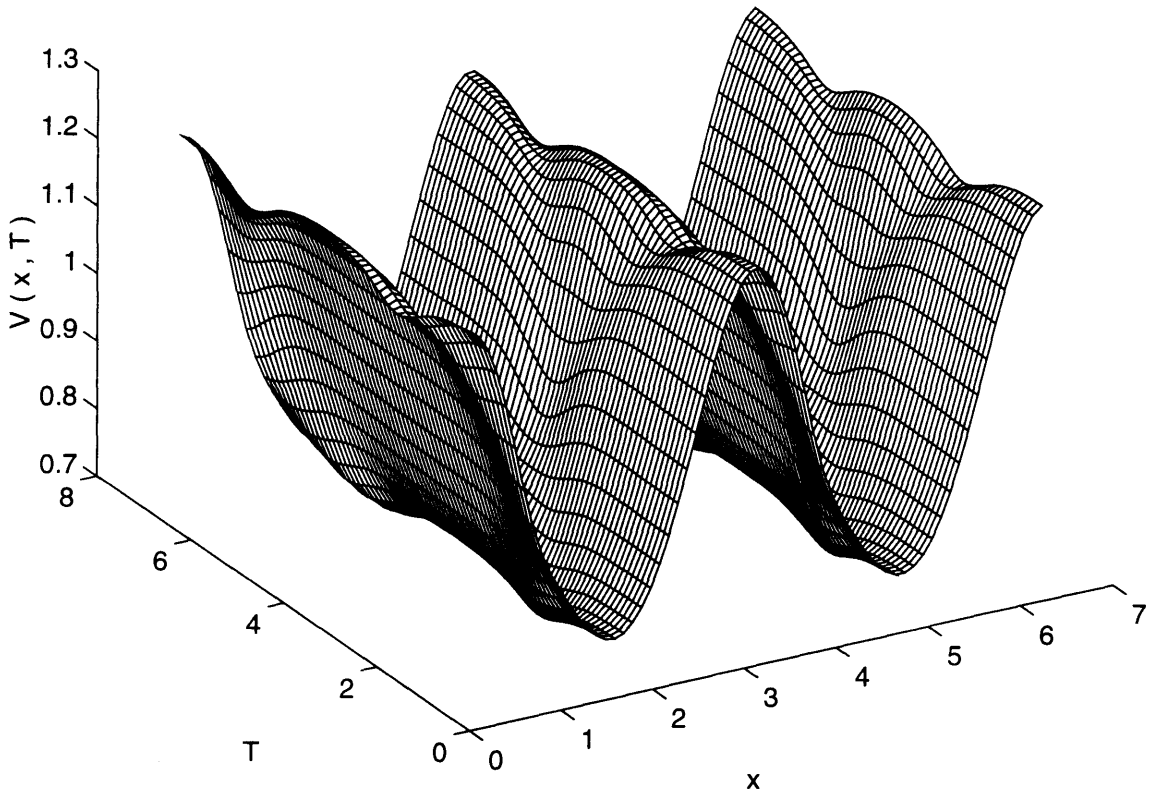

Figure 56: $V(x,\tau)$ for $\epsilon = 0.1237$, $\omega = 2.01723$; $a = 0.00603$, $SPL = 162.0dB$, $M = 0.04306$, (TC 3).

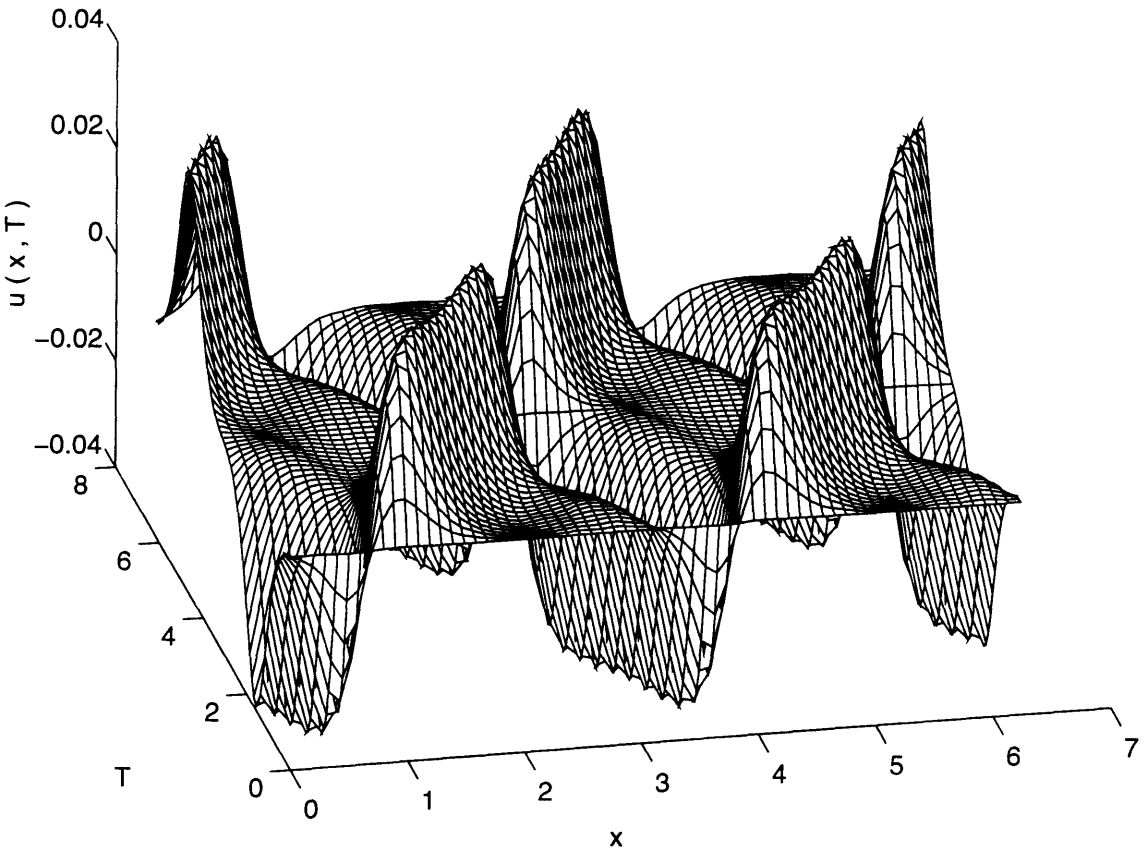

Figure 57: $u(x,\tau)$ for $\epsilon = 0.1237$, $\omega = 2.01723$; $a = 0.00603$, $SPL = 162.0dB$, $M = 0.04306$, (TC 3).

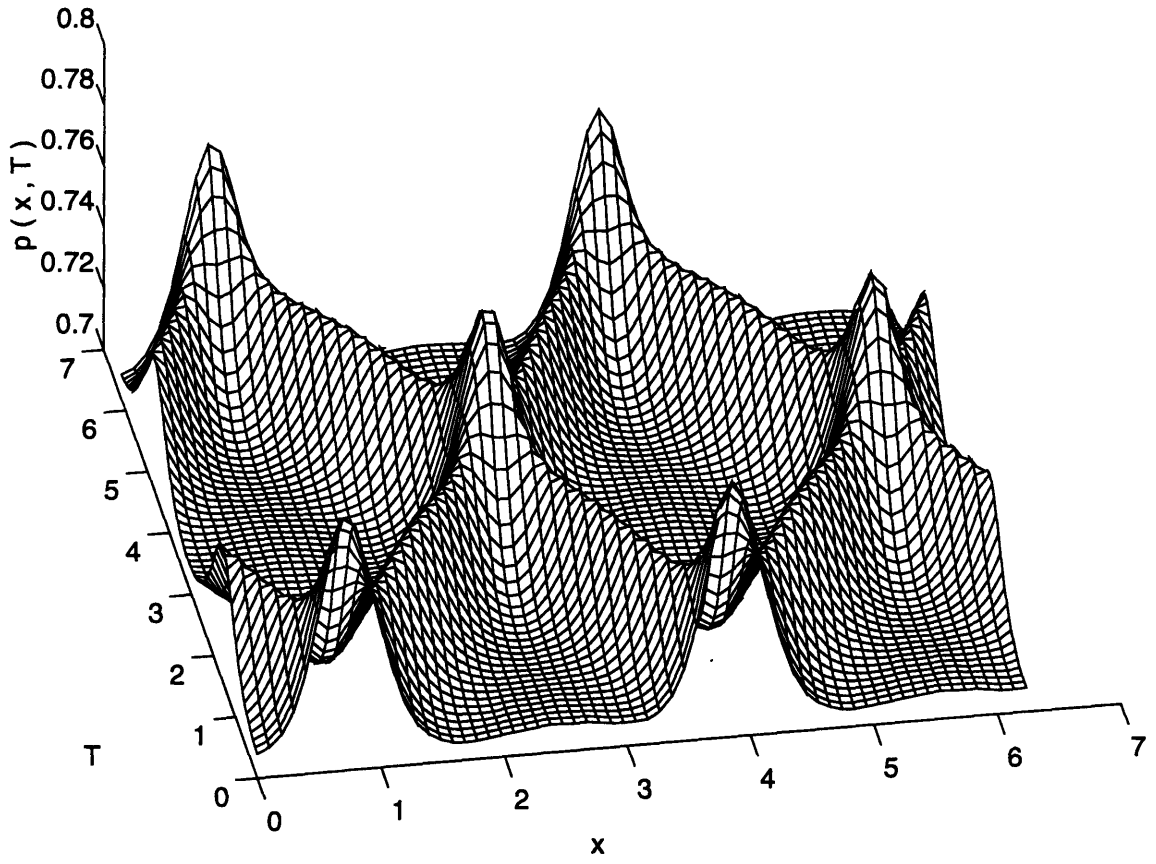

Figure 58: $p(x,\tau)$ for $\epsilon = 0.1237$, $\omega = 2.01723$; $a = 0.00603$, $SPL = 162.0dB$, $M = 0.04306$, (TC 3).

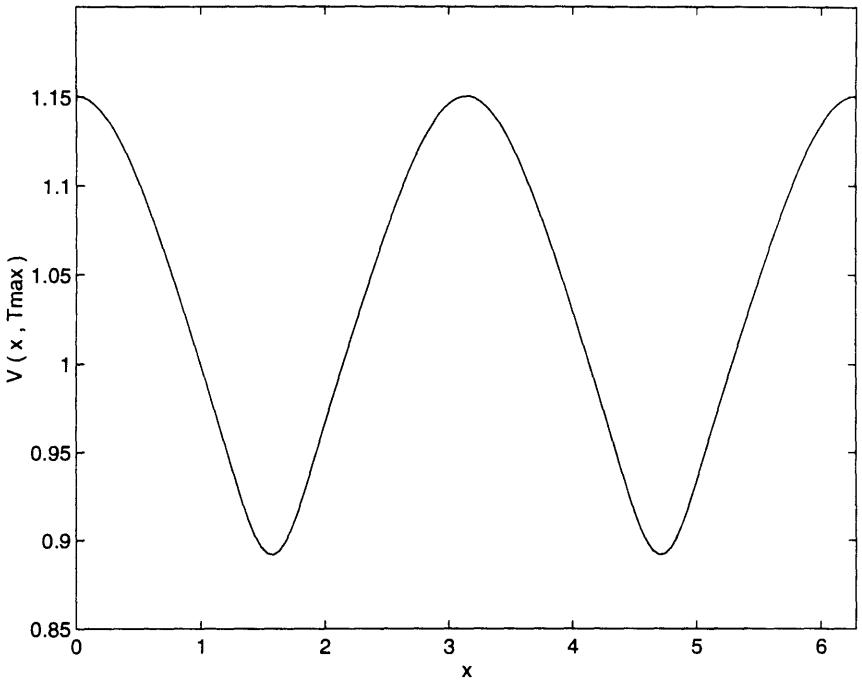

Figure 59: $V(x, \tau_{max})$ for $\epsilon = 0.04562$, $\omega = 1.93115$ (TC 4).

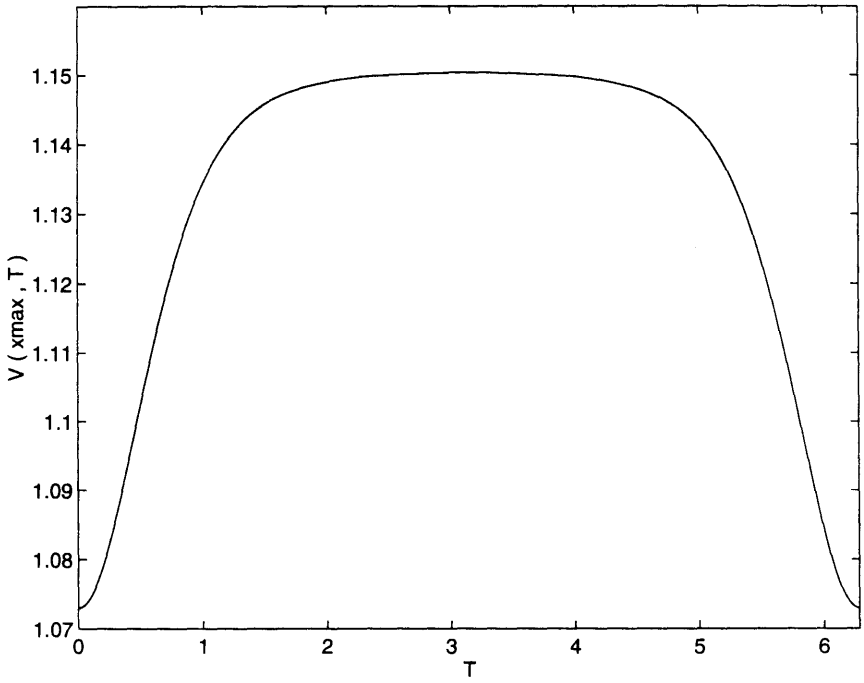

Figure 60: $V(x_{max}, \tau)$ for $\epsilon = 0.04562$, $\omega = 1.93115$ (TC 4).

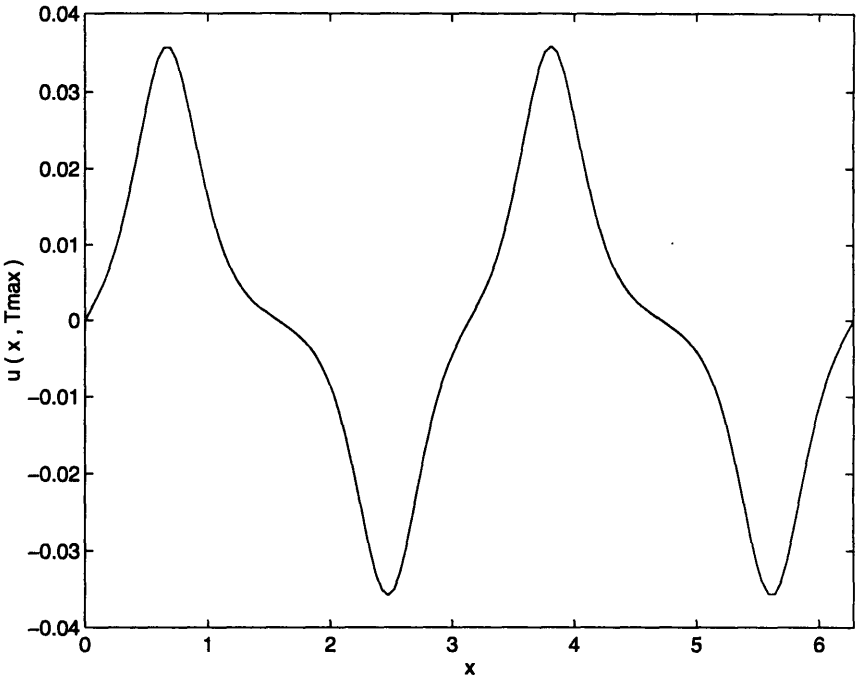

Figure 61: $u(x, \tau_{max})$ for $\epsilon = 0.04562$, $\omega = 1.93115$ (TC 4).

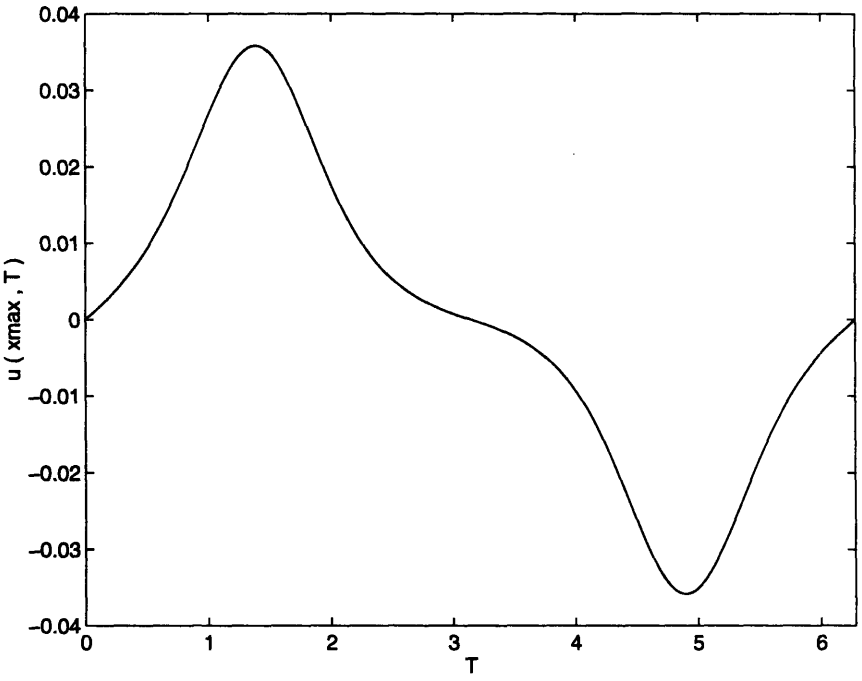

Figure 62: $u(x_{max}, \tau)$ for $\epsilon = 0.04562$, $\omega = 1.93115$ (TC 4).

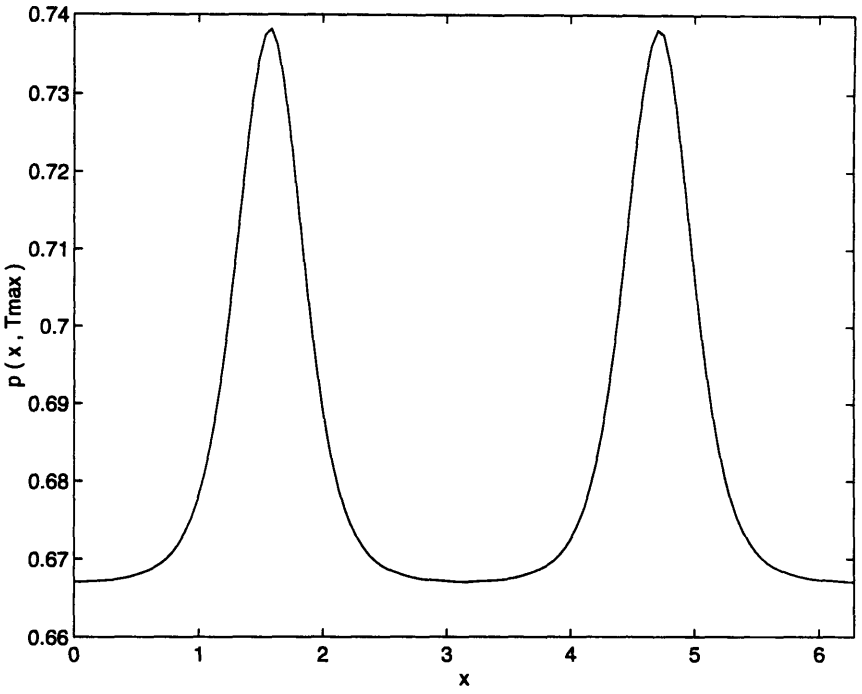

Figure 63: $p(x, \tau_{max})$ for $\epsilon = 0.04562$, $\omega = 1.93115$ (TC 4).

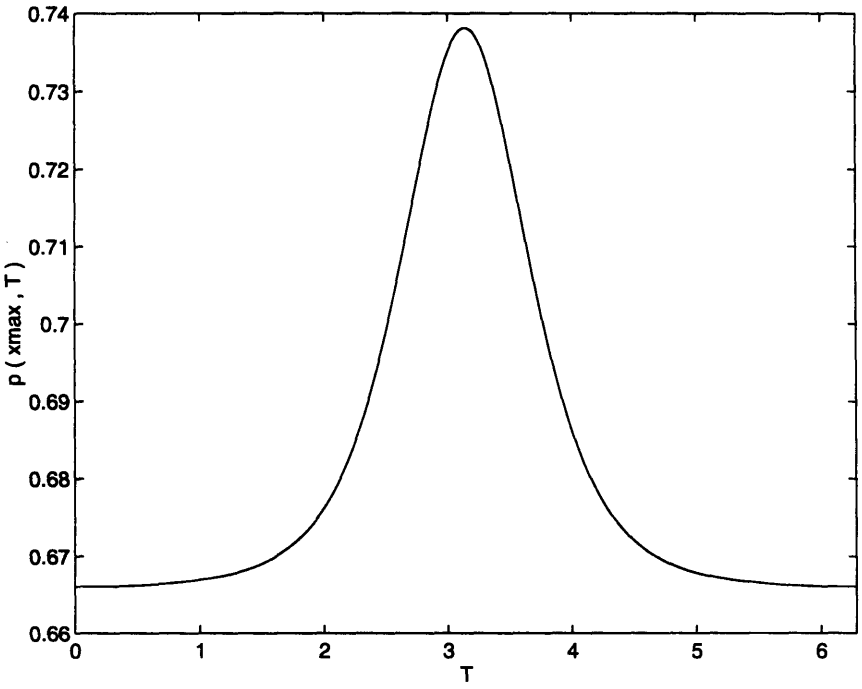

Figure 64: $p(x_{max}, \tau)$ for $\epsilon = 0.04562$, $\omega = 1.93115$ (TC 4).

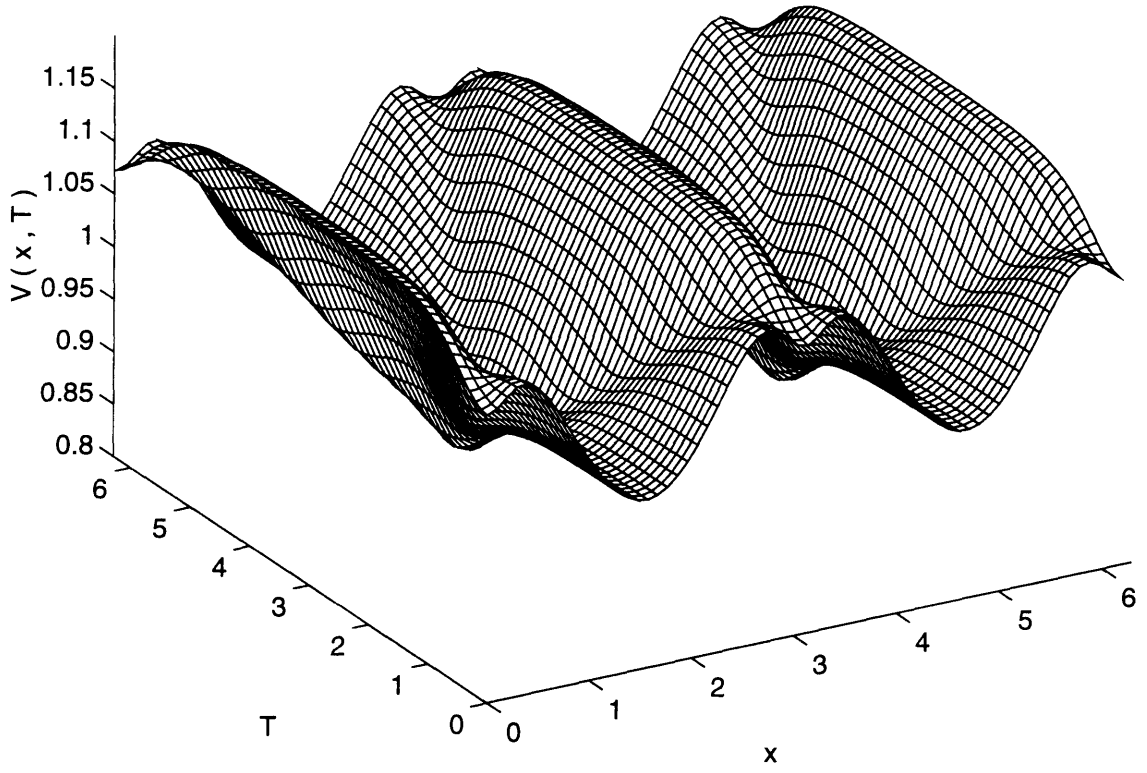

Figure 65: $V(x,\tau)$ for $\epsilon = 0.04562$, $\omega = 1.93115$; $a = 0.00676$, $SPL = 168.4dB$, $M = 0.03709$, (TC 4).

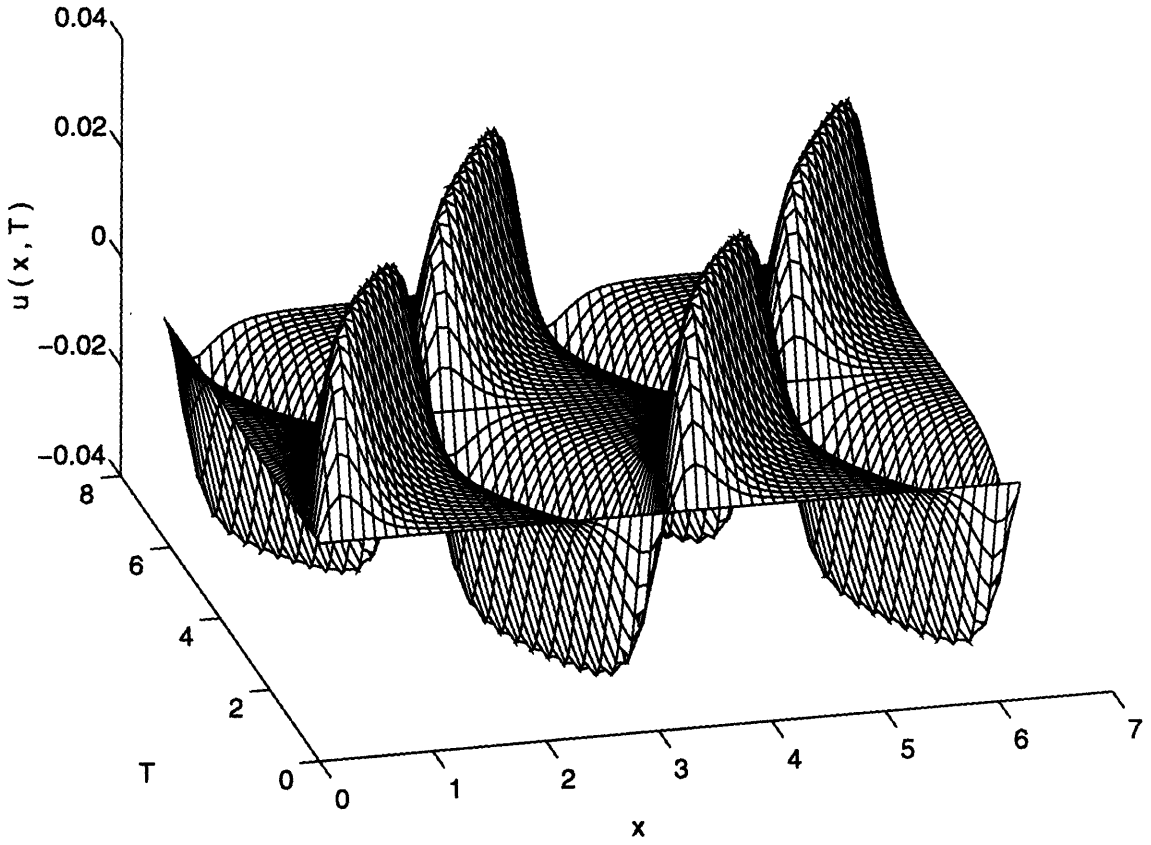

Figure 66: $u(x,\tau)$ for $\epsilon = 0.04562$, $\omega = 1.93115$; $a = 0.00676$, $SPL = 168.4dB$, $M = 0.03709$, (TC 4).

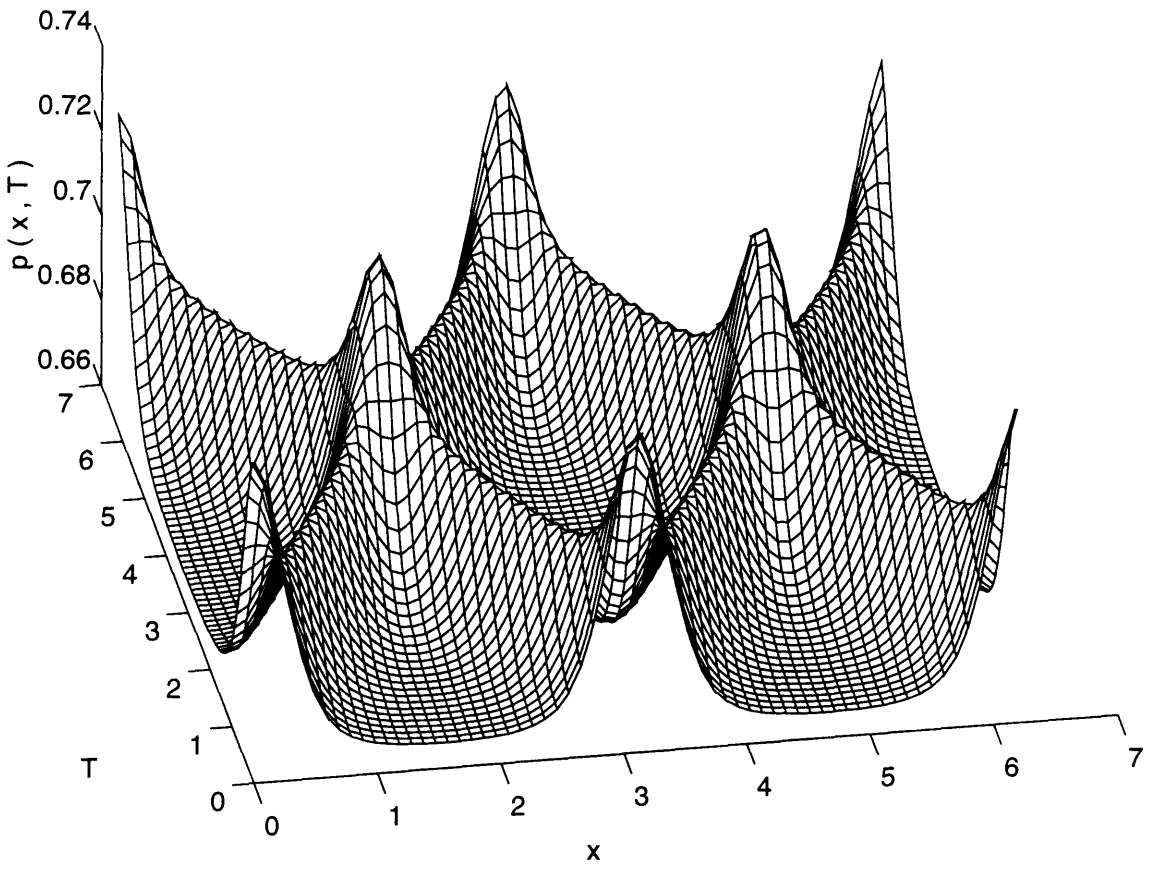

Figure 67: $p(x,\tau)$ for $\epsilon = 0.04562$, $\omega = 1.93115$; $a = 0.00676$, $SPL = 168.4dB$, $M = 0.03709$, (TC 4).

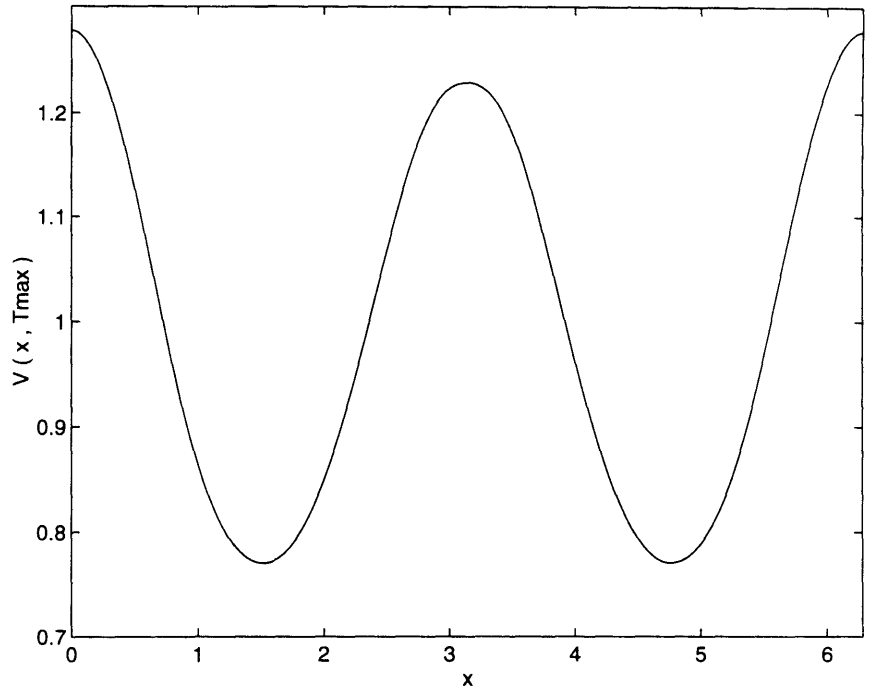

Figure 68: $V(x, \tau_{max})$ for $\epsilon = 0.1237$, $\omega = 3.04496$ (TC 5).

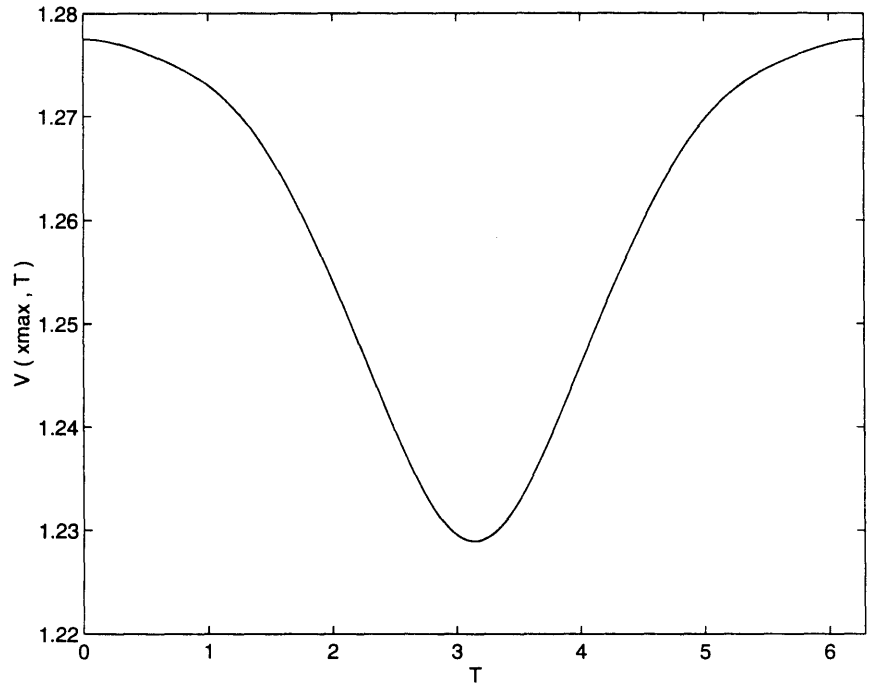

Figure 69: $V(x_{max}, \tau)$ for $\epsilon = 0.1237$, $\omega = 3.04496$ (TC 5).

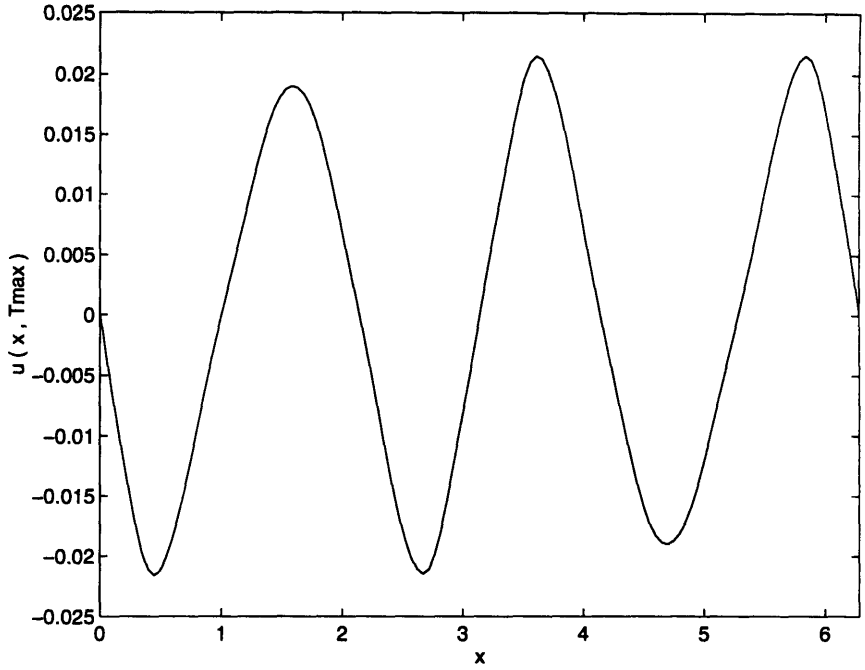

Figure 70: $u(x, \tau_{max})$ for $\epsilon = 0.1237$, $\omega = 3.04496$ (TC 5).

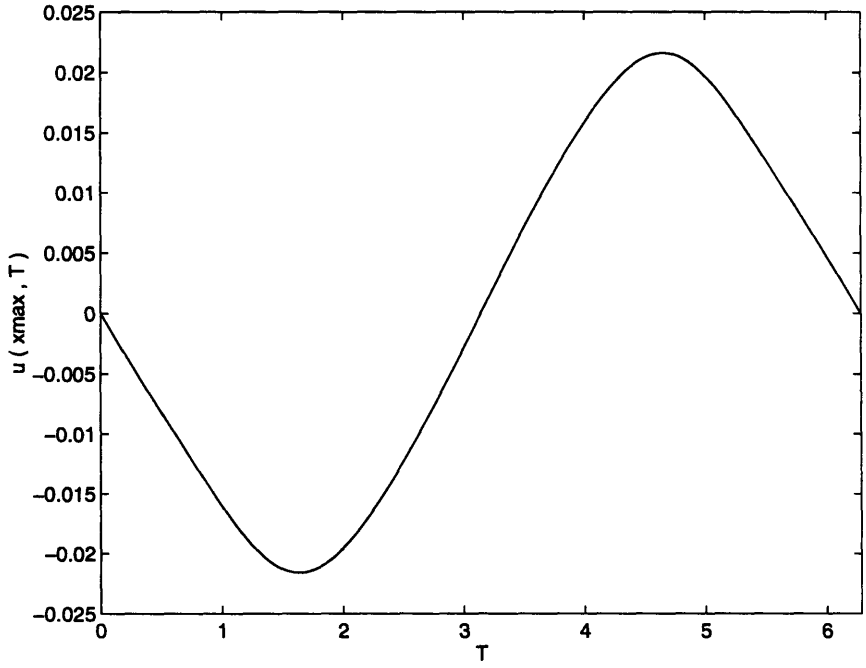

Figure 71: $u(x_{max}, \tau)$ for $\epsilon = 0.1237$, $\omega = 3.04496$ (TC 5).

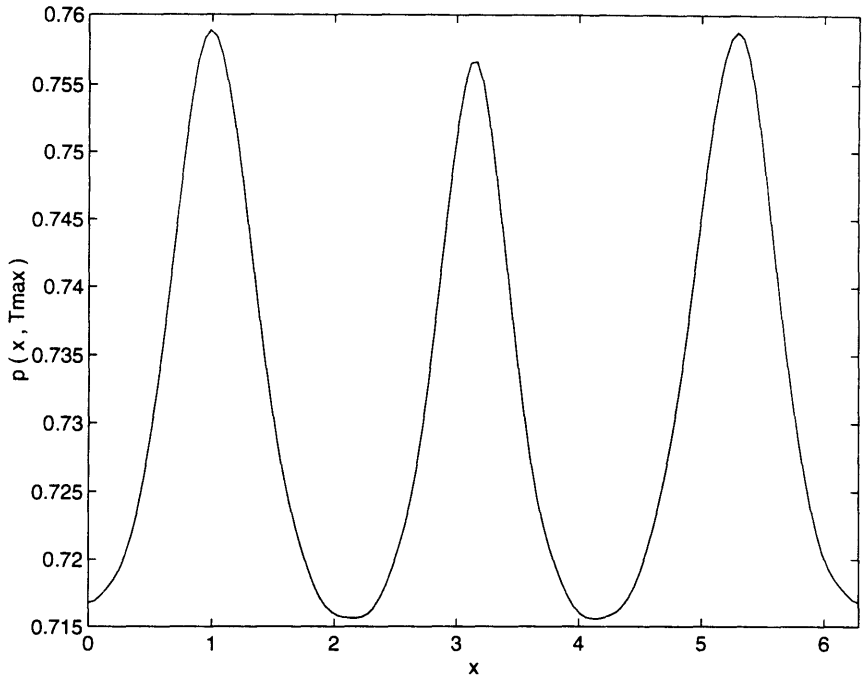

Figure 72: $p(x, \tau_{max})$ for $\epsilon = 0.1237$, $\omega = 3.04496$ (TC 5).

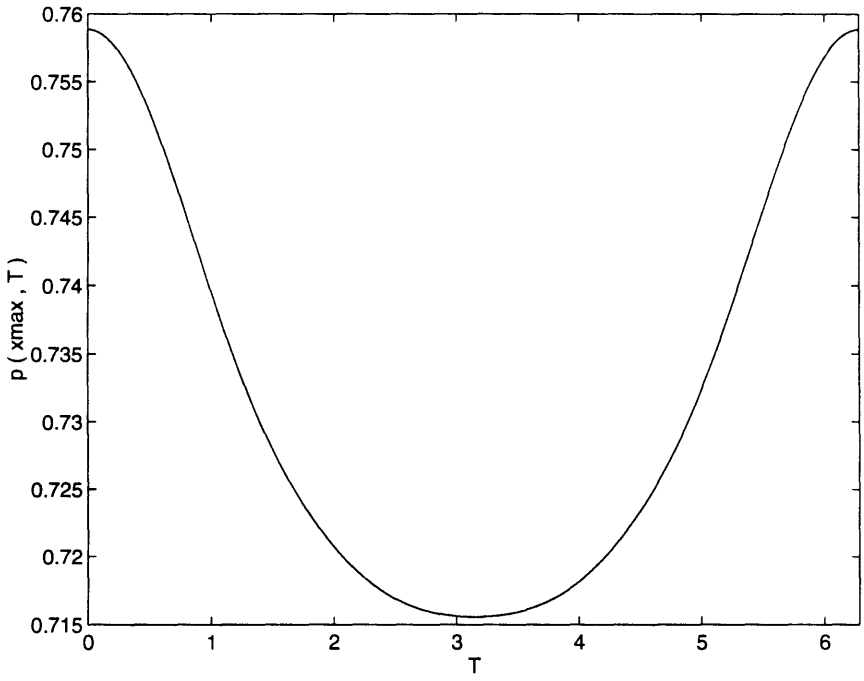

Figure 73: $p(x_{max}, \tau)$ for $\epsilon = 0.1237$, $\omega = 3.04496$ (TC 5).

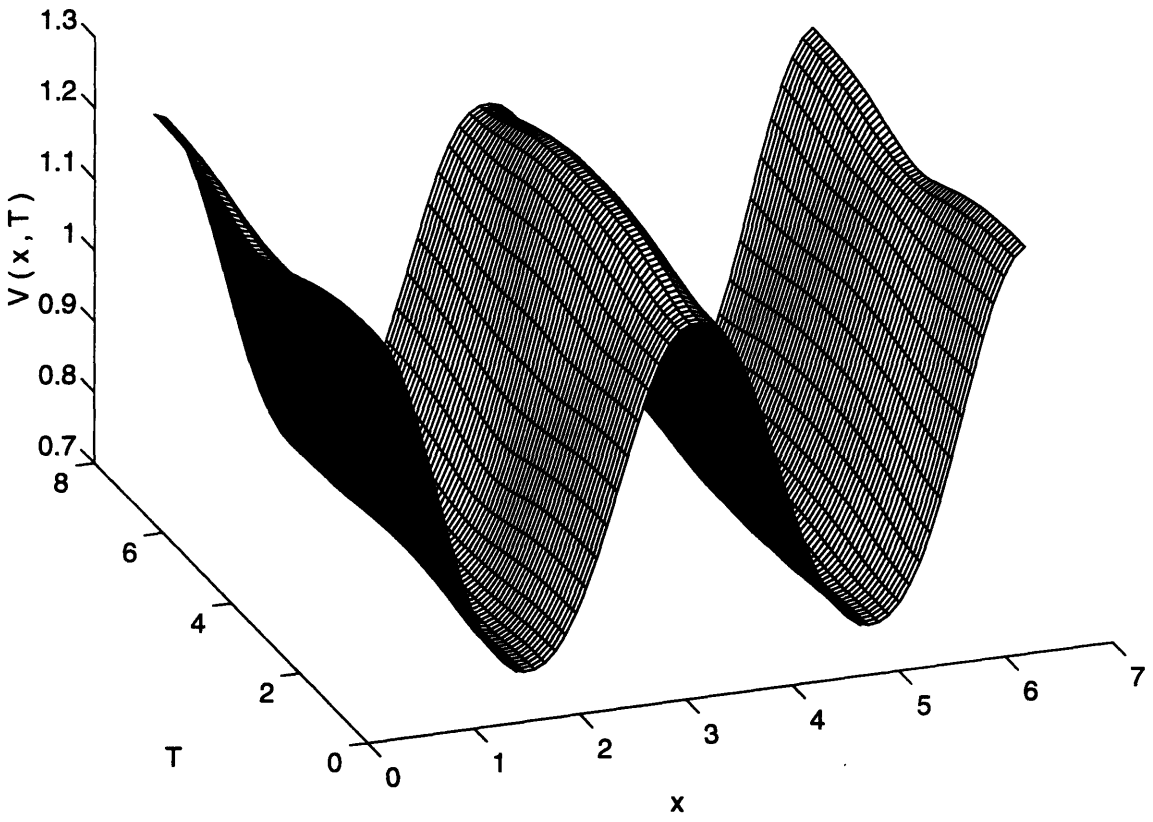

Figure 74: $V(x,\tau)$ for $\epsilon = 0.1237$, $\omega = 3.04496$; $a = 0.00323$, $SPL = 157.3dB$, $M = 0.02277$, (TC 5).

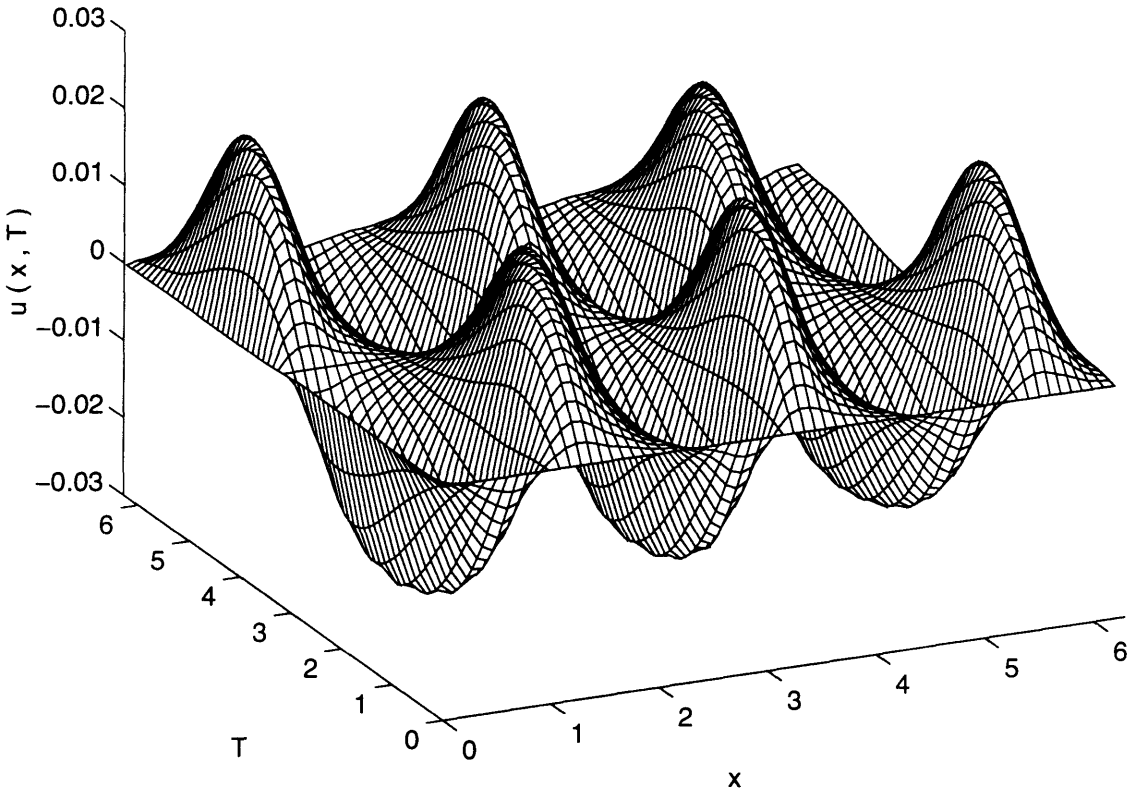

Figure 75: $u(x,\tau)$ for $\epsilon = 0.1237$, $\omega = 3.04496$; $a = 0.00323$, $SPL = 157.3dB$, $M = 0.02277$, (TC 5).

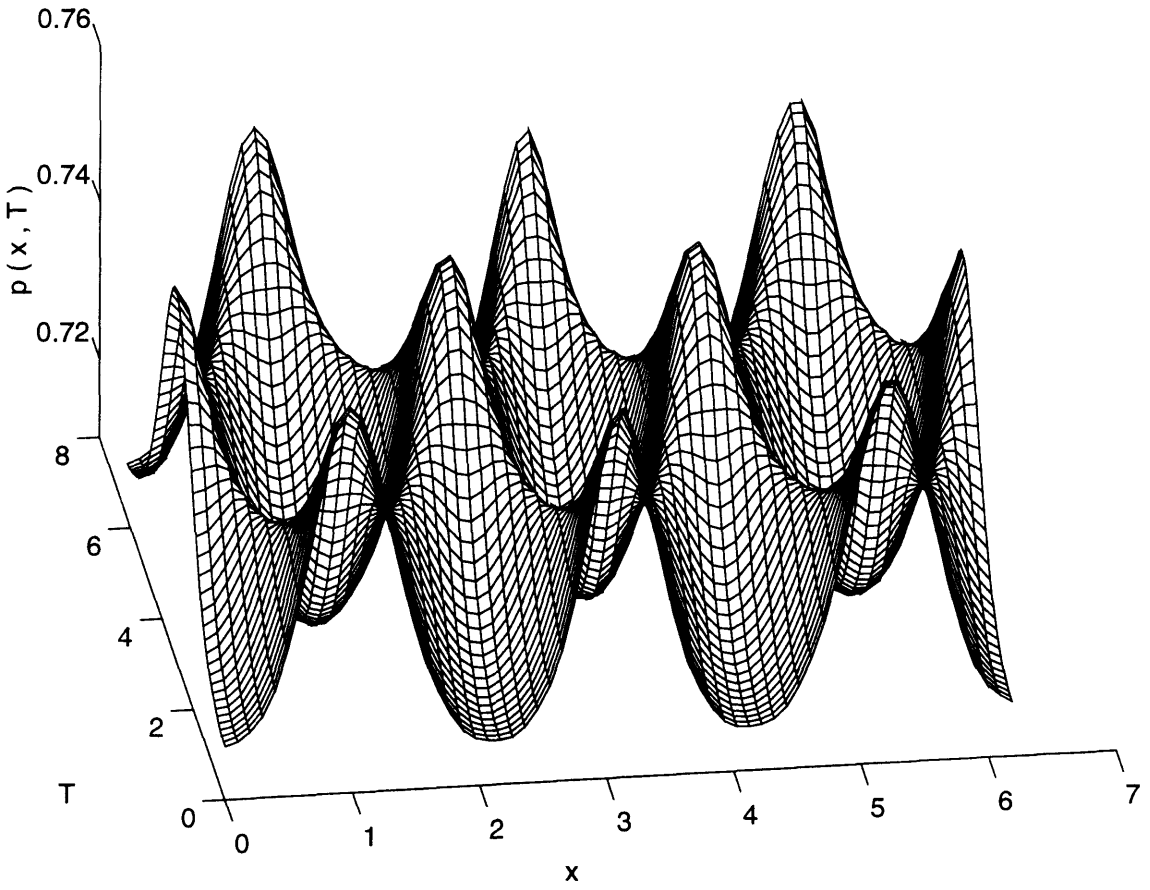

Figure 76: $p(x, \tau)$ for $\epsilon = 0.1237$, $\omega = 3.04496$; $a = 0.00323$, $SPL = 157.3dB$, $M = 0.02277$, (TC 5).

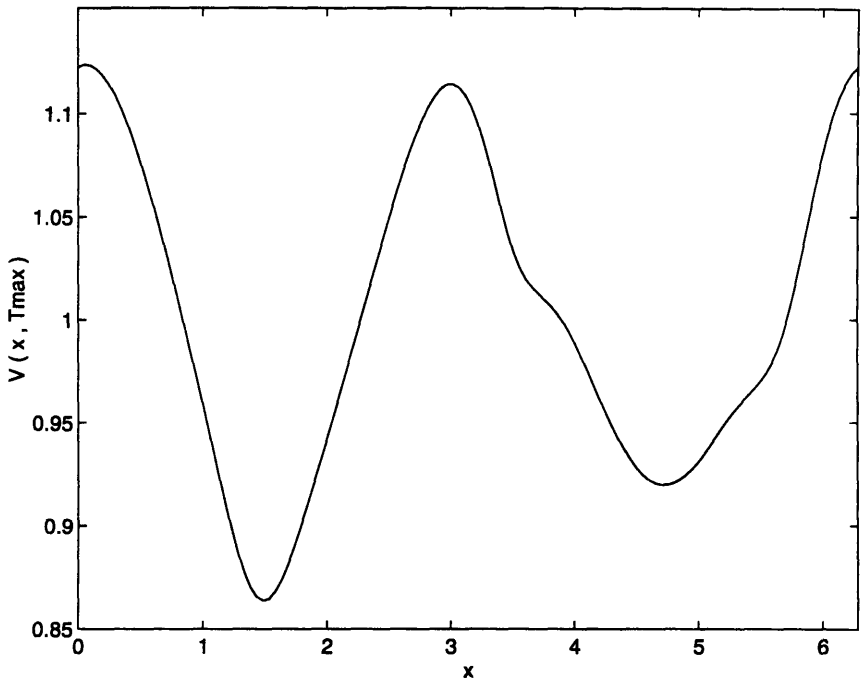

Figure 77: $V(x, \tau_{max})$ for $\epsilon = 0.0513$, $\omega = 3.00561$ (TC 6).

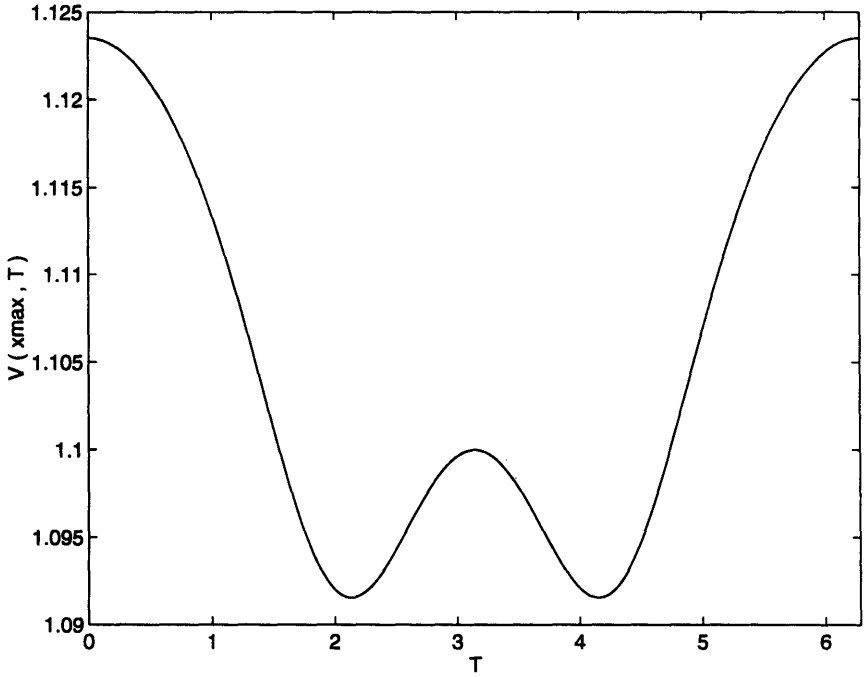

Figure 78: $V(x_{max}, \tau)$ for $\epsilon = 0.0513$, $\omega = 3.00561$ (TC 6).

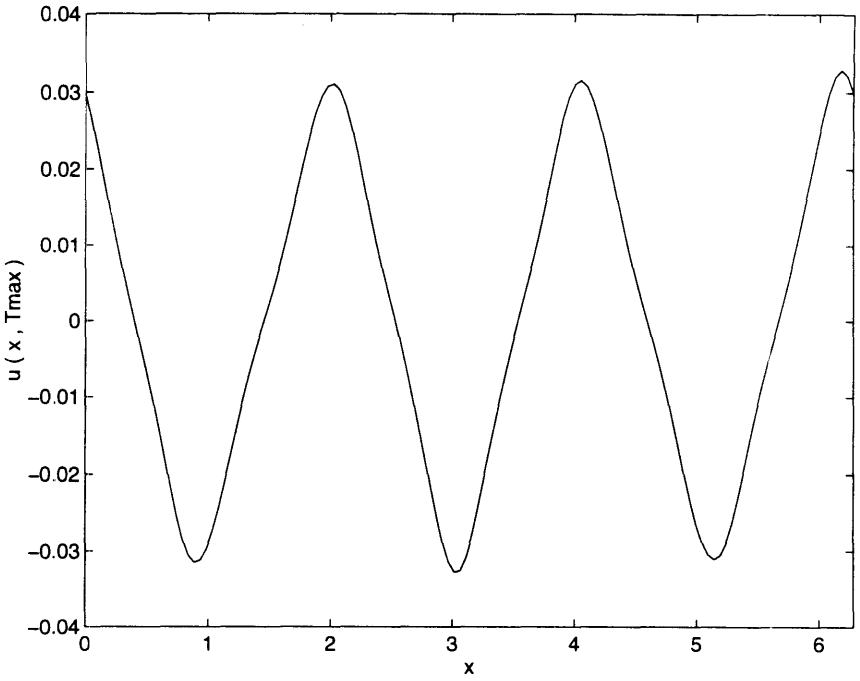

Figure 79: $u(x, \tau_{max})$ for $\epsilon = 0.0513$, $\omega = 3.00561$ (TC 6).

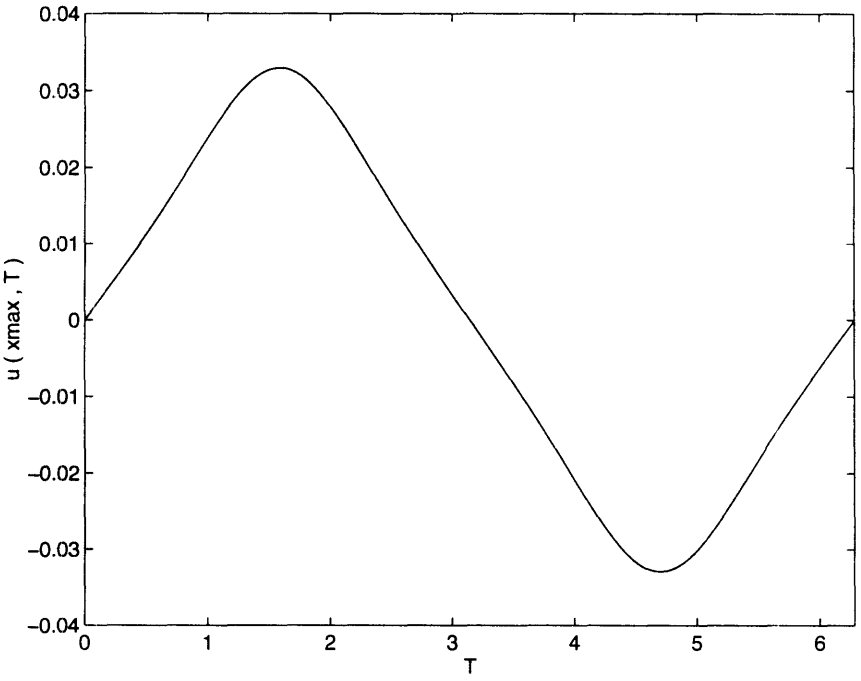

Figure 80: $u(x_{max}, \tau)$ for $\epsilon = 0.0513$, $\omega = 3.00561$ (TC 6).

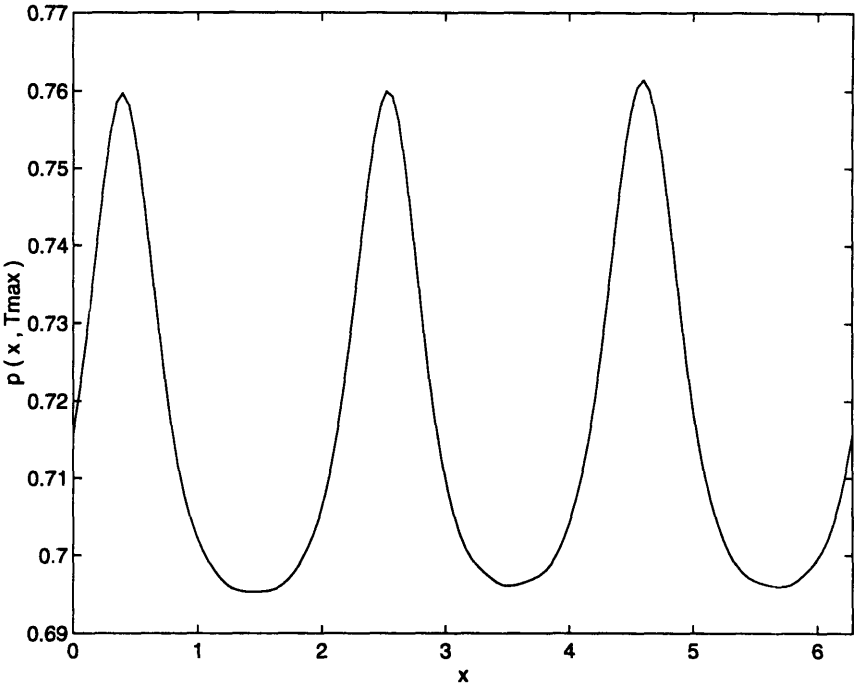

Figure 81: $p(x, \tau_{max})$ for $\epsilon = 0.0513$, $\omega = 3.00561$ (TC 6).

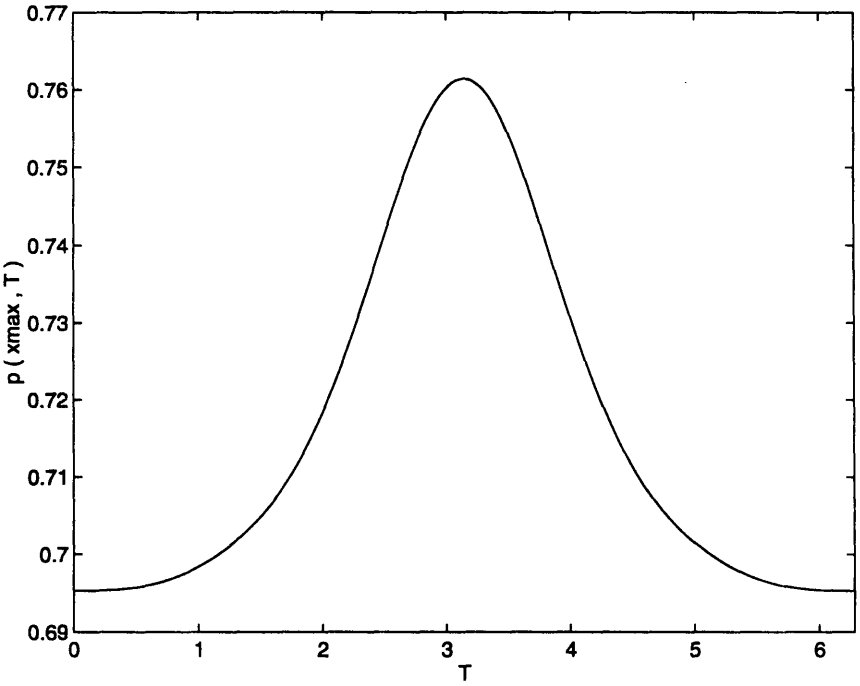

Figure 82: $p(x_{max}, \tau)$ for $\epsilon = 0.0513$, $\omega = 3.00561$ (TC 6).

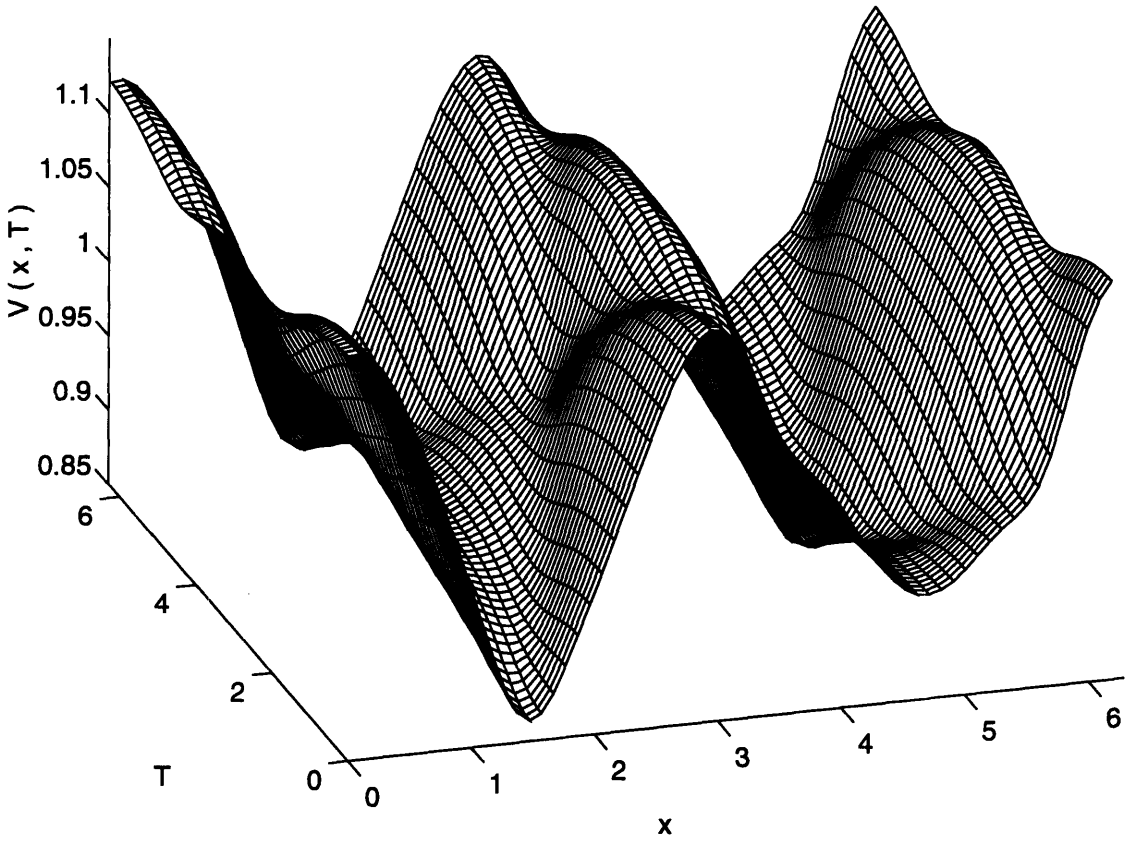

Figure 83: $V(x,\tau)$ for $\epsilon = 0.0513$, $\omega = 3.00561$; $a = 0.00455$, $SPL = 160.6dB$, $M = 0.03408$, (TC 6).

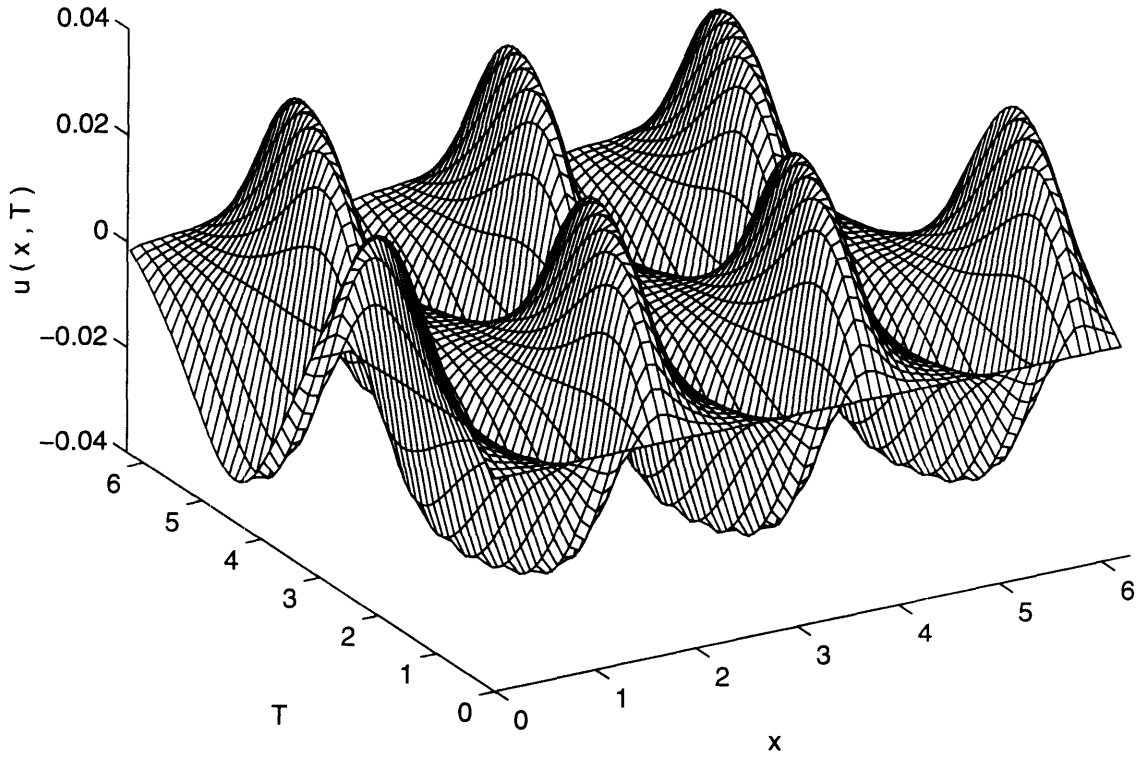

Figure 84: $u(x,\tau)$ for $\epsilon = 0.0513$, $\omega = 3.00561$; $a = 0.00455$, $SPL = 160.6dB$, $M = 0.03408$, (TC 6).

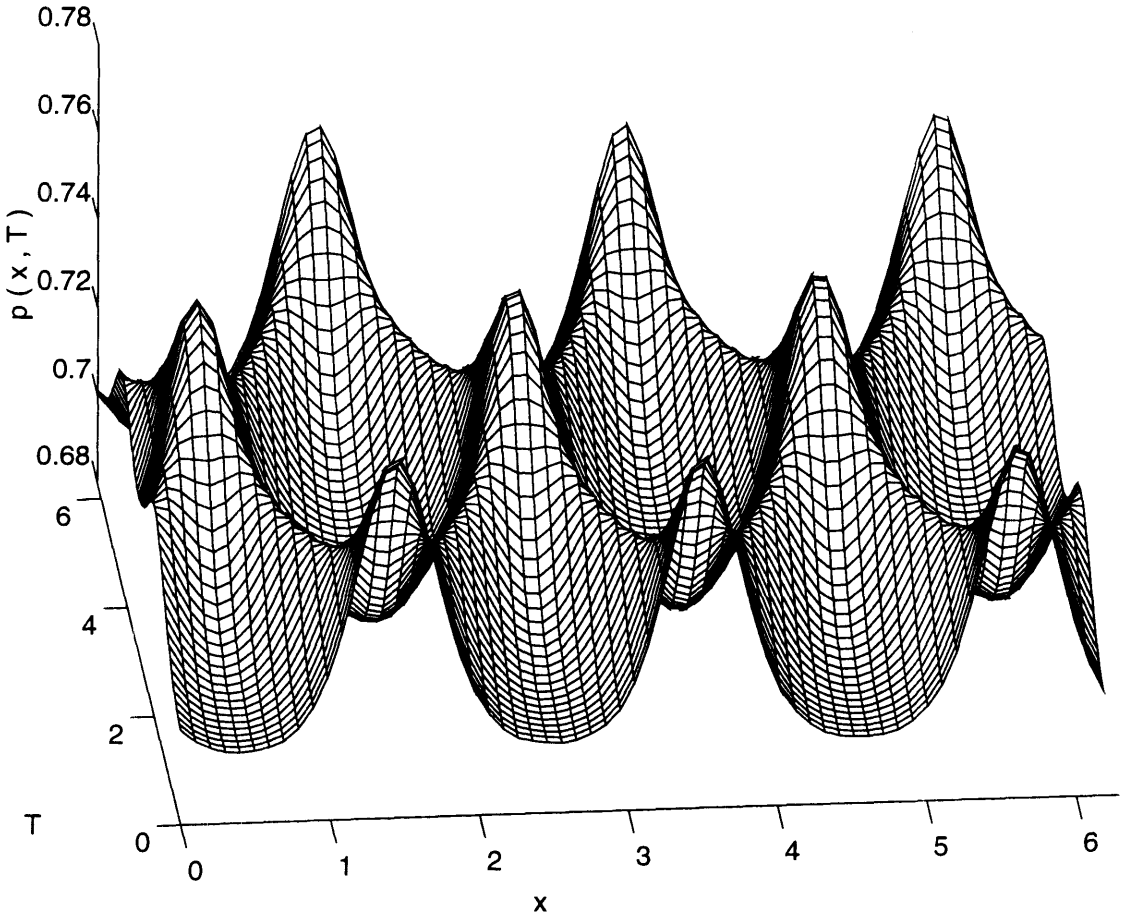

Figure 85: $p(x,\tau)$ for $\epsilon = 0.0513$, $\omega = 3.00561$; $a = 0.00455$, $SPL = 160.6dB$, $M = 0.03408$, (TC 6).

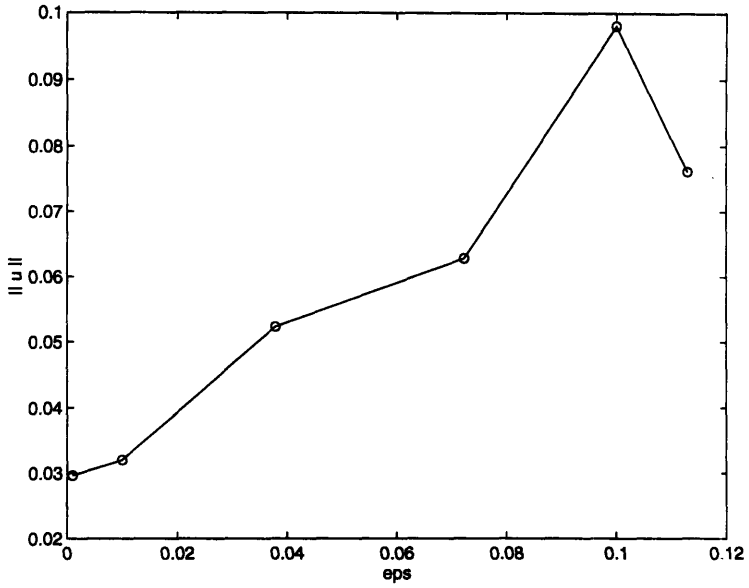

Figure 86: Velocity norm $max|u_j^n|$ of continuous waves of greatest amplitude, for different values of the entropy wave amplitude ϵ. All these solutions bifurcate from the second transition curve (TC 2) whose frequency is $\omega \simeq 1 + \epsilon/2$, for small ϵ.

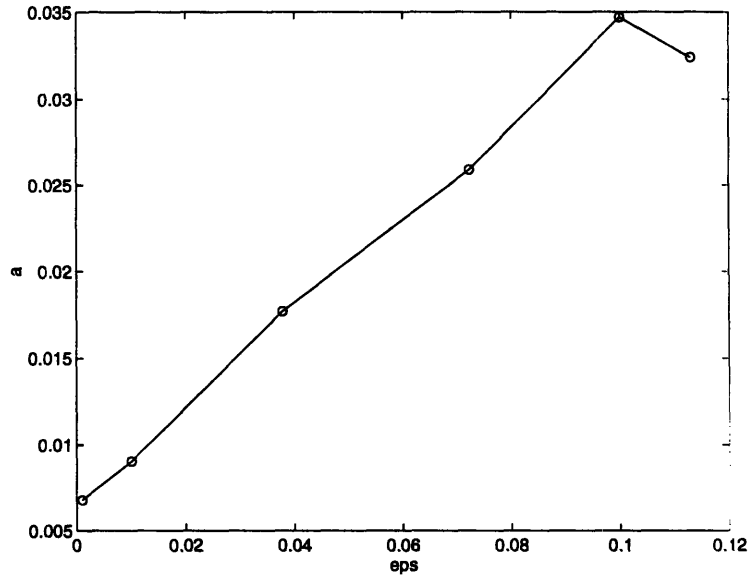

Figure 87: Acoustic amplitude a (eq. (3.39)) of continuous waves of greatest amplitude, for different values of the entropy wave amplitude ϵ. All these solutions bifurcate from the second transition curve (TC 2) whose frequency is $\omega \simeq 1 + \epsilon/2$, for small ϵ.

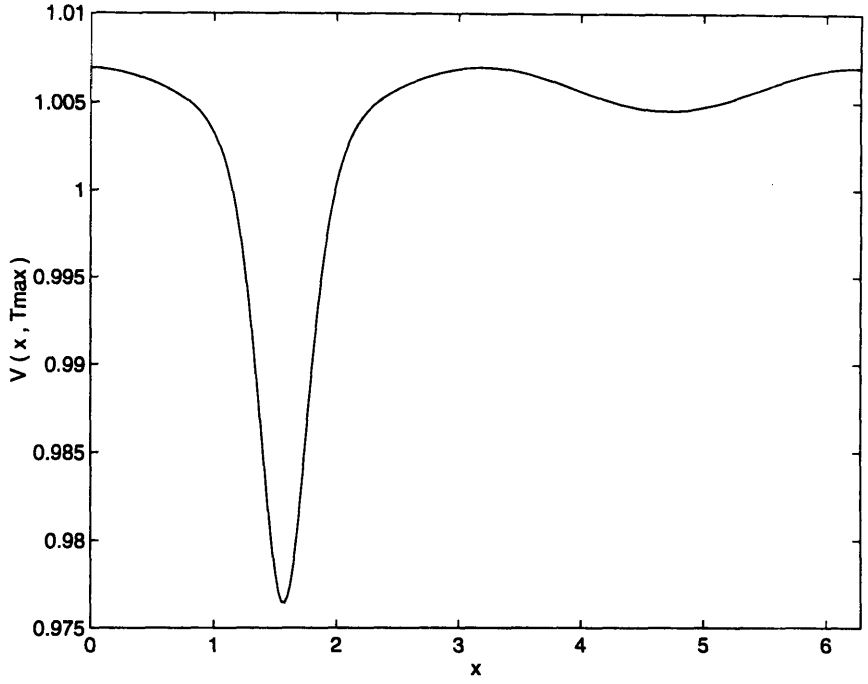

Figure 88: $V(x, \tau_{max})$ calculated using 256 points in x ($J = 255$), for $\epsilon = 0.0006793$, $\omega = 1.00042$ (TC 2).

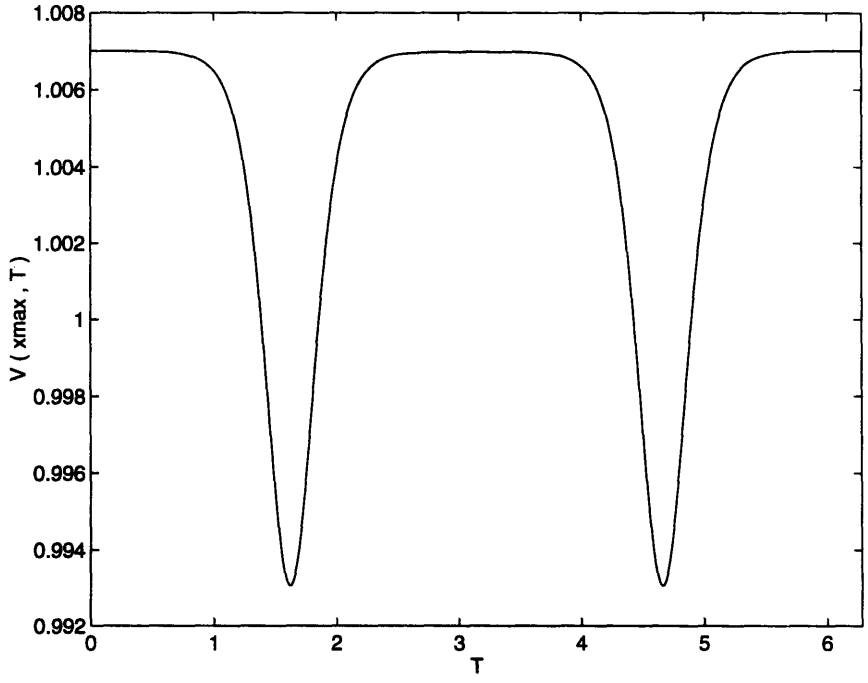

Figure 89: $V(x_{max}, \tau)$ calculated using 256 points in x ($J = 255$), for $\epsilon = 0.0006793$, $\omega = 1.00042$ (TC 2).

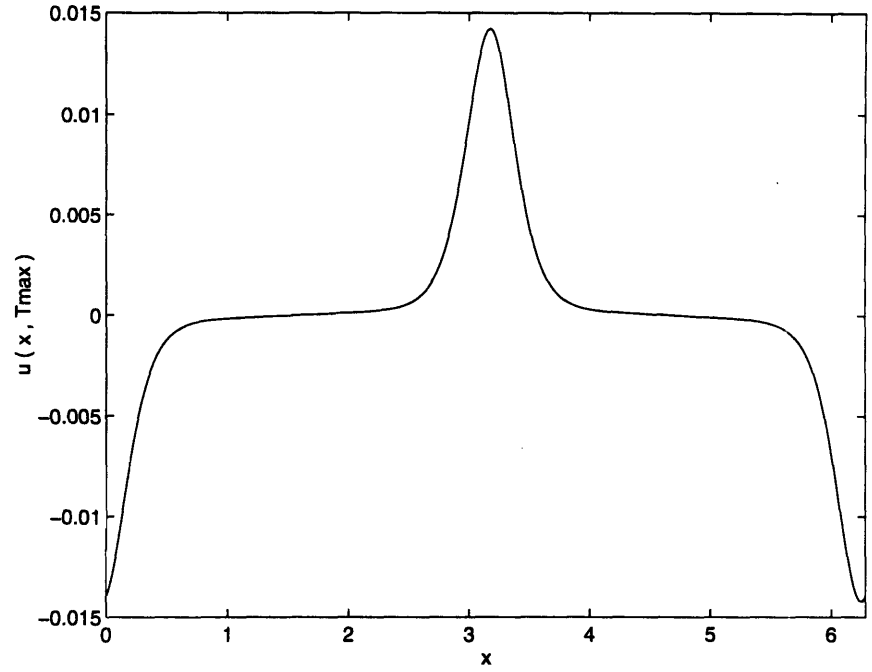

Figure 90: $u(x, \tau_{max})$ calculated using 256 points in x ($J = 255$), for $\epsilon = 0.0006793$, $\omega = 1.00042$ (TC 2).

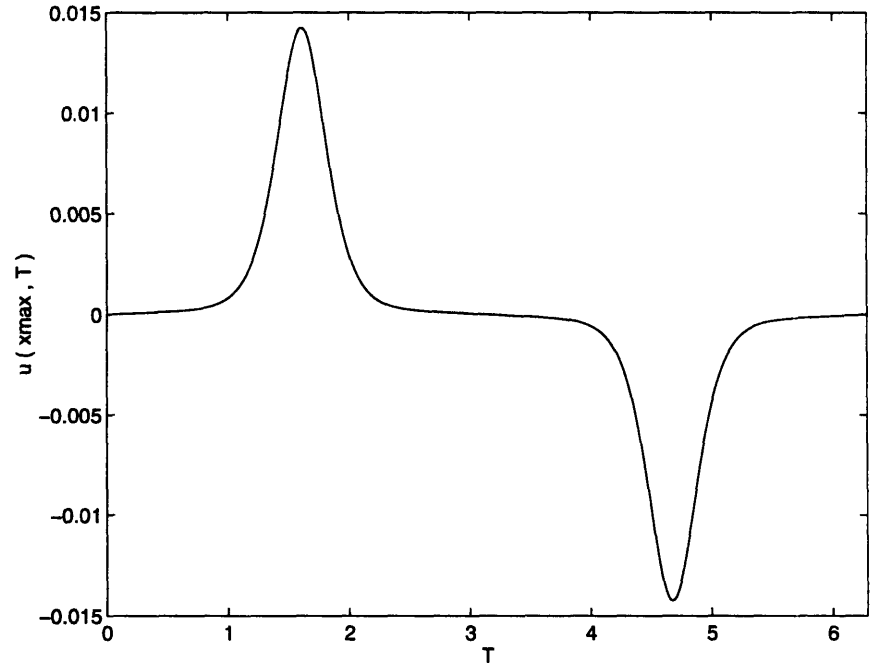

Figure 91: $u(x_{max}, \tau)$ calculated using 256 points in x ($J = 255$), for $\epsilon = 0.0006793$, $\omega = 1.00042$ (TC 2).

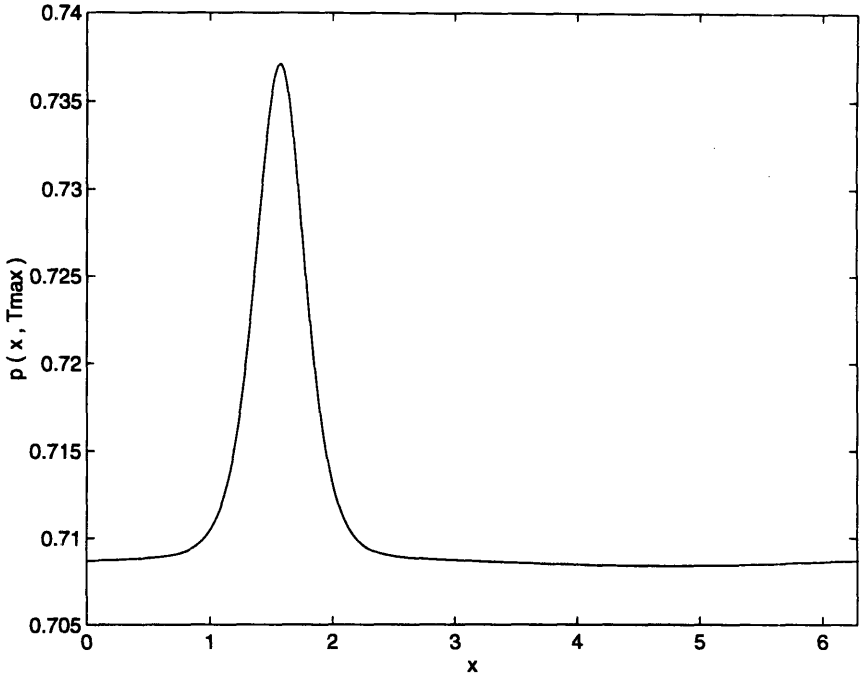

Figure 92: $p(x, \tau_{max})$ calculated using 256 points in x ($J = 255$), for $\epsilon = 0.0006793$, $\omega = 1.00042$ (TC 2).

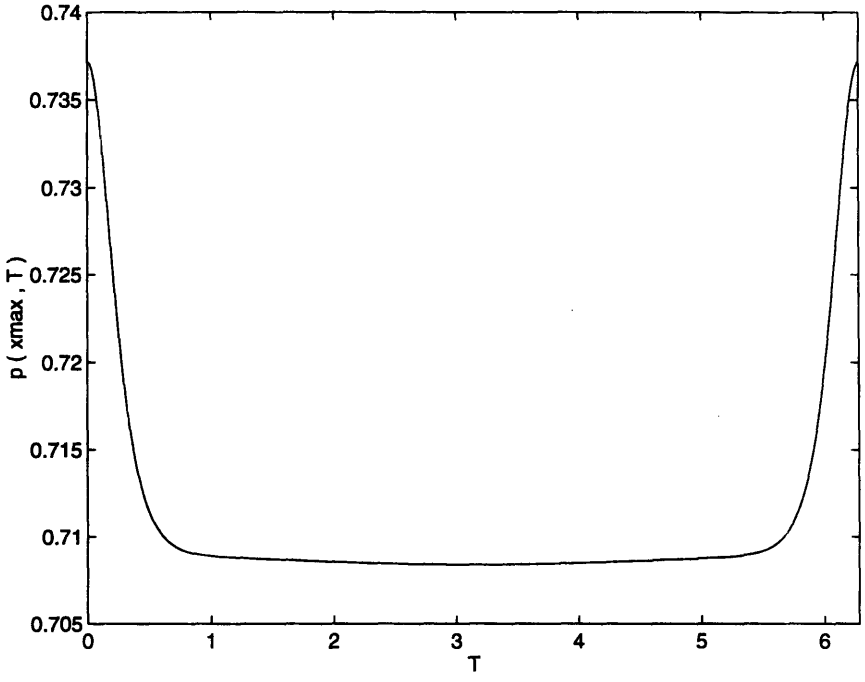

Figure 93: $p(x_{max}, \tau)$ calculated using 256 points in x ($J = 255$), for $\epsilon = 0.0006793$, $\omega = 1.00042$ (TC 2).

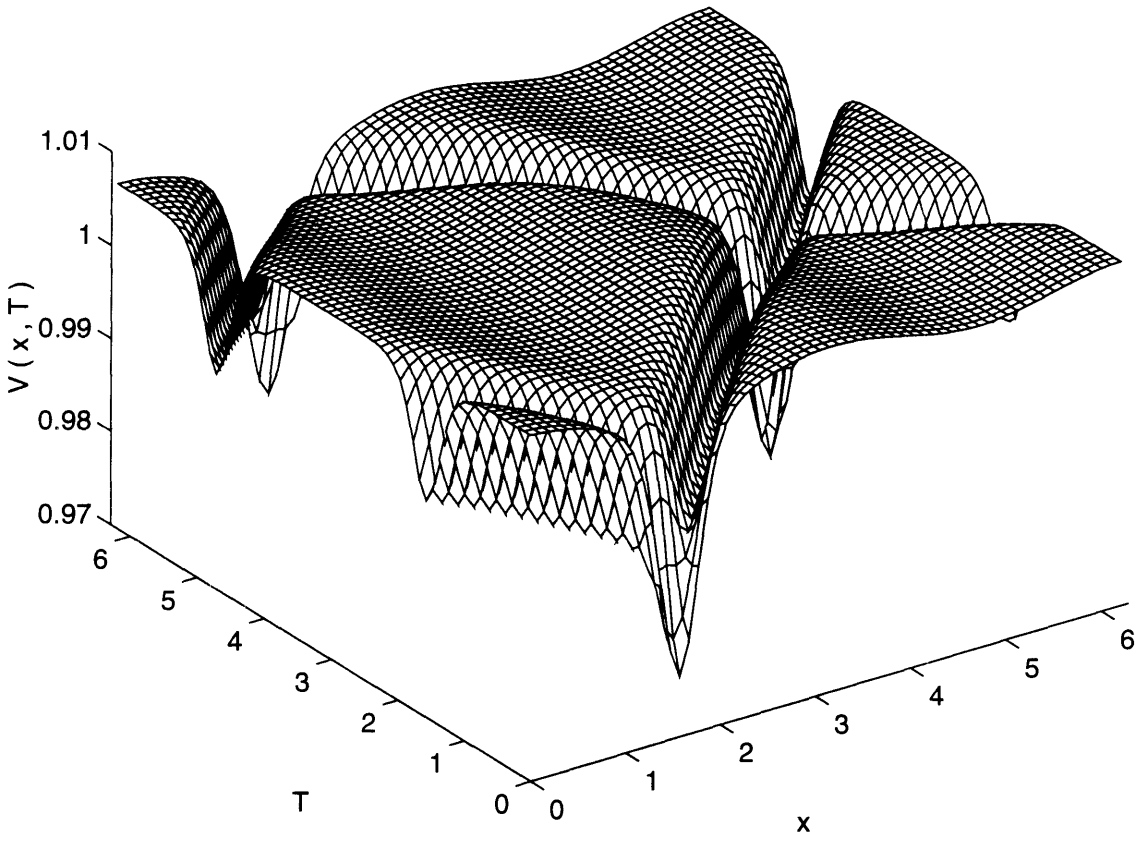

Figure 94: $V(x,\tau)$ calculated using 256 points in x ($J = 255$), $\epsilon = 0.0006793$, $\omega = 1.00042$; $a = 0.00244$, $SPL = 151.7dB$, $M = 0.01411$, (TC 2).

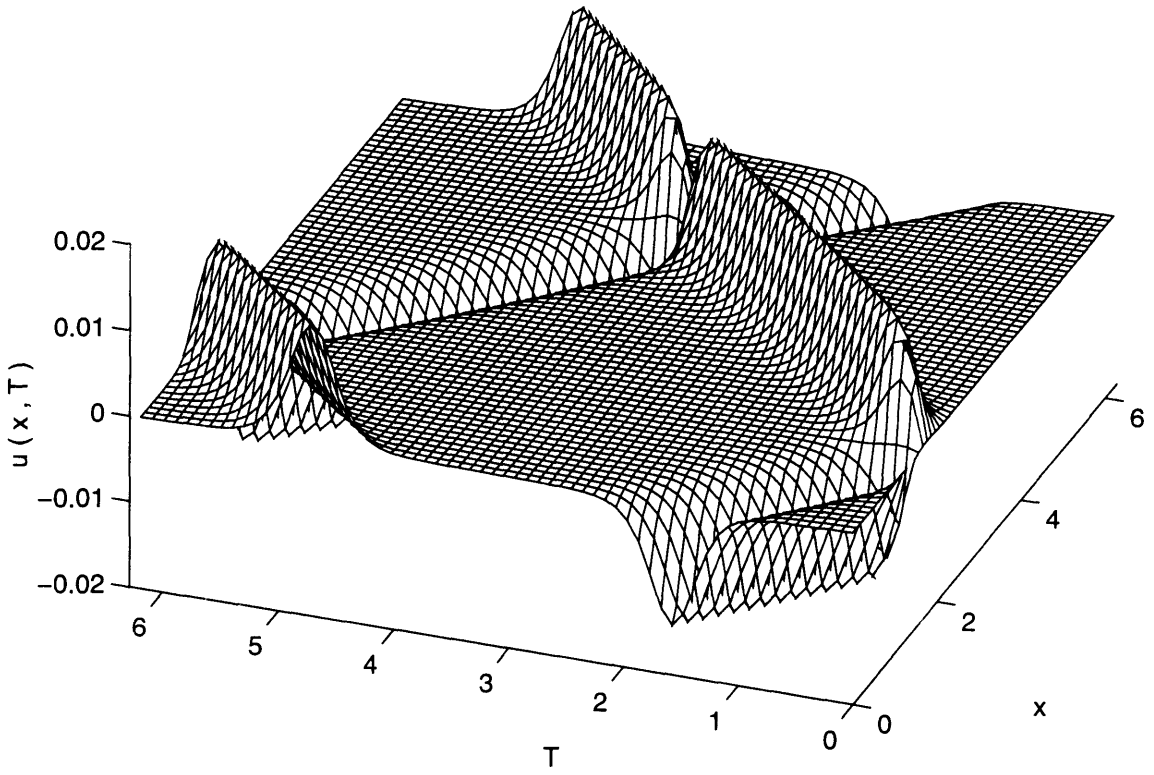

Figure 95: $u(x,\tau)$ calculated using 256 points in x ($J = 255$), $\epsilon = 0.0006793$, $\omega = 1.00042$; $a = 0.00244$, $SPL = 151.7dB$, $M = 0.01411$, (TC 2).

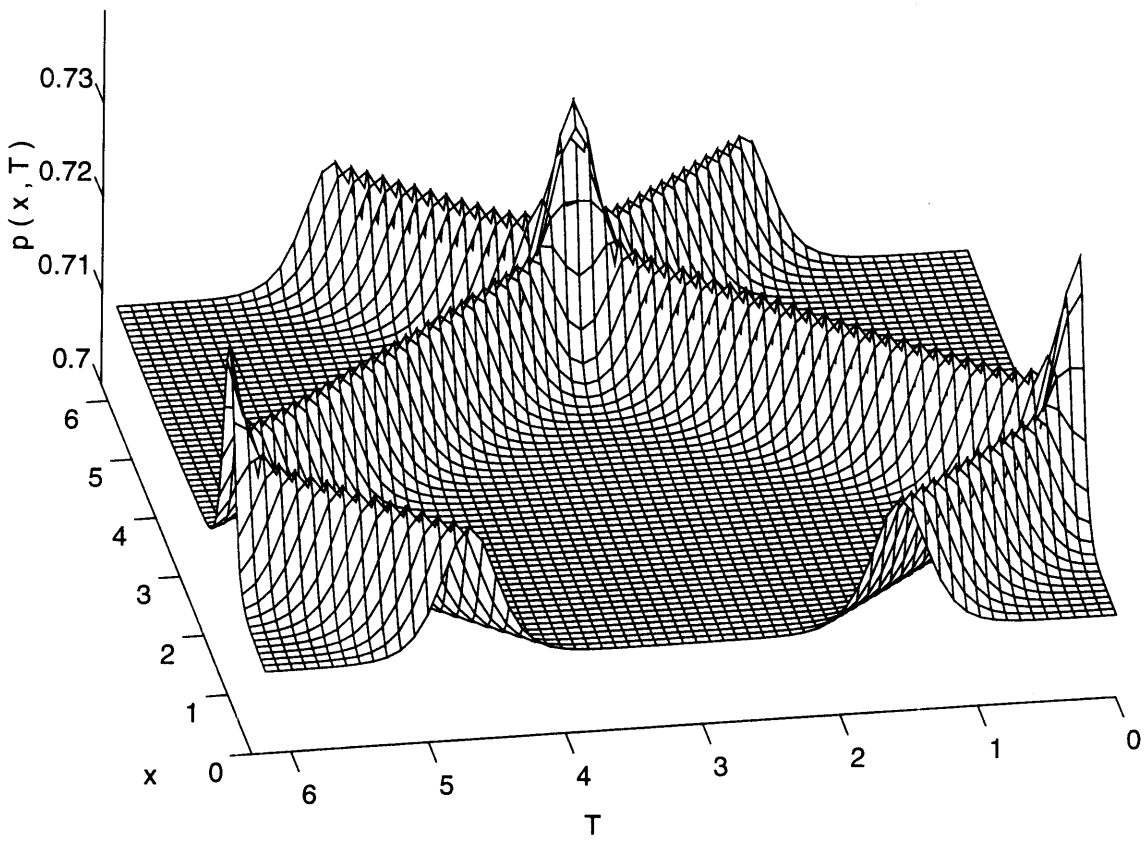

Figure 96: $p(x,\tau)$ calculated using 256 points in x ($J = 255$), $\epsilon = 0.0006793$, $\omega = 1.00042$; $a = 0.00244$, $SPL = 151.7dB$, $M = 0.01411$, (TC 2).

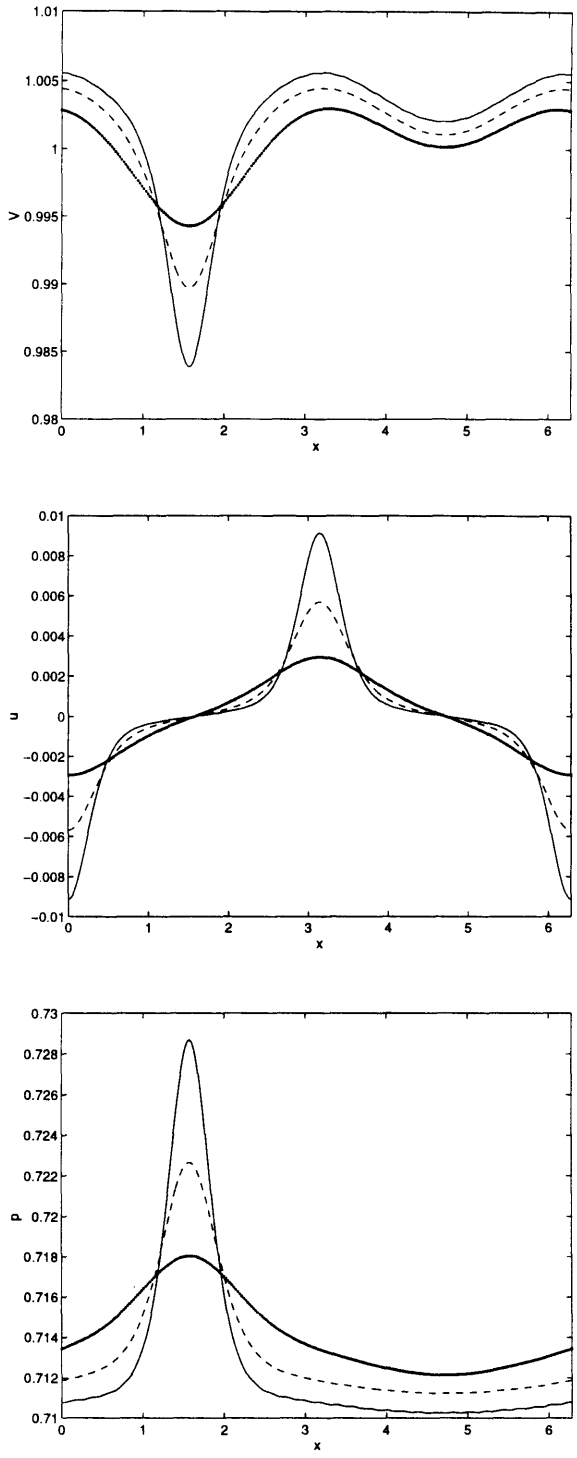

Figure 97: Wave steepening: Specific volume $V(x, \tau = 2\pi)$, velocity $u(x, \tau = \pi/2)$ and pressure $p(x, \tau = 2\pi)$ for $\epsilon = 0.001$ and three different values of a: .... $a = 0.00125$, - - - $a = 0.00165$, — $a = 0.00205$ (TC 2, 256 points).

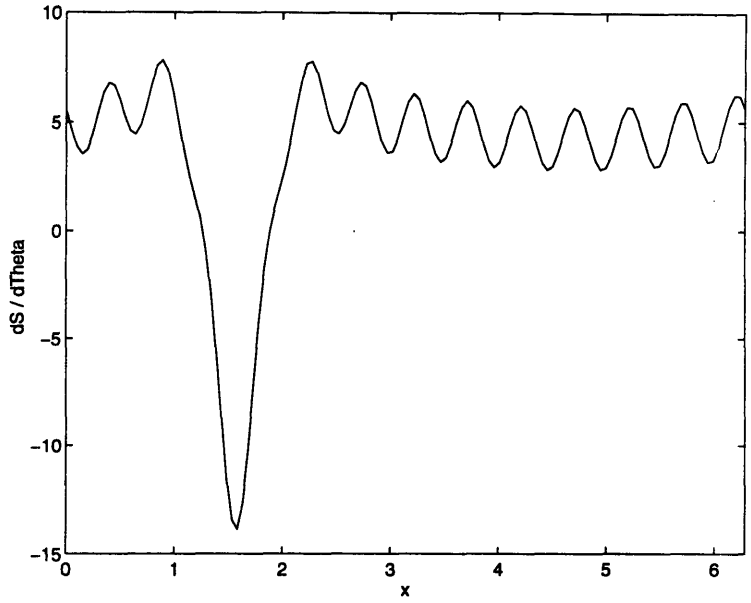

Figure 98: Breakdown of continuous large amplitude acoustic waves as seen in the continuation slope $ds/d\theta$, see equations (3.35)–(3.36); $\epsilon = 0.01$, $\omega = 1.0036$, $u_{max} = 0.0319$, $a_{max} = 0.009$, $SPL = 159.1dB$, (TC 2).

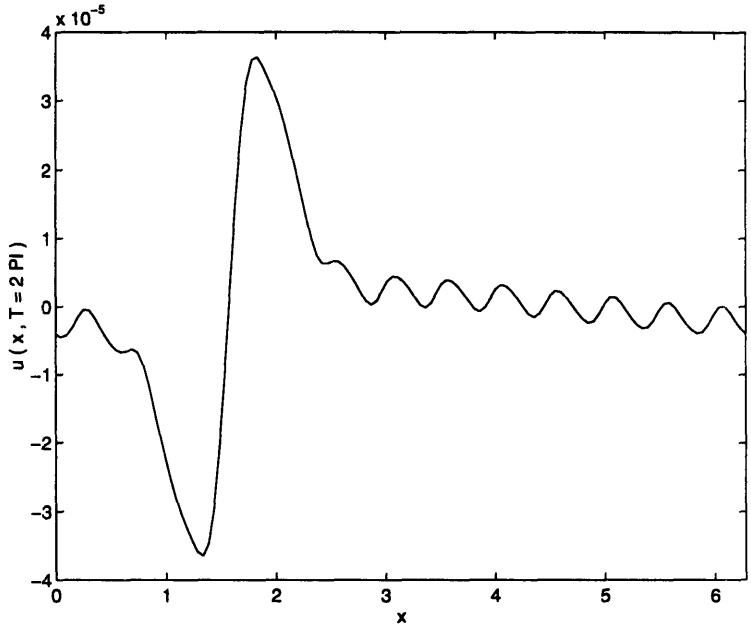

Figure 99: Breakdown of continuous large amplitude acoustic waves as seen in velocity $u(x, \tau = 2\pi)$; $\epsilon = 0.01$, $\omega = 1.0036$, $u_{max} = 0.0319$, $a_{max} = 0.009$, $SPL = 159.1dB$, (TC 2).

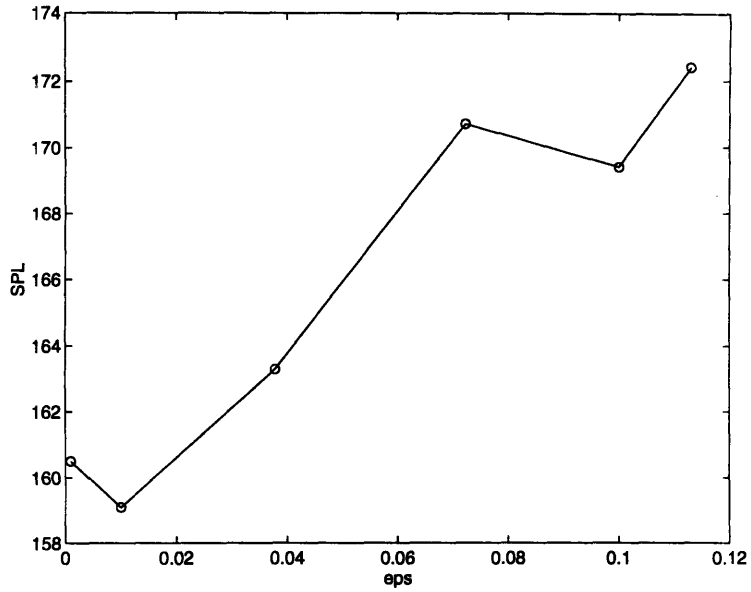

Figure 100: Sound pressure level SPL of continuous waves of greatest amplitude, for different values of the entropy wave amplitude ϵ. All these solutions bifurcate from the second transition curve (TC 2) whose frequency is $\omega \simeq 1 + \epsilon/2$, for small ϵ.

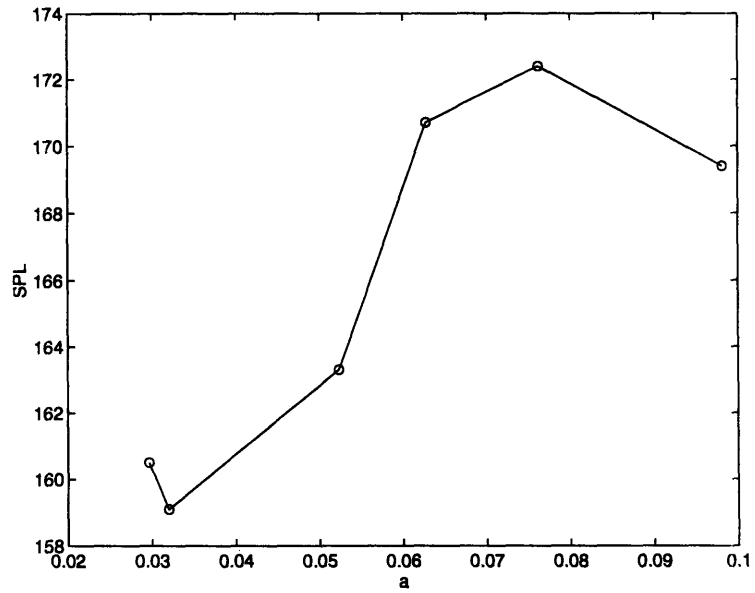

Figure 101: Sound pressure level SPL of continuous waves of greatest amplitude, for different values of the acoustic amplitude a (eq. (3.39)). All these solutions bifurcate from the second transition curve (TC 2) whose frequency is $\omega \simeq 1 + \epsilon/2$, for small ϵ.

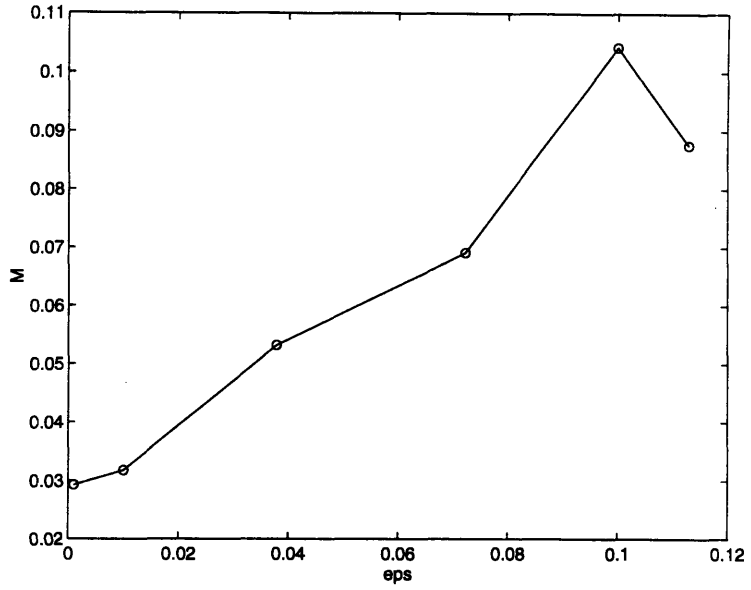

Figure 102: Acoustic Mach number M of continuous waves of greatest amplitude, for different values of the entropy wave amplitude ϵ. All these solutions bifurcate from the second transition curve (TC 2) whose frequency is $\omega \simeq 1 + \epsilon/2$, for small ϵ.

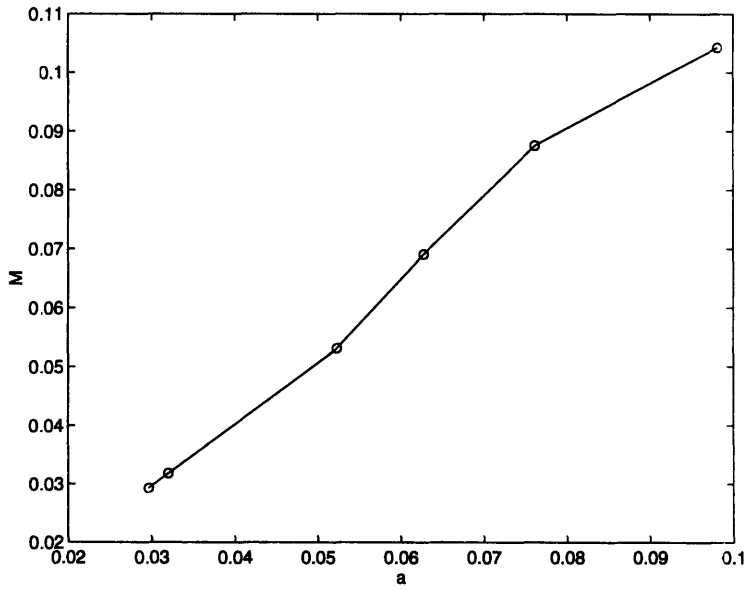

Figure 103: Acoustic Mach number M of continuous waves of greatest amplitude, for different values of the acoustic amplitude a (eq. (3.39)). All these solutions bifurcate from the second transition curve (TC 2) whose frequency is $\omega \simeq 1 + \epsilon/2$, for small ϵ.

Chapter 4

Stability

To complete the characterization of the new class of nonlinear standing periodic acoustic waves, we briefly address in this chapter the issue of their stability properties.

In first place, the stability against infinitesimal perturbations will be considered. The linearized stability evolution equations lead to a Floquet problem in the normalized time τ. This problem will be solved by numerically evaluating the eigenvalues of the associated monodromy matrix, in a way similar to the analysis of Chapter 2.

Next, the long time behavior of standing periodic acoustic waves subject to small arbitrary perturbations will be discussed. The main difficulties for the analysis of this situation will be pointed out. Our limited goal in this area is to test certain general hypotheses concerning the qualitative behavior of such perturbed flows. We will do so by numerical calculations in which we will follow the evolution of perturbed waves in time. These experiments, though not systematic, will confirm a very interesting new and unexpected phenomenon: in certain cases, after shocks form and decay, solutions (apparently continuous for all time) with a nontrivial acoustic content emerge as the final asymptotic state. This result needs more careful study, but if true it would notably expand the class of solutions without shocks (for all times) in Gas Dynamics. A class thought to consist (till this work) only of pure entropy waves.

4.1 Linear Stability

In this section, we analyze the stability of the standing periodic acoustic waves against infinitesimal disturbances.

Let us denote by $[\,\bar{V}(x,\tau), \bar{u}(x,\tau)\,]$ the basic flow corresponding to a nonlinear, smooth and continuous standing acoustic wave, 2π–periodic in both the mass coordinate x and normalized time τ, as calculated by the numerical algorithm of Chapter 3. If $\tilde{V}(x,\tau)$ and $\tilde{u}(x,\tau)$ represent the small infinitesimal perturbations, the flow under consideration can be written as

$$V(x,\tau) \;=\; \bar{V}(x,\tau) \;+\; \tilde{V}(x,\tau), \tag{4.1}$$

$$u(x,\tau) \;=\; \bar{u}(x,\tau) \;+\; \tilde{u}(x,\tau). \tag{4.2}$$

Introducing (4.1)–(4.2) into the equations of motion (2.1)–(2.2), we obtain, after linearization, the equations governing the evolution of the small disturbances $\tilde{V}(x,\tau)$ and $\tilde{u}(x,\tau)$:

$$\frac{\partial \tilde{V}}{\partial \tau} \;-\; \frac{1}{\omega}\,\frac{\partial \tilde{u}}{\partial x} \;=\; 0, \tag{4.3}$$

$$\frac{\partial \tilde{u}}{\partial \tau} \;-\; \frac{1}{\omega}\,\frac{\partial}{\partial x}\left\{ \left(\bar{C}(x,\tau) \right)^2 \tilde{V} \right\} \;=\; 0, \tag{4.4}$$

subject to periodic boundary conditions in x, i.e., $\tilde{V}(0,\tau) = \tilde{V}(2\pi,\tau)$ and $\tilde{u}(0,\tau) = \tilde{u}(2\pi,\tau)$. In (4.4), $\bar{C}^2(x,\tau) = \gamma \bar{p}(x,\tau)/\bar{V}(x,\tau)$ is the sound speed associated with the basic flow, also 2π–periodic in x and τ.

Applying the method of lines to (4.3)–(4.4), we can discretize this system as in Section 3.3. The perturbation equations then yield a system of coupled ordinary differential equations, which in vector notation takes the form

$$\dot{\tilde{\mathbf{V}}}(\tau) \;=\; \mathbf{H}(\tau)\,\tilde{\mathbf{V}}(\tau), \tag{4.5}$$

where the coefficients of the matrix $\mathbf{H}(\tau)$ are 2π–periodic in τ. Thus, we have a Floquet problem for the perturbations superimposed on the basic periodic flow.

The present situation is very similar to that of Chapter 2: in Section 2.3 we found a Floquet problem in x when studying periodic solutions bifurcating from equilibrium, with periodic coefficients due to the static solution field, a pure entropy wave. Now we formulate a Floquet problem in τ to investigate the linear stability of the standing periodic acoustic waves of finite amplitude calculated in Chapter 3.

As we saw before in Section 2.3, if $\tilde{\mathbf{V}}(\tau)$ is an M–column vector, the monodromy matrix $\mathbf{E}$ of the system (4.5) is simply an $M \times M$ matrix whose columns are M linearly independent solutions obtained by integrating (4.5) up to one period, i.e., $\tau = 2\pi$, starting with the identity matrix as initial condition. That is $\mathbf{E} = \Phi(2\pi)$, where

$$\dot{\Phi}(\tau) \;=\; \mathbf{H}(\tau)\,\Phi(\tau), \tag{4.6}$$

$$\Phi(0) \;=\; \mathbf{I}. \tag{4.7}$$

The stability problem then reduces to find the eigenvalues (or Floquet multipliers) λ_i of the monodromy matrix $\mathbf{E}$. For each "normal" eigenvalue λ_i (i.e., algebraic

multiplicity equal geometric multiplicity equal m_i), there correspond m_i linearly independent solutions of (4.5) of the form $\tilde{V}(\tau) = h(\tau)\, e^{\rho_i \tau}$, where $h(\tau)$ is 2π–periodic and $e^{\rho_i 2\pi} = \lambda_i$ defines the Floquet exponent ρ_i. For a "degenerate" eigenvalue λ_i (i.e., algebraic multiplicity equal m_i bigger than geometric multiplicity), again m_i linearly independent solutions as above can be found, but now $h(\tau)$ takes the form of a polynomial in τ with the coefficients 2π–periodic functions of τ. The degree of this polynomial takes any value up to (and including) the "deficiency" of λ_i (see Ince (1956)). Therefore, a basic periodic solution $[\, \bar{V}(x,\tau), \bar{u}(x,\tau)\,]$ will be stable against infinitesimal perturbations if $Re(\rho_i) < 0$ (i.e., λ_i is inside the unit circle) for all the eigenvalues. Instability will result if there is at least one Floquet exponent with positive real part (corresponding multiplier outside the unit circle). The case of zero real part in a Floquet exponent (Floquet multiplier on the unit circle) corresponds to neutral stability if the eigenvalue is normal and mild (algebraic) growth otherwise. Since, in general, the eigenvalues of $\mathbf{E}$ will be distinct, we need not be overly concerned by the possibility of degenerate eigenvalues.

In recent years, the numerical solution of stability problems for time dependent and/or spatially varying flows has been generally performed using spectral collocation methods (cf. Dwoyer & Hussaini (1987)). An important contribution in this area is that of Herbert (see the article by Herbert and collaborators in the book edited by Dwoyer & Hussaini and his review paper of (1988)) concerned with secondary instability and transition from laminar to turbulent flow in viscous boundary layers. However, in our stability problem, the shooting method employed to obtain the monodromy matrix $\mathbf{E}$ considerably simplifies the numerical solution of the disturbance equations. The fact that our basic flow is periodic in two variables, requiring double Fourier series in x and τ for its representation, makes a collocation method unsuited for the numerical task, since it would produce a set of algebraic equations of difficult computational implementation.

To calculate the Floquet exponents ρ_i, we integrate the system (4.3)–(4.4) using the same discretization as in Chapter 3. Starting with the identity matrix as initial condition at $\tau = 0$, we integrate the equations up to $\tau = 2\pi$ and obtain the monodromy matrix $\mathbf{E}$ (equations (4.6)–(4.7)). Its eigenvalues, or Floquet multipliers λ_i, are then calculated by the QR method. Finally, the Floquet exponents are obtained from the relations $e^{\rho_i 2\pi} = \lambda_i$.

The procedure was repeated for decreasing values of the mesh size $\Delta x = 2\pi/J$, to check convergence for the λ_i. (Recall that the specific volume $V(x,\tau)$ and flow velocity $u(x,\tau)$ are discretized as $V_j(\tau)$ and $u_j(\tau)$, with $j = 0, 1, 2, ..., J-1$; thus, the monodromy matrix $\mathbf{E}$ has dimensions $M \times M$, with $M = 2J$). As an additional confidence test, the eigenvector associated with the maximum modulus eigenvalue was evaluated by inverse iteration[39]. Several basic flows, given by nonlinear acoustic

[39]Clearly, an eigenvalue with corresponding eigenvector showing oscillations at the grid level scale is not a "converged" eigenvalue — and should be treated with great suspicion.

waves calculated with the method of Section 3.3, were tested in this way. Growth rates were found to lie in the range $Re(\rho_i) < 4 \times 10^{-7}$. This result consistently held in different regions of the (ω, ϵ, a) parameter space. Therefore, *within our numerical accuracy, standing periodic nonlinear acoustic waves appear to be neutrally stable against infinitesimal perturbations.* This result agrees well with what we expected given the dispersive (Hamiltonian in fact) nature of the time evolution of the full equations for solutions without shocks.

4.2 Absolute Stability

From a practical point of view, it is obviously more relevant to go beyond a linear analysis of the type presented in Section 4.1 and study the stability properties of the standing periodic acoustic waves when subject to perturbations of finite size. However, in our case such a nonlinear stability problem turns out to be a very complicated one, as explained below[40], due to the fact that the basic flow is governed by a hyperbolic system of conservation laws with two genuinely nonlinear characteristics. Therefore, our treatment of this topic will be rather superficial, and will be confined, mainly, to a discussion of various general aspects.

Let us point out to a specific characteristic a nonlinear stability analysis of a periodic acoustic wave does present. Any perturbation added to an exact periodic basic solution will interact with it and propagate in a hyperbolic fashion. Typically, the perturbation will lead to the formation of shocks, whose strength will depend upon the perturbation amplitude. Before shocks form, the evolution is non-dissipative. Afterwards, dissipation occurs, but only at the location of the shocks — which should eventually decay and become negligible. An analysis of this mechanism, with no linear analog, appears extremely hard.

Therefore, regardless of the way in which a periodic solution is perturbed, it seems plausible that, in general, shocks will form and later decay (asymptotically) to zero strength. Consequently, the stability question, when properly formulated, should be about the large-time asymptotic behavior of the perturbed flow after shocks have disappeared. Rather than looking at the growth or decay of disturbances (by a "local in time" linear analysis[41]), a stability analysis in this context should consider the following scenarios (in part anticipated by the discussion of Section 3.2 — fourth paragraph):

(1) A disturbance disrupts the periodic basic solution in such a way that the per-

[40] See also Section 3.2, third and fourth paragraphs.

[41] Which gives no growth or decay — see prior section —, as any such growth or decay must be purely nonlinear.

turbed solution ultimately decays towards a trivial state with no acoustic content, a pure entropy wave ($V = V(x)$, $u \equiv 0$, $p = const$ as $t \to \infty$). This would be the scenario favored by the current ideas regarding the long time behavior of genuinely nonlinear hyperbolic conservation laws, as explained in the Introduction[42].

(2) The (small) perturbation introduced in the solution induces shocks. These shocks produce dissipation and eventually decay and become negligible. The solution thus converges (as $t \to \infty$) to one without shocks. But this limit solution does not need to have — as in the scenario **(1)** above — a trivial acoustic content. As mentioned before in Section 3.2, the set of solutions whose complete time evolution lacks shocks can be very rich. Thus, we could have:

(2a) The limit solution is a standing periodic acoustic wave of the type we have been investigating. This would correspond to the type of behavior observed by Majda, Rosales & Schonbeck (1988) in the context of the weakly nonlinear asymptotic equations they investigated numerically (see the Introduction).

(2b) The limit solution has nontrivial acoustic content, but it is not a standing periodic acoustic wave.

We note that, in case (2a), the limit solution cannot be the same one we started from — because of the decay and extra entropy produced by the shocks. Thus, a notion of "asymptotic stability" would make sense only in some sort of (generalized) "orbital" sense. This is even truer in case (2b). It should be clear then that any stability issue for the kind of solutions we are investigating would involve some very subtle considerations — which we will not attempt to clarify here. Generally we conjecture that small enough perturbations will give rise to a type (2a) scenario. Larger ones should produce any of the three.

In this sense, nonlinear periodic acoustic waves, which are isolated solutions of the Gas Dynamic equations, may nevertheless constitute part of an attractor[43] for arbitrary initial conditions. This feature may enlarge substantially the class of smooth for all times solutions in nonlinear acoustics, which in turn should make them more attractive for practical applications. We suspect that the geometry of such an attractor is very complex and we have not attempted to investigate it.

In Chapter 1, based on the behavior of the leading order traveling wave solutions found by Pego (see Section 1.5), it was argued that the periodic acoustic waves satisfying Euler's equations would present corners in their profiles at the maximum amplitude. This phenomenon would express the limiting balance between nonlinear distortion and dispersion that makes possible continuous finite amplitude sound

[42]Of course, these ideas do not even allow the existence of the object whose stability we want to study.

[43]That would include other solutions with nontrivial acoustical contents and no shocks. Perhaps multiply-periodic (in time) waves, or more complicated.

waves. This conjecture was made stronger by the numerical calculations of Chapter 3.

A similar prediction can now be formulated for the absolute stability problem. As said before, shocks will appear in finite time when a periodic acoustic wave is perturbed. In this situation, nonlinear effects would prevail over the dispersive effects coming from the coupling of acoustic and entropy modes. If the second case mentioned above occurs, the balance between nonlinearity and dispersion will be restored, and continuous waves will appear. It is very likely, then, that the emerging acoustic waves will display corners in the flow quantities' profiles, as the balance just regained will correspond to a limiting case[44].

We have tested these ideas numerically. As pointed out in Section 3.2, an evolution type of calculation can be very helpful for studying the stability of our finite amplitude periodic acoustic waves when subject to arbitrary perturbations. Although this type of approach does not constitute an exhaustive analysis of the topic, it does provide a relatively quick and robust way to test our hypotheses, especially in view of the considerable difficulties an analytical treatment would present.

To solve the initial value problem for the Euler's equations, we employed a pseudospectral or Fourier collocation method to evaluate the flux gradients and a standard fourth order Runge-Kutta method for the time discretization (cf. Vichnevetsky & Bowles (1982) and Canuto et al. (1988)).

The occurrence of shocks in the initial value problem demands some precautions in the formulation of the numerical method (cf. Leveque (1990)). First, we have to use the proper conservation form of the equations of motion (enforcing conservation of mass, momentum and energy), leaving aside equation (1.3) that only holds for adiabatic processes. This condition is satisfied by equations (1.a), (1.b) and (1.c). Second, to guarantee that the numerical scheme "picks out" the physically relevant weak solution, an entropy satisfying method must be employed.

The second condition above must be addressed with special care. It is known that spectral methods can in fact converge to a weak solution satisfying the proper entropy condition (cf. Canuto et al. (1988), cap. 8, and refs. therein). However, as pointed out by Majda et al. (1978), in the presence of discontinuities the global nature of spectral methods induces oscillations of the familiar Gibbs phenomenon type in the solution. High frequency spectral coefficients of discontinuous functions decay very slowly. Therefore, some sort of filtering must be applied to that portion of the spectrum in order to have nonoscillatory shocks and avoid aliasing errors. The filter is, in fact, also responsible for the verification of the proper entropy conditions at the shocks — as it is, actually, a form of viscosity.

[44]Achieved by decaying to it from larger energies. See the next to last paragraph in this Section for more details.

Recently, there has been some progress in the development of filtering techniques for hyperbolic problems with discontinuous solutions. However, convergence analyses have only been provided for linear systems. Despite this limitation, we chose to use a pseudospectral approximation with filtering in our absolute stability problem for two reasons: first, it is a shock-capturing, entropy satisfying method that guarantees a physically correct propagation of discontinuities. Second, since we are mostly interested in the properties of the perturbed flows after the shocks have disappeared, an extremely detailed shock structure representation is not needed. In this context, the filtering technique is simply a necessary intermediate step to obtain the final smooth solutions. And it is precisely at that final stage where the great accuracy of spectral methods can have a competitive advantage over other methods[45]. Thus, although not well-suited in general for nonlinear hyperbolic problems, a spectral method is reasonable for the present absolute stability analysis.

In our calculations, we have employed a standard raised cosine filter applied in Fourier space to smooth the solution at regular intervals in time. The raised cosine filter is algebraically equivalent (at leading order) to a second order artificial viscosity term with $\nu = (\Delta x)^2/4\Delta t N_f$, where N_f is the number of time steps between applications of the filter. To adjust the filtering strength, we calibrated our code on a model problem, namely, the shock tube problem posed by Sod (1978).

Equipped with this numerical solver for the Euler equations (1.a), (1.b) and (1.c), we first tested the accuracy of the finite amplitude periodic acoustic waves calculated in Chapter 3. As initial conditions, we took

$$V(x,0) \;=\; \bar{V}(x,0),$$

$$u(x,0) \;=\; \bar{u}(x,0) \;\equiv\; 0,$$

$$E(x,0) \;=\; \frac{1}{2}\,\bar{u}^2(x,0) \;+\; \bar{e}(x,0) \;=\; \frac{1}{\gamma\,(\gamma-1)}\; e^{\gamma S(x,0)}\;\; \bar{V}^{-\gamma+1}(x,0),$$

where $\bar{V}(x,0)$ and $\bar{u}(x,0)$ correspond to a smooth, continuous and periodic solution calculated by the method of Section 3.3. Notice that, initially the entropy field is given by $S(x,0) = \epsilon K(x)$. Namely, it is just the assumed background used in the calculation of the periodic sound waves. But, in general, as shocks may develop, for $t > 0$ the entropy function $S(x,t)$ must be recovered from the total energy $E(x,t)$ and the equation of state.

Figure 104 compares a smooth, finite amplitude acoustic wave as calculated in Chapter 3 and representing the initial data for the spectral solver, with its evolution

[45]Generally, spectral methods are not very competitive when shocks (particularly strong ones — which we do not have) are involved.

after 500 periods. Figure 105 displays the same comparison, but when a smooth, high intensity acoustic wave is used as initial condition. Considering that the method of Chapter 3 for the solution of a nonlinear boundary-value problem is only second order accurate, these periodicity checks clearly show that the algorithm of Section 3.3 is remarkably robust. It also shows that the standing periodic wave is "stable", as it is not destroyed by the (small) numerical errors the solver introduces.

Going now back to the absolute stability problem, we took again one of the finite amplitude acoustic waves of Chapter 3 as initial condition, and added a small disturbance of the form $\tilde{V} = -A_p\, sin(x)$, $\tilde{u} = A_p\, cos(x)$ with $A_p \simeq 10^{-4}$. We then followed the time evolution of this perturbed flow with our spectral code. A systematic series of numerical experiments aimed at exploring the geometry of the attractor mentioned before, was not performed. With a more limited goal, a reduced number of calculations sufficed to confirm the predicted scenarios as $t \to \infty$. We will present numerical results just for the more interesting one, i.e., case 2.

A natural criterion to detect whether a smooth wave without shocks emerges at large times is given by the stabilization of the total entropy. If the flow field contains shocks, entropy is generated. Conversely, if the total entropy reaches asymptotically a constant value, the flow quantities will be continuous. If in addition, the solution has nontrivial acoustical content, then the balance between nonlinearity and dispersive effects would have been restored. Then the final asymptotic solution, after all finite jumps disappeared, will constitute a smooth wave (without shocks) of which the periodic continuous acoustic waves are an example. This criterion, expressed in terms of the primary dependent variables V, u and E takes the form

$$\langle\, S(t)\,\rangle \;=\; \frac{1}{2\pi}\int_0^{2\pi} S(x,t)\,dx \;=$$

$$= \frac{1}{2\pi}\int_0^{2\pi} \frac{1}{\gamma}\, ln\left\{\gamma(\gamma-1)\left[E(x,t)-\frac{1}{2}u^2(x,t)\right]\, V^{\gamma-1}(x,t)\right\} dx \to const. \quad as \quad t\to\infty.$$

Figures 106 to 109 illustrate the situation described in case 2, when the initial data are given by a large amplitude periodic acoustic wave[46]. Due to a disturbance of the type described above, strong shocks develop rapidly and later decay, as the total entropy $\langle S(t)\rangle$ approaches a constant value (Fig. 106a). Figures 106b and 106c display the L^∞ and L^1 norms of $u(x,t)$: at large times both measures oscillate around finite positive (albeit small) values, thus indicating unmistakably the presence of a nontrivial wave structure. (For a trivial pure entropy solution with no acoustical content, both measures go to zero and there are no oscillations). Finally, Figures 107–109 show the dependent variables at several instants of time (roughly a sixth of a period apart) after the large time standing periodic wave emerged. Notice that

[46]Here the limiting solution appears to be very close to a periodic wave, so we have the scenario (2a).

these profiles do exhibit corners[47] as predicted before, a manifestation of the limiting balance between nonlinear and dispersive effects just before breaking. The velocity profiles, in particular, resemble those corresponding to Pego's solution in weakly nonlinear acoustics depicted in Fig. 2.

A final remark to clarify the behavior of nonlinear acoustic waves in parameter space is in place. Recall that in Chapter 3, when calculating periodic acoustic waves for increasing amplitudes a, at some point we reached the maximum amplitude a_{max} permitted for continuous solutions. That instance defined a threshold in parameter space beyond which the continuous solutions break down and cease to exist. There the calculation proceeded from a region in parameter space where nonlinear and dispersive effects were balanced — yielding continuous, periodic solutions — towards another region where such balance was not possible and shock formation effects dominated. It should be clear that when we approach an absolutely stable periodic acoustic wave in a calculation as described above, we follow a similar path but in a reverse sense: starting from a wave distortion dominated region, where shocks form and decay, we finally end up over the threshold, at a continuous but non-smooth (with corners) periodic sound wave. Notice that this wave cannot be smoothed out any further by penetrating into the dispersive dominated region in parameter space, since no dissipative mechanism is present to reduce its amplitude.

In sum, much work remains to be done regarding the large time behavior of finite amplitude periodic sound waves. For example, it would be interesting to determine in a comprehensive way the amplitude, functional form and frequency of the initial conditions that produce nontrivial acoustic waves for $t \to \infty$, as opposed to those that yield trivial final solutions. Nevertheless, the preliminary evidence presented in this chapter does confirm our presumptions concerning the global behavior of sound waves propagating in an inhomogeneous media and the striking possibility of nontrivial acoustic waves surviving strong shock waves in the long time evolution of the equations.

[47]These are noticeable only in the u and p profiles. In the V profile, the large contribution from the steady equilibrium part of the solution (V_f) dominates and swamps the acoustic component — where the corners occur.

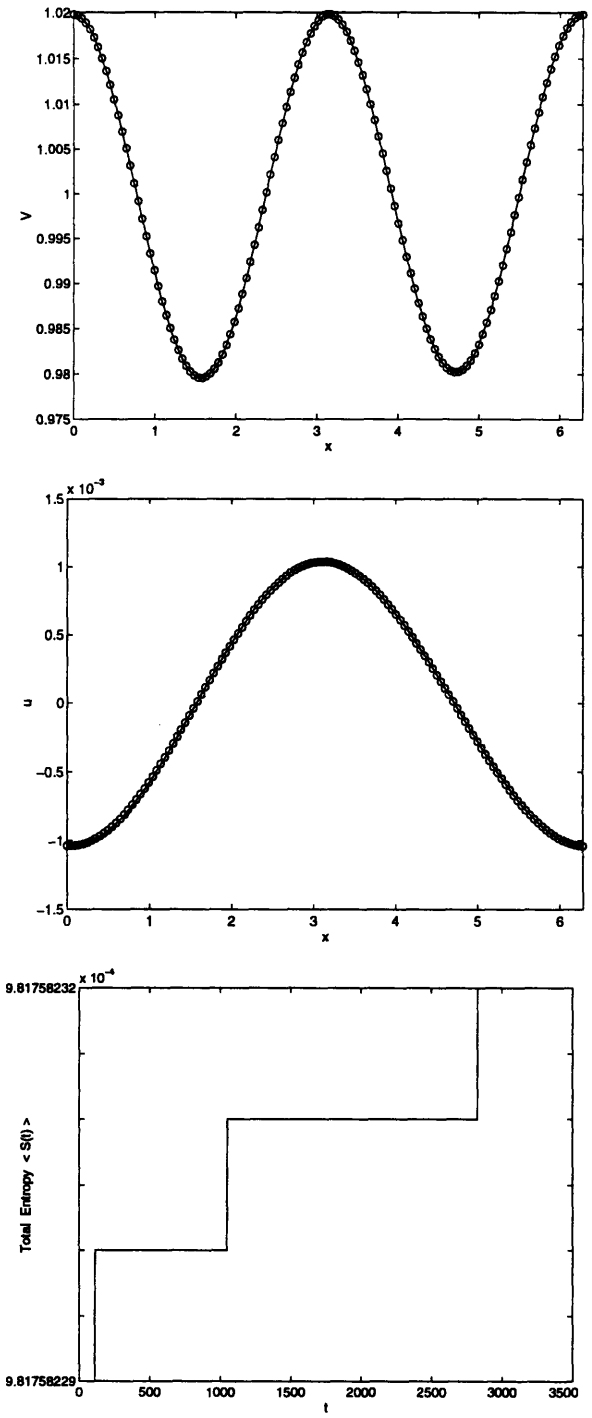

Figure 104: Periodicity check: specific volume V and velocity u at $t = 0$ (ooo) and $t = 500\,T$ (—), and Total Entropy $\langle S(t) \rangle$ between $t = 0$ and $t = 500\,T$, for a smooth sound wave with $\epsilon = 0.01$, $\omega = 1.00511$, $a = 0.00054$, $SPL = 132.5dB$, $M = 0.00110$ (TC 2). Notice that $\langle S(t) \rangle$ changes in the 11th decimal.

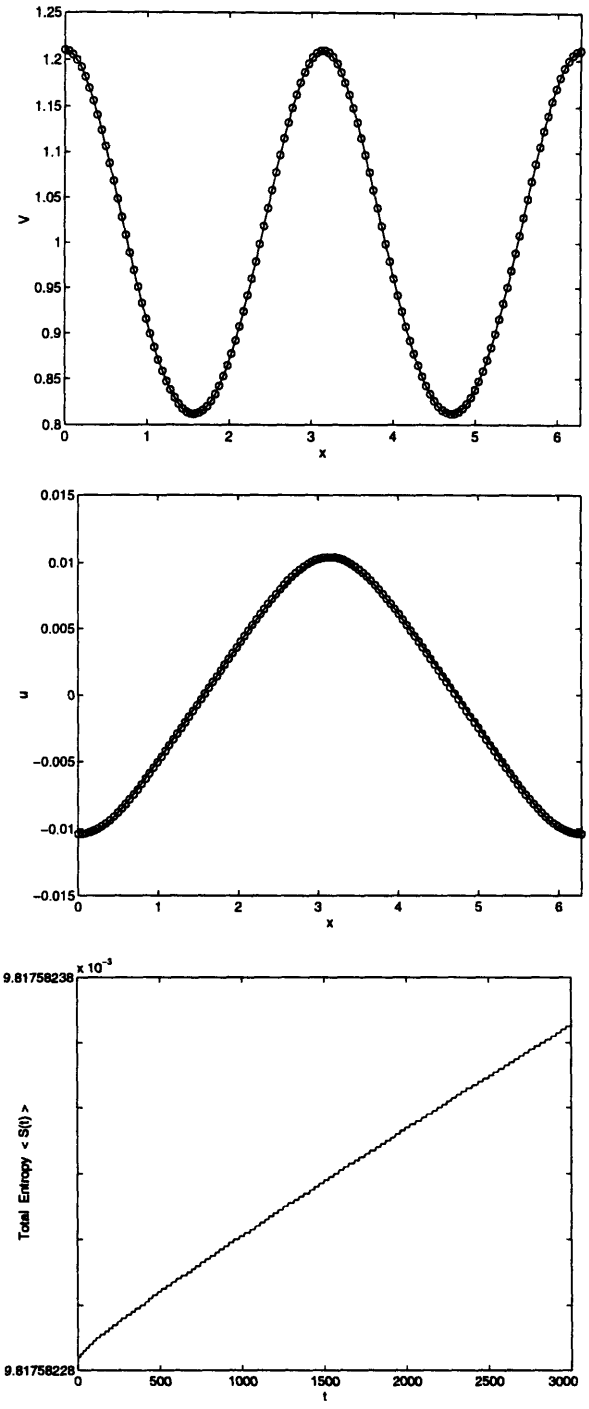

Figure 105: Periodicity check: specific volume V and velocity u at $t = 0$ (ooo) and $t = 500\,T$ (—), and Total Entropy $\langle S(t) \rangle$ between $t = 0$ and $t = 500\,T$, for a smooth, high intensity sound wave with $\epsilon = 0.1$, $\omega = 1.05888$, $a = 0.00471$, $SPL = 151.5dB$, $M = 0.01137$ (TC 2). Notice that $\langle S(t) \rangle$ changes in the 10th decimal.

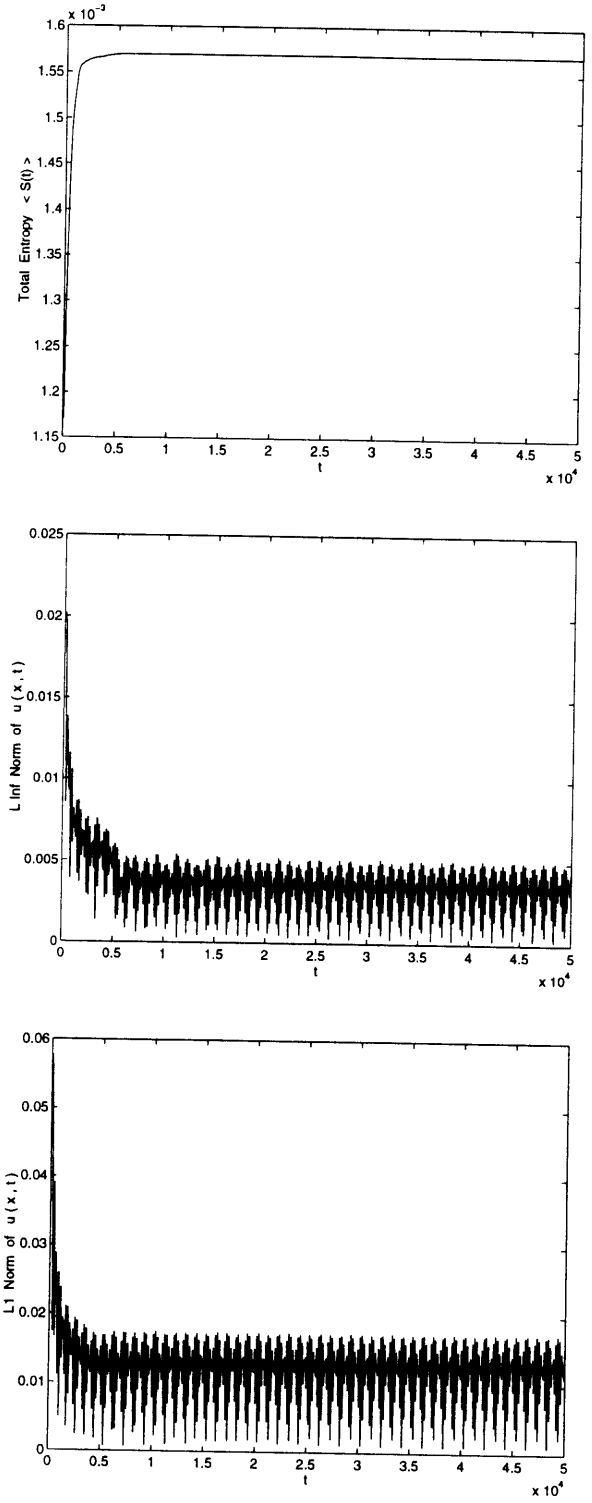

Figure 106: Asymptotic Stability: Total entropy $\langle S(t) \rangle$, L^∞ and L^1 norms of $u(x,t)$, when the high intensity sound wave of figs. 23 to 31 is perturbed initially.

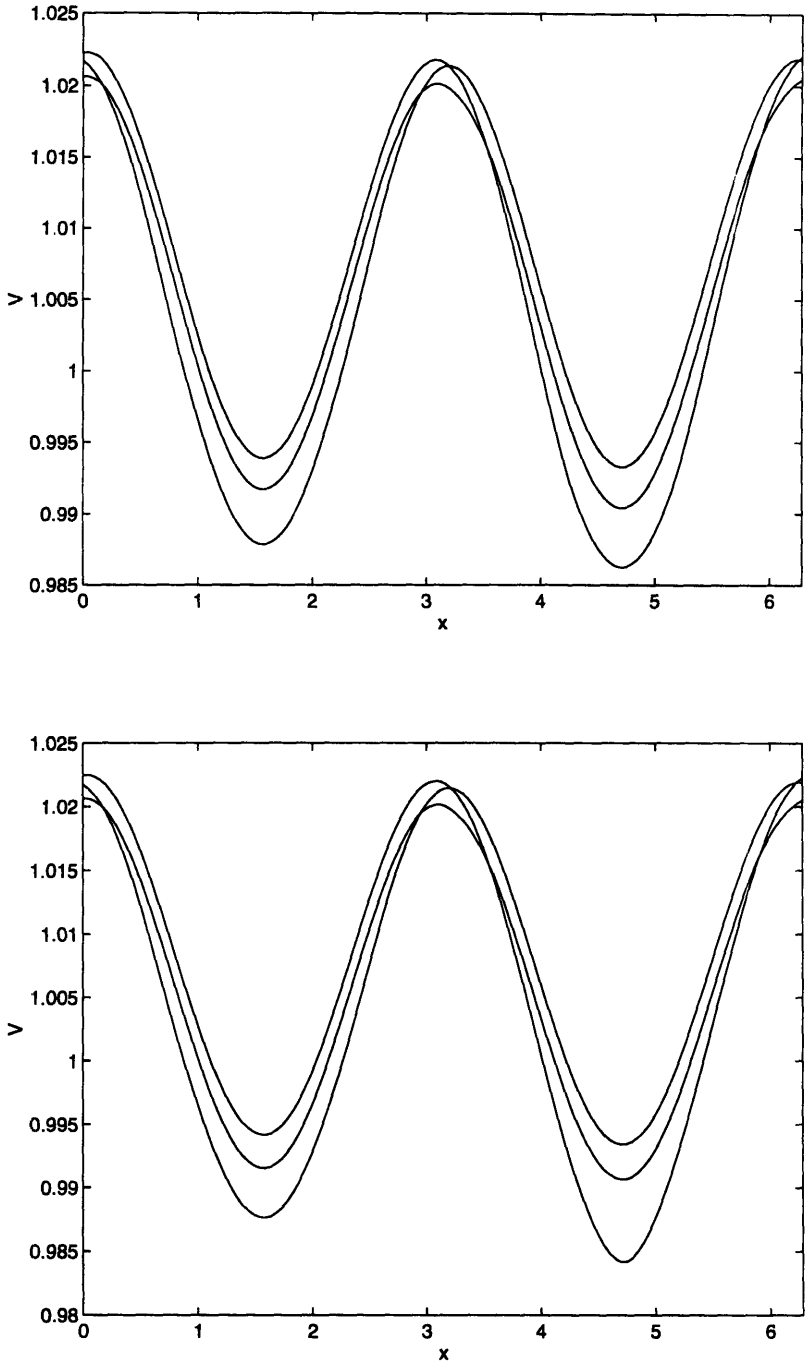

Figure 107: Asymptotic Stability: specific volume V after shocks disappeared, at six different times ($\Delta t \simeq T/6$), when the high intensity sound wave of figs. 23 to 31 is perturbed initially.

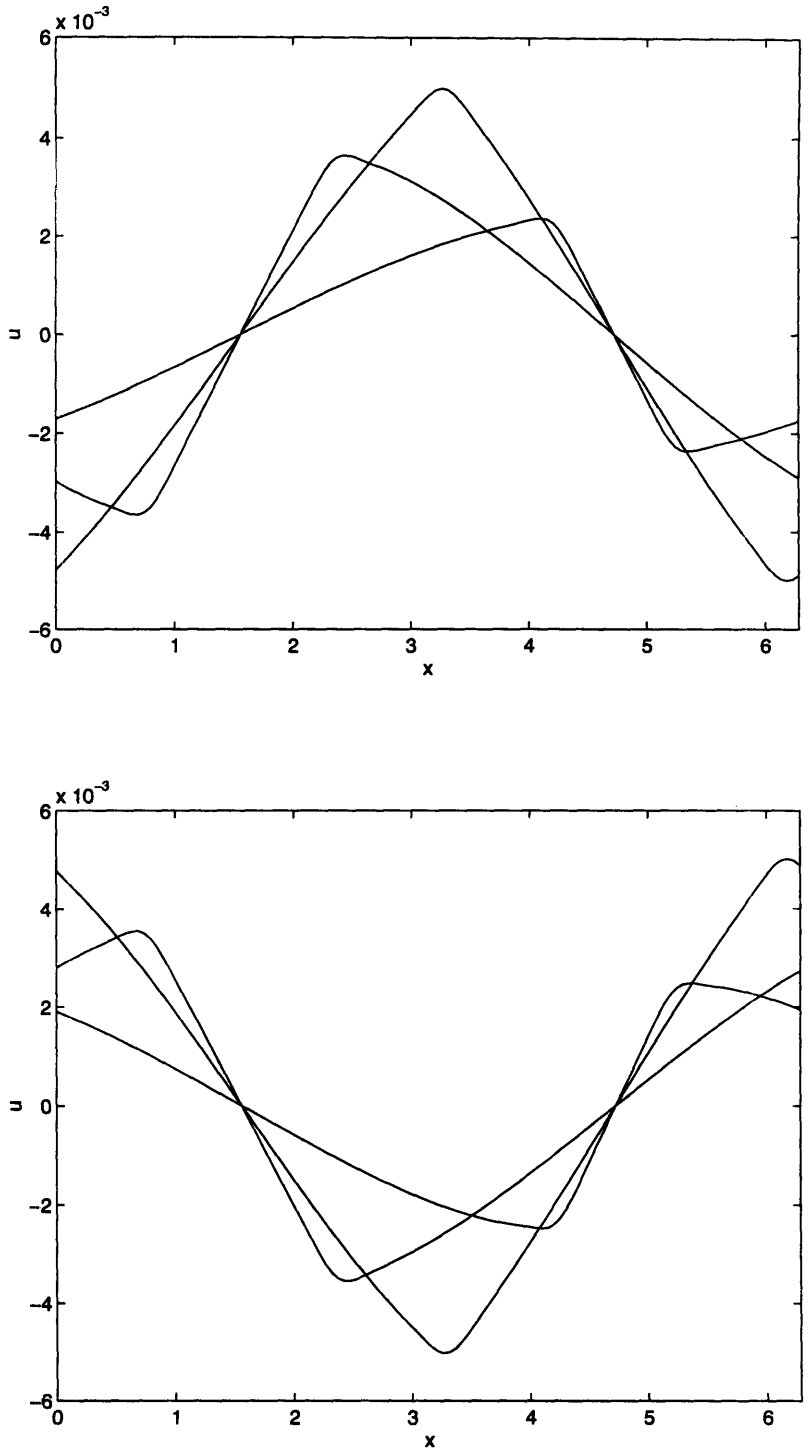

Figure 108: Asymptotic Stability: velocity u after shocks disappeared, at six different times ($\Delta t \simeq T/6$), when the high intensity sound wave of figs. 23 to 31 is perturbed initially.

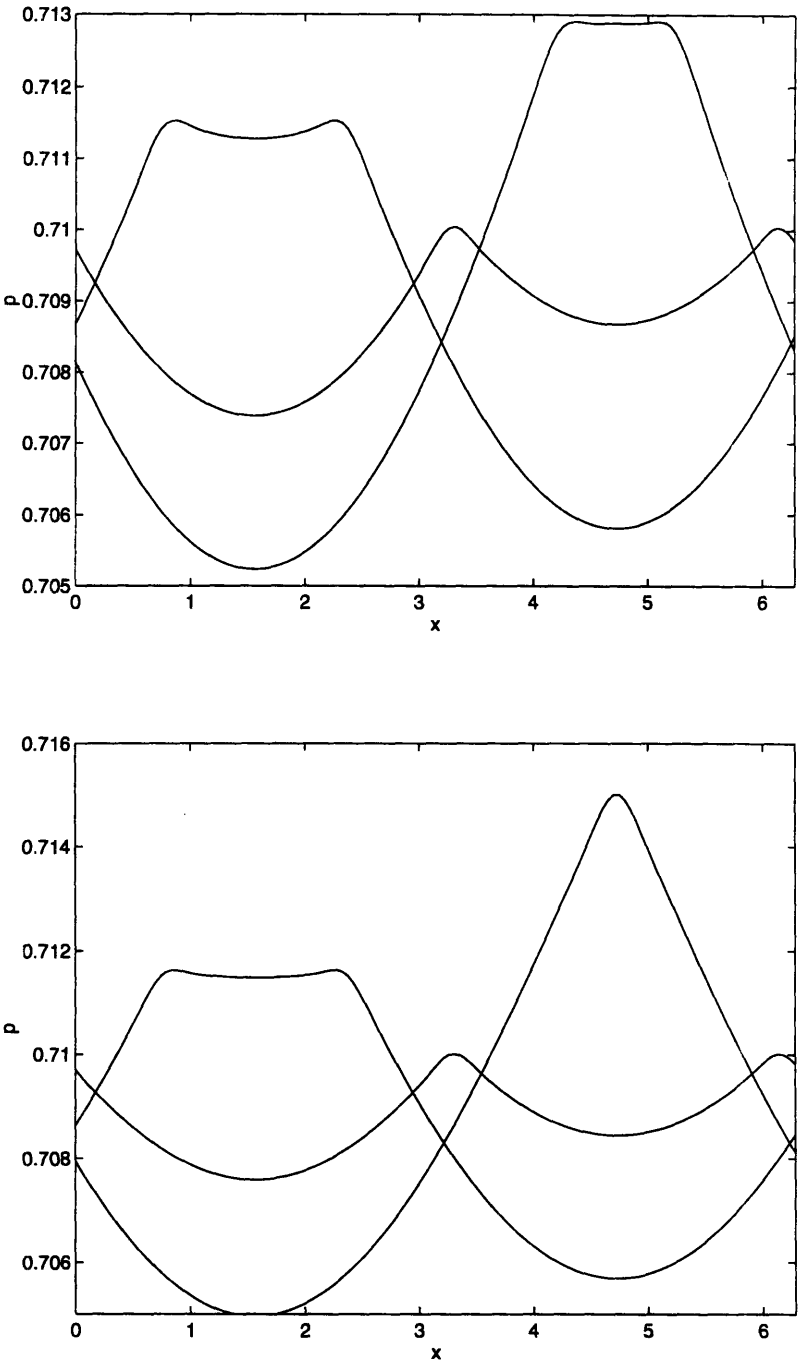

Figure 109: Asymptotic Stability: pressure p after shocks disappeared, at six different times ($\Delta t \simeq T/6$), when the high intensity sound wave of figs. 23 to 31 is perturbed initially.

Conclusions

A new class of solutions in 1D Gas Dynamics was found. Remarkably, these solutions do not develop shocks at any time, even though the genuinely nonlinear modes (acoustic) are excited. These solutions are given as finite amplitude, continuous and time periodic acoustic waves propagating in a nonuniform entropy background.

The fundamental mechanism that prevents hyperbolic wave breaking was identified as a resonant, nonlocal coupling between the acoustic and entropy modes. This interaction has a dispersive character that balances the nonlinear terms in the equations of motion and produces a continuous flow. A complete study of the (formal) conditions that guarantee the existence of small amplitude periodic acoustic waves was performed using weakly nonlinear and bifurcation theories. Although a simple entropy mode was employed in many of our analytical and numerical calculations, the approach is general and can be extended straightforwardly to problems involving very general entropy fields (as shown in various cases). Thus, time periodic sound waves encompass a rich variety of solutions in nonlinear acoustics.

Numerical calculations displayed the domain of existence of these continuous solutions in parameter space. In particular, for a given entropy wave amplitude ϵ, they showed that periodic waves can occur only in a bounded range of acoustic amplitudes $0 < a \leq a_{max}$, with $\omega = \omega(a)$ the fundamental time frequency. The computations also showed that extremely high intensity sound waves are possible in the presence of relatively small entropy fluctuations. At the maximum amplitude a_{max}, these standing acoustic waves exhibit corners in the flow quantities' profiles, similarly to free-surface gravity waves in water.

Furthermore, while neutrally stable against infinitesimal perturbations, it appears that these solutions can be asymptotically stable when subject to small but finite disturbances: a nontrivial periodic acoustic wave, though different from the initial basic periodic flow, may emerge after the shocks have disappeared. More generally, a continuous (for all times) wave with nontrivial acoustic component may emerge. This striking phenomenon enlarges substantially the class of continuous for all time solutions in nonlinear acoustics: in addition to the strictly periodic acoustic waves found by our theoretical and numerical studies, the stability calculations suggest that continuous, almost periodic solutions can also exist. Moreover, this result suggests that, contrary to common belief, strong waves in a cavity with reflecting boundaries may decay to the equilibrium state only due to viscous effects and at a much slower rate than the one shocks would produce. [48].

[48] $O(t^{-1/2})$ as opposed to $O(t^{-1})$ — which is the typical decay for space periodic N-waves. Recall that the decay rate of the inviscid theory is $O(t^{-1/2})$ in unbounded domains.

This result could be important in certain combustion problems and in sound generation by moving objects inside enclosed domains; problems where the balance between dissipation and forcing is crucial in determining the type and amplitude of the waves generated.

Several topics for future research arising from this work can be enumerated. A brief description of some of them follows.

We have studied here the propagation in one space dimension of nonlinear acoustic waves through an entropy background. In two or more space dimensions it is known that, to leading order, entropy and shear modes can couple planar oblique sound waves in the same fashion that entropy variations couple sound waves in one dimension (cf. Majda, Rosales & Schonbeck (1988) and Hunter, Majda & Rosales (1986)). Therefore, it seems possible to apply our ideas to study resonant nonlinear acoustic wave interactions in the presence of a nonuniform background given by a combination of vorticity and entropy fields. In this context, by combining analytical studies with numerical calculations, it would be interesting to explore topics of practical relevance in aero-acoustics, such as sound generation by low Mach number airflows (that can lead to regular oscillations at moderate Reynolds number R or turbulence at high R). This approach may also contribute to a better understanding of the relation between acoustic output and vorticity distributions, so critical in jet noise control and for designing turbomachinery components in aircraft engine propulsion systems.

An important objective in the area of noise reduction, is to achieve reliable calculations of the acoustic output (a very small fraction of the total system energy) of a gas flow. For this purpose, accurate modeling of the fundamental physical processes, even in relatively simple situations, is required to validate numerical codes for more realistic unsteady flow-related noise generation problems. In this context, it is important to note that many of the current numerical methods have the unfortunate feature that they generate (small) spurious entropy variations as shocks and other large waves interact with the numerical mesh. Our one dimensional work in Chapter 3 showed that entropy variations as small as 0.1% can produce very strong couplings in the sound waves. In view of this fact, it is clear that those spurious entropy variations can (potentially) have a very large effect on the computed acoustical field.

Another situation that can be considered is when the resonant couplings of sound waves occur in a reacting flow. Two main areas of possible interest here are the study of the interaction of flames with sound waves (in particular, the production of sound by flames) and DDT (Deflagration-Detonation Transition). In both cases, nonlinear couplings of the acoustical and entropy-vorticity fields appear to be very important, and rather poorly understood. This is further compounded by the strong couplings that result from chemical reactions that are usually very sensitive to either pressure or temperature variations (large activation energies). Many (asymptotic) studies of these effects have been done in the weakly nonlinear regime (see, for example, Almgren, Majda & Rosales (1991a,b)), but it would be worth exploring larger amplitudes

than those accessible by perturbation methods, in the same way that was done here, namely, by a balanced combination of analytical and numerical work.

References

Ablowitz, M. J. & Segur, H. (1981) *Solitons and the Inverse Scattering Transform.* SIAM, Philadelphia.

Almgren, R. F., Majda, A. & Rosales, R. R. (1991a) "Asymptotic analysis of reacting materials with saturated explosion. I. Low-frequency waves". Stud. Appl. Math **84**, 275–313.

Almgren, R. F., Majda, A. & Rosales, R. R. (1991b) "Asymptotic analysis of reacting materials with saturated explosion. II. High-frequency waves". Stud. Appl. Math **84**, 315–360.

Arnold, V. I. (1978) *Mathematical Methods of Classical Mechanics.* Springer-Verlag, New York.

Arscott, F. M. (1964) *Periodic Differential Equations.* The MacMillan Company, New York.

Beranek, L. L. (1949) *Acoustic Measurements.* John Willey & Sons, Inc., New York.

Beyer, R. T. (1974) *Nonlinear Acoustics.* Naval Ship Systems Command, Dept. of the Navy.

Beyer, R. T. (ed.) (1984) *Nonlinear Acoustics in Fluids.* Van Nostrand Reinhold Co., New York.

Brezis, H. & Nirenberg, L. (1978) "Forced vibrations for a nonlinear wave equation". Comm. Pure Appl. Math. **31**, 1–30.

Canuto, C., Hussaini, M. Y., Quarteroni, A. & Zang, T. A. (1988) *Spectral Methods in Fluid Dynamics.* Springer-Verlag, New York.

Cokelet, E. D. (1977) "Steep gravity waves in water of arbitrary uniform depth". Phil. Tran. Roy. Soc. London A **286**, 183–230.

Courant, R. & Friedrichs, K. O. (1948) *Supersonic Flow and Shock Waves.* Wiley (Interscience), New York.

Drennan, W. M., Hui, W. H. & Tenti, G. (1992) "Do Stokes' series converge for large amplitudes ?". In *Breaking Waves*, Banner, M. L. & Grimshaw, R. H. J. (eds), 187–192. Springer-Verlag, Berlin.

Dwoyer, D. L. & Hussaini, M. Y. (eds.) (1987) *Stability of Time Dependent and Spatially Varying Flows.* Springer-Verlag, New York.

E, W. & Yang, H. (1991) "Numerical study of oscillatory solutions of the gas-dynamic equations". Stud. Appl. Math. **85**, 29–52.

Friedman, B. (1990) *Principles and Techniques of Applied Mathematics.* Dover Publications, Inc., New York.

Glimm, J. (1965) "Solutions in the large for nonlinear hyperbolic systems of equations". Comm. Pure Appl. Math. **18**, 697–715.

Goldstein, M. E. (1976) *Aeroacoustics.* McGraw-Hill, New York.

Hardin, J. C. & Hussaini, M. Y. (eds.) (1993) *Computational Aeroacoustics.* Springer-Verlag, New York.

Hayashi, C. (1964) *Nonlinear Oscillations in Physical Systems.* McGraw-Hill, New York.

Herbert, T. (1988) "Secondary instability of boundary layers". Ann. Rev. Fluid Mech. **20**, 487–526.

Hunter, J. K., Majda, A. & Rosales, R. (1986) "Resonantly interacting, weakly nonlinear hyperbolic waves. II. Several space variables". Stud. Appl. Math. **75**, 187–226.

Ince, E. L. (1956) *Ordinary Differential Equations.* Dover Publications, Inc., New York.

Ioos, G. & Joseph, D. D. (1980) *Elementary Stability and Bifurcation Theory.* Springer Verlag, New York.

Jordan, D. W. & Smith, P. (1987) *Nonlinear Ordinary Differential Equations.* Oxford University Press, New York.

Joseph, D. D. (1976) *Stability of Fluid Motions.* Vol 1. Springer-Verlag, Berlin.

Keller, H. B. (1992) *Numerical Methods for Two-Point Boundary-Value Problems.* Dover Publications, Inc., New York.

Keller, J. B. & Ting, L. (1966) "Periodic vibrations of systems governed by nonlinear partial differential equations". Comm. Pure Appl. Math. **19**, 371–420.

Kevorkian, J. & Cole, J. D. (1981) *Perturbation Methods in Applied Mathematics.* Springer-Verlag, New York

Kubicek, M. & Hlavacek, V. (1983) *Numerical Solution of Nonlinear Boundary Value Problems with Applications.* Prentice-Hall, Inc., New Jersey.

Lax, P. D. (1957) "Hyperbolic systems of conservation laws II". Comm. Pure Appl. Math. **10**, 537–566.

Lax, P. D. (1964) "Development of singularities of solutions of nonlinear hyperbolic partial differential equations". J. Math. Phys. **5**, 611–613.

Leveque, R. J. (1990) *Numerical Methods for Conservation Laws.* Birkhauser Verlag, Basel.

Levi–Civita, T. (1925) "Determination rigoureuse des ondes permanentes d'ampler finie". Math. Ann. **93**, 264–314.

Longuet-Higgins, M. S. (1975) "Integral properties of periodic gravity waves of finite amplitude". Proc. Roy. Soc. A **342**, 157–174.

Liu, T. P. (1977a) "Decay to N-waves of solutions of general systems of nonlinear hyperbolic conservation laws". Comm. Pure Appl. Math. **30**, 585–610.

Liu, T. P. (1977b) "Linear and nonlinear large-time behavior of solutions of general systems of hyperbolic conservation laws". Comm. Pure Appl. Math. **30**, 767–796.

Majda, A., McDonough, J. & Osher, S. (1978) "The Fourier method for nonsmooth initial data". Math. Comput. **32**, 1041–1081.

Majda, A. & Rosales, R. (1984) "Resonantly interacting, weakly nonlinear, hyperbolic waves. I. A single space variable". Stud. Appl. Math. **71**, 149–179.

Majda, A., Rosales, R. & Schonbek, M. (1988) "A canonical system of integrodifferential equations arising in resonant nonlinear acoustics". Stud. Appl. Math. **79**, 205–262.

Mason, W. P. (ed.) (1965) *Physical Acoustics.* Academic Press, New York.

McLachlan, N. W. (1947) *Theory and Application of Mathieu Functions.* Clarendon Press, Oxford.

Milne-Thomson, L. M. (1968) *Theoretical Hydrodynamics.* MacMillan & Co., London.

Moser, J. (1973) *Stable and Random Motions in Dynamical Systems.* Princeton Univ. Press, New Jersey.

Murdock, J. (1991) *Perturbations: Theory and Methods.* John Wiley & Sons, Inc., New York.

Nishida, T. & Smoller, J. (1973) "Solutions in the large for some nonlinear hyperbolic conservation laws". Comm. Pure Appl. Math. **26**, 183–200.

Pego, R. L. (1988) "Some explicit resonating waves in weakly nonlinear gas dynamics". Stud. Appl. Math **79**, 263–270.

Penney, W. G. & Price, A. T. (1952) "Finite periodic stationary gravity waves in a perfect liquid". Phil. Trans. Roy. Soc. A **244**, 254–284.

DiPerna, R. J. (1973) "Existence in the large for quasilinear hyperbolic conservation laws". Arch. Rat. Mech. Anal. **52**, 244–257.

Rabinowitz, P. H. (1967) "Periodic solutions of nonlinear hyperbolic partial differential equations". Comm. Pure Appl. Math. **20**, 145–205.

Rabinowitz, P. (ed.) (1977) *Applications of Bifurcation Theory.* Academic Press, New York.

Rabinowitz, P. H. (1978) "Free vibrations for a semilinear wave equation". Comm. Pure Appl. Math. **31**, 31–68.

Rudenko, O. V. & Soluyan, S. I. (1977) *Theoretical Foundations of Nonlinear Acoustics.* Consultants Bureau, New York.

Sattinger, D. H. (1972) *Topics in Stability and Bifurcation Theory.* Lectures Notes in Mathematics No. 762. Springer–Verlag, New York.

Schwartz, L. W. (1974) "Computer extension and analytic continuation of Stokes' expansion for gravity waves". J. Fluid Mech. **62**, 553–578.

Sod, G. A. (1978) "A survey of several finite difference methods for systems of nonlinear hyperbolic conservation laws". J. Comp. Phys. **27**, 1–31.

Stoker, J. J. (1950) *Nonlinear Vibrations.* Interscience, New York.

Taylor, G. I. (1953) "An experimental study of standing waves". Proc. Roy. Soc. A **218**, 44–59.

Temple, J. B. (1981) "Solutions in the large for the nonlinear hyperbolic conservation laws of gas dynamics". J. Diff. Eqs. **41**, 96–161.

Vichnevetsky, R. & Bowles, J. B. (1982) *Fourier Analysis of Numerical Approximations of Hyperbolic Equations.* SIAM, Philadelphia.

Whitham, G. B. (1974) *Linear and Nonlinear Waves.* John Willey & Sons, New York.

Appendix 1.1

Pressure Expansion

The equation of state for a polytropic gas with an adiabatic exponent γ is given by equation (1.4)

$$p = p(S,V) = \frac{1}{\gamma}\, e^{\gamma S}\, V^{-\gamma}.$$

Substituting the entropy wave $S(x)$ as given by equation (1.5) and the specific volume V according to its asymptotic expansion (1.6), we have

$$p = p(S,V) = \frac{1}{\gamma} e^{\gamma\,\epsilon\,K} \left\{ 1 \,+\, \sum_{i=1}^{\infty} V_i\, \epsilon^i \right\}^{-\gamma}.$$

Using notation introduced in (1.8), the pressure expansion can be written

$$p(S,V) = \frac{1}{\gamma} \,+\, \epsilon\,(\,K - V_1\,) \,+\, \sum_{i=2}^{\infty} (\,-V_i + \hat{p}_i\,)\,\epsilon^i,$$

where terms $\hat{p}_i$ have the following structure:

$$\hat{p}_i = KV_{i-1} + P_i, \qquad\qquad P_i = f(K, V_1, V_2, ..., V_{i-2}).$$

If we now make use of the first order solution $V_1 = K$, the functions $\hat{p}_i$ are given by

$$\hat{p}_2 = KV_1 + P_2 = \tfrac{1}{2}K^2,$$

$$\hat{p}_3 = KV_2 + P_3 = KV_2 - \tfrac{1}{3}K^3,$$

$$\hat{p}_4 = KV_3 + P_4 = KV_3 + \tfrac{1}{8}(-2\gamma^3 + \gamma + 2)\, K^4 - \tfrac{1}{2}\,(2+\gamma)\, K^2\, V_2 + \tfrac{1}{2}\,(1+\gamma)\, V_2^2,$$

$$\hat{p}_5 = KV_4 + P_5 = KV_4 - \tfrac{1}{30}\,(6+5\gamma)\, K^5 + \tfrac{1}{6}\,(6+5\gamma)\, K^3\, V_2 + \tfrac{1}{2}\,(2+\gamma)\, K^2\, V_3$$

$$+(1+\gamma)\, K\, V_2^2 + (1+\gamma)\, V_2\, V_3,$$

$$\vdots$$

Appendix 1.2

Weakly nonlinear analysis: $O(\epsilon^3)$ solution

Forcing terms appearing in the integro–differential equations (1.38) and (1.39) are given by

$$R_3(\lambda) = -\frac{1}{4\pi}\,\omega_1\,\frac{\partial}{\partial\lambda}\int_0^{2\pi}\left[\,\mathcal{V}_2+\mathcal{U}_2\,\right]d\mu - \frac{1}{4\pi}\frac{\partial}{\partial\lambda}\int_0^{2\pi}\left[\,K\mathcal{V}_2+P_3\,\right]d\mu,$$

$$T_3(\mu) = -\frac{1}{4\pi}\,\omega_1\,\frac{\partial}{\partial\mu}\int_0^{2\pi}\left[\,\mathcal{V}_2-\mathcal{U}_2\,\right]d\lambda - \frac{1}{4\pi}\frac{\partial}{\partial\mu}\int_0^{2\pi}\left[\,K\mathcal{V}_2+P_3\,\right]d\lambda.$$

Replacing functions $\mathcal{V}_2 = 2cos[2(\lambda-\mu)]$, $\mathcal{U}_2 \equiv 0$ and P_3 as given in Appendix 1.1, we immediately obtain

$$R_3(\lambda) = T_3(\mu) \equiv 0.$$

Therefore, unidirectional waves $\sigma_2(\mu)$ and $\rho_2(\lambda)$ satisfying (1.38)–(1.39) can be written

$$\sigma_2(\mu) = \delta^{(2)}_{1,0}\,cos(\mu-\chi_0), \qquad \rho_2(\lambda) = \delta^{(2)}_{0,1}\,cos(\lambda+\chi_0), \qquad \omega_1 = 1/2, \quad (\chi_0 = \pi/2),$$

$$\sigma_2(\mu) = \delta^{(2)}_{1,0}\,cos(\mu), \qquad \rho_2(\lambda) = \delta^{(2)}_{0,1}\,cos(\lambda), \qquad \omega_1 = -1/2, \quad (\chi_0 = 0),$$

where amplitude coefficients (see notation for Fourier coefficients in Section 1.4) are given by $\delta^{(2)}_{1,0} = \delta^{(2)}_{0,1} = \alpha$, with α a free parameter in the asymptotic expansions.

Interaction terms $\mathcal{V}_3(\mu,\lambda)$ and $\mathcal{U}_3(\mu,\lambda)$ are calculated from

$$\mathcal{V}_3(\mu,\lambda) = \frac{1}{2}\left\{\int M_3(\mu,\lambda) + \int N_3(\mu,\lambda)\right\},$$

$$\mathcal{U}_3(\mu,\lambda) = \frac{1}{2}\left\{\int M_3(\mu,\lambda) - \int N_3(\mu,\lambda)\right\},$$

with

$$M_3 = \frac{1}{2}\,(\,A_3+B_3\,), \qquad N_3 = \frac{1}{2}\,(\,A_3-B_3\,),$$

and

$$A_3 = -\sum_{i=1}^{3-2} \omega_i \left(V_{3-i_\mu} + V_{3-i_\lambda} \right),$$

$$B_3 = -\sum_{i=1}^{3-2} \omega_i \left(u_{3-i_\mu} + u_{3-i_\lambda} + \hat{p}_{3_\mu} - \hat{p}_{3_\lambda} \right).$$

(Recall that arbitrary constants of integration are removed by requiring a zero mean value on x for $\mathcal{V}_3$ and $\mathcal{U}_3$.) Thus, for the solution branch that has the frequency perturbation $\omega_1 = 1/2$ ($\chi_0 = \pi/2$), we have

$$\mathcal{V}_3(\mu,\lambda) = 1/3\, cos(3\lambda - 3\mu + 6\chi_0) - cos(\lambda - \mu + 2\chi_0) + 3/4\, \alpha\, [\, cos(\lambda + \chi_0)$$
$$+cos(\mu - \chi_0)\,] + 9/8\, \alpha\, [\, cos(\lambda + 2\mu + 3\chi_0) + cos(2\lambda - \mu + 3\chi_0)\,],$$

$$\mathcal{U}_3(\mu,\lambda) = \alpha/4\, [\, cos(\lambda + \chi_0) + cos(\mu - \chi_0)\,] - 3/8\, \alpha\, [\, cos(\lambda - 2\mu + 3\chi_0)$$
$$-cos(2\lambda - \mu + 3\chi_0)\,].$$

For the branch $\omega_1 = -1/2$ ($\chi_0 = 0$), the interaction terms take the form

$$\mathcal{V}_3(\mu,\lambda) = 1/3\, cos(3\lambda - 3\mu) - cos(\lambda - \mu) - 3/4\, \alpha\, [\, cos(\lambda) + cos(\mu)\,]$$
$$-9/8\, \alpha\, [\, cos(2\lambda - \mu) + cos(-\lambda + 2\mu)\,],$$

$$\mathcal{U}_3(\mu,\lambda) = -\alpha/4\, [\, cos(\lambda) - cos(\mu)\,] - 3/8\, \alpha\, [\, cos(2\lambda - \mu) - cos(-\lambda + 2\mu)\,].$$

Appendix 1.3

Weakly nonlinear analysis: $O(\epsilon^4)$ solution

Forcing terms appearing in the integro–differential equations at $O(\epsilon^4)$ are given by

$$R_4(\lambda) = -\frac{1}{4\pi}\,\omega_1\,\frac{\partial}{\partial\lambda}\int_0^{2\pi}[\,\mathcal{V}_3+\mathcal{U}_3\,]\,d\mu - \frac{1}{4\pi}\,\omega_2\,\frac{\partial}{\partial\lambda}\int_0^{2\pi}[\,\mathcal{V}_2+\mathcal{U}_2\,]\,d\mu$$
$$-\frac{1}{4\pi}\frac{\partial}{\partial\lambda}\int_0^{2\pi}[\,K\mathcal{V}_3+P_4\,]\,d\mu,$$

$$T_4(\mu) = -\frac{1}{4\pi}\,\omega_1\,\frac{\partial}{\partial\mu}\int_0^{2\pi}[\,\mathcal{V}_3-\mathcal{U}_3\,]\,d\lambda - \frac{1}{4\pi}\,\omega_2\,\frac{\partial}{\partial\mu}\int_0^{2\pi}[\,\mathcal{V}_2-\mathcal{U}_2\,]\,d\lambda$$
$$-\frac{1}{4\pi}\frac{\partial}{\partial\mu}\int_0^{2\pi}[\,K\mathcal{V}_3+P_4\,]\,d\lambda.$$

Replacing interaction and pressure terms as given in Appendices 1.1 and 1.2, we obtain unidirectional waves $\sigma_3(\mu)$, $\rho_3(\lambda)$ and frequency perturbation ω_2 in the form

$$\sigma_3(\mu) = \delta^{(3)}_{2,0}cos[2(\mu-\chi_0)],\quad \rho_3(\lambda) = \delta^{(3)}_{0,2}cos[2(\lambda+\chi_0)],\quad \omega_2 = 5/16+\gamma/2,\quad (\chi_0=\pi/2),$$

$$\sigma_3(\mu) = -\delta^{(3)}_{2,0}\,cos[2\mu],\qquad \rho_3(\lambda) = -\delta^{(3)}_{0,2}\,cos[2\lambda],\qquad \omega_2 = 5/16+\gamma/2,$$

where the amplitude coefficient depends on the free parameter α (appearing at previous order) in the form $\delta^{(3)}_{2,0} = \delta^{(3)}_{0,2} = (1+\gamma)\alpha^2/4$ (see notation for Fourier coefficients in Section 1.4).

Interaction terms $\mathcal{V}_4(\mu,\lambda)$ and $\mathcal{U}_4(\mu,\lambda)$ are calculated from

$$\mathcal{V}_4(\mu,\lambda) = \frac{1}{2}\left\{\int M_4(\mu,\lambda) + \int N_4(\mu,\lambda)\right\},$$

$$\mathcal{U}_4(\mu,\lambda) = \frac{1}{2}\left\{\int M_4(\mu,\lambda) - \int N_4(\mu,\lambda)\right\},$$

with

$$M_4 = \frac{1}{2}\,(\,A_4 + B_4\,), \qquad N_4 = \frac{1}{2}\,(\,A_4 - B_4\,),$$

and

$$A_4 = -\sum_{i=1}^{2} \omega_i \left(V_{4-i_\mu} + V_{4-i_\lambda} \right),$$

$$B_4 = -\sum_{i=1}^{2} \omega_i \left(u_{4-i_\mu} + u_{4-i_\lambda} + \hat{p}_{4_\mu} - \hat{p}_{4_\lambda} \right).$$

(Recall that arbitrary constants of integration are removed by requiring a zero mean value on x for $\mathcal{V}_4$ and $\mathcal{U}_4$.) Thus, for the solution branch that has the frequency perturbation $\omega_1 = 1/2$ ($\chi_0 = \pi/2$), we have

$$\begin{aligned}
\mathcal{V}_4(\mu,\lambda) = {} & 3/16\,(1+\gamma)\,\alpha^2\,\{cos[2(\lambda+\chi_0)] + cos[2(\mu-\chi_0)]\} \\
& +(1/12 - \gamma^3/2)\,cos[4\lambda - 4\mu + 8\chi_0] \\
& -(2/3 + 2\gamma^3)\,cos[2\lambda - 2\mu + 4\chi_0] + (1+\gamma)\,\alpha^2/2\,cos[\lambda - \mu + 2\chi_0] \\
& +(1+\gamma)\,\alpha^2/3\,cos[3\lambda - \mu + 4\chi_0] + (1+\gamma)\,\alpha^2/3\,cos[-\lambda + 3\mu - 4\chi_0] \\
& +(1/32 + 3/4\gamma)\,\alpha\,cos[\lambda + \chi_0] + (1/32 + 3/4\gamma)\,\alpha\,cos[\mu - \chi_0] \\
& -75/64\,\alpha\,cos[2\lambda - 3\mu + 5\chi_0] + 9/64\,\alpha\,cos[\lambda - 2\mu + 3\chi_0] \\
& -125/192\,\alpha\,cos[3\lambda - 2\mu + 5\chi_0] - 9/64\,\alpha\,cos[2\lambda - \mu + 3\chi_0] \\
& -9/32\,\alpha\,cos[-\lambda + 2\mu - 3\chi_0] + 25/48\,\alpha\,cos[-2\lambda + 3\mu - 5\chi_0],
\end{aligned}$$

$$\begin{aligned}
\mathcal{U}_4(\mu,\lambda) = {} & 1/16\,(1+\gamma)\,\alpha^2\,\{cos[2(\lambda+\chi_0)] - cos[2(\mu-\chi_0)]\} \\
& +(1+\gamma)\,\alpha^2/6\,cos[3\lambda - \mu + 4\chi_0] - (1+\gamma)\,\alpha^2/6\,cos[-\lambda + 3\mu - 4\chi_0] \\
& +(3/32 + 1/4\gamma)\,\alpha\,cos[\lambda + \chi_0] - (3/32 + 1/4\gamma)\,\alpha\,cos[\mu - \chi_0] \\
& +15/64\,\alpha\,cos[2\lambda - 3\mu + 5\chi_0] - 15/64\,\alpha\,cos[\lambda - 2\mu + 3\chi_0] \\
& -25/192\,\alpha\,cos[3\lambda - 2\mu + 5\chi_0] + 9/64\,\alpha\,cos[2\lambda - \mu + 3\chi_0] \\
& +3/32\,\alpha\,cos[-\lambda + 2\mu - 3\chi_0] - 5/48\,\alpha\,cos[-2\lambda + 3\mu - 5\chi_0].
\end{aligned}$$

For the branch $\omega_1 = -1/2$ ($\chi_0 = 0$), the interaction terms take the form

$$\begin{aligned}
\mathcal{V}_4(\mu,\lambda) = {} & (1/32 + 3/4\gamma)\,\alpha\,\{cos[\lambda] + cos[\mu]\} \\
& +3/16\,(1+\gamma)\,\alpha^2\,\{cos[2\lambda] + cos[2(\mu - \chi_0)]\} \\
& +(1/12 - \gamma^3/2)\,cos[4\lambda - 4\mu] - (2/3 + 2\gamma^3)\,cos[2\lambda - 2\mu] \\
& +(1+\gamma)\,\alpha^2/2\,cos[\lambda - \mu] + (1+\gamma)\,\alpha^2/3\,cos[3\lambda - \mu] \\
& +(1+\gamma)\,\alpha^2/3\,cos[-\lambda + 3\mu] - 75/64\,\alpha\,cos[2\lambda - 3\mu] \\
& -9/64\,\alpha\,cos[\lambda - 2\mu] - 125/192\,\alpha\,cos[3\lambda - 2\mu] \\
& -9/64\,\alpha\,cos[2\lambda - \mu] + 25/48\,\alpha\,cos[-2\lambda + 3\mu],
\end{aligned}$$

$$\begin{aligned}
\mathcal{U}_4(\mu,\lambda) = {} & 1/16\,(1+\gamma)\,\alpha^2\,\{cos[2\lambda] - cos[2\mu]\} \\
& +(1+\gamma)\,\alpha^2/6\,cos[3\lambda - \mu] - (1+\gamma)\,\alpha^2/6\,cos[-\lambda + 3\mu] \\
& +(3/32 + 1/4\gamma)\,\alpha\,\{cos[\lambda] - cos[\mu]\} \\
& +15/64\,\alpha\,cos[2\lambda - 3\mu] - 25/192\,\alpha\,cos[3\lambda - 2\mu] \\
& +9/64\,\alpha\,cos[2\lambda - \mu] - 9/64\,\alpha\,cos[-\lambda + 2\mu] \\
& -5/48\,\alpha\,cos[-2\lambda + 3\mu].
\end{aligned}$$

Appendix 1.4

Weakly nonlinear analysis: $O(\epsilon^5)$ solution

Forcing terms appearing in the integro–differential equations at $O(\epsilon^5)$ are given by

$$R_5(\lambda) = -\frac{1}{4\pi}\,\omega_1\,\frac{\partial}{\partial\lambda}\int_0^{2\pi}[\,\mathcal{V}_4+\mathcal{U}_4\,]\,d\mu - \frac{1}{4\pi}\,\omega_2\,\frac{\partial}{\partial\lambda}\int_0^{2\pi}[\,\mathcal{V}_3+\mathcal{U}_3\,]\,d\mu$$

$$-\frac{1}{4\pi}\,\omega_3\,\frac{\partial}{\partial\lambda}\int_0^{2\pi}[\,\mathcal{V}_2+\mathcal{U}_2\,]\,d\mu + \omega_2\,\rho_3'(\lambda) - \frac{1}{4\pi}\frac{\partial}{\partial\lambda}\int_0^{2\pi}[\,K\mathcal{V}_4+P_5\,]\,d\mu,$$

$$T_5(\mu) = -\frac{1}{4\pi}\,\omega_1\,\frac{\partial}{\partial\mu}\int_0^{2\pi}[\,\mathcal{V}_4-\mathcal{U}_4\,]\,d\lambda - \frac{1}{4\pi}\,\omega_2\,\frac{\partial}{\partial\mu}\int_0^{2\pi}[\,\mathcal{V}_3-\mathcal{U}_3\,]\,d\lambda$$

$$-\frac{1}{4\pi}\,\omega_3\,\frac{\partial}{\partial\mu}\int_0^{2\pi}[\,\mathcal{V}_2-\mathcal{U}_2\,]\,d\lambda + \omega_2\,\sigma_3'(\mu) - \frac{1}{4\pi}\frac{\partial}{\partial\mu}\int_0^{2\pi}[\,K\mathcal{V}_4+P_5\,]\,d\lambda.$$

Replacing interaction and pressure terms as given in Appendices 1.1 to 1.3, we obtain unidirectional waves $\sigma_4(\mu)$, $\rho_4(\lambda)$ and frequency perturbation ω_3 in the form

$$\sigma_4(\mu) = \delta_{2,0}^{(4)}\,cos[2(\mu-\chi_0)] + \delta_{3,0}^{(4)}\,cos[3(\mu-\chi_0)],$$
$$\rho_4(\lambda) = \delta_{0,2}^{(4)}\,cos[2(\lambda+\chi_0)] + \delta_{0,3}^{(4)}\,cos[3(\lambda+\chi_0)],$$
$$\omega_3 = 459/128 + 41/16\,\gamma + (1+\gamma)^2\,\alpha^2/16, \qquad (\chi_0 = \pi/2),$$

$$\sigma_4(\mu) = \delta_{2,0}^{(4)}\,cos[2\mu] + \delta_{3,0}^{(4)}\,cos[3\mu],$$
$$\rho_4(\lambda) = \delta_{0,2}^{(4)}\,cos[2\lambda] + \delta_{0,3}^{(4)}\,cos[3\lambda],$$
$$\omega_3 = -\{459/128 + 41/16\gamma + (1+\gamma)^2\alpha^2/16\}, \qquad (\chi_0 = 0),$$

where amplitude coefficients (see notation for Fourier coefficients in Section 1.4) are given by

$$\delta^{(4)}_{2,0} = \delta^{(4)}_{0,2} = -(305 + 377\,\gamma + 72\,\gamma^2)\,\alpha^2/96, \qquad \delta^{(4)}_{3,0} = \delta^{(4)}_{0,3} = (1+\gamma)^2\,\alpha^3/8.$$

Interaction terms $\mathcal{V}_5(\mu,\lambda)$ and $\mathcal{U}_5(\mu,\lambda)$ are calculated from

$$\mathcal{V}_5(\mu,\lambda) = \frac{1}{2}\left\{ \int M_5(\mu,\lambda) + \int N_5(\mu,\lambda) \right\},$$

$$\mathcal{U}_5(\mu,\lambda) = \frac{1}{2}\left\{ \int M_5(\mu,\lambda) - \int N_5(\mu,\lambda) \right\},$$

with

$$M_5 = \frac{1}{2}\,(\,A_5 + B_5\,), \qquad N_5 = \frac{1}{2}\,(\,A_5 - B_5\,),$$

and

$$A_5 = -\sum_{i=1}^{3} \omega_i \left(V_{5-i_\mu} + V_{5-i_\lambda} \right),$$

$$B_5 = -\sum_{i=1}^{3} \omega_i \left(u_{5-i_\mu} + u_{5-i_\lambda} + \hat{p}_{5_\mu} - \hat{p}_{5_\lambda} \right).$$

(Recall that arbitrary constants of integration are removed by requiring a zero mean value on x for $\mathcal{V}_5$ and $\mathcal{U}_5$.)

The resulting formulas for $\mathcal{V}_5$ and $\mathcal{U}_5$ are very lengthy and are not reproduced here.

Appendix 2.1

Hamiltonian structure of the equations of motion

Consider the equations of motion governing 1D compressible Gas Dynamics in mass-Lagrangian coordinates:

$$V_t = u_x, \tag{A2.1}$$

$$u_t = -p_x, \tag{A2.2}$$

where $p = p(S, V)$ is the pressure and $S = S(x)$ is a given and periodic (of period 2π, say) function defining the entropy field. We look for solutions of the equations of motion that are 2π–periodic in x and such that the specific volume V and flow velocity u have mean values one and zero, respectively.

Let $e = e(S, V)$ be the specific internal energy of the system. Recalling that $T\,dS = de + p\,dV$, we have $e_S = T$ and $e_V = -p$. Let H be the total energy, which is a constant for each solution; it is given by

$$H = \frac{1}{\pi}\int_0^{2\pi}\left\{\frac{1}{2}u^2(x,t) + e(x,t)\right\}dx.$$

We can now write Fourier series expansions for the solutions in the form

$$V(x,t) = 1 + \sum_{n=1}^{\infty}\sqrt{n}\,[\,q_n(t)\,cos(nx) + P_n(t)\,sin(nx)\,], \tag{A2.3}$$

$$u(x,t) = \sum_{n=1}^{\infty}\sqrt{n}\,[\,Q_n(t)\,cos(nx) + p_n(t)\,sin(nx)\,], \tag{A2.4}$$

and consider the Hamiltonian H as a function of $\{q_n, Q_n, p_n, P_n\}$. Furthermore, let us also expand in Fourier series the pressure:

$$p(x,t) = p_0 + \sum_{n=1}^{\infty}\sqrt{n}\,[\,A_n(t)\,cos(nx) + B_n(t)\,sin(nx)\,]. \tag{A2.5}$$

Then, the equations of motion (A2.1)–(A2.2) can be written as

$$\dot{q_n} = n\,p_n, \qquad \dot{P_n} = -n\,Q_n, \qquad \dot{Q_n} = -n\,B_n, \qquad \dot{p_n} = n\,A_n. \tag{A2.6}$$

On the other hand, a bit of variational calculus shows that

$$\frac{\partial H}{\partial p_n} = \frac{1}{\pi}\int_0^{2\pi} u\sqrt{n}\,sin(nx)\,dx = n\,p_n$$

$$\frac{\partial H}{\partial Q_n} = \frac{1}{\pi}\int_0^{2\pi} u\sqrt{n}\,cos(nx)\,dx = n\,Q_n$$

$$\frac{\partial H}{\partial P_n} = -\frac{1}{\pi}\int_0^{2\pi} p\sqrt{n}\,sin(nx)\,dx = -n\,B_n$$

$$\frac{\partial H}{\partial q_n} = -\frac{1}{\pi}\int_0^{2\pi} p\sqrt{n}\,cos(nx)\,dx = -n\,A_n$$

Thus, using the equations (A2.6), we see that the equations of motion (A2.1)–(A2.2) reduce to

$$\dot{q_n} = \frac{\partial H}{\partial p_n}, \qquad \dot{p_n} = -\frac{\partial H}{\partial q_n}, \qquad \dot{Q_n} = \frac{\partial H}{\partial P_n}, \qquad \dot{P_n} = -\frac{\partial H}{\partial Q_n}, \qquad (A2.7)$$

This is, formally, an infinite dimensional Hamiltonian system.

Of course, this derivation makes sense only as long as the solutions of (A2.1)–(A2.2) are sufficiently smooth so that (A2.3), (A2.4) and (A2.5) converge strongly enough, and in particular, term by term differentiation is allowed.